Study of the molecular mechanisms linking transcription and DNA repair in Saccharomyces cerevisiae

Diyavarshini Gopaul

NNT : 2018SACLS347

Thèse de doctorat

Study of the molecular mechanisms linking transcription and DNA repair in *Saccharomyces cerevisiae*

Thèse de doctorat de l'Université Paris-Saclay
préparée à l'Université Paris Sud

Ecole doctorale n° 577 : Structure et Dynamique des Systèmes Vivants

Spécialité de Doctorat : Sciences de la Vie et de la Santé

Thèse présentée et soutenue à Gif-sur-Yvette,
le 1er octobre 2018,

par

Mme Diyavarshini Gopaul

Composition du jury :

Pr. Capy Pierre	Professeur de l'université Paris Sud	Président
Dr. Lengronne Armelle	Directeur de Recherche, IGH Montpellier	Rapporteur
Dr. Le May Nicolas	Chargé de Recherche, IGBMC Illkirch	Rapporteur
Dr. Marcand Stéphane	Directeur de Recherche, CEA Fontenay-aux-Roses	Examinateur
Dr. Lesage Pascale	Directeur de Recherche, IUH Paris	Examinateur
Dr. Soutourina Julie	Directeur de recherche, CEA Saclay	Directeur de thèse

Acknowledgements

Four years already, time flies indeed! For my PhD, I moved from Lyon to the Paris region. Looking back at those years, I realise that each member of the team has in one way or the other left a mark on me.

First of all, I would like to extend my gratitude to my jury members: Pr. Pierre Capy, Dr. Nicolas Le May, Dr. Armelle Lengronne, Dr. Pascale Lesage and Dr. Stéphane Marcand for accepting to evaluate my work and for the interesting discussion during my defense. A special thanks to Dr. Stéphane Marcand for having accepted to be my thesis tutor and for his constructive comments during my thesis committee.

I would like to thank Julie for welcoming me in the team and without whom my PhD would not have been possible. Thank you for always being available for discussion which have been most enriching. Thank you also for having given me the opportunity to present my work at several seminars and conferences. Michel, thank you for taking the time to participate in my thesis committee and lab meetings and for your valuable inputs. Thank you also for your assistance when I had administrative setbacks for my fourth year funding application. Bénédicte, thank you for sharing with me your technical expertise and being my French professor. I will miss our little talks especially on French culture. Nathalie, thank you for our pleasant conversations and for continuing the project. Arach, thank you for your inputs during lab meetings and continuing the bioinformatic analyses of the different Rad proteins. Diletta, I enjoyed our little talks. You'll be defending next, bonne chance et bon courage! Cyril and Veronica, we were the three angry birds. "The office" was our little reunion place where we talked about science but also joked to enliven long and tiring days. I will miss those little moments. Cyril, we were also bench mates and I enjoyed working with you on different projects. Good luck with your little guys! Veronica, good luck with your experiments and take a chill pill. Thomas, Adrien, Liza, Elodie, Claire P. and M., "les anciens", thank you for sharing my day-to-day laboratory life and making it more enjoyable. Liza, thank you for helping out with the bioinformatic analyses. Olivier A, thank you for introducing me to bioinformatics, for your patience and good humour.

Catherine and Monique, thank you for always being there to facilitate administrative procedures. Catherine, our conversations on your trips made me wanderlust. I hope that one day I'll be able to go to the Galápagos Islands. Thank you Olivier L. for your assistance during my PhD from providing me with informatic support to helping me out with my administrative procedures.

Thanks to all the people of Building 144 that I have crossed path with, during all those years. For all the quick hellos down the hall that sometimes turned into a conversation.

I would like to thank my friends for being there for me and making me laugh at the most stressful time.

Last but not least, I would like to thank my family for always being there for me, for being my pillar. You made me the person I am today. Thank you.

Table of Content
Table of figures
List of abbreviations

Table of Figures

List of Abbreviations

3D DIP	DNA damage detection by DNA immunoprecipitation
6AU	6-Azauracil
6-4 PP	6-Pyrimidine-4-Pyrimidone photoproducts
ABF1	Autonomously replicating sequence binding factor 1
AML	Acute Myeloid Leukaemia
ARR	Access Repair Restore
ATM	Ataxia Telangiectasia mutated
ATP	Adenosine triphosphate
ATR	ATM related
BER	Base Excision Repair
Brd4	Bromodomain-containing protein
BRE	Transcription factor II B recognition element
BRU	Bromouridine
CAF1	Chromosome Assembly factor 1
CAK	CDK Activating kinase
CETN 2	Centrin 2
ChIP	Chromatin Immunoprecipitation
COFS	Cerebro-oculo-facio-skeletal Syndrome
CoIP	Co-immunoprecipitation
CPD	Cyclobutane pyrimidine dimer
CS	Cockayne Syndrome
CSB	Cockayne Syndrome protein B
CSN	CoP9 signalosome
CTD	C-terminal domain
DCE	Downstream core element
DDR	DNA damage response
DEF1	RNA Polymerase II degradation factor 1
DPE	Downstream promoter element
DSC	DeSanctis Cacchione Syndrome
DRB	5,6-Dichloro-1-β-D-ribofuranosylbenzimidazole
DSIF	DRB Sensitivity-Inducing Factor
FEN1	Flap endonuclease 1
GG-NER	Global Genome Nucleotide Excision repair

GTFs	General Transcription factors
GO	Gene Ontology
H3K14	Histone H3 Lysine 14
HA	Human Influenza Hemagglutinin
HAT	Histone Acetyltransferase
HhH2	Helix-Hairpin-Helix
HIRA	Histone regulator A
HR	Homologous recombination
HS Seq	High Sensitivity Damage Sequencing
IEG	Immediate Early Genes
IGB	Integrated genome browser
INO80	Inositol Requiring 80
INR	Initiator
LL	Leucine Latch
MED	Mediator
MMR	Mismatch repair pathway
MPA	Mycophenolic Acid
mRNA	messenger RNA
MTE	Motif Ten Elements
ncRNA	Non-coding RNA
NER	Nucleotide Excision Repair
NELF	Negative Elongation Factor
NHEJ	Non-Homologous End Joining
NLS	Nuclear localization signal
NMR	Nuclear Magnetic Resonance
NPC	Nuclear Pore Complex
NTP	Nucleotide Triphosphate
NSs	Non-Structural protein
ORF	Open Reading Frame
PAF1	Pol II associated Factor 1 complex
PARP	Poly ADP Ribose Polymerase I
PCNA	Proliferating Cell Nuclear Antigen
Pdr1	Pleiotropic drug resistance
PH	Pleckstrin homology
PIC	Pre-initiation complex

P-TEFb	Positive Transcription Elongation Factor
RAD	Radiation Sensitive
RF-C	Replication Factor C
RNA Pol	RNA Polymerase
RPM	Reads Per Million
SEC	Super Elongation Complex
SF2	Super Family 2
TAF	TBP associated protein
TBP	TATA Binding Protein
TC-NER	Transcription Coupled Nucleotide Excision Repair
TF	Transcription factors
TFBs	Transcription Factor Binding Sites
TFIIH	Transcription Factor II H
TGFβ	Transforming Growth Factor β
TPE	Telomere Position Effect
TREX	Transcription Coupled Export
TSS	Transcription Start Site
TTD	Tricho Trio Dystrophy
UAS	Upstream Activating Sequences
UBD	Ubiquitin Binding Domain
URS	Upstream Regulatory Sequences
USP7	Ubiquitin Specific Protease 7
UV	Ultraviolet
UV-DBB	UV radiation DNA Damage Binding Protein
UVSS	UV sensitive Syndrome
UV-SSA	UV Stimulated Scaffold Protein A
XFE	XPF-ERCC1 Progeroid Syndrome
XP	xeroderma pigmentosum
XPC	Xeroderma Pigmentosum Group C
XPE	Xeroderma Pigmentosum Group E
XR-Seq	Excision Repair Sequencing
YPD	Yeast Peptone Dextrose

Introduction

I. DNA repair pathways

The delivery of an intact genetic material to the next generation is a prerequisite to the survival of any species. A human cell endures tens of thousands of DNA lesions on a daily basis (Jackson and Bartek, 2009) and this can have dire effects on the cell, hence DNA damages have to be repaired most faithfully. Lesions can be of exogenous nature (such as sunlight, ionising radiation and genotoxic compounds) or of endogenous nature (such as by-products of the cell's metabolism or cellular processes like replication). It is vital that DNA damages are either repaired or tolerated as they can interfere with fundamental processes like replication and transcription and also have mutagenic effects. When they occur in gametes, mutations can be passed on to the next generation and it is crucial for the species viability that an undamaged genetic material is passed on. Mutations occurring in somatic cells can lead to genome instability which has been associated with cancer and ageing. It is hence essential to resolve DNA lesions and the cell has developed an elaborate and highly coordinated pathway called the DNA damage response (DDR) to detect and trigger an appropriate cellular response to maintain genome integrity. Cellular response to genotoxic stress can be the activation of DNA repair pathways, stimulation of transcriptional programmes, cell cycle arrest or even apoptosis depending on the extent of the damage and cell proliferative status. As of now, all the components of this pathway are not known. However, many genes involved in the DDR pathway are conserved from yeast to mammals (Zhou and Elledge, 2000).

DNA repair pathways can detect a large variety of DNA damages. Figure 1 illustrates the most common DNA damages and their most relevant repair mechanisms (Hoeijmakers, 2001). Although the DNA repair pathways are represented in an independent manner, there are cross-talks in between them and some proteins can be involved in more than one pathway. DNA repair mechanisms are well conserved in eukaryotes but the degree of structural and functional conservation differs between pathways.

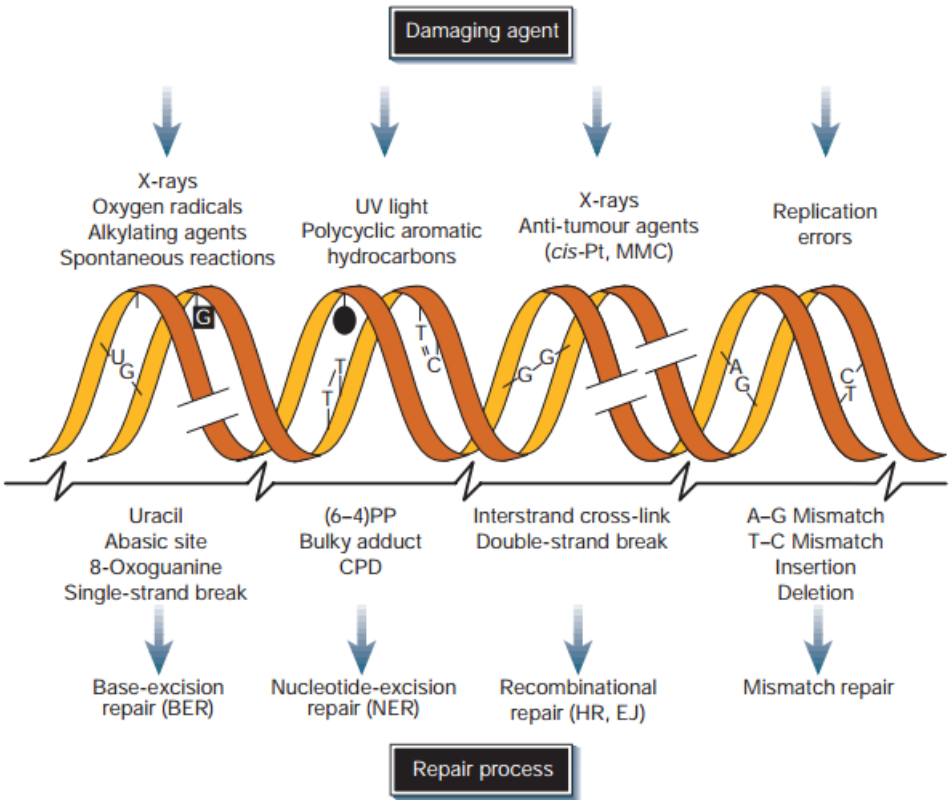

Figure 1: DNA damage, repair mechanisms and consequences.
Common DNA damaging agents (top); examples of DNA lesions induced by these agents (middle); and most relevant DNA repair mechanism responsible for the removal of the lesions (bottom) (Hoeijmakers, 2001).

The main DNA repair pathways are as follows:

1. Base Excision Repair (BER) removes base modifications such as oxidation, alkylation and deamination. These damages are relatively common and can result from the spontaneous decay of DNA and also from environmental sources such as chemicals and cytostatic drugs. DNA glycosylases recognize and remove the damaged base, leaving an abasic site that is further processed by patch-repair to completely resolve the damage (Krokan and Bjøras, 2000).

2. Nucleotide Excision Repair (NER) pathway detects distortion in the DNA helix caused by bulky adducts (refer to "Nucleotide Excision Repair" chapter below).

3. Double strand breaks are typically repaired by homologous recombination (HR) and non-homologous end-joining (NHEJ). HR uses the homologous chromatid and therefore involves strand invasion. NHEJ consists of end ligation independently of sequence homology (Ceccaldi *et al.,* 2016). Double strand breaks can arise from replication fork collapse or some chemotherapeutic agents and ionising irradiation.

4. Mismatch Repair pathway (MMR) recognises base mispairing or small insertions/deletions generated during recombination or that have escaped the proofreading activity of DNA polymerases. Errors that arise during DNA replication can become permanent in dividing cells therefore it is important that they are resolved (Li, 2007).

II. NER (Nucleotide Excision Repair)

In the laboratory we are particularly interested in the NER (Nucleotide Excision Repair) pathway and hence it will be presented in more details. The NER pathway is conserved in eukaryotes, prokaryotes and archaea. One of the particularities of this pathway is that it is able to repair structurally and chemically diverse base lesions, the common point being that the DNA damages are able to create DNA helix distortion. Helix-distorting damages include UV-induced photoproducts, DNA adducts formed from environmental mutagens, for example, polycyclic hydrocarbons (benzo[a]pyrene) and aromatic amines (acetylaminofluorene), certain chemotherapeutic drugs like cisplatin and certain cyclopurines which represent a class of oxidative lesions that are specifically repaired by NER (Gunz *et al.,* 1996; Zhou and Moorthy 2016 and as reviewed in Gillet and Scharer 2006).

II.1 History of NER discovery

The 1960s were a turning point in radiation biology and molecular biology as molecular mechanisms were attributed to the previously observed radiation sensitivity phenotype of *E.coli* strain B/r exposed to UV-irradiation (Hill, 1958). Many laboratories contributed to the understanding of the molecular basis of this radiation sensitivity. Setlow *et al.* reported that DNA synthesis was inhibited in this mutant compared to the radiation resistant strain which was only temporarily inhibited after UV irradiation (Setlow *et al.,* 1963). Hence, the authors proposed that the thymine dimers observed after UV irradiation blocked DNA synthesis *in vivo*. Further study revealed that most of these thymine dimers where part of a sequence with structure pXpTpT where the rate of dimer formation depends on the X base (Setlow *et al.,* 1964). That year, a new enzymatic mechanism that removes intrastrand thymine dimers in the dark was reported (Setlow & Carrier 1964). Similar results were obtained using another UV-sensitive *E.coli* mutant, AB1886 (Boyce and Howard-Flanders, 1964). In the continuity of characterising the molecular mechanisms behind the observed UV-sensitivity, it was demonstrated that the excised single-stranded DNA containing the damage was replaced using the undamaged strand as template in bacteria (Hanawalt 1964).

Parallel experiments carried out in human cells showed similar *de novo* DNA synthesis after UV irradiation (Rasmussen and Painter, 1964). In yeast also, a photoproduct retention in UV-sensitive mutant compared to the wild-type strain was demonstrated in the dark (Unrau *et al.,* 1971). In archaea as well it was demonstrated that the removal of UV-induced DNA damage in the dark requires homologs of the bacterial NER genes (Crowley *et al.,* 2006).

Therefore, the NER pathway is a highly conserved mechanism that can be found in all three branches of life (archaea, bacteria, eukaryotes) attesting its vital importance.

This pathway which comprises the excision of the DNA fragment containing the helix-distorting adduct followed by DNA synthesis to fill the gap using the opposite strand as template was termed nucleotide excision repair (NER) by Friedberg and his colleagues (Duncan *et al.,* 1976).

II.2 UV-induced damages

One of the sources of helix-distorting lesions is non-ionising radiation from sunlight. Therefore, in the laboratory, we use UV-irradiation to induce NER substrates. In this section, the two most common UV-induced damages: CPD (Cyclobutane Pyrimidine Dimers) and 6-4 PP (6-4 Photoproduct) will be discussed. There are also other less prevalent lesions that can be induced such as cytosine hydrate, adenine adducts and adenine dimers. These damages can constitute a block to the progression of the transcription and replication machineries and should therefore be quickly resolved.

Solar radiation can be divided into UV (Ultraviolet) A (315-400 nm), UVB (280-315 nm) and UVC (100-280 nm). At 254 nm, the optimal absorption wavelength of UV radiation by DNA, there is no major direct ionization taking place (Seebode *et al.*, 2016). The use of UVC for the study of the NER pathway in laboratory conditions is hence not aberrant even though it is not the major radiation reaching the Earth due to its short wavelength. UV-light poses a high mutagenic risk even though it is a small fraction of the solar spectrum. Therefore, cells possess diverse mechanisms such as UV-absorbing pigmentation (melanin) and DNA repair mechanisms (NER) to counteract these DNA aggressions.

The absorption of radiation energy by two adjacent pyrimidines (cytosines or thymines) can lead to the formation of a covalent bond between these two bases. This can result in the formation of CPDs and 6-4 PPs, two of the most cytotoxic DNA lesions, generated in a ratio of 8:1 or 3:1, depending on the detection methods (Douki *et al.*, 2001; Perdiz *et al.*, 2000). These two lesions also differ in their persistence time as CPDs are repaired more slowly than 6-4 PPs. The genome-wide repair kinetics were measured in human cells and it was demonstrated that the bulk of 6-4 PP repair was completed within 4h, whereas CPDs removal was slower and persisted after 48h in certain regions (Adar *et al.,* 2016). It is possible that this difference in repair kinetics is due to the chemical structure of these two dimers, the difference in DNA distortion induced and the NER sub-pathway activated (refer to section “NER steps” for details on the sub-pathways).

To note that there is another pathway that can undertake the repair of pyrimidine dimers: the photo-reactivation pathway. This pathway is light-dependent and uses CPD or 6-4 specific photolyases to repair these damages (Kelner, 1949). It has been identified in species of archaea, bacteria, fungi including yeast but is absent in placental mammals.

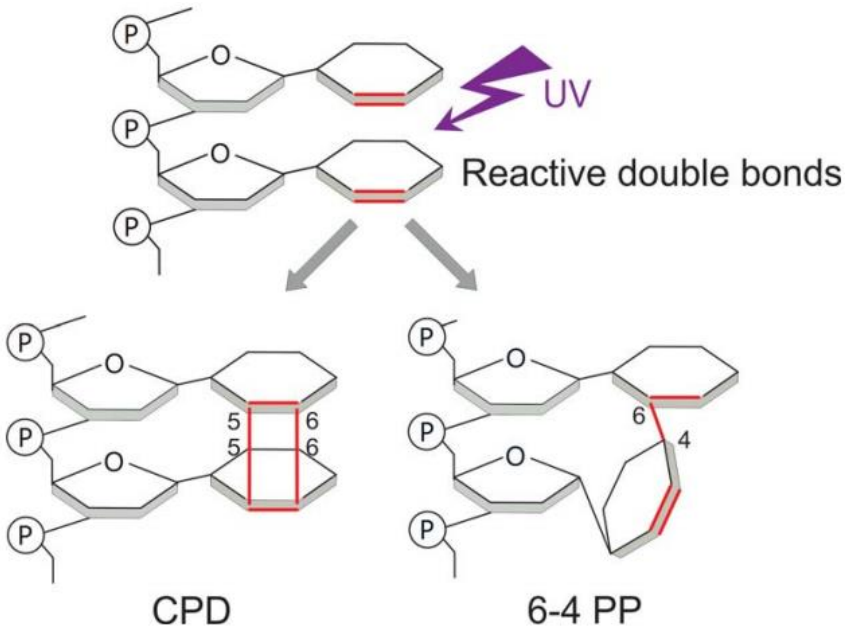

Figure 2: Formation of photoproducts induced by UV-light.
The absorption of solar radiation can lead to the formation of CPD (Cyclobutane Pyrimidine Dimers) and 6-4 PP (6-Pyrimidine-4-Pyrimidone photoproducts) (Seebode *et al*., 2016).

II.2.1 CPD (Cyclobutane Pyrimidine Dimers)

It is the most abundant UV-induced lesion, produced by UVA, UVB and UVC (Ravanat and Douki, 2016). It involves the formation of a covalent bond between the carbon 5 and carbon 6 of adjacent pyrimidines, disrupting the double bonds they were implicated in (Figure 2). Structural analysis showed that CPD caused a helical bending of 9° and did not seem to impact on the stacking of the bases (Kim *et al.,* 1995). Also, the formation of CPD is sequence dependent and the yield of formation is different with TT, TC, CT and CC CPDs being produced in a roughly 10:5:2:1 ratio in isolated as well as in cellular DNA (Ravanat and Douki, 2016).

II.2.2 6-4 PP (6-Pyrimidine-4-Pyrimidone photoproducts)

6-4 PPs are produced by UVB and UVC but not UVA irradiation (Ravanat and Douki, 2016). Their formation involves the double bond between carbon 5 and carbon 6 of the 5' pyrimidine and the C4 of the 3' end pyrimidine (Figure 2). Structural analysis demonstrated that 6-4 caused a helical bending of 44° and there was a disruption of the hydrogen bonds at the 3' side of the 6-4PP (Kim *et al.,* 1995). 6-4 PP formation is also sequence dependent and TC 6-4 PP is the most common 6-4 PP formed (Ravanat and Douki, 2016).

In mouse cell lines proficient in the repair of either type of dimer, it was shown that CPDs were the most mutation-inducing UV-lesions (You *et al.,* 2001) and CPD was also identified as the main cause of skin cancer in transgenic mice (Jans *et al.,* 2005). Therefore 6-4 PP

contribute to a smaller degree to UV mutagenesis despite their mutagenic properties, at least in mouse models as there can be differences between human and rodent cells.

II.2.3 Elements influencing the generation of UV-induced damages

In the above section it was mentioned that the formation of 6-4 PP and CPD is dependent on the sequence, adjacent pyrimidines are required and formation of TT CPD and TC 6-4 PP is favoured. There are other factors that can influence the formation of UV-damage. Single nucleotide damage mapping of CPD genome-wide in yeast showed that these damages are not uniformly distributed and dependent on the chromosome landscape and transcription factors (Mao *et al*., 2016). The authors showed that the presence of nucleosomes drastically influenced the formation of CPD leading to a UV-damage pattern which is not present in naked DNA. CPD was less frequent in DNA located at inward rotational settings within nucleosomes compared to the outward facing DNA. UV damage formation was also inhibited at transcription factor bound DNA thereby protecting important functional DNA sequences. On the contrary, studies carried out in human cells came to different conclusions; transcription factor binding did not inhibit UV-damage formation like in yeast, the results were more complex (Hu *et al.,* 2017; Pfeifer *et al.,* 1992). Indeed, genome-wide mapping of 6-4 PP and CPD showed that, there is a general increase in UV-damage formation in transcription factor binding sites (TFBS). However, case per case analysis showed that for some genes there was an increase in UV-damage formation on the motif carrying DNA but not for other TFBS. The generation of UV-damage in the complementary strand was inhibited in all cases. Therefore, in human cells, there is a variation in UV-damage formation depending on the binding sites of specific transcription factor, damage type, and strand (Hu *et al.,* 2017).

II.3 NER: repair steps

The NER pathway was discovered more than five decades back and new reports are still shedding light on this repair mechanism. It has been shown that NER comprises the following steps:

(i) Recognition of the damage.
(ii) Unwinding of the double helix around the damage.
(iii) Incision on the 3’ and 5’ sides of the single-stranded DNA containing the lesion.
(iv) Excision of the damaged single-stranded DNA.
(v) DNA synthesis to fill the gap of the excised fragment.
(vi) Ligation to seal the nick.

The different steps are presented separately but *in vivo* they can be overlapping.

The NER pathway can be divided into two sub-pathways: GG-NER (Global Genome Nucleotide Excision Repair) and TC-NER (Transcription coupled Nucleotide Excision Repair) (Figures 3 and 4). The two sub-pathways differ at the recognition step. The GG-NER repairs damages in the genome overall, whereas TC-NER repairs damage on the transcribing strand

that blocks the progression of RNA Pol II. The subsequent steps of NER are common to both sub-pathways. The repair rate and damage removal efficiency of these two sub-pathways also differ.

II.3.1 Recognition step:

NER is a versatile pathway that is able to detect a wide variety of structurally and chemically diverse base lesions, all causing DNA distortion. Therefore, the recognition factors are faced with the challenge of recognising these very diverse lesions for efficient NER.

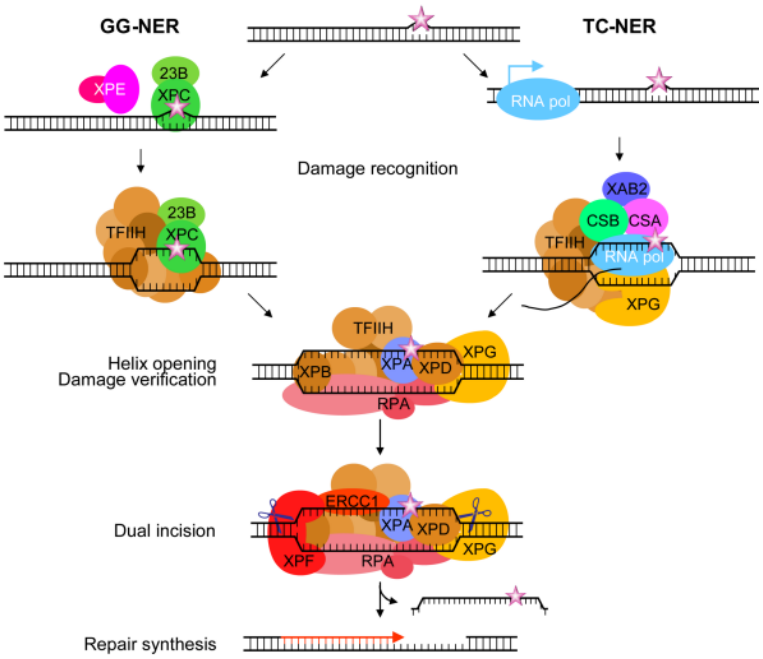

Figure 3: The NER pathway as proposed in human.
In GG-NER, the XPC-RAD23B dimer first recognises the helix-distorting lesion. DDB1/2 (XPE) complex and associated factors aid in the recognition of DNA damages. XPC-RAD23B complex recruits TFIIH to the DNA damge site and the two helicase subunits of TFIIH namely XPB and XPD unwind the DNA around the damage. RPA, XPA and XPG are then recruited to verify the damage and form the pre-incision complex. XPG has a 3' endonuclease activity which does not seem to be active at this step. After the recruitment of the 5' endonuclease dimer ERCC1-XPF, dual incision occurs. ERCC1-XPF cuts on the 5' of the DNA damage while XPG cuts on the 3' side which results in a gap. The replication machinery and DNA ligase I seal the gap. On the other hand, the TC-NER mechanism is less well characterized and is initiated by a RNA polymerase arrested at a DNA lesion site. The recognition step differs from the GG-NER mechanism and appears to involve CSB, CSA, XAB2, TFIIH and XPG proteins. However the subsequent steps: damage verification, dual incision and repair synthesis step are similar to the GG-NER mechanism (Schärer, 2008).

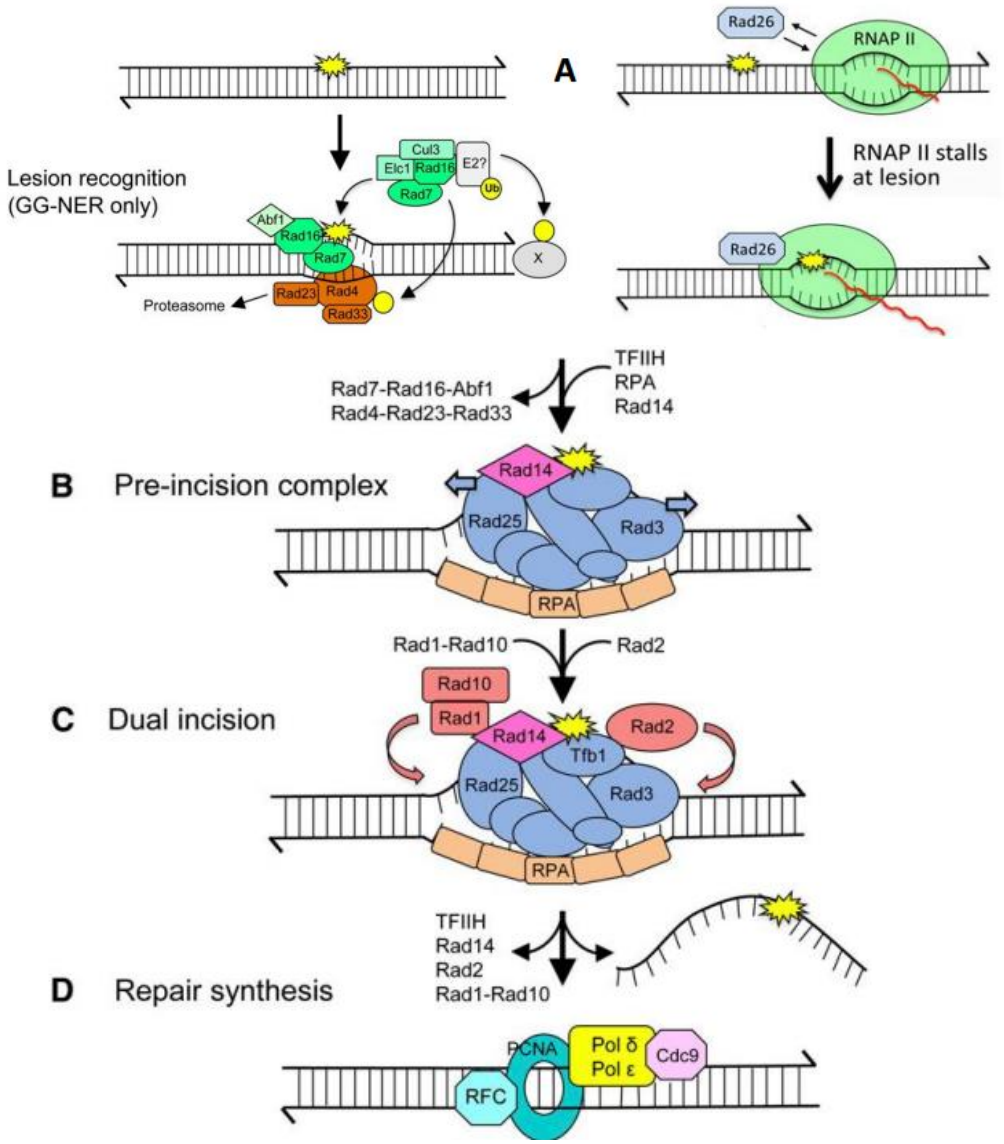

Figure 4: The NER pathway as proposed in yeast.
(A) The recognition step of the GG-NER and TC-NER pathway are shown. During GG-NER, Rad4-Rad23-Rad33 and Rad7-Rad16 complexes recognise a helix-distorting lesion (yellow star). It has been proposed that Rad7-Rad16 as part of a complex with Abf1 has chromatin remodelling activity, whereas as part of a complex with Elc1-Cul3-E2 has Ub ligase activity. These activities allow efficient DNA damage recognition by Rad4 and helix opening. In TC-NER, RNA Pol II is the first factor encountering the DNA damage. The interaction between Rad26 and the stalled RNA Pol II is then stabilised. (B) TFIIH (subunits are in blue), Rad14, and RPA then recruited form a pre-incision complex, verifies the lesion and further opens the DNA around the lesion. (C) The endonucleases Rad1-Rad10 dimer and Rad2 incise the 5' and 3' of the DNA damage, respectively. (D) The lesion-containing oligonucleotide is released from the duplex. The following steps involves DNA resynthesis and ligation to fill the gap (Boiteux and Jinks - Robertson, 2013).

II.3.1.1 Damage recognition in GG-NER

The GG-NER (Global Genome Nucleotide Excision Repair) removes damage throughout the genome independently of transcriptional activity including the non-transcribed strand of transcribed regions (the steps are summarised in Figures 3 (human) and 4 (yeast)).

GG-NER recognition step requires a dimer comprised of XPC and RAD23B (Xeroderma Pigmentosum group C and RADiation sensitive 23B) in human and their homologs Rad4 and Rad23 (RADiation sensitive 4 and 23) in the budding yeast *Saccharomyces cerevisiae* (Sugasawa *at al.,* 1998; Jansen *et al*., 1998). This Rad4/XPC and Rad23/RAD23B complex probes the DNA and recognises the unpaired single-stranded DNA opposite the lesion (Sugasawa *et al.,* 2001). In yeast the structural domains of Rad4 binding the single-stranded DNA was solved by macromolecular crystallography, it shows that Rad4 contacts primarily the undamaged DNA strand and expels the damaged bases out of the double helix (Min *et al.*, 2007). Therefore, instead of direct lesion recognition, it seems that recognition is achieved by strand separation and exclusion of lesions. This could account for the broad variety of substrates recognised by NER. Rad23/RAD23B have been suggested to have a more accessory role in NER by stabilizing the Rad4/XPC protein, aiding in the assembly of the NER complex and protecting Rad4/XPC from proteasomal degradation (Xi *et al*., 2004, Ng *et al.,* 2003, Lommel *et al.,* 2002). Also, genetic studies showed that the DNA binding activity of XPC is potentiated by the binding of CETN2 (centrin 2) to XPC (Nishi *et al.*, 2005). A similar role was reported for the homolog of CETN2 in the budding yeast, Rad33 (de Bulk *et al*., 2008).

However, lesions that only mildly destabilise the DNA helix such as UV-induced CPD (Cyclobutane Pyrimidine Dimer) are poor substrates for Rad4/XPC. Indeed, it was reported that after UV-irradiation, XPC localised only to 6-4 PP sites, therefore XPC does not efficiently recognise CPDs *in vivo* (Fitch *et al.*, 2003). Hence in mammals, an auxiliary recognition complex aids in the recognition of these damages: the UV-DDB complex (UltraViolet radiation–DNA Damage Binding protein), also called XPE (Xeroderma Pigmentosum group E) (Chu and Chang, 1988; Wakasugi *et al.,* 2002).

The mammalian UV-DDB complex, composed of two principal subunits UV-DDB1 and 2, binds to the damage directly and bends the DNA, stimulating the subsequent binding of XPC (Scrima *et al.,* 2008). Indeed, it was reported that *in vivo*, DDB2 localises to CPD and 6-4 PP damages, immediately after UV, ahead and independently of XPC (Fitch et al., 2003; Moser et al., 2005; Wakasugi et al.,2002). It was demonstrated that XPC was recruited to CPD damage by UV-DDB2 *in vivo* (Fitch *et al.*, 2003). A mechanism was proposed where UV-DDB complex forms a stable complex with UV-induced photo-lesions and target NER factors such as XPC-RAD23 complex to allow efficient removal of these damages (Moser *et al.,* 2005). Moreover, it was showed that UV-DDB facilitates repair of 6-4PPs preferably and later that of CPDs *in vivo*. In the absence of UV-DDB, XPC-Rad23B pathway still repaired 6-4 PPs but at a slower rate and CPDs were repaired to a lesser amount. This could be explained by the

fact that 6-4 PPs induce a greater DNA distortion than CPDs and hence may be recognised more easily by XPC-RAD23B complex.

Additionally, the UV-DDB complex is part of an E3 ubiquitin ligase 3 complex and it was demonstrated that after UV irradiation, XPC and UV-DDB complex itself was ubiquitinated by this E3 ligase complex (Sugasawa *et al.,* 2005). This ubiquitination increased the binding affinity of XPC-RAD23 complex to the photo-lesion, whereas the affinity of the UV-DDB complex was reduced. Furthermore, given that UV-DDB in its unmodified form has a higher affinity for UV-induced lesions than XPC, it was suggested that ubiquitination actually played a role in transferring the DNA lesion from UV-DDB to XPC which is essential for the recruitment of downstream factors (Sugasawa *et al*., 2005).

To note that no UV-DDB1 homolog has yet been identified in *S. cerevisiae* but it is present in *S. pombe* and mammals (Tang and Chu, 2002). On the contrary, photolyase exists in *S. cerevisiae*, but not in placental mammals or *S. pombe*. By comparing the binding of UV-damaged DNA from wild-type *S. cerevisiae* extract or from photolyase deletion mutants, it was showed that the UV-binding activity was attributable to photolyase (Patterson and Chu, 1989). Hence it has been proposed that species have evolved to use only one, either UV-DDB1 or photolyase (Tang and Chu, 2002). Therefore, when using *S. cerevisiae* as biological model to study the NER pathway, it is important to shield the cells from light given that the photolyase pathway is light-dependent.

Therefore, there are few differences between human and the budding yeast even though the GG-NER sub-pathway is conserved in both organisms. Another one is that in *S. cerevisiae* there is another GG-NER specific complex comprising of Rad7 and Rad16, with no homolog described in human cells as of yet (Prakash and Prakash, 2000). Rad7 and Rad16 form a stable complex that removes UV-induced damages from non-transcribed regions of the genome including the non-transcribed strand of transcribing genes (Verhage *et al*., 1994, Guzder *et al*., 1997). It was demonstrated that Rad4-Rad23 complex was indispensable for NER *in vitro* whereas Rad7-Rad16 had a more stimulatory role in NER (Guzder et al., 1999). Also, it was shown that Rad4 (yeast homolog of XPC) interacts with Rad7 (Wang *et al.,* 1997) and that there is a synergistic interaction between Rad7-Rad16 complex and Rad4-Rad23 complex to bind UV-damaged sites (Guzder *et al*., 1999).

Rad16 is part of the SWI/SNF2 family and has a DNA-dependent ATPase activity which is markedly reduced by UV-damage (Guzder *et al.*, 1998) and this ATPase activity is essential for Rad7-Rad16 repair activity *in vivo* (Ramsey *et al.*, 2004). Therefore, the authors proposed a model in which the Rad7-Rad16 complex translocate over the DNA molecule using ATP in search of damage and its binding to DNA damage down-regulates its ATPase activity. Rad7 is part of an E3 ligase complex that ubiquitinates Rad4. This UV-specific ubiquitination plays a role in regulating the level of Rad4 in the cell which is also regulated by Rad23 and this modification directly impacts on NER and cell survival. (Ramsey *et al*., 2004).

It was reported that Rad7 and Rad16 interacts with ABF1 (Autonomously replicating sequence-Binding Factor 1) forming a stable complex that plays a role in yeast GG-NER both *in vivo* and *in vitro* (Reed *et al*., 1999). Actually, the Rad7-Rad16-ABF1 complex is implicated in damage DNA superhelical torsion which seems to be important for efficient repair to take place, via Rad16 catalytic activity, *in vitro* (Yu *et al.,* 2004). In addition, it was shown that after UV irradiation of yeast cells, the binding of ABF1 to its associated DNA site aids efficient Rad16-Rad7 dependent GG-NER (Yu *et al*., 2009).

In conclusion, GG-NER is responsible of repairing DNA lesions in the genome overall and the recognition process requires the cooperative actions of GG-NER recognition proteins. Cells carrying mutations in GG-NER specific factors are less UV-sensitive than those mutated for genes that are common to both NER sub-pathways as the transcribing strand of genes is still repaired. To note that the UV sensitivities of yeast cells lacking Rad4 and human cells lacking its human homolog XPC are different (Prakash and Prakash 2000). The UV-sensitivity of Rad4-deficient cells is comparable to that of cells lacking NER proteins common to both sub-pathways (Prakash and Prakash 2000) which indicates that Rad4 might have a role in the common steps of NER apart from its role in recognition in the GG-NER pathway. On the other hand, XPC is specific to the GG-NER sub-pathway. Similar results to Rad4 were obtained for its partner, Rad23 (Mueller et al., 1996).

II.3.1.2 Damage recognition in TC-NER

TC-NER removes lesions from the actively transcribing strand. The stalled RNA Pol II is the initial signal that leads to the assembly of the NER repair machinery (the steps are summarised in figures 3 (human) and 4 (yeast)).

Early experiments were carried out in hamster and human cells and it was showed that the repair of CPDs on the non-transcribed strand was significantly delayed compared to the transcribed strand (Bohr *et al.*, 1985; Mellon *et al.,* 1987), showing the existence of the TC-NER sub-pathway. TC-NER has since been confirmed in other organisms such as yeast (Smerdon and Thoma, 1990), in bacteria (Mellon and Hanawalt, 1989) and recently in archaea (Stantial *et al*., 2016).

This heterogeneity in repair kinetics might be correlated to the functional organisation of the genome; regions that are required for cellular activity are repaired more efficiently. One such example is *Arabidopsis thaliana*, plants are exposed to solar energy throughout the day and are therefore at high risks of acquiring UV-induced damages but they also require sunlight to grow. Therefore, a fine regulation of repair is needed to allow the plant to withstand these damages. Interestingly in *Arabidopsis*, it has recently been reported that TC-NER is influenced by the circadian gene expression with the maximum repair phase coinciding with the maximum transcription phase (Oztas *et al.,* 2018). Therefore, genes that are needed at that point are repaired to maintain normal cellular activity. Furthermore, the same team recently discovered that in mice the removal of cisplatin-DNA adducts was regulated by circadian programmes as well (Yang *et al.,* 2018). The authors showed that the

transcribed and non-transcribed strands were repaired out of phase. The repair of the transcribed strand is dictated by each gene's phase of expression, whereas the maximum repair of the non-transcribed strand occurred at a particular circadian time. Cisplatin is a chemo-therapeutic drug that kills cancer cells by inducing DNA damages. However, it also has severe side effects like nephrotoxicity and hepatotoxicity. Cisplatin, hence, has to be administered carefully and at the optimal dosage for maximum efficiency but low toxicity. Taking into account the circadian cycle can help as most cancers are thought to have defective circadian rhythms and hence can reduce damaging healthy tissues.

The TC-NER pathway is conserved in many organisms, there is however differences between them. For example, in human cells it has been proposed that TC-NER is dependent on CSA (Cockayne syndrome Complementation group A) and CSB (Cockayne Syndrome complementation group B). On the other hand, in *S. cerevisiae*, the homolog of CSB, Rad26, mediate a TC-NER mechanism, but other mechanisms have been proposed.

a. Factors implicated in TC-NER:

- RNA polymerase II

One particularity of TC-NER is that it engages RNA Pol II as the first damage detector. This is different from GG-NER as TC-NER does not require specific factors such as XPC and UV-DDB to recognise the DNA damage, but instead it is the arrested RNA Pol II that triggers repair (Hanawalt and Spivak 2008). This can be a reason for the difference in repair kinetics between the transcribed and non-transcribed strand.

Defects in the TC-NER pathway have been associated to CS (Cockayne Syndrome, refer to "Diseases associated with NER defects" section). One of the characteristics of CS cells is that they exhibit lower transcriptional activity after UV irradiation. *In vitro* transcription system showed that the transcription activity is not solely reduced by a block in elongation due to arrested RNA Pol II at damaged sites but also due to a repression of transcription initiation (Rockx *et al.,* 2000). Indeed, there was a decrease of the hypophosphorylated form of RNA Pol II which is the form recruited in the PIC (Pre-Initiation Complex). It was showed that the hypophosphorylated form of RNA Pol II reappears, in about 6h, after UV irradiation in the wild-type cells but not in CS cells. The change to the hypophosphorylated form of RNA Pol II was proposed to be crucial for transcription restoration after damage repair. This is in accordance with another report showing that there was an accumulation of the hyperphosphorylated form of the large subunit of RNA Pol II after UV irradiation (Luo *et al.,* 2001). These results are suggestive of a UV-induced transcription regulation via modification of RNA Pol II phosphorylation state.

In human, during transcription elongation RNA Pol II interacts transiently with CSB (Cockayne syndrome protein B), UVSSA (UV-stimulated scaffold protein A) and USP7 (ubiquitin-specific-processing protease 7) (Schwertman *et al*., 2013). In case RNA pol II encounters a transcription blocking lesion, the binding with these factors is increased, which allows the recruitment of other NER factors such as CSA (Schwertman *et al*., 2013). These

factors namely CSB, CSA, UV-SSA and USP7 are implicated in regulating the post-translational modifications of RNA Pol II to allow efficient TC-NER to take place and importantly for transcription to restart after repair.

One of the hurdles the NER machinery has to face is accessing the lesion. Even though RNA Pol II triggers repair in TC-NER, its presence can block access to the damaged site. Many studies have addressed the question of the fate of RNA Pol II after damage signalling and three mechanisms have been proposed namely lesion bypass, reverse translocation (backtracking) and degradation (Steurer and Marteijn, 2016). First, for damages causing minimal DNA distortion, the RNA Pol II can bypass the lesion, stimulated by translesional factors. Indeed, RNA Pol II has an intrinsic capacity to bypass lesions by incorporation or misincorporation of nucleotides across the lesions. In yeast, *in vivo* translesion bypass was demonstrated to be correlated with increased UV resistance of cells, in GG-NER deficient context (Walmacq *et al.*, 2012). It was shown that AMPs (Adenosine Mono-Phosphate) is incorporated opposite thymine dimer in a template independent manner. On the contrary, a mutation that abrogates lesion bypass *in vitro* was correlated with increased UV-sensitivity in GG-NER deficient context. The translesion transcription have been suggested to clear RNA Pol II from DNA damage sites and allow access of the NER machinery. Moreover, the UV-resistance provided by translesion proficient RNA Pol II is dependent on a functional *RAD26* gene therefore linking translesion transcription and TC-NER in yeast. In mammals, it was shown that RNA Pol II can bypass cyclopurine, which is a bulky oxidative DNA lesion repaired by the NER pathway, this results in a non-templated AMP insertion (Walmacq *et al.,* 2015). However, the translesional bypass was slow. It should be noted that translesion bypass has also been described in bacteria. Second, RNA Pol II can backtrack providing the space required for the repair of transcription blocking lesions. The molecular mechanism behind backtracking has been proposed in bacteria, but not in eukaryotes. Backtracking is also likely to occur in eukaryotes, given its frequent occurrence during transcription, as a regulatory mechanism to transcription pausing (Steurer and Marteijn, 2016). If backtracking fails, stalled RNA Pol II is degraded to avoid persistent transcription blockage which can be deleterious to the cell. Third in yeast, degradation of elongation arrested RNA Pol II, dependent on Def1 (RNA Pol II degradation factor 1) has been reported *in vivo* (Woudstra *et al.*, 2002; Somesh *et al.*, 2005). Degradation of RNA Pol II has been described as the last recourse when the lesion cannot be rapidly removed by Rad26-dependent TC-NER. Therefore, there is a coordinated action between Rad26 and Def1 to allow cell survival (Woudstra *et al*., 2002). In mammals, the sequential actions of the E3 ubiquitin ligase Rsp5 and Elongin ubiquitin complex lead to RNA Pol II polyubiquitination (Huibregtse *et al.,* 1997; Harreman *et al.*, 1997). The release of ubiquitinated RNA Pol II is dependent on a segregase complex, VCP/p97-Ufd11-Npl4, and facilitates RNA Pol II proteasomal degradation (Verma *et al.*, 2011; He *et al.*, 2017). Recently, it was proposed that CSB influenced the degradation of RNA Pol II by enhancing UV-induced RNA Pol II ubiquitination and the association of VCP/p97 with RNA Pol II (He *et al.*, 2017), in line with previous experiments showing a defect in RNA Pol II ubiquitination in CSB-deficient cells (Groisman *et al.*, 2003).

- Human UV-SSA and USP7

UVSSA is a causative gene for UVSS (UV-Sensitive Syndrome, refer to "Diseases associated with NER defects" section), an autosomal recessive disease that is characterized by UV-hypersensitivity associated with a deficiency in TC-NER. UVSSA forms a complex with the deubiquitinating enzyme USP7 (Ubiquitin-Specific Protease 7) that stabilises UVSSA. Indeed, UVSSA mutant that is defective for the interaction with USP7, is polyubiquinated and degraded by the proteasome, which leads to a deficiency in TC-NER (Higa *et al.,* 2018).

UVSSA and USP7 are part of the TC-NER complex and can be loaded onto RNA Pol II in a CSB and CSA-dependent manner (Zhang *et al*., 2012). In turn, UVSSA and USP7 cooperate to stabilise CSB by protecting CSB from UV-induced proteasome-dependent degradation (Zhang *et al.*, 2012). It has been proposed that UVSSA delivers the USP7 deubiquitinase to the damage-stalled RNA Pol II complex thereby protecting CSB from UV-induced degradation (Schwertman *et al.,* 2012).

Moreover, UVSSA is required for processing stalled RNA Pol II at damage sites (Schwertman *et al., 2013*). As mentioned previously, RNA Pol II can be recycled for a new round of transcription by dephosphorylating the elongating hyperphosphorylated form of RNA Pol II (Rockx *et al*., 2000). In UVSSA-deficient cells, there was a substantial inhibition of dephosphorylation of RNA Pol II (Nakazawa *et al.,* 2012), similar to that observed in CS cells. UVSSA also facilitates ubiquitination of RNA Pol II stalled at the damage sites. Depending on the residue that is ubiquitinated and whether it is mono- or poly-ubiquitinated, it can lead to degradation or regulation of the function of the proteins. Polyubiquitination of lysine 48 triggers proteasomal degradation of the targeted protein, whereas monoubiquitination and lysine 63-linked polyubiquitination contribute to functional changes of various DNA repair factors (Nakazawa*et al.,* 2012). UVSSA-dependent ubiquitination of stalled RNA Pol II does not lead to proteasomal degradation. On the other hand, there are UVSSA-independent ubiquitination pathways that lead to proteasomal degradation of RNA Pol II, as described in "RNA Pol II" section (Nakazawa *et al.,* 2012).

- Rad26/CSB

Human CSB and its budding yeast counterpart Rad26 is a TC-NER specific factor, implicated in the recognition step. In human cells it has been proposed that TC-NER is dependent on CSA and CSB. In *S. cerevisiae*, a Rad26-dependent TC-NER pathway has been proposed.

The roles of both Rad26 and CSB in TC-NER will be discussed below as these proteins exhibit structural and functional differences (schema of Rad26 and CSB domains in Figure 5).

One main difference between Rad26 and CSB is that yeast cells lacking Rad26 do not exhibit any UV-sensitivity (van Gool *et al.,* 1994), but CSB-deficient cells are moderately UV-sensitive (Troelstra *et al*., 1992). Sequence analysis revealed that yeast Rad26 and human CSB are DNA-dependent ATPase of the SWI/SNF chromatin remodelling family, having a putative helicase activity (Troelstra *et al*., 1992; van Gool *et al.,* 1994). Rad26 is a DNA-

dependent ATPase without a helicase activity, whereas CSB has been proposed to have both the ATPase and helicase function. The helicase function has been shown *in vitro* but not yet demonstrated *in vivo* (Citterio *et al.,* 2000). However, both CSB and Rad26 contain a leucine latch domain that autoinhibits its ATPase activity and the C-terminal domain counteracts this autoinhibition, but its implication in TC-NER is unknown (Lake *et al*., 2009, Li, 2015). There are also differences concerning post-translational modifications. CSB contains a UBD (Ubiquitin Binding Domain), absent in Rad26, which is important for triggering damage incision but not for the assembly of the repair complex (Anindya *et al.,* 2010). Therefore, the ubiquitin recognising ability of CSB is essential for TC-NER. Moreover at a late stage in TC-NER, CSB is ubiquitinated and degraded by a proteasome-mediated pathway (Groisman *et al.,* 2006). On the other hand, Rad26 does not seem to be either ubiquitinated or degraded during TC-NER (Li, 2015). Moreover, after DNA damage Rad26 is primarily phosphorylated on serine 27 by DNA damage checkpoint kinase Mec1 (yeast homolog of human ATR) which enhances TC-NER (Taschner *et al.*, 2010). In human, mutation of the residue targeted by ATM (Ataxia Telangiectasia mutated) and ATR (ATM-related) does not lead to an increase in UV-sensitivity indicating that NER is not affected (Matsuoka *et al.*, 2010, Taschner *et al.*, 2010). CSB has other phosphorylation sites that can play a role in regulating its TC-NER activity. For example, a UV-induced CSB dephosphorylation observed *in vivo,* has been correlated with an increase in ATPase activity *in vitro* (Christiansen *et al.,* 2003).

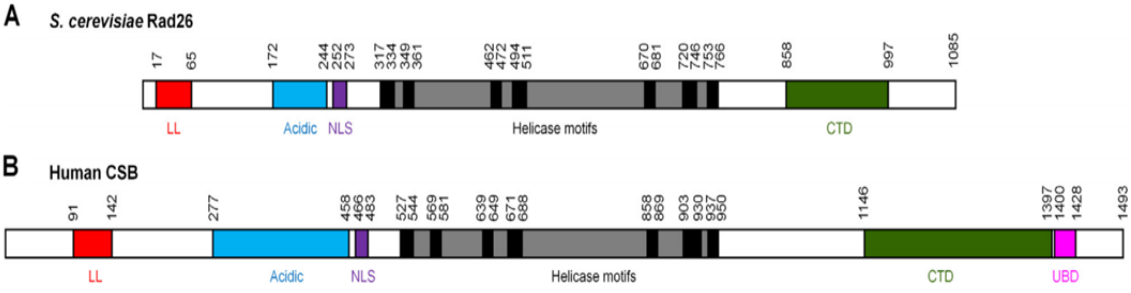

Figure 5: Domain composition of *S. cerevisiae* Rad26 and human CSB domains. The different motifs are shaded. The LL (leucine latch) is indicated in red, NLS (nuclear localization signal) in purple, CTD (C-terminal domain) in green, UBD (ubiquitin-binding domain) and in grey the helicase motifs in grey (Li, 2015).

b. Human CSB and CSA -dependent TC-NER

CSA and *CSB* are two causative genes of Cockayne syndrome and are implicated in TC-NER in human. RNA Pol II that is unable to bypass a lesion might allow enough time for NER factors to be recruited. CSB interacts transiently with elongating RNA Pol II during transcription and CSB's affinity for RNA Pol II increases after stalling of RNA Pol II due to a transcription blocking lesion (Schwertman *et al.,* 2013). CSB is one of the initial sensor of stalled RNA Pol

II. After irradiation, CSA is recruited to RNA Pol II in a CSB- and TFIIH- (Transcription Factor IIH) dependent manner (Saijo *et al*., 2007).

CSA and CSB differentially recruit NER and chromatin remodelling factors. CSB recruits factors such as DDB1 bound to CSA and the histone acetyltransferase p300. CSA is dispensable for recruiting NER proteins but in cooperation with CSB can, for example, recruit TC-NER protein XAB2 (XPA-binding protein 2) (Fousteri *et al.,* 2006).

Moreover, RNA Pol II ubiquitination is deficient in CSA- and CSB-deficient cells and this defect is abolished by complementing with wild-type *CSA* or *CSB* (Bregman *et al.,* 1996). Therefore, there is a pathway of CSA and CSB-mediated RNA Pol II ubiquitination that indicates a connection between RNA Pol II ubiquitination and TCR. In addition, TC-NER-deficient CSA and CSB cells are more likely to trigger the apoptotic programme after UV-irradiation, perhaps because of the ineffective removal of RNA Pol II at UV-induced sites can subsequently lead to transcription blockage (Lee *et al.,* 2002).

This ubiquitination of RNA Pol II can be mediated by the E3 ubiquitin ligase complex, which CSA is a part of, and this complex is recruited by CSB (Fousteri et al., 2006, Groisman *et al.,* 2003). Indeed, CSA can bind to DDB1, similarly to GG-NER DDB2, and integrate a cullin-based ubiquitin E3 ligase (Groisman *et al.,* 2003). This complex is composed of Cul4A (cullin 4A), Rbx1 (or Roc1) and its activity is regulated by the CSN (COP9 signalosome). It has been proposed that CSN is a negative regulator of ubiquitin ligase activity, as a complex devoid of CSN can catalyse ubiquitin polymerisation (Groisman *et al.,* 2003). UV-induced recruitment of CSN will down-regulate the ubiquitin ligase E3 activity and hence CSA-CSN will prevent early degradation of stalled RNA Pol II (Lainé and Egly, 2006).

Furthermore, it was observed that in the absence of CSB, even undamaged genes were not transcribed after UV damage (Proietti-De-Santis *et al.,* 2006). It was demonstrated that, after UV-irradiation, transcription resumption of certain genes and the recruitment of RNA Pol II and other transcription factors at the promoter were dependent on CSB, whereas p53 responsive genes which were activated upon UV irradiation were independent of CSB. This indicates that CSB has a role in transcription restart after repair.

c. *S. cerevisiae* Rad26-dependent TC-NER and other sub-pathways

In *S. cerevisiae,* Rad26 is among the first proteins to be recruited to the lesion-arrested Pol II during the initiation of eukaryotic TC-NER. In yeast, contrary to its human homolog CSA, *rad28* deletion does not lead to defect in TC-NER (Bhatia *et al.*, 1996).

In yeast, the identification of NER factors specific to the TC-NER pathway was tedious as the GG-NER pathway is very efficient and may compensate for a defect in TC-NER. The yeast CSB homolog, designated *RAD26*, was identified through cloning and sequence comparison with human CSB and like CSB, it is not essential for cell survival (van Gool *et al*., 1994) in line with *CSB* mutations found in Cockayne Syndrome (Troelstra *et al.,* 1992). Also, on a phenotypic level, *RAD26* deletion did not lead to any noticeable increase in UV-light or cis-platin

sensitivities (van Gool *et al*., 1994). In this same study, it was however shown that similarly to human CS cells, preferential repair of the transcribing strand was impaired, indicating a role of Rad26 in TC-NER.

Nevertheless, observations that *rad26* deletion mutants still presented residual or even considerable TC-NER in certain genes and that *rad26* cells are not completely NER-defective in a GGR-deficient background (*rad7*Δ or *rad16Δ*) were strong indications that there is a Rad26-independent TC-NER pathway (Verhage *et al.,* 1996; Bhatia *et al.,* 1996). A non-essential subunit of RNA Pol II, Rpb9 was tested (Woychik et al., 1991; Li and Smerdon, 2002). It was shown that *rad16 rad26 rpb9* or *rad7 rad26 rpb9* triple mutants present a very strong UV-sensitive phenotype, even more severe than *rad1* deletion mutant in which NER is completely abolished, and no repair was detected with repair kinetics experiments in these mutants (Li and Smerdon, 2002, 2004). Therefore, it was proposed that there are Rpb9- and Rad26-dependent TC-NER pathways.

Even though Rpb9 is not required for cell viability, it has several roles in transcription including its implication in transcription start site selection (Furter-Graves *et al.,* 1994, Hull *et al.,*1995), its role in promoting transcription elongation by interacting with TFIIS (Hemming *et al.,* 2000) and for maintaining transcriptional fidelity (Nesser *et al.,* 2005) *in vivo*. It was demonstrated that impairing transcription elongation abolishes Rpb9-mediated TC-NER (Li *et al.,* 2006). Therefore, there is a coupling between these two functions for Rpb9.

Repair on the promoter region and non-transcribed strand is dependent on the GG-NER sub-pathway, whilst repair on the transcriptionally active strand is dependent on the TC-NER sub-pathway (Tijsterman *et al.,* 1996). Now within the TC-NER sub-pathway there seems to be a differential requirement for Rpb9 and Rad26. It was reported that very actively transcribing genes (for example, inducible *GAL1-10* genes) are more dependent on Rpb9 than Rad26, whereas slow or moderately transcribing genes (for example *URA3* and *RPB2* genes) are dependent on Rad26 (Li and Smerdon, 2002, Tijsterman *et al*., 1997).

Another non-essential RNA Pol II subunit, Rpb4, has been proposed to regulate Rpb9- and Rad26-dependent TC-NER pathways (Woychik and Young, 1989, Li and Smerdon, 2002). The structure of the complete RNA Pol II structure consists of twelve subunits organised in a ten-subunit core and a Rpb4-Rpb7 heterodimer was resolved in yeast *S. cerevisiae* (Armache *et al*., 2003, Bushnell and Kornberg, 2003). One model proposed that the dissociation of the heterodimer allowed the clamp of RNA Pol II to open and hence allowing the DNA molecule in. The reassociation of Rpb4-Rpb7 closes the clamp (Armache *et al*., 2003). This dissociation of Rpb4-Rpb7 dimer from the catalytic core has been observed *in vitro* (Edwards *et al*., 1991) and the crystal model reveals that the interaction surface between the core and Rpb7 is small which is consistent with a transient interaction (Armache *et al.,* 2003). *In vitro* experiments have also suggested a role for Rpb4-Rpb7 in transcription initiation while dispensable for catalytic RNA Pol II elongation (Edwards et al., 1991). However, the

dissociation of Rpb4 and Rpb7 has not been shown *in vivo*. A second model proposed that Rpb4-Rpb7 stays bound to the core which leads to the DNA being bound further away from the active site. But after DNA melting, the single-stranded template can slip in the active site (Armache *et al.,* 2003). This scenario is in accordance with previously observed RNA Pol II structure, in solution, where the access to the active site is not blocked by the clamp (Craighead *et al.,* 2002) and *in vivo* experiments showing that Rpb4-Rpb7 is part of the DNA-associated RNA Pol II (Jasiak *et al.,* 2008).

The model proposed by Li and Smerdon in their 2002 paper, was that Rpb4 played a regulatory role in TC-NER (Li and Smerdon, 2002). In the absence of Rpb4, RNA Pol II was in an open conformation allowing Rpb9-dependent TC-NER to occur. On the contrary in the presence of Rpb4, RNA Pol II is in a closed conformation, which facilitates Rad26-dependent TC-NER while suppressing Rpb9-dependent TC-NER. The Rpb7-Rpb4 subcomplex presence maintains RNA Pol II in a transcribing, closed complex conformation. This model is in accordance of the previously mentioned structure analysis and *in vitro* experiments in favour of a dissociation of the Rpb4-Rpb7 heterodimer from the catalytic core.

However, we do not have a clear picture of Rad26 and Rpb9 roles in TC-NER. A functional redundancy between Rad26 and Rpb9 has been proposed, as the double mutants are UV-sensitive while the single *rpb9* mutant or *rad26* mutant is not (Li and Smerdon, 2002). However, there are reports of Rad26 and Rpb9 acting as inhibitors of TC-NER repressors (for example, transcription elongation factors) instead of playing a direct role *per se* in TC-NER. When RNA Pol II is stalled in the presence of a transcription-blocking lesion, transcription elongation factors can be a hindrance to repair. They can force RNA Pol II over the lesion and cause RNA Pol II to be arrested over the lesion irreversibly, which could be cytotoxic. It is therefore important for proper repair that these elongation factors are inhibited. RNA Pol II is accompanied by several factors during transcription, for example to facilitate elongation.

The Spt4-Spt5 complex enables processive transcription elongation *in vivo* (Hartzog *et al.,* 1998). It was demonstrated that disrupting *SPT4* gene restored TC-NER in *rad26* and *rpb9* cells and GG-NER was not affected by *SPT4* disruption (Jansen *et al*., 2000; Li *et al*., 2006). These results indicate that Spt4 is a repressor of TC-NER and its disruption is sufficient to restore TC-NER even in the absence of Rad26 and Rpb9. In addition, Spt4 suppresses Rad26-independent TC-NER by preventing the degradation of Spt5 and stabilizing the interaction between Spt5 and RNA Pol II (Ding et al., 2009). It was proposed that Spt5 suppresses Rad26 independent TC-NER by serving as a platform for the assembly of a protein suppressor complex associated to RNA Pol II.

Another factor was identified: Pol II-associated factor 1 complex (Paf1C), which has been shown to function in transcription elongation, 3'-processing of mRNAs, and post-translational modification of histones (Tatum *et al.,* 2011). Paf1C plays a minor role in

facilitating Rad26-dependent TC-NER and a more consequent role in suppressing Rad26-independent TC-NER by cooperating with Spt4-Spt5 (Tatum *et al*., 2011).

An integrated model was proposed (Tatum *et al*., 2011) involving these factors: in the absence of Rad26, the coordinated interactions of Rpb4-Rpb7, Spt4-Spt5 and Paf1C with each other and with the core catalytic RNA Pol II stabilizes the damage blocked in the active site of RNA Pol II. This would explain that disrupting one of these factors could allow repair even in the absence of Rad26.

In support of this competition for RNA Pol II binding, a recent study combining biochemical and electron microscopy approaches showed that there are steric clashes between Spt4-Spt5 and Rad26 (Xu *et al.,* 2017). This suggests that there is an important functional interplay during TC-NER between transcription factors and Rad26 in line with the previously proposed antagonizing role of Rad26 for TCR repressors (Rad26 antagonizes the repression of TCR by Spt5 and Spt4). This study also showed that Rad26 binds to DNA upstream of RNA Pol II and Rad26 ATPase activity associated with its translocase activity was important to promote RNA Pol II forward movement. Interestingly, this function allowed RNA Pol II to move over certain less bulky DNA damages such as poly-A tract or pyrrole-imidazole (Py-Im) polyamide hence stimulating transcription elongation. It did not however promote transcriptional bypass over bulky damages such as CPD lesions, which is in agreement with previous observation with human CSB (Selby *et al.,* 1997). Finally, most of the Rad26–DNA and Rad26–Pol II interaction interfaces identified are highly conserved between yeast and human (Xu *et al.,* 2017).

Another possibility to remove RNA Pol II that can impede proper repair and transcription re-initiation is via Def1 (Woudstra *et al*., 2002). A coordinated rescue mechanism between Def1 and Rad26 was proposed, where Def1 is required for RNA Pol II ubiquitination and degradation in case Rad26-mediated repair is unable to remove the damage.

Furthermore, in response to UV-irradiation Rpb9 can promote ubiquitination and degradation of the largest subunit of RNA Pol II, Rpb1 (Chen *et al.,* 2007). This function of Rpb9 seems to be independent of Rad26 or even Rpb9-mediated TC-NER.

In conclusion, the different reports on Rad26 propose a role in the first DNA damage recognition step, Rad26 gives a certain specificity to the stalled RNA Pol II. Taken together these results highlight the importance of RNA Pol II in TC-NER and its intrinsic capacity of triggering the repair cascade. The exact role of Rad26 and Rpb9 is still debatable but in a GG-NER-deficient context, Rad26 and Rpb9 seem important for efficient TC-NER.

Recently, a new NER factor has been identified: Sen1, the yeast homolog of human senataxin (Li *et al.,* 2016). Sen1 is essential for cell viability and among the different functions proposed for Sen1, it has been shown to be implicated in genome stability by resolving RNA-DNA hybrids formed during transcription and also in the metabolism of different classes of non-coding RNAs. It has been proposed that Sen1 has a role in TC-NER

but seems dispensable for GG-NER (Li *et al.,* 2016). The role of Sen1 in TC-NER is of now not elucidated. Interactions with NER protein Rad2 and RNA Pol II subunit, Rpb1 have been demonstrated (Ursic *et al*., 2004; Chinchilla *et al.,* 2012), but point mutations compromising these interactions do not seem to affect its TC-NER role (Li *et al.,* 2016). Also unlike Rad26 and Rpb9, disrupting *SPT4* does not restore TC-NER in *sen1* cells. Sen1 might therefore play a role in TC-NER that is distinct from Rad26 and Rpb9. In addition, mutants with *rpb9* deletion and *sen1* truncations are non-viable which indicates a functional complementation. Therefore, the mechanism behind Sen1 role as a facilitator of TC-NER still remains to be elucidated and it would be interesting to test if the human senataxin also plays a role in TC-NER. This newly identified NER factor shows that even decades after the discovery of the NER pathway, there are still many aspects of this pathway that needs to be elucidated.

d. The 3' endonuclease XPG as a TC-NER recognition factor

Human XPG is a 3' endonuclease that intervenes in a later step of NER: damage excision. However, *in vitro* experiments carried out in human cells, proposed a non-enzymatic role in damage recognition for XPG in the TC-NER sub-pathway (Sarker *et al.*, 2005). It was reported that a damage independent binding of XPG to arrested RNA Pol II seems to implicate the transcription bubble. It was previously shown that XPG interacts with CSB *in vitro* (Iyer *et al*., 1996). Further characterisation of this interaction suggested that XPG stimulates CSB binding to DNA bubble and its ATPase activity of CSB (Sarker *et al.,* 2005), indicating cooperation between these two proteins for the recognition of stalled RNA Pol II. Still in the absence of CSB, XPG can bind to the stalled RNA Pol II. These results indicate that stalled RNA Pol II recognition in TC-NER implicates the coordinated actions of CSB and XPG, which is further strengthened by the fact that loss of XPG leads to defect in TC-NER and truncation of XPG results in the development of Xeroderma pigmentosum associated with Cockayne syndrome (XP/CS) (Emmert *et al.*, 2002, details on diseases in the "Diseases associated with NER defects" chapter).

In budding yeast as well Rad2, the XPG homolog interacts with RNA Pol II in the absence of UV stress (Eyboulet *et al.,* 2013). It does not however possess the C-terminal domain like XPG. The C-terminal domain together with the spacer (or R (Recognition) domain) of XPG are required for transcription bubble recognition but not for incision (Sarker *et al.,* 2005, Figure 6). The C-terminal domain is also required for interacting with CSB and stimulating its ATPase activity, in yeast as of now there has been no interaction described between Rad26 (CSB homolog) and Rad2.

II.3.2 Post DNA recognition: Bubble Opening

After the damage is recognised, it is important that the DNA damage is accessible to the NER machinery. The TFIIH complex is implicated in DNA unwinding around the damage forming a bubble which allows the downstream factors to access the DNA lesion namely for XPG incision to take place (Sarker *et al.,* 2005).

II.3.2.1 TFIIH

TFIIH (Transcription Factor II H) is a multi-subunit complex that has a role in both transcription and DNA repair. It is composed of ten subunits, six of them forming the core module (Ssl2/XPB, Tfb1/p62, Tfb2/p52, Ssl1/p44, Tfb4/p34 and Tfb5/p8) and a three-subunit kinase module (Kin28/CDK7, Ccl1/Cyclin H and Tfb3/MAT1) in human and yeast. The Rad3/XPD bridges these two modules (Luo *et al*., 2015, for structural details refer to chapter "Transcription"). The kinase module CAK (CDK activating kinase) in human and TFIIK in yeast phosphorylates RNA Pol II and regulates its promoter escape during transcription (more details in transcription chapter). However, this kinase module is not necessary for NER and dissociates from the core module to allow efficient repair (Svejstrup *et al.,* 1995, Coin *et al.,* 2008). On the contrary, the core subunits P8 (Tfb5 in yeast), XPB (Ssl2 or Rad25 in yeast) and XPD (Rad3 in yeast) have been implicated in NER in both yeast and human cells (Rimel and Taatjes, 2018). Rad3/XPD is a DNA helicase with a 5'-3' polarity and ATPase, Ssl2/XPB is a 3'-5' DNA helicase and ATPase and p8/Tfb5 has a structural role.

In yeast, Tfb5 has been proposed to have a role in transcription and DNA repair (Ranish *et al*., 2004). It interacts with another core module protein Tfb2 and confers rigidity to the core TFIIH maintaining the complex in its functional architecture (Zhou *et al*, 2007). Its human homolog p8 is implicated in DNA repair but is dispensable for RNA synthesis (Coin *et al*., 2006). Even if p8 interacts with the CAK module, it does not interfere with its transcriptional activity, therefore minimal conformational change is required for TFIIH to switch between its transcription and DNA repair function. In repair, p8 stimulates the ATPase activity of XPB together with GG-NER complex XPC-HR23B (Coin *et al.,* 2006).

Rad3/XPD and Rad25/XPB are DNA helicases of opposite polarities. In transcription Rad3/XPD seems to have a minor role but both its helicase and ATPase activities are crucial for NER (Oksentyn *et al.,* 2010). It has been reported that XPD scans the DNA strand in a 5' to 3' orientation. In GG-NER, XPD scans DNA from XPC binding site, therefore, TFIIH via XPD is also implicated in damage verification (Sugasawa *et al.,* 2009). Rad3 also binds DNA in an ATP-dependent manner (Guzder *et al*., 1995). Additionally, purified Rad3 has been demonstrated to have the ability to displace the RNA fragment making way for the NER complex (Naegeli *et al.,* 1992).

It was reported that the helicase activity of XPB is dispensable for repair *in vivo* (Coin *et al.,* 2007). Genetic studies with XPD or XPB mutated in their ATPase domain showed that XPB, but not XPD, is required for the proper recruitment of TFIIH to damaged sites (Oksenych *et al.,* 2009). Therefore, the recruitment of TFIIH to DNA damage sites is an active process requiring the ATP hydrolysis activity of XPB, the latter acts as a hook to stabilise TFIIH to damage sites.

In conclusion, DNA opening around the damage site and efficient repair involves the concerted actions of core TFIIH subunits. TFIIH is recruited to the damaged site using the ATPase activity of Rad25/XPB and DNA unwinding is driven by the helicase activity of

Rad3/XPD. Tfb5/p8 enhances the activity of Rad25/XPB and maintains TFIIH in a functional conformation.

a. How is TFIIH recruited to DNA damage sites?

TFIIH is involved in transcription initiation and is not part of the elongating complex, therefore it must be recruited to the damage site in TC -NER and also in GG -NER.

In GG-NER and TC-NER, XPC-RAD23B and UVSSA respectively recruit TFIIH via the pleckstrin homology (PH) domain of its p62 subunit (Yokoi *et al.,* 2000; Okuda *et al.,* 2017). Therefore, the same TFIIH recruitment mechanism is shared by the GG-NER and TC-NER sub-pathways. TFIIH CAK module inhibits TFIIH DNA binding and hence favours TFIIH specific lesion-dependent recruitment by XPC (Li *et al.,* 2015). This shows that a cooperation between TFIIH modules adds another level of specificity to NER response.

TFIIH does not recognise stalled RNA Pol II by itself (Tantin *et al*., 1998), it has to be recruited by other factors in TC-NER. It was demonstrated that TFIIH can be targeted to transcriptionally active DNA via an interaction with RNA Pol II- bound CSB *in vitro* (Tantin *et al*., 1998) and *in vivo* (Tijsterman *et al*., 1997). Another possible recruitment of TFIIH is via an interaction with XPG (Araujo *et al.,* 2001) even in the absence of CSB (Sarker *et al.*, 2005). Also, TFIIH can be recruited to UV lesion sites in the absence of XPG *in vivo* (Thorel *et al.*, 2004). Therefore, CSB and XPG possibly have overlapping and cooperative function to recruit TFIIH to damage sites.

In yeast, Rad2 (homolog of XPG) interacts with and stabilizes TFIIH (Habraken *et al.,* 1996). Yeast Rad4 and Rad23 (homologs of XPC-RAD23B) also interact with TFIIH (Bardwell *et al*., 1994; Guzder *et al.,* 1995). In addition, it has been shown that Rad2 and Rad4 compete to bind the Tfb1 (homolog of P62) subunit of TFIIH in NER (Lafrance-Vanasse *et al.*, 2013).

Moreover, a role for Rad26 in TFIIH recruitment to the stalled transcription elongation complex to allow repair has been proposed (Tijsterman *et al.,* 1997).

II.3.3 Bubble opening and damage verification: RPA and Rad14/XPA

The initial DNA opening by TFIIH favours the recruitment of RPA and XPA, which help in the expansion of the DNA around the lesion and drive the dissociation of the CAK module of TFIIH thereby promoting the repair function of TFIIH (Coin *et al.,* 2008). Footprinting experiments showed that the collaborative actions of these factors lead to the opening of an asymmetrical DNA bubble of about 27 nucleotides around the damage extending to the 3’ and 5’ of the incision sites (Oksentyn and Coin, 2010, Evans *et al*., 1997).

RPA (Replication Protein A) is a heterotrimeric complex that is conserved in eukaryotes capable of unwinding complementary DNA strands (Georkagi *et al.,* 1992). It is composed of three subunits that bind single-stranded DNA with a defined polarity (de Latt *et al*., 1998). A stronger DNA binding domain resides in the 5’ side of its binding region, this polarity is important for the positioning of the 5’ and 3’ endonucleases (de Laat *et al.,* 1998). *In vivo*, a

central role for RPA in coupling incision and DNA repair synthesis was reported, thereby averting further DNA breaks that could lead to genome instability (Overmeer *et al.,* 2011).

RPA interacts with XPA (Xeroderma Pigmentosum complemented group A protein) and stabilise the interaction of XPA to damaged DNA (Guzder *at al.,* 1998). This interaction is conserved in yeast as well: RPA interacts with Rad14, the yeast counterpart of XPA (You *et al.,* 2003). Structural analyses have determined that the zinc-containing subdomain of XPA interacts with the largest subunit of the RPA trimer, RPA70, and that the C-terminal subdomain of XPA binds to DNA (Ikegami *et al.,* 1998). XPA exhibits a preferential binding affinity to damaged DNA (Robins *et al*., 1991) and this is important for further recruitment of the downstream endonucleases. Mutational analyses defined lysine residues on the surface of XPA next to its DNA binding domain that is responsible for recognition of helical kinks, due to increased deformability of damaged sites, contributing to target selectivity in NER (Koch *et al.,* 2016). XPA and RPA cooperate to bind to DNA (He *et al.,* 1995), RPA stabilises XPA on the damaged strand whereas RPA binds specifically to the undamaged strand at the lesion site, in the presence of XPA (Lee *et al.,* 2003). XPA also inhibits the DNA strand separation activity of RPA and hence stabilises RPA binding to DNA (Patrick and Turchi, 2002). In addition, XPA also interacts with the GG-NER recognition protein XPC and in cooperation with RPA helps displace the XPC-HR23B complex from the damaged DNA (You et al., 2003).

II.3.4 NER-mediated DNA excision

Once the pre-incision complex has verified the damage, the next step consists of excising the damage. Dual incision of the damaged DNA is carried out by human XPG (Rad2 in yeast) on the 3' side of the damage and by a dimer composed of XPF (Rad1 in yeast) and ERCC1 (Rad10 in yeast) on the 5' side. It has been recently demonstrated, by the generation of a single-nucleotide repair map in *S. cerevisiae*, that incision occurs 13-18 nucleotides 5' and 6-7 nucleotides 3' to the UV damage generating a 21- to 27-nucleotide-long excision product (Li et al., 2018). The excised fragment is similar in human with a difference in excision mode with 19-21 nucleotides 5' and 5-6 nucleotides 3' to the DNA damage (Hu *et al*., 2016).

II.3.4.1 Rad2/XPG

Rad2/XPG is a structure-specific endonuclease of the FEN1 family. It cleaves DNA at the 3' of the damage at the junction of the single stranded DNA and double stranded DNA (Habraken *et al*., 1995; Hohl *et al.,* 2003).

The identification of the active sites and mutations that specifically abolish the nuclease activities of XPG and XPF has been very useful to understand the mechanism of the dual incision (Wakasugi *et al*., 1997; Enzlin and Scharer, 2002). Human cell free extracts from XPG- or XPF-deficient cells were complemented with either wild-type or nuclease-deficient mutant of XPF or XPG that retains the DNA binding activity, showed that 5' incision is required prior to 3' incision and that the presence of XPG and not its catalytic activity is required for 5' incision (Staresincic *et al*., 2009; Wakasugi *et al.*, 1997). These results

indicate that XPG has an enzymatic role in 3' incision as well as an indirect and non-catalytic role in 5' incision. Thus, there is a distinct order for the dual incision and this coordinated action of the NER endonucleases prevent the prolonged exposure of a single-stranded DNA intermediates which can have detrimental effects.

The sequence similarities between human XPG and *S. cerevisiae* Rad2 is confined to the N and I nuclease domains (Scherly *et al.,* 1993). Mutating the conserved residues in these domains of XPG abolishes its 3' endonuclease activity (Wakasugi *et al.,* 1997, Constantinou *et al.,* 1999). Between these two nuclease domains, the spacer domain is not required for the catalytic function of Rad2/XPG but is still important for the proper progression of NER *in vivo* and *in vitro* (Dunand-Sauthier *et al.,* 2005). Moreover, this domain is important for recruiting and positioning XPG to the damage site and it also mediates the interaction between XPG and TFIIH (Dunand-Sauthier *et al*., 2005; Thorel *et al.,* 2004). It was demonstrated, by live cell imaging in human fibroblasts, that XPG is uniformly distributed throughout the nucleus (Zotter *et al.,* 2006). After induction of global UV-irradiation, XPG is quickly recruited to damage sites in a TFIIH dependent and independent manner (Zotter *et al,* 2006). As mentioned before (section damage recognition), XPG can be recruited in the early steps of TC-NER, which involves interactions with RNA Pol II and CSB (Sarker et al., 2005).

Furthermore, XPG interacts with RPA and TFIIH and can help to stabilise the melted repair intermediate with them (Naegli and Sugasawa, 2011). In yeast as well, the interaction between TFIIH and Rad2 is conserved (Bardwell *et al.*, 1994). In addition, it was shown that TFIIH active in NER lacked the kinase module and is associated with NER proteins Rad1, Rad2, Rad4, and Rad10 (Svejstrup *et al.,* 1995).

The crystal structure of the catalytic core of Rad2 in association with its DNA substrate has been resolved (Mietus *et al*., 2014). It was proposed that the presence of an altered helical arch structure in Rad2 makes the active site more accessible compared to other FEN1 members. This could explain the unique ability of Rad2/XPG to cleave DNA bubbles.

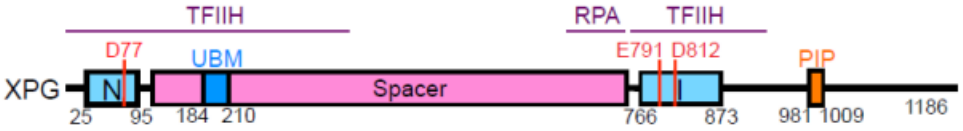

Figure 6: Schematic representation of XPG domains and its interacting partners. N and I nuclease domains in blue are separated by the spacer region in pink. In dark blue the UBM (Ubiquitin Binding Motif) and in proteins interacting with XPG are written in purple (Fagbemi *et al.,* 2011).

II.3.4.2 XPF-ERCC1/Rad1-Rad10

XPF-ERCC1/Rad1-Rad10 complex is a structure-specific DNA-nuclease belonging to the XPF/Mus81 family (Ciccia *et al.,* 2008). Eukaryotic members of this family form a

heterodimeric dimer with one of the subunits having the catalytic activity. For instance it is XPF that has the nuclease activity in XPF-ERCC1 complex. (Sijbers *et al.,* 1996). It has actually been proposed that Rad1/XPF and Rad10/ERCC1 have a common ancestral gene based on their high sequence similarity and Rad10/ERCC1 lost the endonuclease activity as illustrated in Figure 7. The helix-hairpin-helix motif in the conserved C-terminal region is essential for heterodimeric interaction, necessary for protein stability (Gaillard and Wood, 2001).

However, mutations in the active site region do not affect the DNA binding ability of the XPF-ERCC1 complex (Enzlin and Scharer, 2002). Therefore, the endonuclease and DNA binding activities are decoupled similarly to Rad2/XPG. Indeed, it was shown that the XPF-ERCC1 complex has numerous DNA binding domains that regulate its activity (Su *et al.,* 2012).

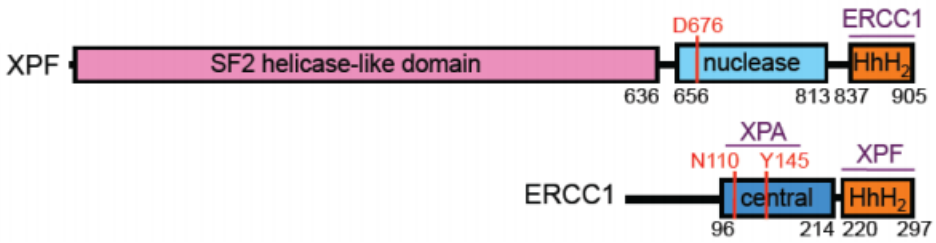

Figure 7: Schematic representation of XPF and ERCC1 domains and their interacting partners.
ERCC1 and XPF interact through their HhH_2 region (helix-hairpin-helix). Residues mediating interactions, with the different partners (purple) are in red. XPF helicase-like domain (pink) belongs to the SF2 family of helicases, but has a defective ATP binding site (Fagbemi *et al.*, 2011).

XPF-ERCC1/Rad1-Rad10 heterodimer is the last factor to join the pre-incision complex (Riedl *et al.,* 2003). This heterodimeric complex is targeted to the damage site via an interaction with Rad14/XPF in human and yeast (Park and Sancar, 1994; Li *et al*., 1995, Guzder *et al*., 2006). Live cell imaging in yeast confirmed these results, since the formation of Rad10 foci, after damage induction, is dependent on Rad14 (Mardiros *et al.,* 2011). Results of human XPF/ERCC1 structure in contact with DNA obtained from NMR (Nuclear magnetic resonance) lead to the establishment of a model where ERCC1 contacts the phosphate backbone of the dsDNA and XPF stabilises the ssDNA (Tripsianes *et al.,* 2005). Moreover, the central domain of ERCC1 is connected to XPA on the NER complex and RPA stimulates the enzymatic activity of XPF-ERCC1 (Tripsianes *et al*. 2005; de Laat *et al.* 1998).

Therefore, the recruitment of Rad1/XPF-Rad10/ERCC1 completes the formation of the pre-incision complex of NER. The complex formed allows dual incision to take place and the removal of a damage-containing oligonucleotide of about 30 nucleotides. The half-life of the

excised oligonucleotide is about 10 minutes before it is degraded by nucleases (Hu et al., 2013).

The fate of the excised oligonucleotide was investigated. *In vitro* and *in vivo,* it was showed that the excised damage-containing fragment was in complex with TFIIH in human, and TFIIH can be dissociated in an ATP-dependent manner (Kemp *et al.*, 2012; Hu *et al*., 2015). Moreover, *in vivo*, it was showed that XPG was also strongly associated with the excision product and to a lesser extent XPF (Hu *et al*., 2015). The binding of XPG might be due to the strong association between XPG and TFIIH, as previously reported (Araújo et al., 2001). Interestingly, it was also demonstrated that in XPC-deficient and CSB-deficient fibroblasts, the excised oligonucleotides were of similar length as the wild-type (25-30 nucleotides). Therefore, the dual incision of DNA-damage containing fragment has the same pattern in GG-NER and TC-NER. The dual incision step is followed by a gap-filling DNA synthesis step.

II.3.5 DNA re-synthesis and ligation

The 5' incision made by XPF-ERCC1 heterodimer is sufficient for inducing the gap-filling DNA synthesis, even before the 3' incision by XPG (Staresincic *et al.,* 2009). This synchronisation between DNA excision and DNA re-synthesis prevents the accumulation of ssDNA gaps that can initiate DNA damage signalling.

The recruitment of factors involved in DNA re-synthesis: PCNA (Proliferating Cell Nuclear Antigen) and RF-C (Replication factor C) depends on a prior 5' incision (Mocquet *et al.,* 2008). RF-C, composed of five subunits, acts as a clamp loader for PCNA and aids the assembly of PCNA trimer (Kelman, 1997). PCNA is the processivity factor for DNA polymerase and tethers the catalytic unit of DNA polymerase to the DNA template (Kelman, 1997). *In vitro*, PCNA is recruited and stabilised by XPG (Mocquet *et al.,* 2008). The NER DNA polymerase and DNA ligase that will be used depend on the proliferative status of the cell.

In replicating human cells, DNA polymerase ε-dependent synthesis occurs and DNA ligase 1 seals the gap. In non-replicating human cells, DNA polymerase δ and DNA polymerase κ are the main NER polymerases and ligation requires the constitutively present XRCC1-DNA ligase 3 complex (Ogi et al., 2010, Moser et al., 2007).

In yeast, DNA polymerases δ and ε are able to perform repair synthesis and can substitute for each other, since mutations in one polymerase do not lead to repair defects (Budd and Campbell, 1995). The ligase activity depends on DNA ligase 1 Cdc9, whose mutations lead to defective DNA ligation in *S. cerevisiae* (Wu *et al.,* 1999).

Mammals	Yeast	Catalytic activity
NER factors		
XPA – DNA damage verification and scaffold for recruitment of other NER factors	Rad14	
XPD (ERCC2) – Promotes opening of DNA around the lesion; DNA damage verification	Rad3	5'-3' helicase/ATPase
XPB (ERCC3) – Promotes opening of DNA around the lesion	Rad25 (Ssl2)	5'-3' helicase/ATPase/ translocase
TTDA, P8 (GTF2H5) – Stimulates the ATPase activity of XPB	Tfb5	
CDK7	Kin28	Kinase activity; the kinase complex of TFIIH is not required for NER
Cyclin H	Ccl1	
RPA – Binds ssDNA revealed after unwinding	Rpa	
XPG – Cleaves damaged strand downstream of lesion	Rad2	Endonuclease
XPF-ERCC1 – Cleaves damaged strand upstream of lesion	Rad10-Rad1	Endonuclease
TC-NER factors		
CSB (ERCC6) – Recognizes damage-stalled RNAPII on upstream side; promotes forward movement of RNAPII	Rad26	Translocase
CSA (ERCC8) – Part of the E3 ubiquitin ligase complex CLR4 Required for recruitment of UVSSA to CSB	Not found	
UVSSA – Promotes stabilization of CSB	Not found	
USP7 – Deubiquitylates CSB	Not found	Ubiquitin protease
GG-NER factors		
XPC – Recognizes helix-distorting lesions	Rad4	
DDB1-DDB2 complex (XPE) – Recognizes DNA lesion directly, kinks the DNA to provide recognition by XPC; also part of the CRL4 E3 ubiquitin ligase complex	Not found	
Gap filling (DNA replication)		
Proliferating cell nuclear antigen (PCNA) – DNA clamp, processivity factor for DNA Pol	Pcna/Pol30	
Replication factor C (RFC) – Clamp loader	Rfc	
DNA Pol δ/ε	DNA Pol δ/ε (Pol3, Pol2)	DNA Pol
DNA ligase 1	DNA ligase I (Cdc9)	DNA ligase

Table 1: NER factors in yeast and mammals and their roles.
(Gregersen and Svejstrup, 2018)

II.4 Chromatin dynamics during NER

In eukaryotic cells, the DNA molecules are packed in a separate compartment, the nucleus. The nucleosome is the fundamental unit of chromatin. A nucleosome comprises of approximately 147 base pairs wrapped around an octamer of histones (two copies of each histone H2A, H2B, H3 and H4). Histones that are part of the nucleosomes are named nucleosomal or core histones. Approximately every 10.4 bp, the positively charged residues of the histones contact the negatively charged phosphate backbone, providing positional stability. The nucleosomes are interconnected via a short linker DNA segment (about 10-50 base pairs) (Clapier and Cairns, 2009). The polynucleosome string is folded into a compact fibre of approximately 30 nm. This fibre is stabilised by the binding of the H1 histone to the nucleosome and the linker DNA (Felsenfeld and Goutine, 2003, Figure 8).

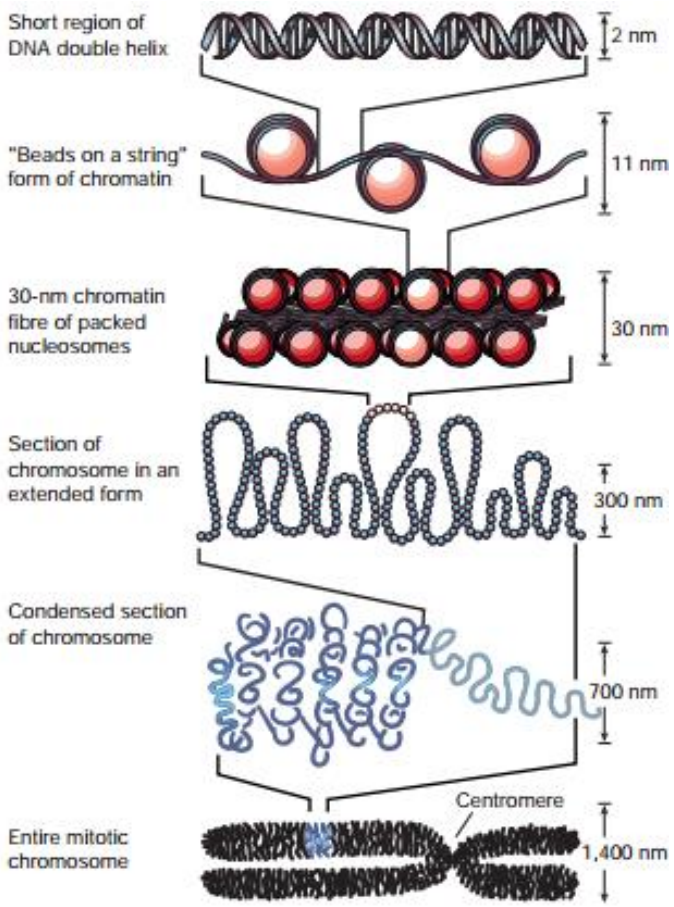

Figure 8: DNA molecule is packaged into chromosomes with the help of histones (Felsenfeld and Goutine, 2003).

The chromatin structure is dynamic and the balance between compaction and accessibility is crucial for the regulation of cellular processes.

Eukaryotes contain histone variants that confer new structural and functional properties to the nucleosome. Histone H2A has a large number of variants with some found in almost all

organisms, for instance H2A.Z and H2A.X. Histone H2A.Z affects histone mobility and replaces H2A at specific genomic sites. Histone H2A.X is distributed throughout the genome and can be phosphorylated in response to DNA damage. A histone variant H3.3 can replace histone H3 in non-dividing cells and seems to be linked to transcriptionally active genes (Felsenfeld and Goutine, 2003).

Moreover, the concerted actions of chromatin modifying enzymes and chromatin remodelling complexes can impact chromatin structure. Histones can undergo post-translation modifications by chromatin modifying enzymes, which exist as pairs with antagonizing functions, for example histone acetylase and deacetylase. Chromatin remodelling complexes use ATP to slide, exchange, and/or evict histones from chromatin. These modifications can render the DNA sequences more or less accessible.

It is important that chromatin remodelling occurs to allow efficient repair and that afterwards it returns to its pre-damaged state so as to preserve the epigenetic codes. The "Access-Repair-Restore" (ARR) model was proposed, which combines chromatin dynamics with DNA repair response. It postulates that, after DNA damage, the chromatin structure is modified which facilitates access to the damage regions by the repair machinery and the native chromatin structure is restored after repair (Smerdon, 1991). An updated version of the ARR model incorporates the fact that there is an added plasticity to the epigenome maintenance, for instance new histones can be incorporated into repaired chromatin (Polo and Almouzni, 2015).

To note that this model is not restricted to the NER pathway as similar nucleosome rearrangements have been described for other damages induced by, for example, methyl methanesulfonate (MMS) and bleomycin (Sidik and Smerdon, 1984, 1990).

During TC-NER, chromatin structure is less of an impediment as the chromatin is transiently in an open conformation due to RNA Pol II translocation. Indeed, TC-NER is rapid, less heterogeneous and do not seem to correlate with chromatin structure in the transcribing stand (Wellinger and Thoma, 1997). It is noteworthy that even though chromatin is transiently in an open configuration due to RNA Pol II translocation in TC-NER, a role in the recruitment of chromatin remodelling factors has been demonstrated for CSB and CSA (Fousteri *et al.,* 2006), these TC-NER specific proteins recruit HMGN1. HMGN1 is a nuclear architectural protein that binds to nucleosome and negatively affects the binding of linker histone H1 and modulates post-translational modifications of nucleosomal histone tails (Bustin, 2001). CSB is required to recruit the histone acetyltransferase p300 to UV-arrested RNA Pol II (Fousteri *et al.,* 2006). CSB, part of the SWI/SNF family, has itself a chromatin remodelling activity associated with its ATPase activity *in vitro* (Citterio *et al.,* 2000), but this activity has not yet been confirmed *in vivo*.

In the case of GG-NER, the chromatin has to be remodelled to allow the repair machinery to access the damaged DNA, as demonstrated by the heterogeneity in the removal of UV-

induced damages from the genome. Heterochromatic non-transcribed DNA seems to be repaired less efficiently than the bulk DNA (Zolan *et al.,* 1982; Leadon *et al.*, 1983).

II.4.1 Histone modifications

Histone post-translational modifications play a major role in modulating the chromatin structure. Some histone modifications implicated in the NER pathway are described below.

II.4.1.1 Histone acetylation

Studies have shown that in response to UV irradiation, there is a wave of nucleosomal histone hyperacetylation, which was correlated with enhanced repair synthesis (Ramanathan and Smerdon, 1986, Ramanathan and Smerdon, 1989). In human cells after UV irradiation, it was demonstrated that the histone acetyltransferase (HAT), GCN5 mediated the rapid acetylation of histone H3 on lysine 9 and promoted the recruitment of NER factors (XPC, XPA, TFIIH subunit, p62) to photo-lesion sites (Guo *et al.,* 2011). In UV-irradiated yeast cells, it was shown that the occupancy of Gcn5 is dependent on GG-NER factors Rad16 and Rad7 (Teng *et al.,* 2008, Yu *et al.,* 2011). However, in the absence of Gcn5, cells were mildly UV-sensitive and elevated H3 acetylation (Lysine 9 and 14) was still observed, suggesting that another HAT can substitute for Gcn5, in yeast (Teng *et al*., 2002; Yu *et al.,* 2011).

Another component that affects Gcn5 occupancy is the Htz1 histone variant, which enhances Gcn5 chromatin presence and promotes H3 acetylation at specific gene locus (Yu *et al.,* 2013). This resulted in an increased binding of NER protein Rad14 to damaged DNA. The positive effect of Htz1 on repair, after UV damage, is restricted to Htz1-bearing nucleosomes.

II.4.1.2 Histone methylation

In addition to acetylation, histone methylation has also been demonstrated as facilitating NER (Chaudhuri *et al.,* 2009). Methylation of histone H3 on lysines 4 and 79 is essential for proper repair of UV-induced damage in the silenced HML locus in *S. cerevisiae* (Chaudhuri et al., 2009). Indeed, mutation of H3K9 and H3K79 residues lead to a highly UV-sensitive phenotype and the effect of these mutations predominantly affected silenced chromatin.

II.4.1.3 Histone ubiquitination

In mammalian cells, the UV-DDB damage recognition complex consists of UV-DDB1 and UV-DDB2. UV-DDB1 strongly associates with the CUL4-RBX1/ROC1 complex to form an E3 ubiquitin ligase complex of the cullin family (Scrima *et al.,* 2008). Ubiquitination of histone H2A, H3 and H4 at the site of UV-damage weakens the interaction between DNA and nucleosomes, facilitating the recruitment of NER proteins (Kapetanaki *et al.,* 2006; Lan *et al.,* 2012; Wang *et al.,* 2006).

II.4.1.4 Histone phosphorylation

Phosphorylation of histone variant H2AX was originally associated with DNA breaks, however, new evidence suggests a broader role in various genotoxic stress. It has been demonstrated that H2AX phosphorylation by ATM and ATR was observed after UV-irradiation (Ibuki and Toyooka, 2005). Moreover, the recruitment of ATM and ATR was dependent on NER factors DDB2, XPC and XPA (Ray *et al*., 2013, 2016).

II.4.1.5 Chromatin PARylation

Poly(ADP-ribosyl)ation of UV-damaged chromatin by the PARP1 (Poly(ADP-Ribose) Polymerase 1) results in the recruitment of the SWI/SNF chromatin remodelling enzyme ALC1 in whose absence cells are UV-sensitive and defective for NER (Pines *et al.,* 2012). This poly(ADP-ribosyl)ation is facilitated by UV-DDB2 (Pines *et al.,* 2012). Additionally, UV-DDB2 can itself be regulated by poly(ADP-ribosyl)ation which increased UV-DDB2 stability and its chromatin retention time. This PARP1 dependent large-scale chromatin unfolding is independent of UV-DDB2 association to CUL4 (Luijsterburg *et al.,* 2012). PARP polymerization of ADP-ribose unit activity is absent in yeast (Kim *et al.,* 2005).

Therefore, inscribing epigenetic marks as well as removing repressive epigenetic marks is crucial to potentiate efficient repair.

II.4.2 Chromatin remodelling complexes

The SWI/SNF is required for chromatin remodelling in GG-NER *in vivo*. In *S. cerevisiae,* the Rad4-Rad23 damage recognition complex has been proposed to recruit the SWI/SNF complex to DNA lesions (Gong *et al.,* 2006). Similarly in human cells, SWI/SNF interacts with GG-NER specific factor XPC and they colocalise at damage sites (Ray *et al.,* 2009). Moreover, the ATPase subunit of SWI/SNF complex, Brg1 is implicated in UV-induced chromatin decondensation (Zhao *et al.,* 2009). Brg1 is recruited in a XPC- and DDB2-dependent manner and Brg1 is required for the recruitment of downstream NER factors (XPG and PCNA) (Zhao *et al.,* 2009).

In human, the INO80 (Inositol requiring 80) remodelling complex interacts with the UV-DDB complex and promotes the removal of photo-lesions. Loss of INO80 leads to UV-sensitivity and defects in assembly of NER factors (XPC and XPA) (Jiang *et al.,* 2010). In *S. cerevisiae*, Ino80 complex is recruited to the chromatin via an interaction with damage recognition complex Rad4-Rad23 (Sarkar *et al.,* 2010). Additionally, Ino80 does not seem to be required for photoproduct removal globally but it contributes to repair in regions of high nucleosome occupancy like the *HML* locus. Interestingly, Ino80 complex is also required at a later stage for the restoration of nucleosomes after repair. These results show that the Ino80 chromatin remodelling complex intervenes at different stages of NER in yeast.

II.4.3 Chromatin structure restoration and epigenome plasticity

Previously, we have discussed about Ino80's role in restoring the chromatin structure after repair. Another factor has also been reported to have a role in chromatin structure restoration: the histone chaperone CAF1 (Chromatin Assembly Factor 1) (Gaillard *et al.,* 1996; Green and Almouzni, 2003). CAF1 was locally recruited to damage sites that had undergone the dual incision step of NER as the presence of damage was not enough to recruit it (Green and Almouzni, 2003). This late recruitment of CAF1 is consistent with a role of CAF1 in locally restoring chromatin structure disrupted during repair.

But to what extent is the epigenetic information maintained after repair?

In 2006 Polo *et al*., gave an *in vivo* demonstration of incorporation of new histones H3.1 at NER sites in human cells (Polo *et al.*, 2006). Histone H3.1 is an isotype of histone H3 whose deposition is coupled to DNA synthesis during DNA replication and repair (Tagami *et al.,* 2004). This deposition of new histone H3.1 is dependent on histone chaperone CAF1. Another recent study used live cell imaging in human cells and showed that there was a removal and incorporation of new histone dimer H2A/H2B, triggered by UV-irradiation (Dinant *et al.,* 2013). This exchange facilitated by the SPT16 subunit of the histone chaperone FACT (Facilitates Chromatin Transcription) and this role of SPT16 is independent of RNA Pol II stalling. These results indicate that there is some degree of epigenetic plasticity that can contribute to repair memory.

II.4.4 Chromatin remodelling in transcription restart in TC-NER

DNA damage inhibits transcription, therefore after repair it is essential to restart transcription as emphasised by the development of diseases (such as Cockayne Syndrome) in its absence. As mentioned above, FACT subunit SPT16 was involved in H2A/H2B turnover in response to UV damage independently of transcription (Dinant *et al.,* 2013). Furthermore, it was showed that SPT16 was implicated in restart of transcription as demonstrated by the impairment of RNA synthesis in its absence. Another study implicated the histone chaperone HIRA (HIstone Regulator A) in transcription restart (Adam *et al.,* 2013). Upon UV irradiation, HIRA deposited histone H3.3, which is normally present in transcription active chromatin, and primed damaged chromatin for transcription restart once repair is complete. In mouse fibroblasts, knockdown of histone methyltransferase DOT1L lead to UV sensitivity and impaired RNA synthesis recovery (Oksenych *et al.,* 2013). Moreover, it was observed that these cells do not recover H4 acetylation, linked to open chromatin, and there was a stabilisation of di-methylation of lysine 9 of histone 3, associated with transcription silencing. In addition, RNA Pol II and transcription factor TFIIB did not get back to UV-repressed genes in the absence of DOT1L. It was hence suggested that DOT1L ensures an open chromatin conformation in order to reactivate RNA Pol II transcription initiation after a genotoxic attack.

In conclusion, chromatin organisation results from the concerted actions of numerous actors namely chromatin modifying enzymes, chromatin remodelling complexes and histone

variants. These events are important for opening the chromatin structure to the repair machinery as well as restoring it after repair. They also contribute to epigenome plasticity that adds to repair memory.

II.5 Contribution of genomic approaches to NER study

In this section, genome-wide approaches that have added a new dimension to the study of cellular response to genotoxic stress will be discussed. Prior to the development of affordable and fast high throughput sequencing techniques, many experiments were carried out on model genes, however for the past few years there are several articles that have been published that gave a more global description of the mechanisms underlying the cellular response to genotoxic stress.

Indeed, genome-wide approaches have been developed to visualise DNA damages and subsequent repair. The 3D-DIP-chip (DNA Damage Detection (3D) by DNA ImmunoPrecipitation (DIP) on microarray chips (Chip)) developed in yeast as well as human cells can be used to locate and measure the DNA damages (Powell *et al.*, 2015). This approach consists of immunoprecipitating damaged DNA with damage-specific antibody or post-translationally modified histone. The mean theoretical distribution was modelled taking into consideration the mean length of the sheared DNA fragment, the CPD yield and the efficacy of microarray probe binding on genomic DNA. The CPD yield is influenced by DNA composition and the probability of CPD occurring at pyrimidine sites (TT, TC, CT, and CC sites in the ratio 28:16:13:3, measured in plasmid DNA (Mitchell *et al.*, 1992). In general, a good concordance was observed between the predicted and the microarray profiles. Interestingly, the 3D-DIP-chip analysis can also be combined with other ChIP on chip data, for example, it was used to investigate the acetylation of histone H3 lysine 14 (H3K14) in response to DNA damaging agents in *S. cerevisiae*. The authors confirmed that H3K14 acetylation occurs in the genome globally in response to UV-irradiation (Powell *et al.*, 2015).

Another technique to visualise DNA damage is through CPD-sequencing (Mao *et al*., 2016). Briefly, this technique involves the use of an enzyme that cuts specifically at CPD sites, the T4 endonuclease V. Bioinformatics analysis of the sequencing reads places the dinucleotide sequence upstream of the 5’ end of the read, which is used to find the CPD dinucleotide sequence on the opposite sequence of the *S. cerevisiae* genome. Combining the CPD-seq results with available nucleosome maps and transcription factors binding sites, revealed that the chromatin landscape influenced CPD formation. Indeed, CPD were more frequent on exposed nucleosomal DNA compared to DNA located at inward rotational settings within nucleosomes. Moreover, CPD formation was inhibited on transcription factor bound DNA, thereby protecting important functional DNA sequences in yeast (Mao *et al*., 2016).

A study, conducted in human cells, investigated the influence of chromatin structure on CPD formation and repair (Hu *et al*., 2017). A technique termed HS-seq (High-Sensitivity-Damage-Sequencing) involves a first step of immunoprecipitation with a lesion specific antibody to enrich in damage-containing DNA fragments. The authors showed that the

binding of transcription factors did not inhibit the formation of UV-induced damage, as there was a variation depending on the specific transcription factor, damage type, and strand (the results of this paper were discussed in "Elements influencing the generation of UV-induced damages" section).

Recently an approach, adapted from the XR-seq (eXcision Repair-sequencing) method was developed, which allowed the generation of a single-nucleotide resolution dynamic repair maps (Li *et al*., 2018). XR-seq, previously described in human cells, was adapted for yeast cells. Briefly, it consists of isolating excised oligomers and immunoprecipitating using damage-specific antibodies. The results obtained confirmed that TC-NER on the transcribed strand occurs at early time points while the bulk repair on the non-transcribed strand occurs later. Moreover, the point of incisions was defined to occur 13-18 nucleotides 5' and 6-7 nucleotides 3' to the UV damage generating a 21- to 27-nucleotide-long excision product. In addition, repair of the transcribed strand occurred in a 5' to 3' direction within genes in accordance with previous studies using *URA3* as model gene (Tijsterman *et al.*, 1999). Therefore, a genome-wide view of repair dynamics can be obtained *in vivo*.

Different studies have tried to address the question of RNA Pol II fate after UV-irradiation. The distribution of RNA Pol II on the chromatin was linked to its phosphorylation level after UV-irradiation, in human fibroblasts (Gyenis *et al.,* 2014). A decrease of RNA Pol II from the promoter regions was observed that was independent of its degradation. Concomitantly, there was an increase of RNA Pol II in the gene bodies associated with an increase of hyper-phosphorylated form of RNA Pol II. Therefore, there seems to be a negative regulatory mechanism that removes promoter-paused RNA Pol II.

Another study conducted in human cells, also addressed the question of RNA Pol II fate and the importance of transcription elongation during DNA repair. Lavigne *et al.* recently analysed the genome-wide distribution of the different forms of RNA Pol II (hypo- and hyper-phosphorylated) by ChIP-seq in human fibroblasts (Lavigne *et al.,* 2017). In mammals, RNA Pol II can pause in the proximity of the promoter, close to the TSS (Transcription Start Site), and be released in a regulated and coordinated manner in response to different developmental or environmental cues. It was observed that in response to UV stress, there was a wave of *de novo* released proximal promoter paused RNA Pol II. Indeed, there was an increase of elongating RNA Pol II on the gene bodies and a concomitant decrease of promoter bound RNA Pol II in active genes but no significant change in inactive genes. Furthermore, RNA Pol II wave was described at almost all active genes irrespective of gene size and expression levels. The wave of elongating RNA Pol II has been proposed to allow faster sensing of damage and also favouring a more open chromatin conformation due to the progression of RNA Pol II, which facilitates TC-NER and indirectly GG-NER on the non-transcribed strand. Accordingly, the repair rates on the non-transcribed strand in inactive regions were lower than in active regions.

In yeast, no such accumulation of RNA Pol II is observed near the TSS, till now (Steinmetz *et al.*, 2006) and hence promoter pausing might be absent or it is quickly resolved. Therefore, the afore proposed mechanism of UV-induced *de novo* release of RNA Pol II from the promoter proximal pausing sites might be specific to mammalian cells and be absent from yeast cells.

The combination of RNA Pol II genomic profile with that of nascent RNA can give a more accurate picture of RNA Pol II's fate after genotoxic stress and its effect on transcription. A first genome-wide study using nascent Bru-seq which uses bromouridine (Bru) to label nascent RNA followed by deep sequencing of the immunoprecipitated nascent Bru-RNA was carried out in human fibroblasts (Andrade-Lima *et al.,* 2015). The observation of nascent RNA will give a more accurate view of RNA synthesis than total RNA measure, which are dependent on RNA stability as well as synthesis. It was showed that there is a UV-induced dose-dependent effect on RNA synthesis. For instance, it was showed that in UV-irradiated cells there was an accumulation of transcription reads on the 5' of genes and decrease in the gene bodies while transcription reads were uniformly distributed from the TSS into the gene bodies in unirradiated cells. The decrease of transcription read in the 3' side of long genes was correlated with a slower repair of lesions at the 3' end of long genes. TC-NER operates in a 5' to 3' direction as well as transcription recovery which is linked to damage removal. This study also provided genome-wide transcription recovery data in CSB-deficient fibroblasts (mutation in TC-NER specific factor) and, XPC-deficient fibroblasts (mutation in GG-NER specific factor). It was observed that CSB-deficient cells had a substantially retarded transcription recovery, whereas XPC-deficient cells were less affected compared to wild-type cells.

These new techniques open new possibilities in the analysis of huge set of data from patients and associate phenotypes to mutations and mutations to an underlying mechanism. As such, genome-wide sequence analysis of over 500 tumours revealed that there is a mutational strand asymmetry namely in UV- and tobacco smoke-associated somatic mutations (Haradhvala *et al.,* 2016). Indeed, it was observed that the mutational densities on the non-transcribed strand are increased in transcribed regions in these tumours, indicating a key role of transcription in maintaining genome integrity.

In this section, a few approaches developed in recent years to study NER on a genome-wide scale was presented. These studies complement *in vivo* studies conducted on few model genes. They also aid in giving a more global view to different mechanisms observed and data from different studies can be combined to give a more in-depth analysis. For instance, repair efficiency can be linked to chromatin structures.

In conclusion, the NER pathway is an evolutionarily conserved mechanism that exhibits some particularities between species as has been described for yeast and human. This mechanism is the only pathway in human that has been descried to remove UV-induced damages and UV-irradiation is one of the most common sources of DNA damage. Hence, it

is crucial that the NER pathway is fully functional as defects in this pathway lead to severe pathologies.

II.6 Diseases associated with NER defects

Defects in the NER pathway is associated with a large family of diseases which include XP (Xeroderma Pigmentosum), CS (Cockayne Syndrome), TTD (TrichoThioDystrophy) as summarised in Table 2. Patients affected by these diseases present overlapping clinical features like UV-sensitivity. They also present distinct clinical features associated with mutations of genes implicated in the GG-NER or TC-NER sub-pathways.

II.6.1 Xeroderma pigmentosum (XP)

XP is a rare autosomal disease that was discovered at the end of the 19th century by Moritz Kaposi. The name XP comes from the Greek terms *xero* meaning dry and *derma* meaning skin which described the aspect of the patients' skin. To it was added the Latin word *pigmentosum* meaning stained, due to pigmentation abnormalities presented by the patients (Bukowska and Karwowski, 2018). Indeed, these patients are hypersensitive to sunlight resulting in sunburn and changes in skin pigmentation and they also have a strong predisposition to develop skin cancer (2000 or more times higher than the average population depending on the cancer type) and internal tumours are 10 times more frequent, associated with mutation accumulation (Menck and Munford, 2014).

Patients were categorised into seven different complementation groups, XPA to XPG, based on cell fusion experiments. Once the genes mutated in these different groups of XP were identified they were assigned the name of the corresponding complementation group (Cleaver, 2005). Patients from the XPA to XPG groups presented defects in the NER pathway, however there were other cases reported where cells from XP patients showed normal level of damaged nucleotide excision after UV irradiation. These cells presented defects in post-replication repair (Lehmann *et al.*, 1975), which is the inability of cells to synthesise daughter DNA strands using damaged templates. This type of XP with translesional DNA synthesis defect was termed XPV (V for variant). Translesional DNA synthesis allows the cell to survive despite the damage but does not repair the lesion. XPV encodes a DNA polymerase η (eta) (Masutani *et al.*, 1999a), which has the ability to add adenines opposite to thymine dimers (Masutani *et al.*, 1999b).

XP patients usually contain mutations in genes involved in the GG-NER pathway or in the steps common to both pathways. A minority of these patients, 20-30%, also develop progressive neurological abnormalities and premature ageing (Menck and Munford, 2014). These more severe symptoms are associated with XP combined with CS and are linked to mutations in XPD, XPB, XPF or XPG genes (Laugel *et al.*, 2013). These genes have been described as implicated in the GG-NER as well as TC-NER pathway.

II.6.2 Cockayne Syndrome (CS)

CS (Cockayne Syndrome) was named after Edward Alfred Cockayne who first described it in 1936. It is an autosomal recessive disease like XP. It affects numerous organs with symptoms such as stunted growth, microcephaly, neurological impairment and prematurely aged appearance (Bukowska and Karwowski, 2018). Remarkably no heightened risk of skin cancer is detected, unlike XP, despite the cells being hypersensitive to UV and displaying increased mutagenesis. Therefore, DNA mutagenesis may be necessary but not sufficient for cancer development.

CS has been associated with a failure to recover RNA synthesis after UV irradiation rather than a defect in the repair mechanism *per se* (Mayne and Lehmann, 1982). Defects in genes implicated in TC-NER are found mutated in these patients.

CS includes a variety of developmental disorders from mild UVSS (UV-sensitive syndrome), in which the only symptom is photosensitivity, to the more severe neonatal lethal COFS (Cerebro-Oculo-Facio-Skeletal) syndrome whose name refers to the organs affected namely the brain, eyes, face and skeletal system (Cleaver *et al.,* 2009; Bukowska and Karwowski, 2018).

Animal models have been developed to better characterise CS but care should be taken on the interpretation of these studies, as there are differences in phenotype between human and mice. For example, CS mice models show heightened predisposition to skin cancer unlike CS patients (van der Horst *et al.,* 1997). It was proposed that this difference could be due to a more efficient GG-NER pathway in human than mice.

II.6.3 TTD (Trichothiodystrophy)

TTD is a rare, autosomal recessive disorder linked to defects in NER associated genes. The term 'trichothiodystrophy' comes from Latin tricho-thio-dys-trophe means hair-sulphur-faulty-nourishment as these patients have lower content of sulphur-rich proteins such as keratin (Bukowska and Karwowski, 2018). These patients exhibit clinical features such as increased photosensitivity, brittle hair, intellectual impairment and short stature, but no cancer development (Bukowska and Karwowski, 2018).

The photosensitive form of TTD has been linked with mutations in NER genes: XPB, XPD, TTDA (Bukowska and Karwowski, 2018). These are subunits of the transcription factor TFIIH, which has a dual role in transcription and NER and, these subunits are required for TFIIH formation and stability. It has been proposed that genetic alterations in XP is mainly due to NER defect, whereas mutations observed in TTD might impact transcription as well as NER (Stefanini, 2006).

It should be noted that NER proteins could also be implicated in other repair pathways or other cellular processes (refer to "Transcription" and "Discussion" chapters). It is therefore possible that the clinical features observed are due to the combination of more than one defective pathway. For instance, CSB deficient cell lines have mitochondrial defects with an increased in mitochondrial content and ROS (Reactive Oxygen Species) production observed (Scheibye-Knudsen *et al.,* 2013). This could partly explain the accelerated ageing feature observed in CS patients as mitochondrial deficiencies are tightly linked to the ageing process (Scheibye-Knudsen et al., 2013). In addition in cases of XP associated with CS, it has been demonstrated that the XP-D/CS cells, for example, exhibit chromosome segregation defects due to early engagement in mitosis (Moriel-Carretero *et al*., 2015). Therefore, the molecular mechanisms behind these pathologies are complex and cannot only be restricted to the impairment of the NER pathway. Moreover, different mutations in the same gene can lead to diverse clinical features by namely affecting different activities of the gene product. Some mutations may also go unnoticed because of functional redundancy or compensation by other DNA repair pathways.

Although we have advanced in the molecular characterisation of these pathologies, there is currently no cure. The patient's life and living condition can be improved by proper protection from sunlight. Therefore, DNA damages can have harmful consequences for an organism and DNA repair act to prevent mutation and maintain genome stability and delay the appearance of cancer, neurodegeneration and premature ageing.

II.6.4 Drug resistance conferred by NER pathway

DNA repair help resolve damages to prevent mutagenesis but in cancer treatment, it can hinder the efficacy of the chemotherapeutic drugs. Cisplatin and carboplatin are often used in chemotherapy for their cytotoxic effects but mutations and epigenetic events can reduce their efficacy. Resistance can be acquired due to an exceeding amount of a resistance factor, or mutation of a factor required for tumour cell toxicity. Platinum damage is mainly resolved by the NER pathway. Indeed, it has been shown that an increased in NER, for example, by the overexpression of NER genes (such as XPA) can confer drug resistance to cells and hence, be deleterious for therapy (States and Reed, 1996). On the contrary, polymorphisms in NER gene XPD conferring reduced repair capacity can lead to increased platinum sensitivity associated with decreased repair efficiency (Stewart, 2007).

These experiments give a better insight into acquired drug resistance and possible therapy that can involve altering the repair capabilities of cancer cells to render them more sensitive to therapy.

Gene	Disease	Pathway affected	Clinical symptoms
XPA	*XP, DSC*	NER	Exaggerated Sunburn; Skin cancer; mild to severe neurological abnormalities
XPB/ERCC3	XP, XP/CS	NER	Exaggerated sunburn; Skin cancer; mild to severe neurological abnormalities
XPC	XP	GG-NER	No abnormal sunburn reaction; Skin cancer; No neurological abnormalities
XPD	XP, XP/CS, TTD	NER	Exaggerated sunburn; Skin cancer; No neurological abnormalities
DDB2	XP	GG-NER	No abnormal sunburn; Skin cancer; No neurological abnormalities
XPF	XP, CS, COFS, XFE	NER	Exaggerated sunburn; Skin cancer; No neurological abnormalities to severely affected patients
XPG	XP, XP/CS	NER	Exaggerated sunburn; Skin cancer; May present developmental abnormalities
XPV	XP	TLS	No abnormal sunburn reaction; Skin cancer; No neurological abnormalities
CSA	CS, UVSS	TC-NER	Mental retardation, microcephaly and growth failure
CSB	CS, COFS, UVSS, DSC	TC-NER	Mental retardation, microcephaly and growth failure
UVSSA	UVSS	NER	Mild sun sensitivity; No neurological abnormalities
TTDA (TFIIH subunit)	TTD	NER	Brittle hair; delayed development; significant intellectual disability and recurrent infections
ERCC1	COFS, XFE	NER	Mental retardation; growth failure

Table 2: NER genes and associated diseases.
Xeroderma pigmentosum (XP). Cockayne syndrome (CS), Trichothiodystrophy (TTD), Cerebro-oculo-facio-skeletal syndrome (COFS), XPF-ERCC1 progeroid syndrome (XFE), UV-sensitive syndrome (UVSS), DeSanctis-Cacchione syndrome (DSC) (Menck and Munford, 2014).

In conclusion, the NER pathway is a multi-step repair process that requires the cooperate actions of many proteins and the post-translational modifications of these proteins are important to regulate their functions. Proper execution of this pathway allows the removal of helix-distorting lesions and in the case of the TC-NER pathway, restoration of transcription. However, the inability to remove the lesions can induce apoptosis or increase the mutation rate. Dysfunctions of this pathway is implicated in numerous incurable pathologies therefore a better understanding of this pathway is key to finding potential therapeutic targets.

III. RNA Pol II transcription

III.1 Transcription and RNA polymerases

The NER pathway is linked to transcription, therefore in this chapter the RNA Pol II transcription will be discussed along with factors having a dual role in transcription and DNA repair.

The different steps of transcription will not be presented in details, as it is not the pivotal focus of this work. I will however elaborate on RNA Pol II, Mediator and TFIIH due to their implication in transcription and DNA repair.

The DNA molecule encodes functional information and transcription helps to decipher this information which is needed for regulation of cellular processes, for adaptation to environmental stimuli and for cell viability. It also allows multicellular organisms to engage cells into various differentiation pathways by triggering specific transcriptional programmes.

Transcription is conserved in eukaryotes, archaea and bacteria and is carried out by evolutionary conserved multi-subunit enzymes: RNA polymerases (RNA Pols). The latter polymerises nucleoside triphosphate (NTP) units into a RNA molecule using DNA as template with the help of transcription factors. The RNA molecules can be of various forms such as messenger RNAs, structural and regulatory non-coding RNAs. DNA-dependent RNA Pols are hence the engines of transcription and in eukaryotes there are three nuclear RNA polymerases whereas bacteria and archaea have only one RNA Pol to transcribe their whole gene repertoire. In the eukaryotic kingdom, plants represent an exception as they have two more RNA Pols (RNA Pol IV and V) that synthesize noncoding RNAs required for transcriptional gene silencing via the RNA-directed DNA methylation (Zhou and Law, 2015).

RNA Pols share a catalytically competent core, composed of five subunits, that is conserved in all three domains of life (Murakami and Darst, 2003). The similar structural framework and associated molecular mechanisms have led to the hypothesis of a common ancestor that had a very similar form to that of the contemporary bacterial RNA Pol which is the simplest form with only a catalytic core (subunits α_2, β, β' and ω) (Werner and Grohmann, 2011).

Eukaryotic RNA Pols were first isolated from sea urchin embryos and rat liver by chromatography and named RNA Pol I, II and III (also known as RNA Pol A, B, C) according to their order of elution (Roeder and Rutter 1969; 1970). The function of these RNA Pols was determined based on their difference in sensitivity to a mushroom toxin, α-amanitin. Indeed, seminal studies showed that RNA synthesis catalysed by RNA Pol II is inhibited even at low doses α-amanitin, which acted by binding to RNA Pol II and blocking chain elongation (Redinger *et al*., 1970). Moreover, only high doses of α-amanitin had a negative effect on RNA synthesis by RNA Pol III (Weinmann *et al.*, 1974). However, α-amanitin had no effect on

RNA synthesis by RNA Pol I at all inhibitor concentrations (Gniazdowski *et al.*, 1970). It was hence found that RNA Pol I and Pol III are responsible for the transcription of non-coding genes, such as genes encoding transfer RNAs or ribosomal RNAs and RNA Pol II is involved in the transcription of all protein-coding genes (messenger RNAs) and of multiple long and short non-coding RNAs.

III.2 Eukaryotic RNA Pol II

The complexity of understanding the transcription process stems from the fact that it is a very dynamic system that employs a plethora of factors. Another layer of regulation and complexity is added by the post-translational modifications and significant conformational changes of RNA Pol II as it advances through the transcription cycle. Therefore, before addressing RNA Pol II transcription, it is important to get a better understanding of the structural as well as functional traits of RNA Pol II.

III.2.1 Structure of RNA Pol II

The resolution of the structures of RNA Pol II from the three domains of life (eukaryotes, bacteria and archaea) have provided insights on the structural and functional evolution of RNA Pols. RNA Pol II is composed of twelve subunits named Rpb1-12, from increasing to decreasing molecular weight. Two of the twelve subunits are not essential for cell viability: Rpb4 and Rbp9. Five RNA Pol II subunits (Rpb1, Rpb2, Rpb3, Rpb6, and Rpb11) share partial sequence homology and structural similarity with archaeal and bacterial RNA polymerases. Rpb5, Rpb6, Rpb8, Rpb10, and Rpb12 subunits are common to the other two eukaryotic RNA Pols (I and II) (Cramer, 2004).

The complexity of determining a high-resolution structure of RNA Pol II stems from the fact that RNA Pol II is a bulky multi-subunit complex of a molecular weight of 0.5 MDa, which has a very dynamic conformation. Initial structural analyses of RNA Pol II alone or in complex with other transcription factors or nucleic acids were obtained by the laboratory of R. Kornberg.

The first high-resolution structure of RNA Pol II was resolved in yeast by X-ray crystallography, but the model only consisted of ten subunits (Cramer *et al.,* 2000). The authors purposefully used a RNA Pol II lacking Rbp4 and 7 as these two subunits are present in substochiometric levels and associate reversibly with the rest of the complex, which was an impediment to crystallisation. A few years later, a complete structure of RNA Pol II with its twelve subunits was published, namely made possible by pulling on tagged Rpb4 and hence enriching the preparation with complete RNA Pol II complexes (Armache *et al.*, 2003; Bushnell and Kornberg, 2003). RNA Pol II complex structure is divided into a ten-subunit core (Rpb1, Rpb2, Rpb3, Rpb5, Rpb6, Rpb8, Rpb9, Rpb10, Rpb11 and Rpb12) with the two largest subunits Rpb1 and Rpb2 forming a central mass and bordering the cleft containing the active centre. Rpb1 and Rpb2 are connected by Rpb3, Rpb10, Rpb11, and Rpb12. The limit of the enzyme is composed of Rpb5, Rpb6, Rpb8 and Rpb9, which are assembled

around Rpb1 and Rpb2. The Rpb4/Rpb7 heterodimer protrudes from the base of the enzyme as illustrated in Figure 9 (Cramer, 2004).

Structural elements of functional significance have been given different names. Indeed, Rpb1 and Rpb2 form a positively charged “cleft” and DNA molecule enters the cleft passing through the upper and lower mobile “jaws”. The active centre is located at the end of the cleft and contains a magnesium ion. The active site is formed by the “wall”, “protrusion” and “clamp”. The “wall” acts as a barrier to the DNA-RNA duplex progression and because the active site is well beneath the level of the downstream DNA, the duplex is forced to incline relative to the axis of the downstream DNA. Consequently, the newly synthesised RNA molecule extrudes the enzyme through a “pore” situated beneath the active site, which widens towards the outside, creating an inverted “funnel”. The template DNA can also re-hybridise with the upstream DNA. The “stalk” located at the bottom of the enzyme is formed by Rpb4/Rpb7 heterodimer. The stalk is mobile and it is in an open conformation in the absence of a DNA template. When RNA Pol II is active, the stalk closes and helps to maintain the DNA-RNA duplex in place. This change of conformation is important for RNA Pol II to move from initiation to elongation (Cramer *et al*., 2000, Cramer, 2004).

The structural features described for yeast RNA Pol II are pertinent to human RNA Pol II as well. Indeed, about half of the amino acid sequence of the twelve subunits are identical between yeast and human. Moreover, most RNA Pol II yeast subunits can functionally replace their human counterparts, even the human Rpb4/Rpb7 heterodimer can functionally substitute their yeast homologs (Khazak *et al.,* 1995). This indicates that the interface between the core and Rpb4/Rpb7 is conserved.

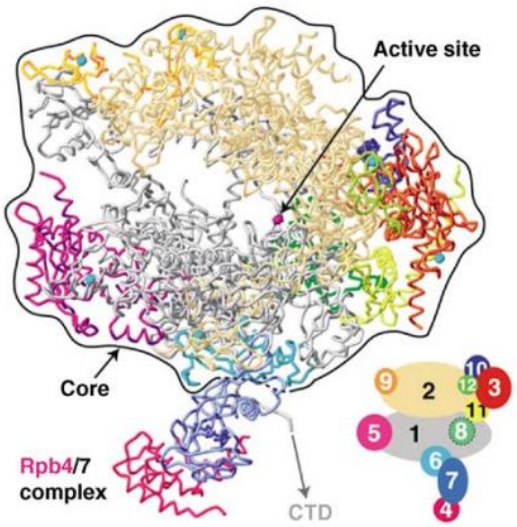

Figure 9: View of the complete yeast Pol II obtained by X-ray crystallography.
On the right is a schematic representation of the RNA Pol II complex (Cramer, 2004).

III.2.1.1 Carboxy terminal domain (CTD) of Rpb1

The CTD of Rpb1 is a conserved structure specific to RNA Pol II, essential for cell viability, composed of heptad repeats with consensus motif Tyr1-Ser2-Pro3-Thr4-Ser5-Pro6-Ser7 and various numbers depending on the organism. In mammals, the CTD is composed of consensus and also significant number of non-consensus heptad repeats, on the contrary, almost all of the heptad repeats in *S. cerevisiae* are consensus repeats. Moreover, human cells with a CTD with only consensus repeats is viable, indicating that the non-consensus repeats have evolved to carry out supplementary functions (Zaborowska *et al*., 2016).

The consensus repeats can be phosphorylated or glycosylated on the serine, tyrosine and threonine residues and prolines can be isomerised. Lysines in the non-consensus repeats can be methylated, acetylated and ubiquitinated and arginines can be methylated. The reversible modifications on the CTD generate a code that change throughout the transcription cycle and can be read by CTD-binding factors (Zaborowska *et al*., 2016).

The pattern of RNA Pol II CTD phosphorylation is modified during the transcription cycle in *S. cerevisiae* and mammals. There are three main cyclin-dependent CTD kinases: CDK7, CDK8 and CDK9.

Inhibition studies have identified a subunit of TFIIH, CDK7 in mammals and Kin28 in yeast, as a major serine 5 and serine 7 kinase (Akthar *et al*., 2009; Glover-Cutter *et al*., 2009). Inhibition of the kinase activity of CDK7 *in vivo* suppressed RNA Pol II accumulation at 5' ends of several genes and has been linked to reduced proximal-promoter pausing. Consistently, there was a defect of NELF (Negative ELongation Factor) recruitment which is required for proximal-promoter pausing (Glover-Cutter *et al*., 2009). RNA Pol II CTD serine 5 phosphorylation by Kin28 is required for promoter escape of RNA Pol II and facilitates the dissociation of Mediator from promoters (Wong *et al.*, 2014; Jeronimo *et al.*, 2014).

In vitro, serine 2 and serine 5 can be phosphorylated by CDK8 subunit of Mediator (more details in Mediator section) (Galbraith *et al*., 2010; Hengartner *et al.*, 1998). CDK8 is a cyclin-dependent serine-threonine kinase involved in transcriptional regulation in yeast and mammals. It has a serine 2 and serine 5 phosphorylation activity *in vitro.* However, its role in CTD phosphorylation *in vivo* remains unclear.

CDK9 is the major serine 2 kinase and can also phosphorylate serine 5 *in vitro* and *in vivo* (Eick and Geyer, 2013) and the phosphorylation of RNA Pol II CTD enhances transcription elongation (Kim *et al.,* 2002) by regulating the association of elongation factors with RNA Pol II.

CTD phosphatases reverse CTD phosphorylation and allow recycling of RNA Pol II. Several phosphatases are implicated. For instance, phosphorylated serine 5 residues are specifically dephosphorylated by Ssu72, conserved from yeast to humans, which is enriched at promoters and 3' of genes. Another serine 5 phosphatase is the yeast Rtr1 which is localised at the 5' end of genes. At the end of the transcription cycle, the level of phosphorylated

serine 2 is moderated by the Fcp1 phosphatase, which aids the recycling of RNA Pol II for PIC re-integration. Fcp1 also acts on phosphorylated serine 5, it is accordingly present at the 5' and 3' of active genes (Eick and Geyer, 2013).

In conclusion, the phosphorylation state of RNA Pol II CTD changes throughout the transcription cycle (Figure 10) and finely regulates transcription as well as RNA Pol II interaction with other proteins, for example to regulate RNA splicing and mRNA export. Hence, coordination between kinases and phosphatases is necessary. Different phosphorylated forms of RNA Pol II predominate at different stages of transcription. A hypophosphorylated form of RNA Pol II is included in the PIC and elongating RNA Pol II is hyperphosphorylated.

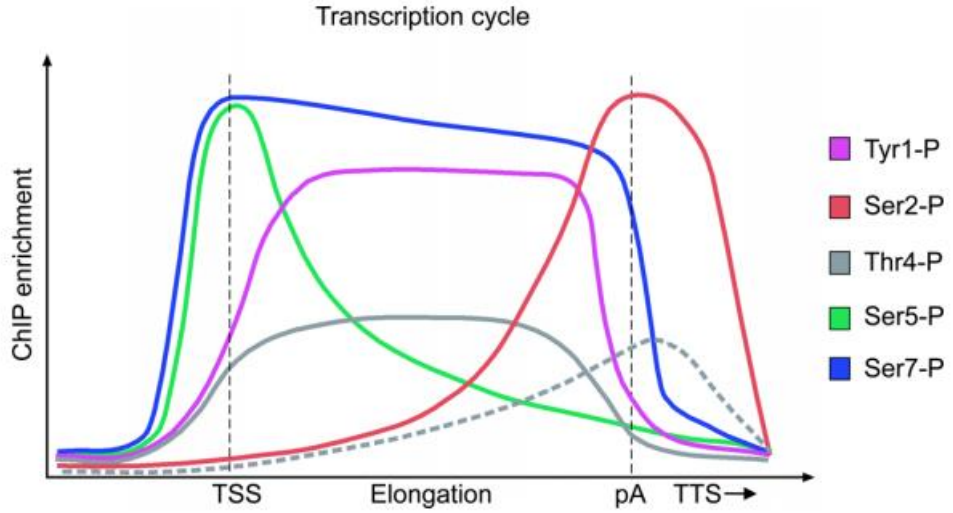

Figure 10: Changes of CTD modifications along the transcription cycle.
Signals were obtained by ChIP experiments in *S. cerevisiae*, with similar results obtained for mammalian cells. TSS: transcription start site, pA: polyadenylation site, TTS: transcription termination site (Eick and Geyer, 2013).

III.2.2 RNA Pol II transcription

The transcription process is composed of three steps: initiation, elongation and termination and each step is finely regulated.

- Transcription initiation involves recruitment of sequence-specific transcription activator which stimulate RNA Pol II transcription via co-activators. It involves the recruitment of GTFs (general transcription factors) and RNA Pol II to form the PIC.
- Transcription elongation involves the progression of RNA Pol II along the transcribed strand of the gene to produce a RNA molecule.
- Transcription termination signals the end of the transcription cycle with RNA Pol II detaching from the DNA template and the newly synthesised RNA is taken over by complexes involved in RNA biogenesis.

III.2.2.1 Promoter region of RNA Pol II transcribed genes

Genes transcribed by RNA Pol II are termed class II genes. Transcription of class II genes requires the assembly of a complex comprising of RNA Pol II on a portion of DNA termed promoter. A promoter region comprises two distinct parts: a core promoter and regulatory region.

The core promoter is defined as the minimal sequence required for transcription initiation *in vitro*. Analyses of the core promoter region have, thus far, identified seven elements which are required for proper transcription initiation, illustrated in Figure 11 (Thomas and Chiang, 2006). The core promoter elements include, upstream of the Inr sequence (Initiator), a TATA-box, BRE (TFIIB-Recognition Element). The DCE (Downstream Core Element) is located downstream of the Inr. The DCE itself consists of two motifs: MTE (Motif Ten Element) and DPE (Downstream Promoter Element). The core promoter elements are bound by GTFs as depicted in Figure 11. These core promoter elements are not systematically present at all gene promoters which allows a fine regulation of gene expression. The described sequences correspond to consensus sequences. In *S. cerevisiae*, the motifs do not exist as such, with the exception of the consensus TATA box, though there are sequence similarities. For example, the Inr sequence is specific to pluricellular eukaryotes, and hence absent in *S. cerevisiae*. It has been proposed that the Inr defines the TSS (Transcription Start Site), consequently in *S. cerevisiae* the TSS is less well defined.

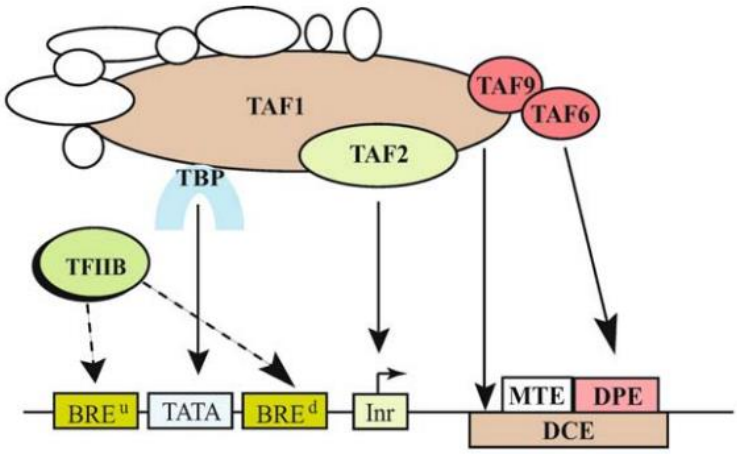

Figure 11: Schema of eukaryotic core promoter.
The seven core promoter elements are represented: BRE (TFIIB-Recognition Element), TATA box, Inr (Initiator), DCE (Downstream Core Element), MTE (Motif Ten Element) and DPE (Downstream Promoter Element). Promoter regions recognised by general transcription factors TFIIB and TFIID (consisting of TBP (TATA-Binding Protein), TAFs (TBP-associated factors) is indicated by arrows (Thomas and Chiang, 2006).

The regulatory region of the promoter can be proximal or distal. These sequences are bound by transcription regulators and are present in yeast and pluricellular eukaryotes. In yeast,

the regulatory elements are termed URS (Upstream Regulatory Sequence), situated a few hundred of bases from the TSS. Regulatory elements bound by transcription activators are UAS (Upstream Activating Sequence). URS are found upstream of the core promoter and in nucleosome-free regions (Hahn and Young, 2011). In pluricellular eukaryotes, the regulatory regions can be found upstream or downstream of the core promoter and kilobases away from the core promoter. Activator regulatory sequences are termed enhancers (Hahn and Young, 2011).

Regulatory regions can have more than one sequence for binding transcription factors, allowing a fine regulation of gene expression. Moreover, regulatory regions can be found far from the core promoter, site of assembly of the general transcription machinery, therefore these two regions need to be brought into close proximity namely by DNA looping.

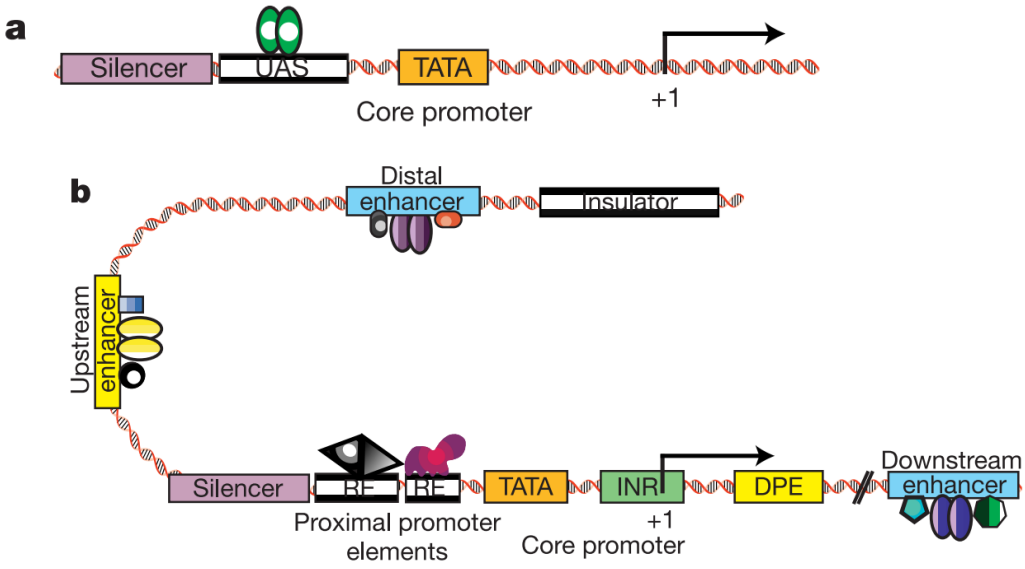

Figure 12: Schematic representation of unicellular eukaryote and metazoan promoters.
a. Simple eukaryotic transcriptional unit, represented by a core promoter (TATA), upstream activator sequence (UAS) and silencer element spaced within few hundred bases of the TATA box that is typically found in unicellular eukaryotes. b. A more diversified metazoan transcriptional unit. A complex arrangement of multiple clustered enhancer modules interspersed with silencer and insulator elements which can be located 10–50 kb either upstream or downstream of a composite core promoter containing TATA box (TATA), Initiator sequences (INR), and downstream promoter elements (DPE) (Levine and Tjian, 2003).

III.2.2.2 Transcription initiation

RNA Pol II requires numerous factors for proper transcription and *in vitro* transcription systems derived from nuclei or whole cell extracts of yeast or mammalian cells (Luse and Roeder, 1980; Lue and Kornberg, 1987; Woonter and Jening, 1989) have been instrumental in identifying transcription factors and defining their roles. It was shown that purified RNA Pol II is capable of transcribing DNA but is unable to initiate specific transcription from the

promoter. However, soluble cell extracts can direct accurate transcription initiation. Therefore, additional factors are required to drive specific RNA Pol II transcription. Several studies led to the identification of factors that aids selective and efficient transcription initiation in yeast and mammalian cells (Matsui *et al.*, 1980; Sayre *et al.*, 1992; Henry *et al.,* 1994 and reviewed in Hahn, 2004). These factors can be divided into two categories: gene-specific and general transcription factors.

GTFs (General Transcription Factors) are required for the proper initiation of all genes. These include TFIIA, TFIIB, TFIID, TFIIE, TFIIF and TFIIH. In vitro transcription assays showed that GTFs are sufficient for basal transcription, in the absence of specific transcription factors. GTFs bind to the core promoter, the minimal sequence required for basal transcription, during transcription initiation.

Gene-specific factors bind promoters at their specific target sequence and can either have a positive effect or negative effect on the gene expression in response to cellular stimuli, adding a regulatory layer to gene expression. Co-regulators bridge the specific transcription factors and the basal transcription machinery (Figure 13). Co-regulators can act on the chromatin structure around promoter (chromatin remodelers and chromatin modifiers) or can stimulate the assembly of the PIC. Some complexes can have both activities. To note that TFIID containing TAFs is a co-regulator as well as GTF (Guermah *et al.,* 2001). Mediator complex is of particular interest to our study and is discussed in detail in "Mediator" chapter.

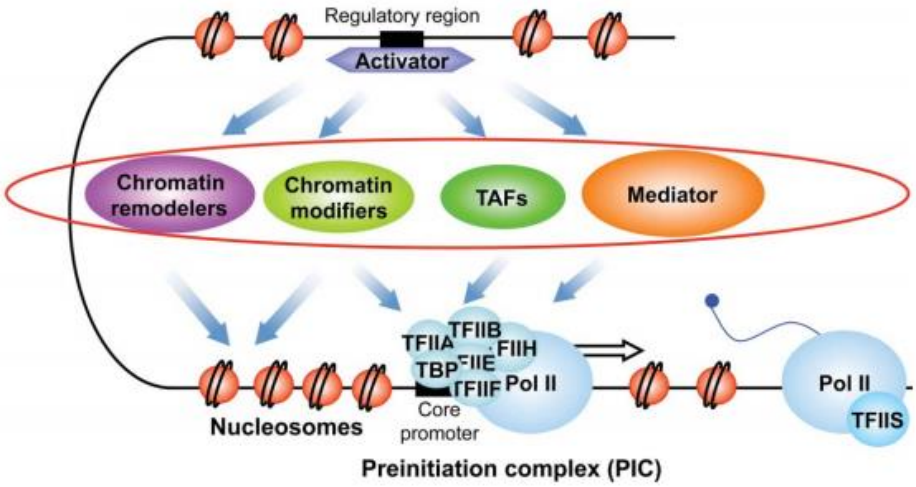

Figure 13: Schema representing the regulation of RNA Pol II transcription initiation. Eukaryotic co-regulators, encircled in red, operate between the basal RNA Pol II transcription machinery and co-activators. These multi-subunit complexes include chromatin remodelers and chromatin modifiers that act on the promoter chromatin structure or TAFs-containing TFIID and Mediator that stimulate assembly of the pre-initiation complex. Some complexes can have both activities (Eychenne *et al*., 2017).

III.3 TFIIH

TFIIH (Transcription Factor II H) is a multi-subunit complex that has a role in transcription, repair and cell cycle. It is composed of ten subunits, forming the core TFIIH module (Ssl2/XPB, Tfb1/p62, Tfb2/p52, Ssl1/p44, Tfb4/p34 and Tfb5/p8) and a kinase module (Kin28/CDK7, Ccl1/Cyclin H and Tfb3/MAT1) in human and yeast, with the Rad3/XPD subunit bridging the two modules (Luo *et al.,* 2015).

The role of TFIIH in DNA repair has been described in the NER chapter section TFIIH. Here, its structure and role in transcription will be discussed.

III.3.1 TFIIH structure

In *S. cerevisiae*, cryo-electron microscopy structure of TFIIH within the PIC and in association with Mediator has been obtained (Schilbach *et al.*, 2017). This study provides structural data on the organisation of the different subunits of TFIIH relative to other protein/complexes of the PIC as well as the positioning of TFIIH domains within the structure. It was shown that TFIIH has a crescent-shape, spanning from Ssl2 to Rad3, with the other TFIIH subunits arranged in between the two ATPases/helicases (Figure 14), showing similarities with the structure previously proposed by electron microscopy (Gibbons *et al*., 2012). This study also gave insights into TFIIH function in opening the DNA molecule and in RNA Pol II phosphorylation. Indeed, the authors proposed a model where Ssl2 translocates on DNA away from RNA Pol II leading to DNA opening, consistent with its function in transcription. The model is based on the fact that Ssl2 binds to downstream DNA, it has a 3'-5' DNA helicase directionality and the fixed Ssl2 position in the PIC. On the other hand, Rad3 is located further away from the DNA molecule, in accordance with its ATPase activity being dispensable for transcription (Schilbach *et al.*, 2017).

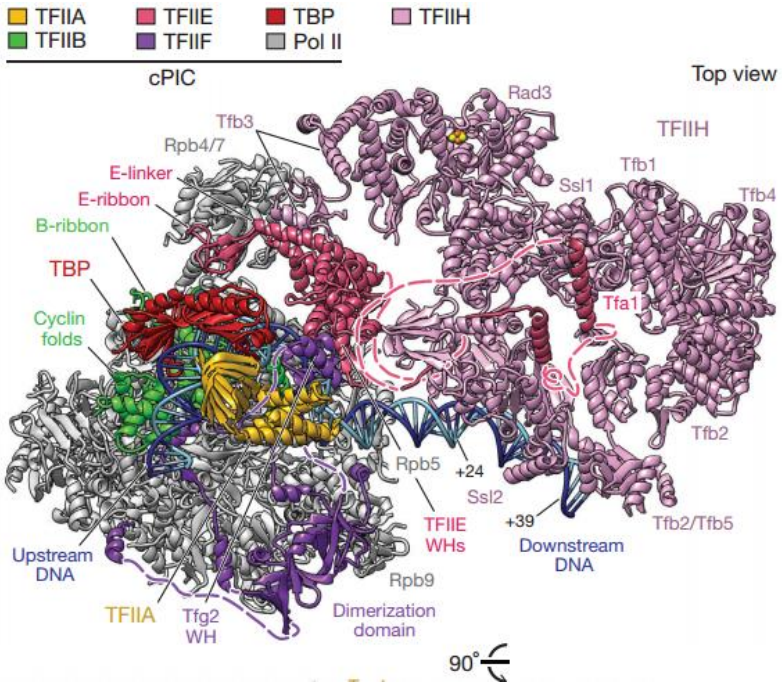

Figure 14: The yeast TFIIH structure with other components of the pre-initiation complex.
The different components of the pre-initiation complex (PIC) are colour-coded: TFIIA, TFIIB, TFIIE, TFIIF, TFIIH, TBP and RNA Pol II. The DNA molecule is represented in blue and flexible linkers in TFIIE and TFIIF are represented in dashed lines. The crescent moon structure of TFIIH, in contact with the DNA molecule and other PIC components is represented in purple (Schilbach *et al.*, 2017).

Moreover, to provide insights on RNA Pol II phosphorylation by TFIH, facilitated by Mediator, the PIC-cMed (core Mediator, details in "Mediator" chapter) structure was solved (Figure 15; Schilbach *et al.*, 2017). In contact with the PIC, there is a change in Mediator conformation. The CTD of RNA Pol II is mobile and extends towards the inner surface of Mediator represented in Figure 15. It was reported that the CTD crosslinks to the inner surface of Mediator (Nozawa *et al.*, 2017), suggesting that the CTD is accommodated in a compact globular form in the cradle formed between Mediator and RNA Pol II (Figure 15; Cramer, 2004). It was proposed that TFIIH could then access the CTD through the openings at the interface between the head and middle modules of Mediator. CTD phosphorylation would cause a repulsion between accumulating negative charges on the CTD leading to its expansion and a weakening of Mediator-RNA Pol II interaction. The dissociation of Mediator from RNA Pol II can destabilise the PIC, facilitating RNA Pol II promoter escape (Schilbach *et al.*, 2017).

The human TFIIH structure was also reconstructed from cryo-electron microscopy data, a horseshoe-shaped assembly of core TFIIH was reported, with the XPD and XPB ATPases/helicases situated next to each other (Greber *et al.*, 2017; Figure 16). This structure is in agreement with previously reported lower-resolution reconstruction data (Schultz *et al.,* 2000). The human TFIIH structure shows similarities with the yeast structure (compare

Figures 14 and 16). Moreover, it was showed that the conformation of TFIIH in the PIC with RNA Pol II compared to free TFIIH changes with the distance between XPD and XPB increased. XPB RecA-like domain moves away from XPD when binding DNA, which also leads to the relocation of other TFIIH subunits bound to XPB.

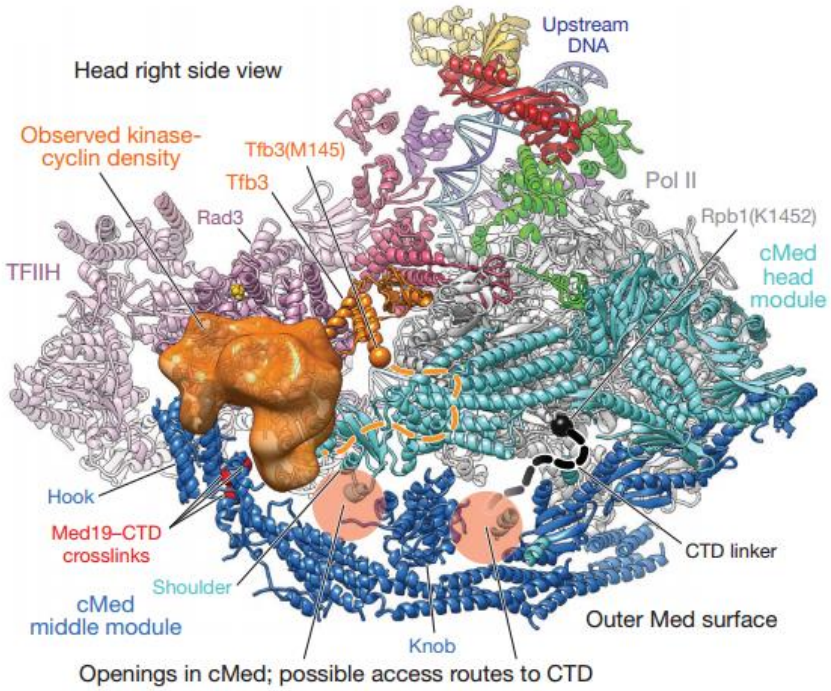

Figure 15: Model for RNA Pol II CTD phosphorylation by TFIIH.
PIC–core Mediator (cMed) structure with the mobile TFIIH Kinase module (Kin28, Ccl1 and Tfb3) in orange. The orange sphere depicts the Tfb3 linker last modelled residue (Met145) in the Tfb3 linker (dotted orange line) to the kinase–cyclin pair, Kin28-Ccl1. The dotted black line represents the CTD linker, with the last ordered residue, Lys1452, as a black sphere. Mediator middle and head modules are represented in blue. Residues of Mediator Med19 subunit that crosslink to the CTD C-terminal end, are in red. Filled transparent red circles indicate two openings at the interface of Mediator head and middle modules (Schilbach *et al.*, 2017).

Interestingly, this study also gives insights on how disease-causing mutations of TFIIH can impact on the conformation of TFIIH. For instance, mutations of XPD implicated in XP, CS and XP combined with CS were mapped on the XPD structure. The mutations were mainly confined to the DNA- or ATP-binding sites of XPD, in agreement with reported defect in helicase activity and NER (Dubaele *et al.*, 2003).

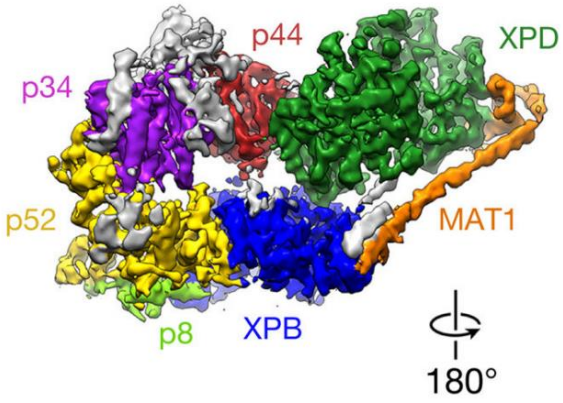

Figure 16: Reconstruction of the human TFIIH by cryo-electron microscopy.
The different subunits of the core TFIIH, with the exception of p62, was unambiguously assigned. The structure also includes the CDK-activating kinase (CAK) component, MAT1. Unassigned density in grey (Greber *et al.*, 2017).

III.3.2 Function in transcription

Three subunits of TFIIH possess catalytic activities: DNA dependent ATPase/helicases Ssl2/XPB (1) and Rad3/XPD (2), the cyclin-dependent kinase Kin28/CDK7 (3) which is associated with the cyclin subunit Ccl1 (Tirode *et al*., 1999).

The ATP-dependent 3'-5' DNA helicase activity of XPB is implicated in the opening of the transcription bubble at the promoter (Douziech *et al*., 2000). An alternative mechanism has been proposed for yeast Ssl2 which uses its translocase activity to push DNA into RNA Pol II leading to gradual DNA unwinding (Grünberg *et al*., 2012).

Recently, it was reported that the depletion of XPB does not lead to major defect in transcription nor transactivation of nuclear receptors, however inhibiting its ATPase activity did (Alekseev *et al.*, 2017). Moreover, mutating helicase motif of XPB lifted the transcription block of XPB ATPase mutant. Therefore, it was proposed that the ATPase activity of XPB is required to overcome the transcription block enforced by its own helicase motifs.

TFIIH kinase module, CAK (CDK activating kinase) in human and TFIIK in yeast, phosphorylates RNA Pol II CTD and this regulates RNA Pol II promoter escape during transcription (Holstege *et al.,* 1997; Ohkuma *et al.*, 1995). Mediator promotes the phosphorylation of the CTD (Kim *et al.*, 1994). The interaction between Mediator Med11 subunit and TFIIH Rad3 subunit is important, *in vivo*, for the TFIIH recruitment to the PIC and for TFIIK presence on promoters and subsequent phosphorylation of serine 5 of RNA Pol II CTD (Esnault et al., 2008). Furthermore, Mediator Cdk8/Cyclin C regulates transcription by targeting the mammalian Cdk7/Cyclin H. The phosphorylation of Cyclin C inhibits the TFIIH ability to activate transcription and also its ability to phosphorylate CTD, which is required for RNA Pol II promoter escape (Akoulitchev *et al.,* 2000).

III.4 The Mediator complex

In the late 1980s, it was observed the transcription activator of one gene can interfere with that of another unrelated gene and that stronger activators inhibit more strongly, independently of their DNA activating domain (Gill and Ptashne, 1988). This phenomenon was termed activator interference in which two transcription activators compete for the same target factor. The addition of a nuclear extract reversed this phenomenon in *S. cerevisiae* (Kelleher *et al*., 1990). These studies led to the identification of the Mediator complex that stimulates transcription activation *in vitro* by bridging transcription activators and the RNA Pol II machinery (Flanagan *et al.,* 1991). Concomitantly, genetic studies identified SRB proteins (Suppressor of RNA polymerase B), which are able to suppress mutations in the CTD of RNA Pol II and are part of a multi-protein complex involved in transcription initiation *in vitro* and *in vivo* (Nonet and Young, 1989; Thompson *et al*., 1993; Hengartner *et al.,* 1995). These SRB proteins were identified as subunits of the Mediator complex. Several biochemical and genetic studies led to the identification of a 25 subunit multi-protein Mediator complex in *S. cerevisiae* and 30 subunits in human (Bourbon *et al.*, 2004). A unified nomenclature for Mediator subunits was proposed for all eukaryotes.

Indeed, Mediator is a highly conserved complex that has been identified in numerous eukaryotes including yeast, mammals, flies and plants. Comparison of Mediator subunits from unicellular eukaryotes to metazoans have led to the identification of a conserved 17 subunit framework around which other subunits have assembled, supporting an ancient eukaryotic origin for Mediator (Bourbon, 2008; Figure 17). The conservation of the primary sequence of Mediator subunits is relatively limited, still, several homology blocks can be defined (Boube *et al.,* 2002; Bourbon, 2008). Moreover, even though the primary sequence has diverged, the general structure of Mediator is conserved in eukaryotes.

III.4.1 Mediator composition and structure

Mediator is large multi-subunit complex with conformational flexibility and relatively low cellular abundance, making structural studies challenging. Therefore, to date the complete structure of Mediator at high resolution has not been obtained.

Electron microscopy experiments showed a modular structure for the yeast and mammalian Mediator complexes (Asturias *et al.*, 1999; Dotson *et al.,* 2000). In addition, it was showed that Mediator had a compact conformation when alone but in the presence of RNA Pol II, it had a more extended conformation in mammals and yeast, and hence indicating a conservation in structure (Asturias *et al*., 1999). This study was also the first evidence of conformational variability of the Mediator complex. Further analysis defined a head, middle and tail modules (Figure 18). The head module appears to be the most structurally conserved compared to the tail and middle modules. Consistently, subunits that are not conserved between yeast and mammals are located in the tail module (Dotson *et al*., 2000). The Mediator complex is also composed of a fourth kinase (Cdk8) module that can dissociate from the rest of the Mediator complex. It was found that the interaction between

the kinase module and the middle module obstructs Mediator interaction with RNA Pol II, indicating that a combination of conformational changes and competitive interactions is required for Mediator function (Tsai *et al*., 2013). Therefore, the Mediator complex is assembled in modules and the different components have been proposed to have different functions (refer to "Functions of Mediator" section).

Biochemical and genetic studies established an interaction network between the different subunits of the Mediator complex in *S. cerevisiae,* in agreement with the previously described general topology of the Mediator complex comprising a head, middle, tail and kinase module (Kang *et al.*, 2001; Guglielmi *et al.*, 2004). For example, a link between the head and middle modules was described via the head Med17 subunit and middle Med21 subunit. Moreover, Med14 has been, recently, described as a core structural component of the complex linking the head, middle and tail modules (Wang *et al.,* 2014; Tsai *et al*., 2014).

A 15-subunit core Mediator was reconstituted in *S. cerevisiae,* which was functional in transcription and active in stimulating CTD phosphorylation (Plaschka *et al.*, 2015). The core Mediator consists of all conserved subunits including the essential head and middle subunits, Med14 and Med19 (non-essential head subunit). Med14 subunit was required to bind the head and middle subunits, suggesting a key role for Med14 in Mediator structure and function. Recently, a high-resolution crystal structure of the core Mediator was obtained in the fission yeast *S. pombe* (Nozawa et al., 2017; Figure 19), which is the largest high-resolution sub-complex of Mediator characterised to date. This structure revealed the organisation of head and middle modules within the core Mediator, the intricate folding and organisation of the subunits within the modules and the positioning of Med14 'backbone' relative to the modules.

Altogether, recent high-resolution structural data of Mediator sub-complexes has helped better understand its organisation, which can aid in better understanding the impact of its conformational changes of Mediator's function.

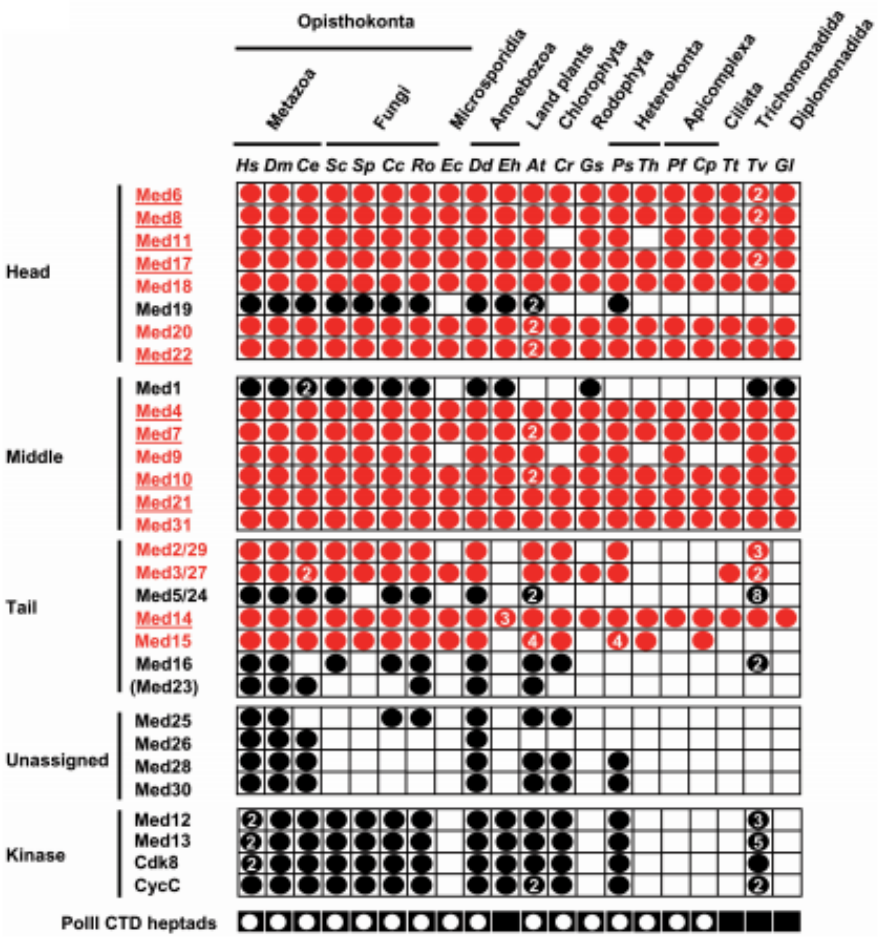

Figure 17: Conservation of Mediator subunits in eukaryotes (Bourbon, 2008).
Essential subunits are underlined. Every dot represents one homolog of that subunit discovered. If more than one homolog, the number is indicated in the dot. In red are represented the most conserved subunits.

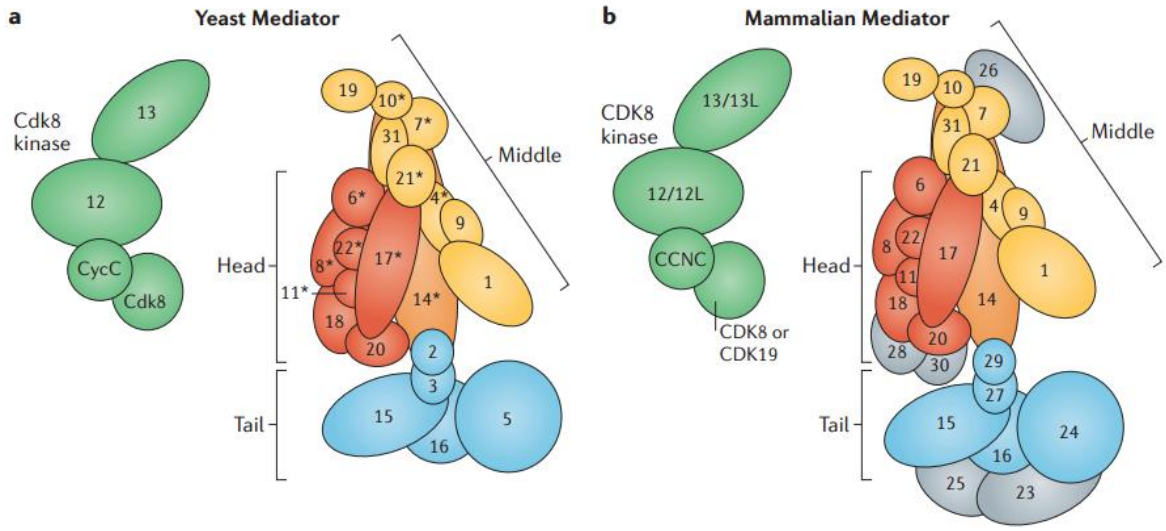

Figure 18: Organisation and subunit composition of the Mediator complex in (a) yeast and (b) mammals
(Soutourina, 2018).

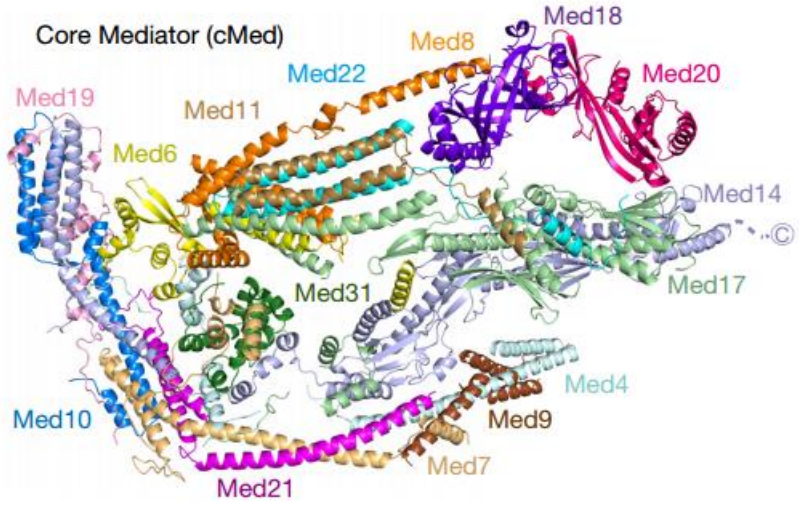

Figure 19: Crystal structure of S. pombe core Mediator.
Ribbon model of the cMed structure refined at 3.4 Å resolution with the 15 subunits shown in different colours. (Nozawa et al., 2017)

III.4.2 Functions of Mediator complex

III.4.2.1 Transcription activation

RNA Pol II transcription is regulated namely by the binding of transcription activators on enhancers (enhancer or UAS (Upstream Activating Sequence)) that activate specific genes. The Mediator complex acts as a physical bridge and transmits the signal from transcription activators to the RNA Pol II machinery. In line with Mediator role in transcription activation, numerous interactions have been found between transcription activators and Mediator and between RNA Pol II and Mediator. Consistently, artificial recruitment of Mediator results in a strong transcriptional activation *in vitro* (Gaudreau *et al*., 1998) and *in vivo* (Barberis *et al.,* 1995). Moreover, Mediator has been shown to physically interact with transcriptional activators in yeast and in human cells (Eychenne *et al*., 2017). However, Mediator does not bind directly to the DNA molecule.

In yeast, it has been proposed that Mediator contacts the activators through the tail module, highlighted by mutations in the tail module which selectively abolish transcription stimulation by activators. For example, deletion of tail subunit Med2 in yeast resulted in a decrease in inducible gene expression genome-wide but had a minor effect on basal transcription *in vivo*, indicating a gene-specific implication of Med2 in transcription activation (Myers *et al.,* 1999). Moreover, structural experiments by NMR spectroscopy showed that tail Med15 subunit contains a KIX domain that is required for interaction with fatty acid gene activator (Thakur *et al.,* 2009). However, Mediator interaction with activators is not restricted to the tail module, as demonstrated by the binding of head Med17 subunit to Gal4 transcriptional activator (Koh *et al.,* 1998).

In mammals, the discovery of Mediator itself was through its interaction with nuclear receptors (Fondell *et al*., 1996). Tail subunits or subunits that are close to the tail module have been implicated in the interaction with transcription activators. Indeed, Med15 tail subunit has a domain that presents similarity to the KIX domain is implicated in interaction with sterol regulatory element binding protein (SREBP) family of transcription activators (Yang *et al*., 2006). Med1, the middle module subunit, has been shown to interact with nuclear receptors, for instance, receptors that regulate energy metabolism and regeneration in liver cells (Jia *et al.,* 2015). Med1 is part of the middle module that is in close proximity to the tail module as illustrated in Figure 18.

The intrinsic flexibility of Mediator is key to its function. Electron microscopy and 3-D reconstruction show that there is a conformation difference between free human Mediator and Mediator bound to transcription activators, suggesting that an activator-induced conformational change of Mediator can potentiate transcription activation. In addition, another study showed that other transcription co-activators interact with activator-bound Mediator but not with free Mediator which suggests that activator binding triggers new interactions between Mediator and co-activators (Ebmeier and Taatjes, 2010).

Therefore, Mediator is recruited by transcription activators which leads to a conformational change in Mediator, important for Mediator interaction with other co-activators and for transcription activation.

Towards the core promoter side, Mediator contacts the RNA Pol II transcription machinery. One point of contact is RNA Pol II itself and numerous subunits have been identified to be important for this interaction. Moreover, Mediator in complex with RNA Pol II was found to be one of the major forms of Mediator detected (Liu *et al.,* 2001).

Electron microscopy studies have been crucial in visualising RNA Pol II and Mediator interaction and also to demonstrate the RNA Pol II-induced rearrangement in Mediator. Indeed, Asturias e*t al.,* 1999 gave the first evidence of conformational variability of the Mediator complex, using electron microscopy, in particular the remarkable structural changes that occurred when Mediator contacts RNA Pol II. In continuation with this work, free Mediator structure was compared to that of Mediator bound to RNA Pol II using cryo-electron microscopic reconstruction in yeast (Cai *et al*., 2009). The results showed that the Mediator complex is intrinsically flexible allowing modular reorganisation to create a network of contacts with RNA Pol II. This structural rearrangement shows parallels to the structural reorganisation triggered by human Mediator interaction with a nuclear receptor. In line with the structure similarity showed between yeast and human Mediator despite low sequence homology (Cai *et al*., 2009).

A role for Mediator in transcription repression has also been proposed. Studies showed that some genes are upregulated in certain Mediator mutants namely mutations of kinase module subunits (Holstege et al., 1998; van de Peppel *et al.,* 2005; Koschubs *et al.,* 2009). However, very less data is available on the mechanisms behind the observed repression.

III.4.2.2 Mediator as a GTF (General Transcription Factor)

General transcription factors are characterised by their requirement for global transcription of all genes and the formation of the PIC. Mediator has been proposed to be a general transcription factor as it is capable to stimulate, *in vitro*, basal and activated transcription in human and yeast (Baek *et al.*, 2006; Takagi and Kornberg, 2006). Basal and activated transcription are *in vitro* concepts as *in vivo,* it is difficult to abolish the effect of transcription activators. For instance, one gene may be under the dependence of more than one activator. Hence, purified proteins and *in vitro* transcription system have been used to study the basal transcription.

To study basal transcription *in vivo*, an artificial system, termed activator bypass, was constructed in yeast (Lacombe *et al.,* 2013). This system allows a transcription activator-independent recruitment of the basal transcription machinery. The general transcription factor (TFIIB) was fused to a human transcription factor (RFX), which does not have an activity in yeast. The binding site of RFX was introduced upstream of a gene promoter, allowing the recruitment of TFIIB on the promoter. The authors showed that in this artificial

system, Mediator could be recruited independently of transcription activators to the PIC, via its interaction with other GTFs and RNA Pol II (Lacombe *et al.,* 2013).

Moreover, *in vivo*, Mediator cooperates with other GTF (TFIIB, TFIID and TFIIH) and RNA Pol II to promote the assembly of the PIC. The head and middle modules of Mediator have been implicated in regulating the formation of the PIC *in vivo* (Soutourina, 2018).

In addition, Mediator is required for global transcription of RNA Pol II transcribed genes which is a characteristic of GTF. For instance, mutation of *med17* lead to similar level of transcription impairment as RNA Pol II *rpb1* mutant (Holstege *et al.*, 1998). *In vitro* analysis showed that this mutant was defective in basal transcription stimulation, which was restored by addition of purified Med17 (Takagi and Kornberg, 2006). Consistently, *in vivo* experiments showed a direct interaction between Rpb3 subunit of RNA Pol II and the Med17 head subunit of Mediator (Soutourina *et al*., 2011). This interaction was showed to be essential for global RNA Pol II recruitment *in vivo*. Ten yeast Mediator subunits (Med4, Med6, Med7, Med8, Med10, Med11, Med14, Med17, Med21 and Med22) have been now identified as essential for cell viability.

III.4.2.3 Regulation of RNA Pol II promoter pausing

In metazoans, Mediator has been implicated in a post-initiation regulation of promoter-paused RNA Pol II. Indeed, genome-wide data of RNA Pol II showed an enrichment near the TSS in mammals and Drosophila (Kwak and Lis, 2013). NELF (negative elongation factor) and DSIF (DRB sensitivity-inducing factor) have been implicated in RNA Pol II pausing around 20 to 60 nucleotides from the TSS. Phosphorylation by P-TEFbs (Positive Transcription Elongation Factors) of DSIF, NELF and the serine 2 of the CTD of RNA Pol II is required for the release of paused RNA Pol II. P-TEFb is recruited as part of the Brd4 (bromodomain-containing protein) and SEC (Super Elongation Complex) complexes by Mediator (Chen *et al*., 2018). Indeed, it has been reported that the metazoan-specific MED26 subunit of Mediator interacts with TFIID during formation of the pre-initiation complex and then exchanges TFIID for PTEFb-containing complexes to facilitate RNA Pol II's transition into productive elongation (Takahashi *et al*., 2011).

To note that RNA Pol II genome-wide distribution profile in the budding yeast does not show an accumulation near the TSS, suggesting that promoter pausing does not occur in yeast or that it is quickly resolved (Steinmetz *et al.*, 2006).

III.4.2.4 Mediator in DNA looping and chromosome compaction

Transcription factors need to transmit regulatory signal to the transcription machinery, they are however localised on regulatory regions that can be far away from the core promoter. Transcription factors hence bind co-regulators such as Mediator that can in turn bind to the RNA Pol II transcription machinery. This indicates a DNA loop formation for proper transcription regulation.

It was reported that Mediator and cohesin, an architectural protein conserved in eukaryotes, physically and functionally connect enhancers and core promoters in murine embryonic stem cells (Kagey *et al.,* 2010). Mediator interacts with cohesin that can form rings connecting the two DNA regions. Mediator and cohesin co-occupy different enhancer and promoter regions in different cells providing cell-type specific loops that regulate gene expression. However, it has recently been reported that DNA looping in erythroid cells can occur independently of Mediator and cohesin and requires lineage specific factors (Krivega and Dean, 2017).

Recently, Mediator has been implicated in chromosome folding in yeast (Hsieh *et al.,* 2015). Indeed, it was showed that deletion of *med1* causes a global loosening of chromosome structure by micro-C. This technique uses micrococcal nuclease to fragment chromatin to generate nucleosome resolution chromosome folding maps. This implication of Mediator in chromatin compaction is interesting as afore mentioned a role for Mediator and cohesin has been described in local chromosome folding in murine embryonic stem cells (Kagey *et al.*, 2010), suggesting that this role of Mediator in chromosome domain compaction may be conserved.

III.4.2.5 Role in telomere maintenance

Mediator is essential for RNA Pol II transcription but it is also implicated in other cellular processes such as telomere maintenance.

Telomeres are repetitive sequences that make up the end of linear chromosomes. Telomeres are in complex with proteins that shelter telomeres from degradation or being processed by the DNA repair machinery. Genes near the telomeric regions can be transcriptionally repressed by an epigenetic mechanism known as telomere position effect (TPE) and this silencing is dependent on Sir2-4 (Silent Information Regulator proteins 2-4) (Loney *et al.,* 2009). Sir2 is an evolutionary conserved histone deacetylase that is required for silencing in yeast. It was demonstrated that Sir2 is implicated in establishing a histone H4 lysine 16 acetylation gradient, from a hypoacetylated state near the telomeric regions to a hyperacetylated state in more distant regions (Kimura *et al.,* 2002). Sas2 histone acetyltransferase antagonises Sir2 activity which is required for gradient formation, shielding against gene silencing. The H4 Lys 16 acetylation gradient also influences the replicative lifespan of cells.

The Mediator subunits Med3 and Med15 were shown to affect TPE in yeast (Suzuki *et al.,* 1994; Piruat *et al.*, 1997). Indeed, deletion of *med15* decreased the telomere length and derepressed the subtelomeric *URA3* gene (Suzuki *et al*., 1994). Similarly, deletion of *med3* caused silencing of *URA3* gene (Piruat et al., 1997). However, deletion of either *med3* or *med15* did not affect the repression of the mating-type loci. Mediator role in TPE was consolidated by the demonstration that Mediator binds the tail of histones H3 and H4 and that Mediator interaction was specifically affected by the acetylation at histone H4 lysine 16 (Zhu *et al.*, 2011). Furthermore, a negative correlation was observed between acetylation of

H4 lysine 16 and Mediator occupancy *in vivo* by ChIP on chip assay. Further analysis showed that deletion of Mediator tail subunits reduced Sir protein binding which results in increased acetylation at H4 lysine 16 and compromised telomere silencing (Peng and Zhou, 2012), indicating that Mediator can participate in regional regulation of transcription via modulation of chromatin structure. The conservation of Mediator role in telomere maintenance remains to be investigated in other eukaryotes, as it involves evolutionary conserved proteins.

III.4.2.6 Mediator and mRNA export

Messenger RNAs are translated in the cytoplasm and hence have to be transported out of the nucleus through NPCs (Nuclear Pore Complexes). NPCs, composed of nucleoporins, control nucleocytoplasmic traffic of macromolecules. Apart from its transport function, NPCs also play an evolutionarily conserved role in gene expression regulation and chromosome attachment sites (Ibarra and Hetzer, 2015). NPC bind a conserved TREX-2 complex (Transcription-coupled EXport) and can, namely, influence its mRNA and gene expression function. A structural and functional link was established between TREX-2 and Mediator in yeast *in vivo* (Schneider *et al.*, 2015). It was demonstrated that Mediator Med31-Med7 subunits (middle module) bind a conserved region of TREX-2 subunit Sac3. Furthermore, the functional characterisation of this interaction, by monitoring the localisation of genes relative to the NPC, showed that Mediator-Sac3 interaction was required for targeting genes to NPC. A role in mRNA export and gene regulation was also suggested. Sac3 can also modulate the serine 5 phosphorylation level of the RNA Pol II CTD as demonstrated by the deletion of *sac3* which leads to an increase of the ser5 phosphorylated form of RNA Pol II CTD and a decrease of Mediator-RNA Pol II interaction. Moreover, the Sac3 can influence the recruitment of Cdk8 (kinase module) to Mediator and it was proposed that, *in vivo*, Sac3 and Cdk8 have a joint regulatory effect on RNA Pol II CTD phosphorylation.

III.4.2.7 Role in DNA repair

As discussed in the previous chapter, NER is closely linked to transcription, and recently, the laboratory has uncovered a novel role for the Mediator complex in NER via a functional interaction with 3' endonuclease Rad2, in *S. cerevisiae* (Eyboulet *et al*., 2013). A physical interaction between Med17 subunit of Mediator and Rad2 was shown by two-hybrid assay. The interaction between the Mediator complex and Rad2 was further confirmed by co-immunoprecipitation experiments. An *in vitro* interaction between XPG (homolog of Rad2) with human Med17 was also reported (Kikuchi et al., 2015). Furthermore, it was observed that Rad2 was present on UAS (Upstream Activating Sequence) and on the transcribed regions of RNA Pol II-transcribed genes. On the UAS, there was a strong correlation between Mediator and Rad2. It was showed that there was a strong decrease of Rad2 occupancy on transcribed regions in an RNA Pol II mutant, *rpb1-1,* in which transcription is rapidly stopped. The presence of Rad2 on the transcribed regions was hence dependent on RNA Pol

II transcription. Moreover, *med17* mutants that were UV-sensitive in a GG-NER background were identified. In these UV-sensitive mutants, a decrease of Rad2 on transcribed regions, and a concomitant decrease of Rad2-Mediator interaction were observed. Altogether, these results suggest that Mediator facilitated Rad2 recruitment to RNA Pol II-transcribed regions in NER.

In yeast, Rad2 implication in transcription was proposed for galactose-inducible genes (Lee *et al*., 2002). However, in our study, we did not observe any effect of *rad2* deletion on transcription of inducible GAL1 gene or constitutively expressed genes (Eyboulet *et al*., 2013). Moreover, no growth phenotypes, except UV-sensitivity, or transcriptional defects were observed in *rad2* deletion strain. Therefore, it was proposed that Rad2 does not play a major role in yeast transcription.

In human, XPG was reported to be required for transcription of nuclear receptor dependent genes (Ito *et al*., 2007). It was shown that XPG and TFIIH formed a stable complex, which was required for transactivation of nuclear receptors. Moreover, XPG recruited on promoters and terminator of nuclear receptor gene was required for DNA breaks and DNA methylation, two events needed for the recruitment of chromatin organiser CTCF (CCCTC binding factor). Subsequently leading to the formation of DNA looping between promoter and terminator which allows efficient transcription (Le May *et al*., 2010; 2012).

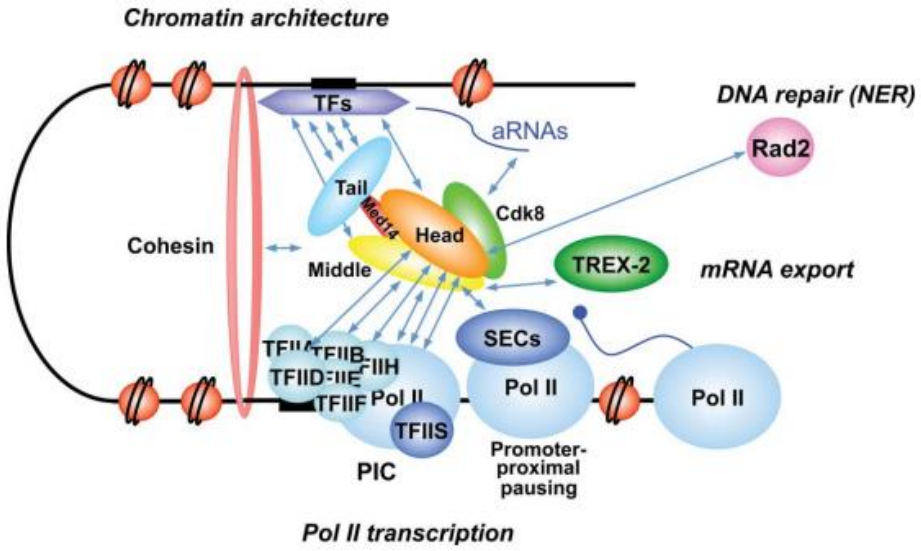

Figure 20: Mediator interactions with nuclear proteins.
Mediator functions are closely related to its physical and functional interactions with nuclear proteins. This schema represents a combined view from different studies in yeasts and metazoans, focusing on RNA Pol II transcription: Transcription factor (TF), PIC assembly and promoter proximal pausing. The interactions with proteins involved in chromatin architecture, mRNA export or DNA repair are also shown. Interaction identified between Mediator and ncRNA (non-coding RNA) are shown. In metazoans, Mediator contacts with SECs (Super Elongation Complexes), cohesin and ncRNAs were reported. Mediator modules are shown in different colours with Med14 (in red) linking the three main modules (head, middle and tail) (Eychenne *et al*., 2017).

III.4.3 Mediator genomic occupancy and functional interplay with RNA Pol II

In vivo genome-wide occupancy profiles of Mediator were obtained by ChIP-seq and ChIP on chip (Chromatin immunoprecipitation followed by sequencing). These experiments showed that Mediator predominantly occupies UAS regions (Upstream Activating Sequences), upstream of the core promoter in *S. cerevisiae* (Andrau et al., 2006, Eyboulet et al., 2013). Moreover, the genomic distribution of the different Mediator modules seem uniform. However, the colocalisation of the kinase module with the other Mediator modules does not imply that this occurs simultaneously in individual cells. To resolve this point, sequential ChIP (re-ChIP) was performed in which a first antibody is used to immunoprecipitate a protein and this immunoprecipitate is subjected to another immunoprecipitation step with a different antibody. Hence, the DNA regions that concomitantly bind the two proteins are obtained. Re-ChIP results indicate that the kinase module associates transiently with Mediator on the UAS (Andrau et al., 2006). Furthermore, Mediator was detected on some transcribed regions of genes, particularly in actively transcribed genes, but it was showed that this signal is artefactual in *S. cerevisiae* (Eyboulet et al., 2013; Jeronimo and Robert, 2014). Indeed, the use of negative controls such as performing ChIP experiments using an untagged strain or the use of non-specific antibodies showed similar signals in the transcribed regions. It was therefore proposed that the observed Mediator presence within

the gene bodies was not specific and due to an open chromatin conformation around active genes. Moreover, no strong signal of Mediator on the core promoter regions has been obtained even though Mediator has been implicated in the recruitment of RNA Pol II and the assembly of the PIC which occurs on the core promoter.

Therefore, in yeast, a clear picture of Mediator genomic presence relative to its function was absent. Two groups addressed this question by thoroughly investigating the occupancy of Mediator *in vivo* (Wong et al., 2014; Jeronimo and Robert, 2014). Similar results were obtained using different conditional mutants of TFIIH Kin28 subunit. TFIIH is a general transcription factor whose kinase Kin28 phosphorylate serine 5 of the RNA Pol II CTD important for RNA Pol II promoter escape and the initiation-elongation transition. Therefore, inhibition of the kinase activity of Kin28 leads to a decrease of RNA Pol II going into elongation. It was demonstrated that in *kin28* mutants, there was a drastic decrease of RNA Pol II on the coding regions and a stabilisation on the 5' region of genes. Interestingly in these mutants, there was a stabilisation of Mediator on the UAS and also on the core promoter. No other CTD kinase mutants affected Mediator's genomic occupancy. Based on these results, a model was proposed in with Mediator contacts the core promoter via an interaction with RNA Pol II, controlled by the serine 5 phosphorylation activity of Kin28 (TFIIH).

These two laboratories then addressed the question of Mediator's compositional change *in vivo* in yeast (Jeronimo et al., 2016; Petrenko et al., 2016). The authors showed that the tail module is indeed required for the interaction with activators but tail-less Mediator could still interact with core promoters. Occupancy of Mediator subunits belonging to the four modules was compared in wild-type and *kin28* conditional mutants and it was found that the kinase module does not associate with the core promoter contrary to all the other Mediator modules. Furthermore, a Mediator lacking the kinase module can still associate to the core promoter. Finally, using sequential ChIP approach, it was shown that a single Mediator complex bridges the enhancer and core promoter region. Altogether these results suggest that the Mediator complex undergoes a compositional change during transcription activation and the kinase module dissociates to permit association of Mediator with RNA Pol II.

Moreover, the fact that one Mediator complex contacts both the enhancer and promoter regions is in favour of the previously proposed role of Mediator in DNA looping via an interaction with cohesin (Kagey *et al.,* 2010; refer to "Mediator in DNA looping and chromosome compaction" paragraph).

III.4.3.1 Mediator in development and diseases

The implication of Mediator in human diseases is rather recent and has been, in part, possible with the development of genotyping and sequencing techniques and the establishment of animal models. Mediator has been implicated in the regulation of genes implicated in cell growth, differentiation and tissue development pathways. Examples of

Mediator's role in these pathways will be discussed as mutations or modification in the expression of Mediator subunits can lead to dysregulation of these pathways and development of pathologies.

Studies on animal model were conducted to get insights into Mediator's role in gene regulation in development employing techniques such as RNA interference or gene overexpression. In mice, knock out strains, in which the gene of interest is deleted, can be constructed via homologous recombination.

It was shown that KO of some Mediator subunits can lead to embryonic lethality in mice, though the stage of development leading to death varies. For illustration, the KO of *MED1* subunit leads to death in early gestational stage E11.5 (Embryonic day 11.5) and the null mutants display cardiac defects, impaired neuronal development with extensive apoptosis (Ito *et al.*, 2000). On the other hand, *Med21* null animals die at blastocyst stage, indicating that MED21 is essential for viability and early embryonic development and hence, the animal survival till blastocyst stage was due to maternal stock of the protein. Moreover, a mutagenesis screen identified a mutation in MED31 that leads to degradation of the protein (Risley *et al.*, 2010). *Med31* mutant embryos have fewer proliferating cells in rapidly developing regions such as forelimb buds. Likewise cultured embryonic fibroblasts, with *MED31* mutation, presented severe proliferation impairment.

It was also demonstrated that master regulators, which are transcription factors that can trigger lineage-specific programs, recruit Mediator to carry out their transcriptional programs. For example, in mice, it was shown that Mediator functions via its MED1 subunit, as a co-activator for GATA-1 to determine blood cell lineage development (Stumpf *et al*., 2006). Moreover, Mediator MED23 subunit presence or absence, in mesenchymal mouse stem cells, can oppositely regulate genes implicated in adipocyte differentiation and smooth muscle cells differentiation (Yin *et al*., 2012), thereby playing antagonistic roles in cell fate determination. Furthermore, Mediator has been proposed to be implicated in the formation of super-enhancers, which are clusters of enhancers that are densely occupied by master regulators and Mediator (Whyte *et al.*, 2013). Moreover, it was shown that reduced levels of master regulators and Mediator lead to reduced expression of super-enhancer-associated genes. Therefore, the ability of Mediator to integrate signals from multiple master regulators supports the notion of Mediator being a master coordinator for developmental gene regulation.

As illustrated above, Mediator plays a key role in gene regulation in various developmental processes, therefore mutations or defect in expression of some Mediator subunits severe have been associated with developmental pathologies and cancer. Table 3 summarizes different pathologies in which the Mediator complex has been implicated.

Mutations in Mediator subunits can lead to the development of several pathologies. For example, congenital heart diseases have been associated with mutations in Mediator subunits. *MED15* is deleted in patients with DiGeorge syndrome, who present

cardiovascular defects (Berti *et al.*, 2001). Another example, is the implication of Mediator mutations in neurological disorders, for example, a missense mutation in *MED23* has been associated with non-syndromic autosomal recessive intellectual disability (Hashimoto *et al.*, 2011). This mutation alters the interaction between transcription activators and Mediator, impairing the response of JUN and FOS immediate early genes (IEGs) to serum mitogens.

Examples of diseases where Mediator subunit expression level is modified include lung and breast cancers (Yin and Wang, 2014). Indeed, an overexpression of MED23 was observed in lung cancer patients with overactive Ras oncogene activities, whereas a lower expression of MED23 predicts better survival in Ras-active cancer patients. Therefore, MED23 is a potential diagnostic marker as well as a therapeutic target. In breast cancer tissues from patients, MED15 was overexpressed and was correlated with a hyperactive TGFβ (transforming growth factor β) signalling. In conclusion, Mediator seems to control different signalling pathway implicated in cancer development.

It is noteworthy that Mediator subunits have been reported to interact with viral proteins and can be potential therapeutic targets. For instance, an interaction between Mediator subunit MED8 and NSs, a non-structural protein, of Bunyamwera virus has been linked to the inhibition of host transcription and interferon response. Moreover, deleting the domain of NSs required for interaction with MED8 reduced the ability of the recombinant virus to carry out these two processes (Léonard *et al.*, 2006). In addition, Mediator association with the herpes simplex transactivator VP16 is required for the latter's activation *in vitro* and in mammalian cells (Mittler *et al.*, 2003).

The implication of Mediator in these different nuclear processes places the complex at the heart of many diseases and targeting specific Mediator subunits have been proposed in therapy. For instance, Mediator is part of super-enhancers which predominantly control gene expression of tumour suppressive genes. Indeed, it has been shown that the inhibition of the kinase module of Mediator enhanced the expression of tumour suppressive genes in AML (Acute Myeloid Leukaemia) (Soutourina, 2018). Moreover, targeting the interaction between specific transcription factors and Mediator can disrupt expression of specific genes. One such example is a drug resistance pathway dependent on Pdr1 (Pleiotropic drug resistance) transcription factor. The inhibition of the Mediator-Pdr1 interaction disrupted expression of genes dependent on Pdr1 and restored sensitivity to anti-fungal drug (Nishikawa *et al.*, 2016). Therefore, Mediator is a potential therapeutic target in fungal infections as well.

Disease/Disorder	Mediator Subunit	Molecular Disposition
Neurodevelopmental disorders		
X-Linked Mental Retardation Syndromes FG syndrome	MED12	missense mutation (R961W)
Lujan syndrome	MED12	missense mutation (N1007S)
Infantile Cerebral and Cerebellar Atrophy	MED17	missense mutation (L371P)
Congenital Retinal Folds, Microcephaly, and Mental Retardation	CDK19	haploinsufficiency (pericentric inversion)
Non-syndromic autosomal recessive intellectual disability	MED23	R617Q
Cardiovascular disorders		
Transposition of the Great Arteries (TGA)	MED13L	haploinsufficiency (chromosomal translocation)
	MED13L	missense mutation (E251G; R1872H; D2023G)
DiGeorge Syndrome	MED15	deletion
Behavioral disorders		
Schizophrenia, Psychosis	MED12	polymorphism (HOPA12bp; HOPA−15bp)
Cancer		
Bladder	MED19	overexpression
Breast	MED1	overexpression (with/without gene amplification)
	MED19	overexpression
	MED28	overexpression
	MED15	overexpression
Colon	MED28	overexpression
	CDK8	overexpression(gene amplification)
Lung	MED1	reduced expression
	MED23	overexpression
	MED19	overexpression
Melanoma	MED1	reduced expression
	MED23	loss of heterozygosity (chromosomal deletion)
	CDK8	overexpression (secondary to mH2A loss)
Pancreas	MED29	overexpression (gene amplification)
Prostate	MED1	overexpression (without gene amplification)
	MED28	overexpression

Table 3: Molecular Disposition of Human Mediator Subunits Linked to Pathological Disorders
(Spaeth *et al.*, 2011; Yin and Wang, 2014)

IV. Basis of project and results summary

IV.1 Basis of project: Mediator links transcription and NER via a functional interaction with Rad2

A recent work in our laboratory revealed a novel role for the Mediator complex in NER via a functional interaction with the 3' endonuclease, Rad2, in *S. cerevisiae* (Eyboulet *et al.,* 2013). Mediator is a transcriptional co-regulator that is generally required for RNA Pol II transcription in all eukaryotes (refer to section "Mediator complex" for more details).

Briefly, a physical interaction between Mediator and Rad2 was shown by two-hybrid and co-immunoprecipitation experiments. Moreover, the genome-wide occupancy of Rad2 was highly correlated with that of Mediator on the regulatory regions (UAS) of RNA Pol II-transcribed genes. Furthermore, Rad2 occupancy of RNA Pol II-transcribed genes was shown to be transcription-dependent. However, no major role in yeast transcription for Rad2 was observed. In addition, the UV-sensitivity phenotype of *med17* mutants was correlated with a reduced occupancy of Rad2 on RNA Pol II-transcribed regions and a concomitant decrease in Mediator-Rad2 interaction.

Based on these results, a novel role for Mediator in DNA repair was proposed in which Mediator facilitates the recruitment of Rad2 on transcribed regions, hereby consolidating the link between transcription and NER. Our general objective is to uncover the molecular mechanisms underlying the link between transcription and DNA repair, and more particularly the novel link between the Mediator complex and the NER machinery.

IV.2 Project aims and result summary

The functional link between Rad2/XPG and Mediator discovered in the laboratory (Eyboulet *et al*., 2013), constitutes the basis of my PhD project. My work aimed at investigating the functional interplay between Mediator and the NER machinery.

First, we sought to better define the functional link between Rad2, Mediator and RNA Pol II. To address this purpose, we used *kin28* TFIIH, *rpb9* RNA Pol II and *med17* Mediator mutants. I was particularly involved in the characterization of Rad2, Mediator and RNA Pol II interplay in *kin28* TFIIH mutant in which Mediator is stabilized on the core promoter and RNA Pol II promoter escape is affected. Genomic analysis of Rad2, Mediator and RNA Pol II binding to the chromatin, in all three mutants, led us to propose a model where Rad2 shuttles between Mediator on regulatory regions and RNA Pol II on transcribed regions, through a transient Mediator/RNA Pol II intermediate formed on the core promoter. Our results also suggest that Mediator functions in transcription and DNA repair are closely related (refer to "Article 1").

Second, we investigated whether the functional link between Mediator and Rad2 could be extended to other proteins of the NER machinery. This led to the identification of new

physical interactions between Mediator and other NER proteins namely the 5' endonuclease dimer, Rad1/XPF and Rad10/ERCC1, and the TC-NER specific factor, Rad26/CSB, in the absence of UV stress. Similarly to Rad2, we demonstrated that Rad1 and Rad10 do not have a major role in yeast transcription. To further study the functional link between Mediator and the NER machinery, we obtained the genomic distribution profiles of different NER proteins by ChIP-seq. It was found that a portion of promoter regions are co-occupied by Mediator and these NER proteins. Further bioinformatics analyses will allow us to characterize the different genomic regions according to the presence of Mediator and NER proteins. Using *rpb1-1* RNA Pol II mutant in which transcription is rapidly stopped after a shift to the non-permissive temperature, we showed that the presence of these NER proteins on RNA Pol II-transcribed genes is dependent on transcription. We investigated the change in Rad1, Rad10 and Rad26 genomic occupancies when Mediator is stabilized on promoter regions and RNA Pol II promoter escape is hindered and compared it to Rad2. Our results showed that the relationship between Mediator and these NER proteins is more complex than for Mediator and Rad2.

We have observed that NER proteins (Rad1, Rad10, Rad26 and Rad2) interact with Mediator in the absence of genotoxic stress. We showed that post-UV irradiation, Mediator-NER proteins interactions persisted with no detectable change. Furthermore, we investigated whether chromatin binding profiles of our proteins of interest were changed after UV stress.

In conclusion, we have strengthened the link between Rad2/XPG, Mediator and RNA Pol II. Moreover, we have provided results showing that the link between Mediator and the NER machinery can be extended to other NER proteins namely Rad1/XPF, Rad10/ERCC1 and Rad26/CSB proteins.

Results

I. Functional interaction between RNA Pol II, Mediator and Rad2 in *S. cerevisiae*

Our laboratory has been working for years now on the Mediator complex, a well-characterized transcription co-regulator necessary for RNA Pol II transcription, and has helped in better characterizing its role in transcription. Indeed, many interactions between Mediator and the basal transcription machinery have been found namely with TFIIH, TFIIB and RNA Pol II *in vivo*, important for the recruitment of these factors to promoters for transcription initiation (Esnault *et al.*, 2008; Soutourina *et al.*, 2011; Eychenne *et al.,* 2016).

Moreover, the laboratory discovered a role for Mediator in NER via a functional link with NER protein Rad2 in *S. cerevisiae* (Eyboulet *et al.,* 2013). Analysis of Rad2 and Mediator genomic occupancies showed a strong correlation on regulatory regions of RNA Pol II transcribed genes. However, Rad2 is also present on the transcribed regions unlike Mediator. Moreover, it was found that both Mediator and Rad2 interact with RNA Pol II which is localized on the transcribed region (Soutourina e*t al*., 2011; Eyboulet *et al.*, 2013). RNA Pol II is the main component of the transcription machinery as well as the first complex in TC-NER that encounters the DNA damage. Hence, there is an interaction network involving RNA Pol II, Mediator and Rad2. We aimed to better characterise the interplay between these factors, in particular we investigated how Rad2 recruited on the regulatory regions is loaded on transcribed regions. To address this question, *kin28* TFIIH, *rpb9* RNA Pol II and *med17* Mediator mutants were used. The results of this study are presented in the paper hereafter “Article 1”.

In this project, my work consisted of analysing the effect of *kin28* mutation on the functional interplay involving RNA Pol II, Mediator and Rad2. It was previously showed that inhibition of the kinase activity or nuclear depletion of Kin28 (TFIIH) hinders RNA Pol II promoter escape allowing the stabilization of the transient association of Mediator with the PIC on the core promoter (Wong *et al.*, 2014; Jeronimo and Robert, 2014, Jeronimo *et al*., 2016; Petrenko *et al.,* 2016).

In the laboratory, a *kin28 ts* (thermo-sensitive) was used and a shift from 25°C to 37°C considerably decreased RNA Pol II CTD phosphorylation that regulates its promoter escape. Therefore, we sought to determine how Rad2 occupancy changes, by ChIP-seq, when the presence of Mediator is stabilized on core promoters and RNA Pol II promoter escape is hindered. We showed that there was a global decrease in RNA Pol II occupancy on transcribed regions. A less pronounced decrease was observed at the 5’ side of genes, by comparing the occupancy ratio of wild-type and *kin28 ts* mutant. These results are in agreement with RNA Pol II CTD phosphorylation defect that is associated with an impaired promoter escape. In comparison to the wild-type, we observed an increase of Mediator occupancy on UAS as well as a very strong enrichment on core promoters, suggesting the stabilization of a Mediator-containing intermediate on the core

promoters. Interestingly, there were distinct changes in Rad2 occupancy in *kin28 ts* mutant compared to the wild-type. Rad2 occupancy was decreased on transcribed regions, accompanying a RNA Pol II occupancy decrease. Moreover, Rad2 occupancy was increased on UAS around Mediator peaks and also on core promoter regions similarly to Mediator, but Rad2 increase was less pronounced.

Next, to determine if the observed changes in Rad2, Mediator and RNA Pol II chromatin binding could be partly explained by modified interactions between these protein/complexes, we performed co-immunoprecipitation (CoIP) experiments with crude extracts from *kin28* ts mutant compared to the wild type. In *kin28 ts* mutant, more Mediator co-immunoprecipitated with RNA Pol II and inversely, less RNA Pol II co-immunoprecipitated with Rad2, in line with ChIP-seq results.

Altogether, our results showed that the presence of Rad2 on the chromatin is influenced by both Mediator and RNA Pol II. Rad2 seems to follow Mediator on promoter regions and RNA Pol II on transcribed regions.

Mutants of two other components, Mediator and RNA Pol II, a *med17* mutants defective for Mediator-Rad2 interaction and *rpb9* (RNA Pol II subunit) deletion mutant were also investigated.

The laboratory had previously reported that the UV-sensitivity of *med17* mutants was correlated with a decrease of Rad2 occupancy on RNA Pol II-transcribed regions, and a concomitant decrease of the interaction between Mediator and Rad2 protein. In this study, we analyzed on a genome-wide scale, the effect of *med17* mutations on Rad2 occupancy. We used a *med17* mutant that was only slightly UV-sensitive and a strongly UV-sensitive mutant. Metagene analysis of Rad2 chromatin binding revealed that there was increase of Rad2 occupancy on UAS accompanying Mediator occupancy increase. A decrease of Rad2 occupancy on transcribed regions was observed concomitantly to a decrease of RNA Pol II, the effect in the strongly UV-sensitive mutant was more pronounced than the slightly UV-sensitive mutant. In addition, genetic screening experiments showed that the thermo-sensitive phenotype, associated with transcriptional defect, cannot be dissociated from the UV-sensitive phenotype. However, all temperature-sensitive Mediator mutants are not UV-sensitive, indicating that the UV-sensitive phenotype is not a consequence of transcriptional defects. Moreover, since the UV-sensitive phenotype of *med17* mutants is only visible in a GG-NER-deficient context, we previously proposed that Mediator might play a role in TCR. Hence, it was tested whether Mediator is epistatic to *rad26* mutation, the TC-NER specific factor in yeast. It was observed that *med17* UV-sensitive mutant presented a synthetic UV-sensitive phenotype with *rad26Δ* in a GG-NER deficient context, suggesting that Mediator function might be in part independent of Rad26-related NER.

There are several studies suggesting a Rad26-independent TC-NER pathway in *S. cerevisiae* (Jansen *et al.,* 2002; Verhage *et al.,* 1996). Rpb9, a non-essential subunit of

RNA Pol II, was suggested to be required for Rad26-independent TCR in yeast (Li and Smerdon, 2002). Moreover, given the strong link between Mediator and RNA Pol II, we tested whether *med17* mutant and *rbp9* mutant were epistatic. Interestingly, we observed an allele-specific co-lethality between *rpb9Δ* and UV-sensitive *med17* mutants, indicating a functional link between Mediator and Rpb9 in TC-NER. Furthermore, Rad2, Mediator and RNA Pol II chromatin occupancies were investigated in *rpb9* mutant. Remarkably, no global decrease of RNA Pol II occupancy on transcribed regions was observed, but rather a gene-specific defect. The effect of *rpb9* deletion on Rad2 occupancy was also gene-specific. Furthermore, Rad2 occupancy was increased on Mediator-bound UAS but no significant change in Mediator binding was observed on UAS in the mutant compared to the wild-type.

Altogether, results from the three mutants, *kin28* TFIIH, *rpb9* RNA Pol II and *med17* Mediator, allowed us to propose a model in which Rad2 is first recruited on Mediator-bound upstream regulatory regions, and then transferred to transcribed regions in a RNA Pol II-dependent manner.

Rad2 shuttles between regulatory and transcribed regions through a transient Mediator/RNA polymerase II intermediate

Adrien Georges[1,2#], Diyavarshini Gopaul[1#], Cyril Denby Wilkes[1], Nathalie Giordanengo Aiach[1], Elizaveta Novikova[1,3], Marie-Bénédicte Barrault[1], Olivier Alibert[4], and Julie Soutourina[1*]

[1]*Institute for Integrative Biology of the Cell (I2BC), CEA, CNRS, Univ. Paris Sud, University Paris Saclay, F-91198 Gif-sur-Yvette cedex, France;*

[2]*Present address: PARCC, Hôpital Européen Georges Pompidou, 56 Rue Leblanc, F-75015 Paris, France;*

[3]*Present address: IBENS, ENS, PSL Research University, F-75005 Paris, France;*

[4]*CEA, iRCM, LEFG, Genopole G2, F-91057 Evry cedex, France.*

[#]*equal contribution*

**Corresponding author and Lead Contact: julie.soutourina@cea.fr*

Abstract
A link between Rad2/XPG endonuclease of nucleotide excision repair and Mediator complex, an essential coregulator of RNA polymerase (Pol) II transcription, was previously discovered. However, the functional interplay between Rad2/XPG, Mediator and Pol II remains to be determined. In this study, we investigated how these components work together using *kin28* TFIIH, *med17* Mediator and *rpb9* Pol II mutants. When Mediator is stabilized on promoters, Rad2 genome-wide occupancy follows that of Mediator, but decreases on transcribed regions together with Pol II. Specific Mediator mutations increase UV sensitivity, reduce Rad2 recruitment to transcribed regions and lead to uncoupling of Rad2, Mediator and Pol II. Moreover, these mutations are colethal with deletion of Rpb9 Pol II subunit involved in transcription-coupled repair. We propose that Rad2 shuttles between regulatory and transcribed regions through a transient Mediator/Pol II intermediate. Our work suggests that Mediator functions in transcription and DNA repair are closely related.

Keywords: Rad2/XPG, Mediator, RNA polymerase II, transcription-coupled repair, transcription, nucleotide excision DNA repair, genome-wide distribution

Introduction
Maintenance of genome integrity is essential for the normal cell function. A number of mechanisms have evolved to repair DNA damages induced by genotoxic agents or cellular metabolism. Nucleotide excision DNA repair (NER) is a unique evolutionarily conserved pathway that specifically removes bulky and/or helix-distorting DNA lesions including photoproducts induced by UV light (Lagerwerf et al., 2011; Marteijn et al., 2014). These DNA lesions can interfere with replication and transcription, emphasizing the importance of NER for cellular physiology. NER factors recognize the DNA lesions, incise and excise the damaged DNA fragment from the genomic DNA allowing repair synthesis. As expected given an essential role of NER for cell physiology, inherited NER defects lead to the severe diseases including xeroderma pigmentosum (XP) and Cockayne syndrome (CS). Two subpathways have been proposed for NER mechanisms. Global genome repair (GGR) removes the DNA lesions in the genome overall, and transcription-coupled repair (TCR) removes the DNA lesions interfering with the RNA polymerase II (Pol II) progression through actively-transcribed regions (Hanawalt and Spivak, 2008; Mullenders, 2015; Svejstrup, 2002, 2007; Vermeulen and Fousteri, 2013). TCR-specific Rad26/CSB protein was shown to bind the stalled Pol II to initiate the TCR complex assembly. In yeast, the existence of Rad26-independent TCR was also proposed (Verhage et al., 1996).
Rad2/XPG is a DNA-repair 3'-endonuclease involved in NER. In human, mutations in XPG gene constitute one of the complementation groups found in XP patients with XP or combined XP/CS syndromes. Together with Rad1-10/XPF-ERCC1 5'-endonuclease, Rad2/XPG ensures the dual incision of the damaged DNA in both NER pathways. Crystal structure of catalytic core of Rad2 in complex with DNA substrate has been reported (Mietus et al., 2014). In addition to its nuclease activity, a non-catalytic function for human XPG in coordinated recognition of stalled transcription together with CSB has been proposed in TCR initiation (Sarker et al., 2005). Previously, links of human XPG with transcription of nuclear receptor (NR)-dependent genes have been suggested. It has been shown that XPG formed a stable complex with TFIIH allowing transactivation of nuclear receptors (NR) (Ito et al., 2007). In addition, XPG was present on active promoters and distal regions of NR-dependent genes and participated in chromatin looping between the promoter and the terminator of the activated NR-dependent gene (Le May et al., 2012; Le May et al.,

2010). XPG roles have been also proposed in other DNA repair mechanisms. For example, a catalytic role in processing of RNA-DNA hybrids into DNA double-strand breaks (Sollier et al., 2014) or a non-catalytic function in homologous recombination (Trego et al., 2016) were reported.

Recently, we identified a novel link between Rad2/XPG and Mediator complex (Eyboulet et al., 2013). Mediator is a multisubunit coactivator complex conserved from yeast to human cells (Kornberg, 2005; Malik and Roeder, 2010; Poss et al., 2013; Soutourina, 2018). This complex plays a crucial role in Pol II transcription regulation. It is recruited to regulatory regions via direct interactions with specific transcription factors. Mediator is also in a direct contact with Pol II serving as a functional bridge between specific regulators and Pol II basal transcription machinery. Mediator acts in cooperation with general transcription factors (GTFs) in preinitiation complex (PIC) assembly on core promoters (Eychenne et al., 2017). It has been shown recently that depletion or inactivation of Kin28 kinase subunit of TFIIH, one of the GTF, stabilizes a transient association of Mediator with the PIC assembled on core promoters (Jeronimo et al., 2016; Petrenko et al., 2016). In human, Mediator subunits have been involved in many diseases including several types of cancer (Schiano et al., 2014; Spaeth et al., 2011). A modular organization of Mediator in head, middle, tail and Cdk8 kinase modules contributes to Mediator function. Crystallographic models have been reported for several yeast Mediator submodules (Lariviere et al., 2012b), the head module (Imasaki et al., 2011; Lariviere et al., 2012a; Robinson et al., 2012) and more recently for core Mediator composed of head and middle modules (Nozawa et al., 2017). Our recent discovery of a Mediator link to NER suggested the Mediator functions beyond the transcription process per se (Eyboulet et al., 2013). Two-hybrid and coimmunoprecipitation experiments show that the essential Med17 Mediator subunit interacts with Rad2/XPG DNA repair protein. Binding of human MED17 to XPG was also observed *in vitro* (Kikuchi et al., 2015). Genome-wide location analyses revealed that Rad2 was associated with upstream activating sequences (UAS) and transcribed regions of class II genes in the absence of exogenous genotoxic stress. Moreover, Rad2 occupancy of UAS was highly correlated with that of Mediator. Rad2 occupancy of Pol II-transcribed genes was strongly decreased in *rpb1-1* Pol II mutant when transcription was rapidly stopped, demonstrating that Rad2 binding to the chromatin was transcription-dependent. This decrease in Rad2 occupancy was observed on promoter and transcribed regions. However, no growth phenotypes, except UV sensitivity, or transcriptional effects were observed in the *rad2*Δ context suggesting that Rad2 does not play a major role in the transcriptional process in yeast. On the contrary, specific *med17* Mediator mutants were UV-sensitive in a GGR deficient genetic background and were epistatic with a TCR deficient *rad26*Δ mutant. This UV sensitivity of *med17* mutants was correlated with reduced Rad2 occupancy of Pol II-transcribed genes, and a concomitant decrease of the interaction between Mediator and Rad2 protein. Taken together, these results strongly suggested that Mediator is involved in TCR by facilitating Rad2 recruitment to transcribed genes.

RNA polymerase II is the main component of transcription machinery and the first complex in TCR that encounters the DNA damage (Mullenders, 2015; Svejstrup, 2002, 2007; Vermeulen and Fousteri, 2013). Rpb9 Pol II subunit is non-essential in yeast. Rpb9 modulates transcription start site selection (Ziegler et al., 2003) and is required, together with TFIIS, to stimulate the intrinsic RNA cleavage activity of Pol II (Ruan et al., 2011). In addition, Rpb9 subunit was proposed to be involved in TCR, since in yeast its deletion increased the UV sensitivity of *rad26* strain in a GGR-deficient context (Gaillard et al., 2009; Li and Smerdon, 2002). It should be noted that Rad2/XPG interacts with Pol II in yeast and in human cells. Indeed, XPG protein was reported to coimmunoprecipitate

with Pol II in crude extracts from undamaged HeLa cells (Sarker et al., 2005). In yeast, we showed that Rad2 also coimmunoprecipitated with Pol II (Eyboulet et al., 2013). Mediator is well known to directly interact with Pol II and these contacts are essential for transcription regulation (Koleske and Young, 1994; Nonet and Young, 1989; Plaschka et al., 2015; Robinson et al., 2016; Soutourina et al., 2011; Thompson et al., 1993; Tsai et al., 2017). It remains to be determined how Mediator link to Rad2/XPG is related to Pol II and how Rad2 recruited by Mediator to UAS arrives on transcribed regions in regards to physical interactions and functional interplay between Mediator, Rad2/XPG and Pol II. It is also unknown if Mediator implication in TCR is Rad26- and/or Rpb9-dependent.

In this work, we used *kin28* TFIIH, *med17* Mediator and *rpb9* Pol II mutants to precisely decipher the functional interplay between Mediator, Rad2 and Pol II related to transcription-coupled repair. We show that in a *kin28* mutant, in which a transient association of Mediator with Pol II and the PIC is stabilized on core promoters, Rad2 genome-wide occupancy follows that of Mediator but is decreased on transcribed regions. We then performed extensive mutational analysis of Rad2-interacting domain of Med17 and showed that specific *med17* mutations are involved in UV sensitivity, reduce Rad2 recruitment to transcribed regions and lead to uncoupling of Rad2 with Mediator and Pol II. Finally, we deleted Rpb9 Pol II subunit involved in TCR, which leads to allele-specific colethality with UV-sensitive Mediator mutants, supporting Mediator implication in TCR mechanisms. Rpb9 deletion also leads to Rad2 stabilization on regulatory regions. Taken together, our data provide mechanistic insights into the functional interplay between Mediator, Rad2 and Pol II related to TCR and allow us to propose a model in which Rad2 shuttles between regulatory regions bound by Mediator and transcribed regions where its presence is dependent on elongating Pol II, through an instable Mediator/Pol II intermediate formed on core promoters. Our work suggests a close relation between Mediator functions in transcription and in NER, two fundamental processes dysfunction of which leads to human diseases.

Results

Rad2 is blocked on promoter regions in a kin28 *mutant*

Previously, we showed that Rad2 and Mediator occupancies are well correlated on the regulatory regions genome-wide and that Rad2 is also present on transcribed regions together with Pol II (Eyboulet et al., 2013). Moreover, Rad2 and Mediator physically interact with each other and with Pol II (Eyboulet et al., 2013; Koleske and Young, 1994; Nonet and Young, 1989; Plaschka et al., 2015; Robinson et al., 2016; Soutourina et al., 2011; Thompson et al., 1993; Tsai et al., 2017). To analyse Rad2-Mediator-Pol II functional interplay, we sought to determine how Rad2 occupancy changes when the presence of Mediator is stabilized on core promoters and Pol II promoter escape is affected. We therefore used a temperature-sensitive mutant in Kin28 TFIIH subunit, *kin28-ts16* (Cismowski et al., 1995). In this mutant, shifting from 25°C to 37°C decreased Pol II CTD phosphorylation that regulates the promoter escape of the enzyme. Previously, Mediator stabilization on core promoters where PIC is assembled was evidenced after depletion or inhibition of Kin28 (Jeronimo et al., 2016; Jeronimo and Robert, 2014; Petrenko et al., 2016; Wong et al., 2014). We examined Mediator (Med17 subunit), Rad2 and Pol II (Rpb1 subunit) occupancy on promoters and transcribed regions of

Figure 1

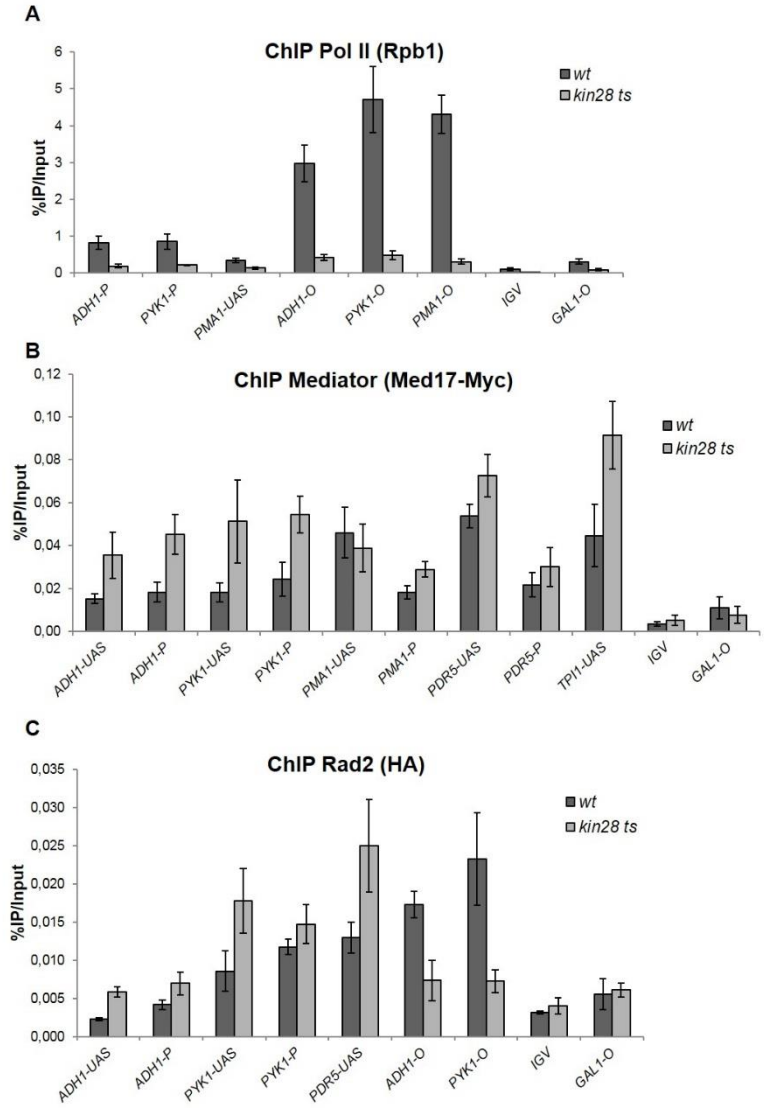

Figure 1. Effects of *kin28* temperature-sensitive mutation on Mediator, Rad2 and Pol II occupancy on the chromatin.

(**A-C**) Quantitative ChIP analysis of Pol II, Mediator and Rad2 occupancies following a 75 minutes shift at 37°C, after reaching exponential phase at 25°C. Sonicated chromatin from exponentially growing yeasts expressing tagged versions of Med17 (Myc) and Rad2 (HA) in wild type or *kin28 ts* context was precipitated using α-Rpb1 (**A**), α-Myc (**B**), or α-HA (**C**) antibodies. Quantitative PCR was performed on the precipitated DNA, using primer pairs designed to amplify either regions in open reading frames (O), core promoters (P) or upstream activating sequences (UAS). Relative quantity of an amplicon was determined by comparing the obtained Ct to a standard curve made on the same qPCR plate. Quantities were reported to qPCR performed on Input DNA and are expressed as a percentage. *GAL1-O* and *IGV* amplicons were used as controls. The indicated value is the mean of three biological replicates, and error bars represent the standard deviation.

selected genes after a transfer of the cells to 37°C for 75 minutes. As expected, Pol II occupancy was strongly decreased on promoter and transcribed regions in *kin28-ts16* mutant compared to the wild type strain (**Figure 1A**). Mediator occupancy was strongly increased on UAS and on core promoter regions, in agreement with previous observation of Mediator stabilization in Kin28-depleted or inhibited contexts (Jeronimo et al., 2016; Jeronimo and Robert, 2014; Petrenko et al., 2016; Wong et al., 2014) (**Figure 1B**). Similarly to Pol II occupancy, Rad2 occupancy was strongly reduced on transcribed regions in *kin28* mutant compared to the wild type (**Figure 1C**). However, together with Mediator stabilization, the presence of Rad2 was increased on core promoter regions and upstream activating sequences (UAS) where it is normally found (**Figure 1C**).

To get genome-wide insights on Mediator, Pol II and Rad2 distribution in *kin28* mutant, we performed ChIP followed by high throughput sequencing (ChIP-seq). Bioinformatic analyses of Mediator (Med17 subunit) profile in *kin28* mutant showed the appearance of peaks corresponding to core promoter regions that aligned with TFIIH (Rad3 subunit) peaks, whereas these peaks were low or absent in the wild type strain (**Figure 2A, C**). Metagene average density profiles show an increase in Med17 enrichment on regulatory regions (UAS) (**Figure 2B**) and a clear enrichment of Med17 in the vicinity of Rad3 TFIIH peaks, corresponding to core promoter regions (**Figure 2C**). This suggests the stabilization of a Mediator-containing intermediate on the promoters, due to the decrease in Pol II phosphorylation (Jeronimo et al., 2016; Jeronimo and Robert, 2014; Petrenko et al., 2016; Wong et al., 2014). Stronger Mediator enrichment on regulatory regions seemed mostly due to its stabilization on corresponding core promoters, as indicated by the Mediator occupancy ratios between the *kin28* mutant and the wild type (**Figure 2B, C,** ratio panels). Interestingly, our results show clear changes in Rad2 distribution in *kin28* mutant compared to the wild type. Rad2 association was increased on regulatory regions (UAS) in the vicinity of Mediator enrichment peaks defined in the wild type context (**Figure 2B**). Rad2 occupancy was also increased on core promoters in the *kin28* context, following the Mediator stabilization on these regions although to a lesser extent (**Figure 2C**). Compared to Mediator which was stabilized mostly on core promoters, the maximum of the Rad2 occupancy ratios between the mutant and the wild Taken together, our results show that Rad2 chromatin binding is influenced by both Mediator stabilized on promoter regions and Pol II whose occupancy is decreased within the gene bodies, suggesting that type was located between the UAS and the core promoter (**Figure 2B, C,** ratio panels). Finally, the presence of Rad2 was reduced on transcribed regions genome-wide, together with a global decrease in Pol II association (**Figure 2D** and **Supplementary Figure S1**). We noted that a global decrease in Pol II occupancy was less pronounced at the beginning of transcribed regions, when the Pol II occupancy ratios between *kin28 ts* mutant and the wild-type were analysed (**Figure 2B, C**, ratio panels and **Supplementary Figure S1,** right panels). This fact is consistent with Pol II promoter escape defect in *kin28* mutants (Jeronimo & Robert, 2014, Wong et al., 2014).

To determine if a part of the observed changes in Rad2, Mediator and Pol II chromatin binding could be explained by modified interactions between these protein/complexes, we performed coimmunoprecipitation experiments with crude extracts from *kin28 ts* mutant compared to the wild type (**Figure 2E**). We confirmed a large decrease in Ser5-phosphorylated Pol II in *kin28* mutant by Western blot analysis of crude extracts prepared from the cells after a transfer to a non-permissive temperature. Pol II was immunoprecipitated via its Rpb1 subunit and coimmunoprecipitated Rad2 and Mediator (Med17 subunit) were analysed in both contexts. We observed that less Rad2 was coimmunoprecipitated in *kin28* mutant. Interestingly, more Mediator was coimmunoprecipitated with Pol II in *kin28* mutant. Our results suggest that interactions between Mediator, Rad2 and Pol II are modified when Ser5 phosphorylation of Pol II is impaired with an increase for Mediator-Pol II contact and a decrease for Pol II-Rad2 interaction.

Rad2 recruitment on upstream regulatory regions and its loading on transcribed regions are connected and depend on Mediator-Pol II-Rad2 interaction network.

Figure 2. Effects of *kin28 ts* mutation on genome-wide Mediator, Rad2 and Pol II occupancy and Mediator/Rad2/Pol II interactions.

(**A**) ChIP-seq tag density profile of Med17, Rad2, Rpb1 and Rad3 in ChrXV:77500-99500 region, in wild type and *kin28 ts* context. ChIP-Seq was done on yeast chromatin extracts prepared as in Figure 1, *i.e.* following a 75 minutes shift from 25°C to 37°C. Mapped reads were extended to 150bp, and the number of reads for each position of the genome was counted to determine tag density. Densities were scaled per millions reads, and normalisation step was performed as described in Experimental procedures. Alignment of Med17 peaks present in *kin28-ts* mutant, and low or absent in wild type strain, with Rad3 peaks in core promoters regions is shown. (**B-D**) Average tag density in Med17 Mediator ChIP (upper panel), Rad2 ChIP (middle panel) and Rpb1 Pol II ChIP (lower panel), around Med15 peaks (**B**, UAS, 1000bp window), Rad3 peaks (**C**, Core promoter, 1000bp window), and on transcribed regions (**D**, 500bp before TSS, scaled window between TSS and TES, and 500 bp after TES, 10% Pol II most-enriched regions in wild-type). Average tag density in wild type strains is indicated in black, whereas average tag density in *kin28-ts* strains is indicated in blue. The right panels (Ratio, in pink) in **B** and **C** show Mediator, Rad2 or Pol II occupancy ratio between *kin28-ts* mutant and the wild-type. For clarity, the background of the plot for ratios >1 is coloured in clear red and the background of the plot for ratios <1 is coloured in clear green. (**E**) Effect of *kin28-ts* mutation on Mediator/Rad2/Pol II interactions. Western blot analysis of Mediator interaction with Rad2 and Pol II. Crude extracts were prepared from yeasts expressing tagged versions of Med17 (Myc) and Rad2 (HA) in the wild type strain and *kin28-ts* mutant following a 75 min-shift at 37°C, after reaching exponential phase at 25°C. Samples were immunoprecipitated with α-Rpb1 (Pol II) antibody (IP). Immunoprecipitates and Inputs were analysed by Western blotting with α-Myc, α-HA and α-Rpb1 antibodies. The effect of *kin28-ts* mutation on Ser5 phosphorylation of Pol II CTD was verified by Western blotting with an antibody against Ser5P-CTD (H14, Abcam).

Figure 2

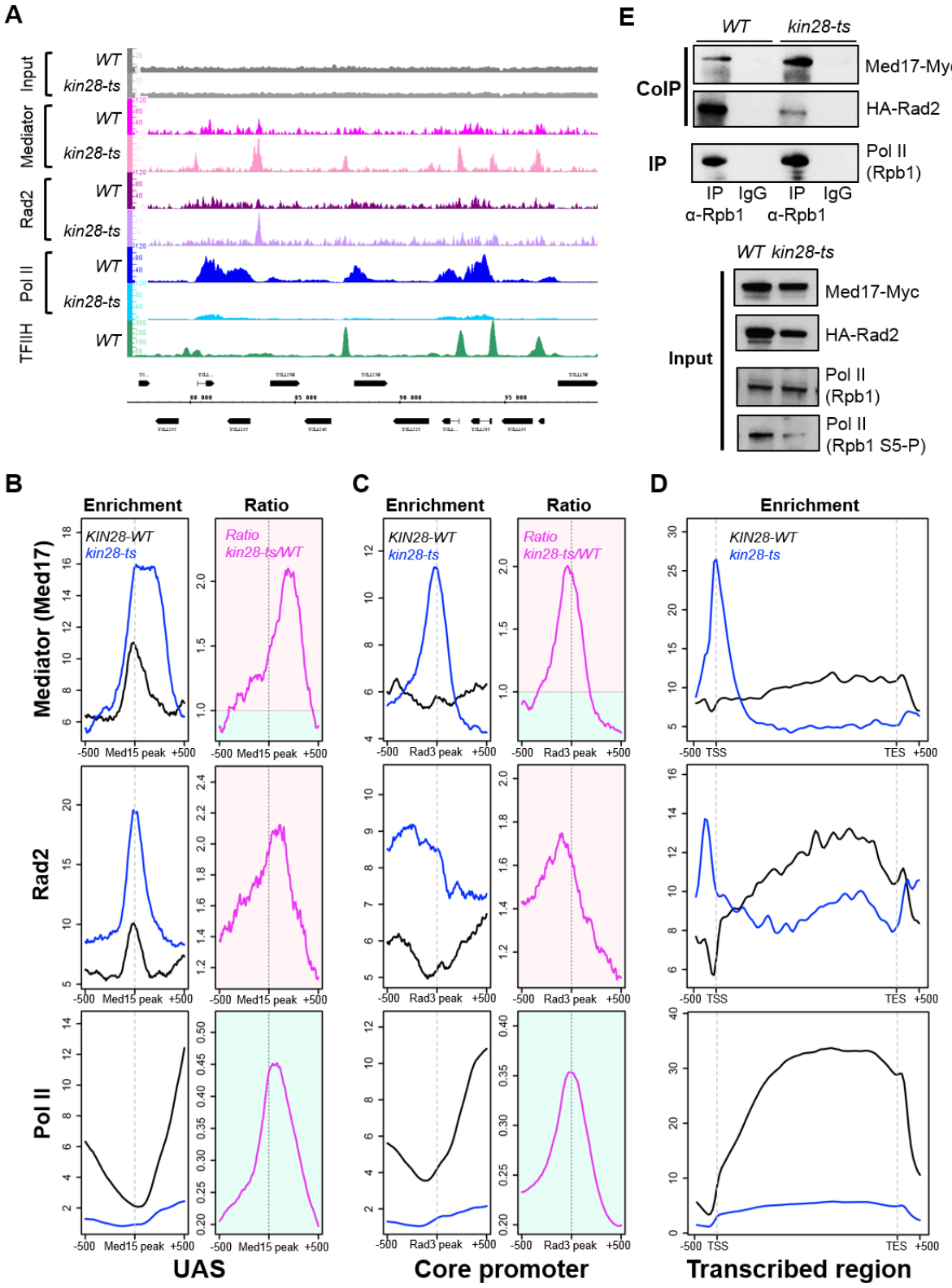
A
Input
Mediator
Rad2
Pol II
TFIIH
WT
kin28-ts
E
WT
kin28-ts
CoIP
Med17-Myc
HA-Rad2
IP
Pol II (Rpb1)
IP IgG IP IgG
α-Rpb1 α-Rpb1
Input
Pol II (Rpb1 S5-P)
B
C
D
Enrichment
Ratio
KIN28-WT
kin28-ts
Ratio kin28-ts/WT
Mediator (Med17)
Rad2
Pol II
-500 Med15 peak +500
-500 Rad3 peak +500
-500 TSS
TES +500
UAS
Core promoter
Transcribed region

Mutational analysis of Med17 C-terminal domain interacting with Rad2

To investigate in more details the role of Mediator in Rad2 recruitment and to obtain further mechanistic insights into Mediator/Rad2/Pol II functional relationship, we decided to analyse the implication of Mediator-Rad2 interaction in these mechanisms. To identify *med17* mutants specifically affecting the interaction with Rad2 *in vivo*, we first used yeast two-hybrid approach (Y2H) to determine interaction domains in Med17 and Rad2 proteins. Previously, our yeast two-hybrid screening of Mediator subunits identified the interaction between full length Med17 and Rad2 (Eyboulet et al., 2013). The isolated fragment of *RAD2* gene encoded amino acids 549 to 857 of its protein product. Two series of Med17 truncation mutants were analysed for their interactions with Rad2 fragment and Med22 Mediator subunit (**Figure 3A, B**). We conclude that Med17 domain (381-681) is necessary and sufficient for Med17 interaction with Rad2 fragment. Further truncations likely affect Med17 secondary structure, impairing also the interactions with Med22 and Med11 Mediator subunits. We performed a similar analysis to identify which Rad2 fragment is the most important for the interaction with Med17. We found that Rad2 catalytic I domain (amino acids 756 to 857) is necessary and sufficient for the interaction with Med17 (**Supplementary Figure S2A, B**).

Our previous studies showed that UV sensitivity of *med17* mutants in *rad7*Δ GGR-deficient context was correlated with an impaired interaction between Med17 and Rad2. We therefore decided to perform a random mutational screening of Med17 C-terminal domain based on *in vivo* phenotypes as described in Experimental procedures (**Supplementary Figure S2C**). We identified and sequenced 88 new *med17* mutants, excluding 33 nonsense mutants, which were UV-sensitive (UV^s) and/or temperature-sensitive (ts) in a *rad7*Δ GGR-deficient context. This set of mutants completed a collection of 27 previously characterized *med17* mutants (**Supplementary Figure S2C-G** and **Supplementary Table S2,** (Eyboulet et al., 2015)).

Among all these *med17* mutants, UV^s phenotype was systematically associated with ts phenotype (**Supplementary Figures S2C-G** and **Supplementary Table S2**). This suggests that the UV^s phenotype in *med17* mutants is closely related to transcription defects associated with ts phenotypes. Conversely, not all Med17 ts mutants were UV^s, further suggesting that UV sensitivity of Mediator mutants could not be the systematic indirect consequence of transcription defects. In most cases, several mutations co-occurred in *med17* mutants, making difficult to find exact correspondence between amino acid changes and ts and UV-sensitive phenotypes. However, we identified that some positions were more frequently mutated and generally associated to UV sensitivity (**Figure 3C** and **Supplementary Figures S2G,** residues indicated in green).

Direct mutagenesis allowed us to identify point *med17* mutations that specifically affected Med17-Rad2 interaction in Y2H system. Interestingly, the corresponding residues are closely located on the *S. cerevisiae* Mediator head structure (Robinson et al., 2012) (**Figure 3D**). However, these *med17* point mutations do not lead to UV^s or ts phenotype (**Supplementary Figure S3**), suggesting that the Y2H system is extremely sensitive to detect Med17-Rad2 interaction changes and that stronger defects with additional mutations are required for UV sensitivity phenotypes of *med17* mutants.

We identified several cases where one additional mutation distinguished a UV-sensitive mutant from a non UV-sensitive mutant (**Figure 3E**). In particular, we found that *med17-Q444P* mutant is temperature-sensitive but does not have a

pronounced UV-sensitive phenotype in *rad7*Δ context, whereas *med17-Q444P/M442L* is both ts and strongly UV^s. The latter mutant is also more sensitive to 4-NQO, further showing its sensitivity to genotoxic stress (**Supplementary Figure S3C**). Another example is the double mutant *med17-M442V/V670E,* which is both UV^s and ts, whereas *med17-M442V* and *med17-V670E* are neither UV^s nor ts. Interestingly, M442 is one of the most frequently mutated positions in our screening, and in all but one case the corresponding mutants are UV^s (**Figure 3C** and **Supplementary Figure S2G**). Mutations in M442 also decreased Med17-Rad2 interaction in Y2H system. Two mutants carrying *med17-Q444P* single and *med17-Q444P/M442L* double mutations were therefore selected for further study.

med17 *UV-sensitive mutations lead to a decrease in correlation between Rad2 occupancy and those of Mediator and Pol II genome-wide*

We first examined the effect of Med17 mutations on Mediator interaction with Rad2 and with Pol II by CoIP experiments. Med5-Myc subunit was used to immunoprecipitate Mediator and the co-immunoprecipitation of Rad2 and Rpb1 Pol II subunit were analysed by Western blotting (**Figure 4A**). We found that less Rad2 was coimmunoprecipitated with Mediator in the UV^s *med17-Q444P/M442L* mutant, in line with a correlation between UV sensitivity of *med17* mutants and a decrease in Mediator-Rad2 interaction (Eyboulet et al., 2013). Surprisingly, we found that an increased amount of Rpb1 was coimmunoprecipitated with Mediator in *med17-Q444P* and *med17-Q444P/M442L* mutants compared to the wild type strain. We observed a similar situation in another *med17* UV^s mutant and another *med17* ts/non UV^s mutant (**Supplementary Figure S3D**). This suggests that Mediator-Pol II interaction is modified in these mutants independently on their UV sensitivity.

We then analysed by ChIP how *med17* mutations affected Rad2, Mediator and Pol II occupancy on promoter and transcribed regions. Med5 Mediator subunit occupancy was not affected or slightly increased in *med17* mutants (**Figure 4B**). We found that Rad2 occupancy was decreased on transcribed regions in *med17-Q444P/M442L* mutant, especially for *PYK1* transcribed region (**Figure 4C**). On promoter regions, we observed an increase in Rad2 occupancy in *med17* mutants. Pol II occupancy was strongly affected in both mutants (**Figure 4D**). Our results thus indicate a strong transcriptional defect in both *med17* mutants and a reduced Rad2 occupancy on transcribed regions in the double mutant, at least on a subset of genes.

To extend the ChIP analysis of *med17* mutants to the whole yeast genome, we performed ChIP-seq experiments for Mediator (Med5 subunit), Pol II (Rpb1 subunit) and Rad2 in the *med17* mutant and the wild type strains. Genome-wide analysis shows a global 3-fold decrease in Pol II occupancy in both *med17* mutants compared to the wild type (the slope of regression line is equal to 0.33 and 0.32 for *med17-Q444P* and *med17-Q444P/M442L*, respectively), with a high coefficient (R^2 is equal to 0.97 and 0.92 for *med17-Q444P* and *med17-Q444P/M442L*, respectively) (**Figure 5A**). This global effect on Pol II occupancy was very similar between the two mutants, with a high R^2 coefficient equal to 0.97 and the slope of the regression line equal to 0.97 (**Figure 5A,** right panel).

Figure 3. Mutation analysis of Med17 region interacting with Rad2 fragment.

Serial truncations of Med17 were assayed for interaction with Med22 and a Rad2 fragment (549-857) identified in a yeast two-hybrid screening using Med17 as a bait. (**A**) Gal4 DNA binding (Gal4-DBD) domain, alone (empty) or in fusion with full length Med17, 5 C-terminal truncations or 5 N-terminal truncations of Med17, was co-expressed with Gal4 Activation Domain (Gal4 AD), alone or in fusion with Med22 or residues 549 to 857 of Rad2. Yeast cells were spotted on SD+2A medium supplemented with 25mM 3-AT, grown for 3 days (left panel) and then stained with X-Gal for 24h (middle panel). Residues 346 to 687 appear necessary and sufficient to have an interaction of Med17 with both Med22 and Rad2 fragment. (**B**) This minimal interaction domain was subjected to further N-terminal or C-terminal truncations, and N-terminal and C-terminal fragments of this domain were also tested for the interaction with Med22 and Rad2 fragment, using the same protocol as in panel **A**).
(C) Pile histogram for occurrence of mutations affecting each residue in Med17 region interacting with Rad2, and the associated UV sensitivity phenotype. A graph for a complete Med17 protein is shown on **Supplementary Figure S2G**. The number of mutation occurrences is indicated for each amino acid position. Only mutants predicted to express full length Med17 were considered. The colours correspond to the associated phenotypes as follows: UV-sensitive in green, mild UV-sensitive in clear green and UV-insensitive in red. More frequently mutated residues F437, M442, I541 were more frequently associated with UV sensitivity (in green), whereas K517 and nearby residues were more frequently found with temperature-sensitive only mutants (UV-insensitive in red).
(D) Med17 residues represented in Supplementary Figure S3, panel A, are highlighted in the structure of Mediator head module from Robinson and colleagues (PDB 4GWP). Residues, mutations of which impaired or reduced Y2H Med17 interaction with Rad2 fragment specifically are in green (M442, K446, I541, N639). Residues, mutations of which impaired Y2H interaction of Med17 with Med22, Med11 and Rad2 fragment (K433, I445, I562) are in red. Residues, mutations of which impaired Y2H Med17 interaction with Med11 and Rad2 fragment, but not Med22, are in yellow (S409, V457, T509, I647) with the exception of M442. Other residues were not depicted.
(E) Spotting assay to determine UV and temperature sensitivity of yeast strains expressing either wild type or mutant versions of Med17 in *rad7*Δ context. Yeast cells were spotted on YPD agar plates, irradiated or not with 30 J/m^2 UV-C (254 nm) and incubated at 30°C or 37°C for 3 days.

Figure 3

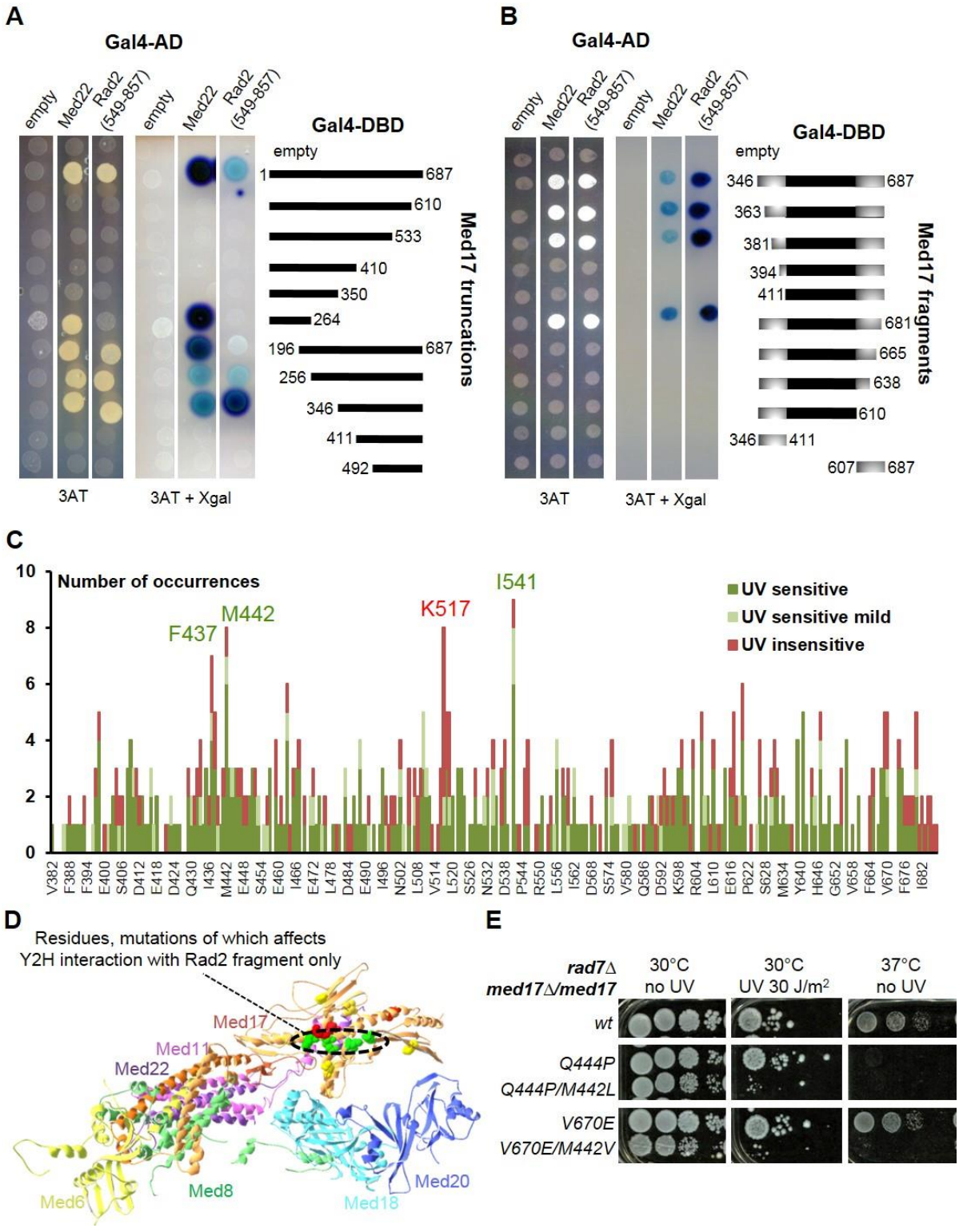
A
Gal4-AD
empty
Med22
Rad2 (549-857)
Gal4-DBD
Med17 truncations
1 687
610
533
410
350
264
196 687
256
346
411
492
3AT
3AT + Xgal
B
Gal4-AD
Gal4-DBD
Med17 fragments
346 687
363
381
394
411
681
665
638
610
346 411
607 687
C
Number of occurrences
UV sensitive
UV sensitive mild
UV insensitive
F437
M442
K517
I541
D
Residues, mutations of which affects Y2H interaction with Rad2 fragment only
Med17
Med11
Med22
Med6
Med8
Med18
Med20
E
rad7Δ
med17Δ/med17
30°C no UV
30°C UV 30 J/m²
37°C no UV
wt
Q444P
Q444P/M442L
V670E
V670E/M442V

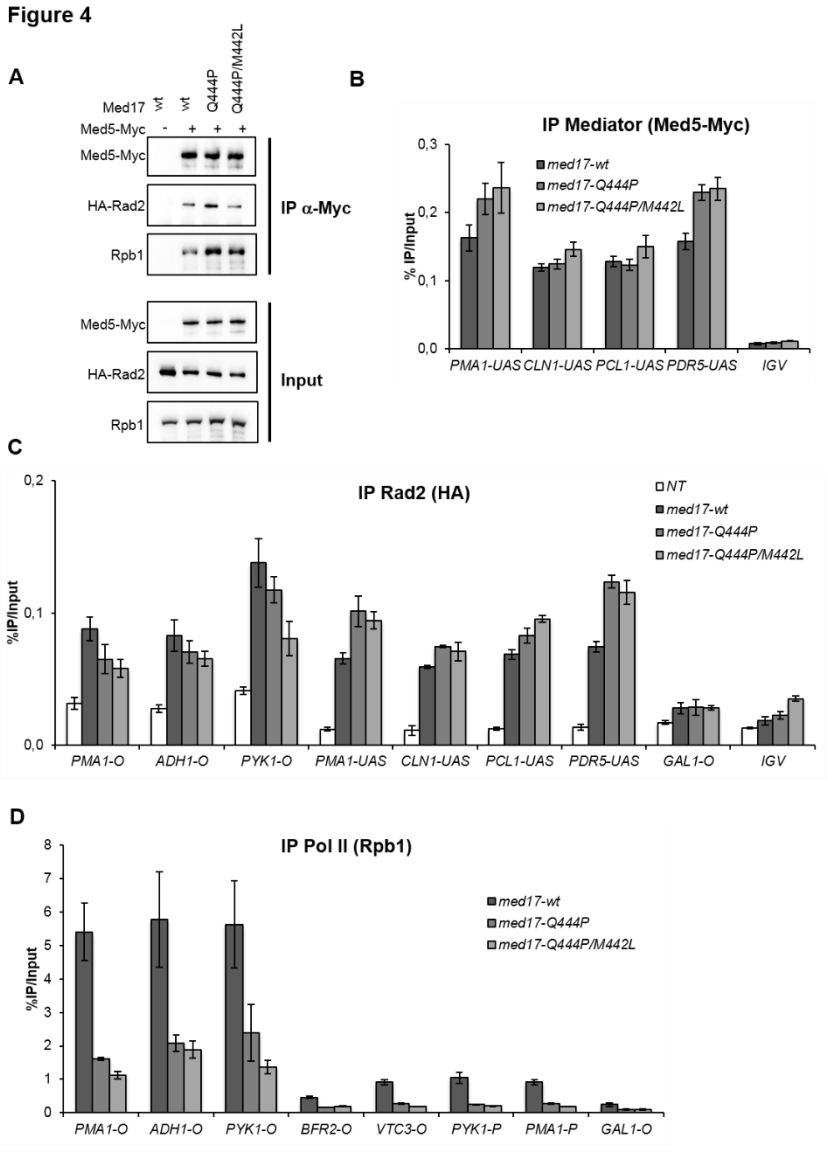

Figure 4. Effects of Med17 mutations on Mediator interactions with Rad2 and Pol II and on the binding of Mediator, Rad2 and Pol II to the chromatin.

(A) Western blot analysis of Mediator interaction with Rad2 and Pol II in standard growth conditions. Crude extracts were prepared from yeasts expressing tagged (+) or untagged (-) versions Med5 (Myc) in *MED17-wt*, *med17-Q444P* or *med17-Q444P/M442L* context in exponential phase, and samples were immunoprecipitated with α-Myc antibody (IP Myc). Immunoprecipitates and Inputs were analysed by Western blotting with α-Myc, α-HA and α-Rpb1 antibodies. (**B-D**) Quantitative ChIP analysis of Mediator, Rad2 and Pol II occupancies under standard growth conditions. Sonicated chromatin from exponentially growing yeasts expressing tagged or untagged (NT) versions of Med5 (Myc) and Rad2 (HA) in *MED17-wt*, *med17-Q444P* or *med17-Q444P/M442L* context was immunoprecipitated using α-HA (**B**), α-Rpb1 (**C**) or α-Myc (**D**) antibodies. Quantitative PCR was performed on the precipitated DNA, using primer pairs designed to amplify either regions in open reading frames (O) or in upstream activating sequences (UAS). Relative quantity of an amplicon was determined by comparing the obtained Ct to a standard curve made on the same qPCR plate. Quantities were reported to qPCR performed on Input DNA and are expressed as a percentage. *GAL1-O* and *IGV* amplicons were used as controls. The indicated value is the mean of three biological replicates, and error bars represent the standard deviation.

Figure 5

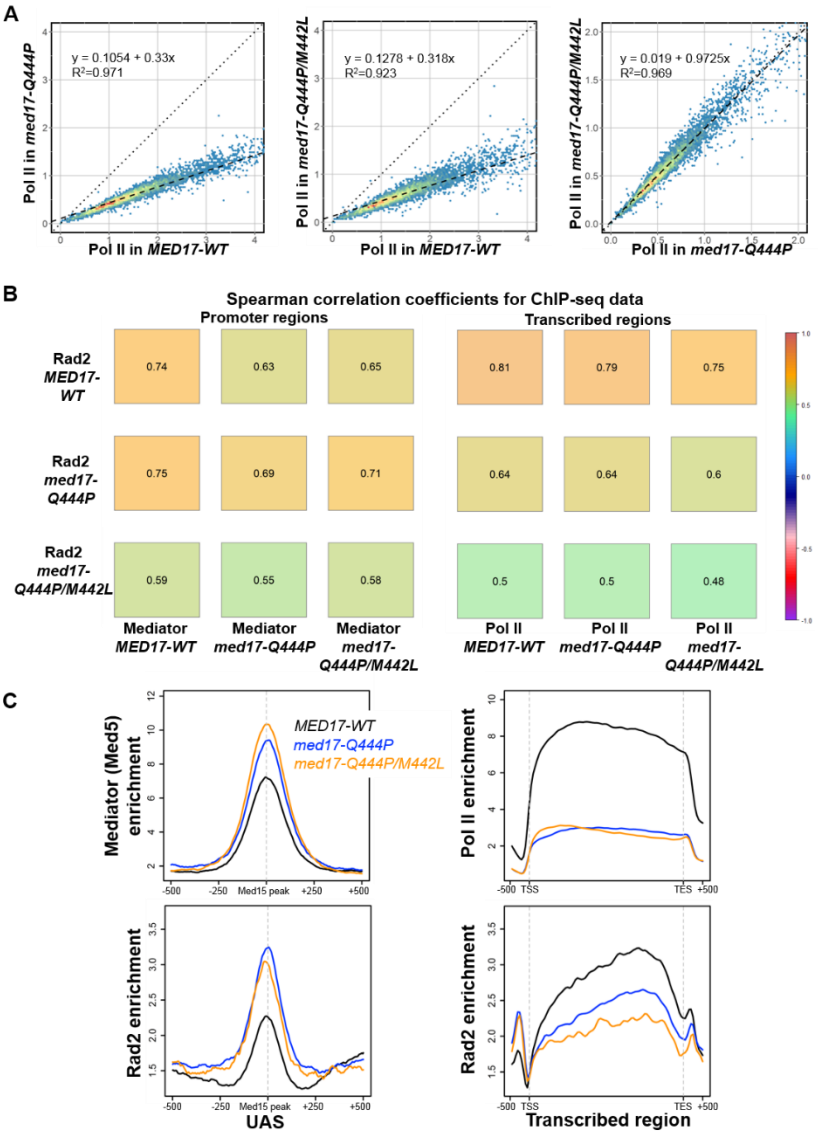

Figure 5. Effects of *med17* mutations on genome-wide Mediator, Rad2 and Pol II occupancy.

(**A**) The tag densities in the Pol II ChIP-seq experiments were calculated for the Pol II-transcribed mRNA genes. Tag densities were normalized relative to qPCR data on a set of selected genes. Each point on the plot corresponds to one transcribed region. A linear regression (dotted line) for ChIP-seq density in the *med17-Q444P* or *med17-Q444P/M442L* mutant versus ChIP-seq density in wild type or in *med17-Q444P* versus *med17-Q444P/M442L* and an R^2 linear regression coefficient are indicated. The dashed line corresponds to $y = x$.

(**B**) Pair-wise Spearman correlation coefficients of ChIP-seq data between *med17* mutants and wild-type were calculated for Rad2 and Mediator on promoter regions (left panel) or for Rad2 and Pol II on transcribed regions (right panel). The colours correspond to the scale for Spearman correlation coefficients indicated on the right.

(**C**) Average tag density in Med5 Mediator ChIP (upper left panel), Rad2 ChIP (lower panels) and Rpb1 Pol II ChIP (upper right panel), around Med15 peaks corresponding to UAS (left panels, 1000bp window), and on transcribed regions of 10% Pol II most-enriched genes (right panels, 500bp before TSS, scaled window between TSS and TES, and 500 bp after TES). Average tag density in wild type, *med17-Q444P* and *med17-Q444P/M442L* strains is indicated in black, blue and orange, respectively.

As previously shown, Rad2 and Mediator occupancies correlated well on promoter regions in the wild-type context (Eyboulet et al., 2013). This Rad2 - Mediator correlation on promoter regions in *med17-Q444P* mutant remains almost the same compared to the wild type, but decreases in *med17-Q444P/M442L* (Spearman correlation coefficients equal to 0.74, 0.69 and 0.58 for the wild type, *med17-Q444P* and *med17-Q444P/M442L*, respectively) (**Figure 5B,** left panel). For Rad2 genomic occupancy, we observed less correlation between *med17-Q444P/M442L* and the wild type or *med17-Q444P* **(Supplementary Figure S4).** Correlation analysis was then performed between Rad2 and Pol II occupancy on transcribed regions in *med17* mutants and the wild type (**Figure 5B,** right panel, and **Supplementary Figure S5**). The correlation between Rad2 and Pol II starts to decrease in a single mutant and strongly decreases in a double mutant, which is strongly UV^s (Spearman correlation coefficients equal to 0.81, 0.64 and 0.48 for the wild type, *med17-Q444P* and *med17-Q444P/M442L*, respectively).

A metagene analysis was then done to compare Mediator, Rad2 and Pol II distributions in *med17* mutants and the wild type (**Figure 5C**). On UAS regions, as determined by Mediator enrichment peaks, our analysis shows some stabilization of Mediator in a single and further in a double mutant and also a slight increase in Rad2 association to these regions in the *med17* mutants (**Figure 5C,** left panels). In accordance with our linear regression analysis, a large decrease in Pol II occupancy was observed on transcribed regions for the both *med17* mutants (**Figure 5C,** right panels, and **Supplementary Figure S6A, B**). We noted some differences in Pol II profiles between *med17* mutants with the enzyme accumulation at the beginning of transcribed regions in the double mutant, as illustrated by Pol II occupancy ratios between *med17-Q444P/M442L* mutant and the wild-type on transcribed regions for all Pol II enrichment quantiles (**Supplementary Figure S6A)**. Importantly, Rad2 occupancy on transcribed regions of 10% Pol II most-enriched genes was gradually decreased in *med17* mutants (**Figure 5C,** right panels and **Supplementary Figure S6B**). In line with our previous results on selected regions (Eyboulet et al., 2013), we showed that UV^s phenotype was correlated with a decrease in Rad2 presence within the gene bodies on the genomic scale. Moreover, using a single Med17 mutant (Q444P*)* with ts phenotype and a double mutant with additional M442L mutation leading to strong UV sensitivity phenotype, we revealed a gradual uncoupling of Rad2 and Mediator on promoter regions and especially of Rad2 and Pol II on transcribed regions.

Rpb9 deletion is colethal in combination with* med17 *UV-sensitive mutations

To determine in which specific NER subpathway Mediator would be involved, we decided to perform genetic interaction analyses of Mediator and NER components. Given that the phenotype of *med17* UV^s mutants is only visible in *rad7*Δ GGR-deficient context, we proposed that Mediator might play a role in TCR (Eyboulet et al., 2013). We therefore tested whether *med17* mutants would be epistatic with the deletion of *rad26*, the homolog of CSB and the most prominent TCR factor. It was the case in GGR-proficient background (Eyboulet et al., 2013). Surprisingly, we found that *med17* UV^s mutants had synthetic UV sensitivity phenotype with *rad26* deletion in *rad7*Δ GGR-deficient context (**Figure 6A** and **Supplementary Figure S7A**). Indeed, a combination of *med17* UV^s mutations with *rad26* deletion in *rad7*Δ context leads to an increase in UV sensitivity compared to the *med17* UV^s *rad7*Δ or *rad26*Δ *rad7*Δ. For example, *med17-Q444P/M442L rad26*Δ *rad7*Δ mutant is more UV-sensitive than *med17-Q444P/M442L rad7*Δ or *MED17*

*rad26*Δ *rad7*Δ. This suggests that the UV sensitivity of *med17* mutants could be at least in part independent of Rad26-related NER.

We then focused on Rpb9 Pol II subunit that was previously suggested to be required for Rad26-independent TCR (Chen et al., 2007; Li and Smerdon, 2002). Given the strong link of Mediator with Pol II, we tested whether *med17* mutants would be epistatic with *rpb9* deletion. We found that the introduction of *med17* double mutation *Q444P/M442L* in *rad7*Δ *rpb9*Δ context completely impaired growth at 30°C and moderately slowed growth at 25°C (**Figure 6B**). In contrast, *med17-Q444P* single mutant grew as a wild-type *MED17* in this context (**Figure 6B**). Similar observations were made with other *med17* UV^s and non-UV^s mutants (**Supplementary Figure S7B**). All tested *med17* UV^s mutants were colethal with *rpb9* deletion at 30°C, whereas none of the non-UV^s mutants were. Similar phenotypes were also observed in *RAD7 rpb9*Δ context (right panels, **Figure 6B** and **Supplementary Figure S7B)**. This suggests a specific defect of *med17* UV^s mutants that is enhanced by *rpb9* deletion, in line with a functional link between Mediator and Rpb9 Pol II subunit related to TCR.

Next, we analysed Mediator, Pol II and Rad2 occupancy on promoters and transcribed regions in *rpb9*Δ context. We showed that *rpb9* deletion did not affect the Med17 recruitment to promoters (**Figure 6C**). Surprisingly, we did not observe a strong decrease of Pol II recruitment to transcribed regions, but rather gene-specific changes (**Figure 6D**). Similarly, we did not find a strong decrease of Rad2 recruitment to transcribed regions, but rather gene-specific effects (**Figure 6E**). However, we found a stronger Rad2 ChIP signals on promoter regions. These results indicate that changes in Pol II composition could affect Rad2 chromatin binding both on promoter and transcribed regions.

To obtain a genome-wide view of *rpb9* mutation effect on Rad2, Mediator and Pol II occupancy, we performed ChIP-seq experiments in *rpb9*Δ and the wild-type strains. On the genomic scale, a clear stabilization of Rad2 on UAS regions was observed (**Figure 6F,** left panel). We did not detect any major changes in Mediator occupancy in *rpb9* mutant. Surprisingly, a metagene analysis of Pol II distribution on transcribed regions demonstrated a slight increase and a change in Pol II profile with the enzyme stabilization at the beginning of the transcribed regions (**Figure 6F**, right panel and **Supplementary Figure S7C**). This potentially points out on more complex and gene-specific effects of *rpb9* deletion on different steps of transcriptional cycle. Rad2 occupancy on transcribed regions was slightly increased in *rpb9* mutant compared to the wild type, especially on the Pol II most-enriched regions (**Figure 6F**, right panel and **Supplementary Figure S7D**). Our ChIP-seq results indicate some gene-specific effects on Pol II occupancy in *rpb9*Δ context (**Supplementary Figure S7E**). Further studies using different approaches are needed to precisely define complex mechanistic consequences of the absence of Rpb9 subunit on gene-specific transcription and TCR.

Figure 6. Effects of *rpb9* deletion on the viability of Med17 mutants and on Mediator, Rad2 and Pol II chromatin occupancy.

(**A**) Spotting assay to determine UV and temperature sensitivity of yeast strains expressing wild type or mutant versions of Med17 in *rad7*Δ or *rad7*Δ *rad26*Δ contexts. Yeast cells were spotted on YPD agar plates, irradiated or not with 10, 20 or 30 J/m^2 UV-C (254 nm) and incubated at 30°C or 25°C for 3 days. (**B**) Spotting assay to determine UV and temperature sensitivity of yeast strains expressing wild type or mutant versions of Med17 in *rad7*Δ, *rad7*Δ *rpb9*Δ or *rpb9*Δ contexts. Yeast cells were spotted on YPD agar plates, irradiated or not with 30 J/m^2 UV-C (254 nm) and incubated at 30°C or 25°C for 3 days. Med17 mutants unable to grow after UV treatment in *rad7*Δ context are also unable to grow at 30°C, in the absence of UV treatment, in *rad7*Δ *rpb9*Δ and *rpb9*Δ contexts. (**C**-**E**) Quantitative ChIP analysis of Mediator, Pol II and Rad2 occupancies under standard growth conditions. Sonicated chromatin from exponentially growing yeasts expressing tagged versions of Med17 (Myc) and Rad2 (HA) in wild type or *rpb9*Δ context was precipitated using α-Myc (**C**), α-Rpb1 (**D**) or α-HA (**E**) antibodies. Quantitative PCR was performed on the precipitated DNA, using primer pairs designed to amplify either regions in open reading frames (O) or in upstream activating sequences (UAS). Relative quantity of an amplicon was determined by comparing the obtained Ct to a standard curve made on the same qPCR plate. Quantities were reported to qPCR performed on Input DNA and are expressed as a percentage. *GAL1-O* and *IGV* amplicons were used as controls. The indicated value is the mean of three biological replicates, and error bars represent the standard deviation.

(**F**) Effects of *rpb9* deletion on genome-wide Mediator, Rad2 and Pol II occupancy. Average tag density in Med17 Mediator ChIP (upper left panel), Rad2 ChIP (lower panels) and Rpb1 Pol II ChIP (upper right panel), around Med15 peaks corresponding to UAS (left panels, 1000bp window), and on transcribed regions of 10% Pol II most-enriched genes (right panels, 500bp before TSS, scaled window between TSS and TES, and 500 bp after TES). Average tag density in wild type and *rpb9*Δ strains is indicated in black and blue, respectively.

Figure 6

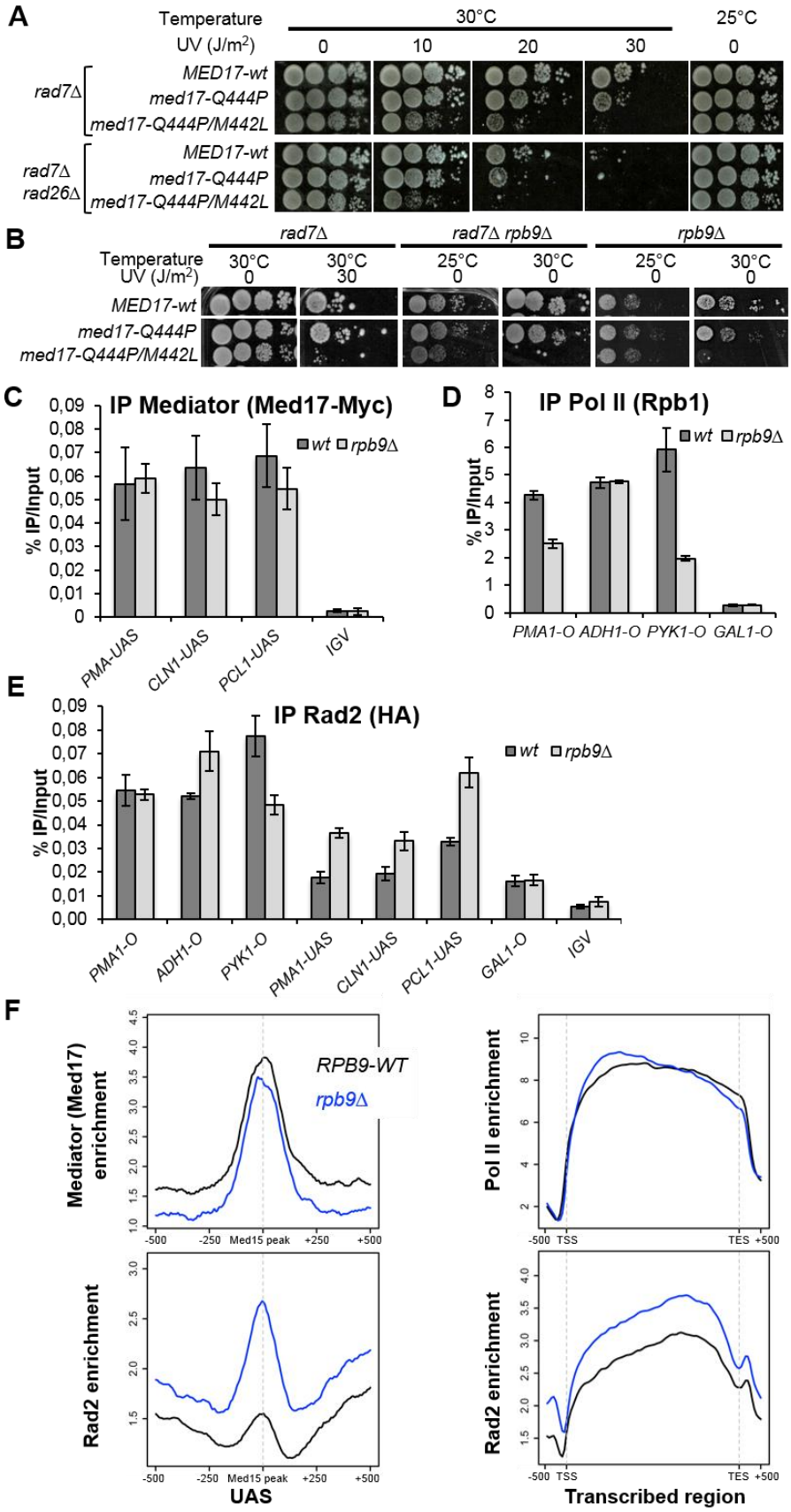
A
Temperature
30°C
25°C
UV (J/m2)
0
10
20
30
0
rad7Δ
MED17-wt
med17-Q444P
med17-Q444P/M442L
rad7Δ rad26Δ
MED17-wt
med17-Q444P
med17-Q444P/M442L
B
rad7Δ
rad7Δ rpb9Δ
rpb9Δ
Temperature
UV (J/m2)
30°C 0
30°C 30
25°C 0
30°C 0
25°C 0
30°C 0
MED17-wt
med17-Q444P
med17-Q444P/M442L
C
IP Mediator (Med17-Myc)
wt rpb9Δ
% IP/Input
PMA-UAS
CLN1-UAS
PCL1-UAS
IGV
D
IP Pol II (Rpb1)
wt rpb9Δ
% IP/Input
PMA1-O ADH1-O PYK1-O GAL1-O
E
IP Rad2 (HA)
wt rpb9Δ
% IP/Input
PMA1-O
ADH1-O
PYK1-O
PMA1-UAS
CLN1-UAS
PCL1-UAS
GAL1-O
IGV
F
RPB9-WT
rpb9Δ
Mediator (Med17) enrichment
Pol II enrichment
Rad2 enrichment
Rad2 enrichment
-500 -250 Med15 peak +250 +500
-500 TSS TES +500
UAS
Transcribed region

Discussion

Model for Rad2 recruitment on regulatory and transcribed regions

The results presented in this work provide strong evidence for a model in which Rad2 shuttles between Mediator bound to regulatory regions and elongating Pol II on transcribed regions in the yeast *Saccharomyces cerevisiae* (**Figure 7**). In this model, Rad2 is first recruited to the UAS by Mediator and is then transferred to the transcribed regions through Mediator/Rad2/Pol II intermediate(s) formed at core promoters. Using mutants that affect Pol II phosphorylation and therefore Mediator chromatin binding, as well as Mediator or Pol II, we obtained several lines of evidence suggesting a mechanism for Rad2 loading on transcribed regions and showing how the presence of Rad2 on the yeast genome is influenced by Mediator and Pol II. At this stage, we could not exclude the possibility that several mechanisms might co-exist for Rad2 recruitment.

We showed that inhibition of Pol II Ser5 phosphorylation in *kin28 ts* mutant, which leads to stabilization of Mediator on core promoters, results in a Rad2 accumulation on regulatory regions and to a lesser extent on core promoters. On the contrary, Rad2 decreases on transcribed regions, together with Pol II decrease. This demonstrates that Rad2 distribution on the chromatin is dependent, at least in part, on the transient interaction between Pol II and Mediator at core promoters. These observations cannot be only explained by the transcriptional defects in *kin28 ts* mutant since it was previously shown that an arrest of transcription in *rpb1-1* mutant leaded to a decrease of Rad2 on both promoter and transcribed regions (Eyboulet et al., 2013). In addition to our ChIP-seq results, coimmunoprecipitation experiments revealed important modifications of interactions between Rad2, Pol II and Mediator when Pol II Ser5 phosphorylation was impaired. Mediator-Pol II interaction was increased in *kin28* mutant, in line with the fact that this phosphorylation promotes Mediator-Pol II dissociation (Schneider et al., 2015; Sogaard and Svejstrup, 2007). An opposite effect was observed for Rad2-Pol II interaction, emphasizing the importance of this phosphorylation step in the interplay between Rad2, Pol II and Mediator.

The two Mediator mutants we chose to study in details (*med17-Q444P* and *med17-Q444P/M442L*) present different UV^s phenotypes and modifications of Rad2 occupancy. Interestingly, Pol II occupancy is globally decreased in a similar way in both mutants (**Figure 5A**, right panel). However, the strongly UV^s mutant *med17-Q444P/M442L* shows lower Rad2 occupancy on transcribed regions and lower correlation between Mediator and Rad2 on promoter regions and especially between Rad2 and Pol II on transcribed regions. In this *med17* UV-sensitive mutant, Rad2 interaction with Mediator is reduced and Mediator interaction with Pol II is increased, in line with our model implying Mediator/Rad2/Pol II intermediate(s). Finally, deletion of Rpb9 Pol II subunit involved in TCR increases Rad2 occupancy on regulatory regions bound by Mediator. In this mutant, a global change in Pol II profile with gene-specific effects is accompanied to some extent by Rad2 repartition on transcribed regions. Consistent with Rad2 shuttling model, our results demonstrate that changes in Pol II composition affect Rad2 chromatin binding both on regulatory and transcribed regions and that the Rad2 loading on regulatory regions is connected to that on transcribed regions. Taken together, our results suggest that Rad2 shuttling is affected by changes in Mediator/Rad2/Pol II interfaces.

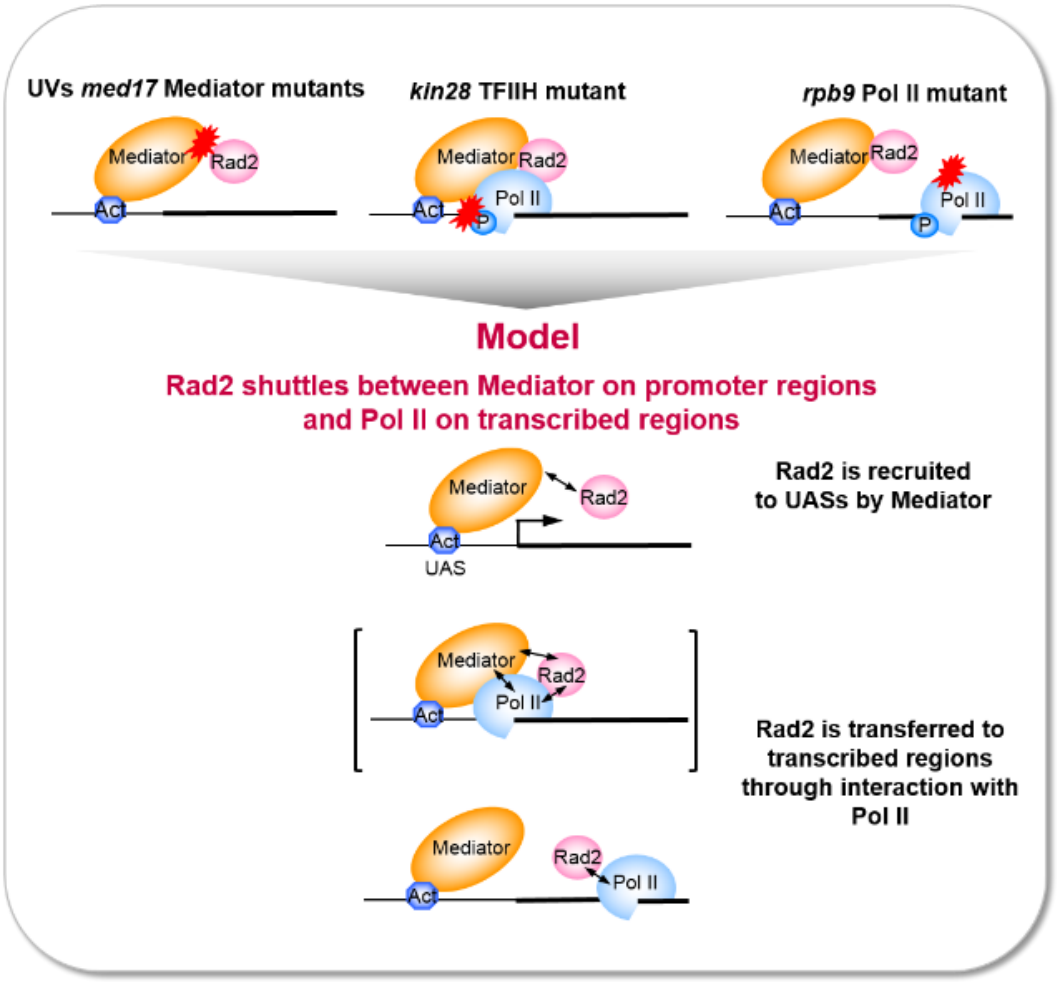

Figure 7. Model for Rad2 recruitment on regulatory and transcribed regions. Using mutants that affect Pol II Ser5 phosphorylation and therefore Mediator chromatin binding (*kin28* TFIIH mutant), Mediator (*med17 UV*^{s} mutants) or Pol II (*rpb9*Δ mutant), we propose a model in which Rad2 shuttles between Mediator bound to regulatory regions and elongating Pol II on transcribed regions. Rad2 is recruited to UAS by Mediator and then transferred to the transcribed regions through Mediator/Rad2/Pol II intermediate(s) (shown in brackets) formed at core promoters. The colour code used is as follows: blue, Activator (Act); orange, Mediator; pink, Rad2; light blue, Pol II. P indicates Ser5 Pol II CTD phosphorylation. Mutated components (Mediator or Pol II) or affected modification (Pol II phosphorylation) are presented as a red star. Double-headed arrows show interactions between Mediator, Rad2 and Pol II.

Interaction interface between Med17 and Rad2

Using Y2H approach, we identified interaction domains between Med17 Mediator subunit and Rad2 protein. Interestingly, Med17 381-681 domain interacting with Rad2 is similar to a Med17 fragment with a globular structure that was crystallized in complex with Med11-Med22 C-terminal helices (Lariviere et al., 2012a). We also specified a 100 amino-acid domain of Rad2 interacting with Med17. This domain is within a crystal structure of catalytic core of Rad2 that however lacks a linker between the two catalytic domains of the protein, making difficult the prediction of possible conformation of the Med17-interacting part (Mietus et al., 2014).

We observed that all Med17 residues affecting Med17-Rad2 Y2H interaction are quite closely located according to *S. cerevisiae* Mediator head structure (Robinson et al., 2012) (**Figure 3D**). This suggests a potential Med17-Rad2 interaction interface, at least in the yeast two-hybrid assay. Recent structural studies also suggest that this region of Med17 may be involved in the interaction with Med14 (Nozawa et al., 2017; Robinson et al., 2015; Tsai et al., 2014; Tsai et al., 2017). Therefore, it is possible that the identified mutants may affect Mediator conformation.

Based on our identification of Med17 domain interacting with Rad2, we performed an extensive mutagenesis analysis demonstrating that UV sensitivity and temperature-sensitivity of Med17 Mediator mutants are highly connected. Our results therefore suggest that Mediator functions in transcription and DNA repair are closely related. We identified specific residues of Med17 (F437, M442, I541) mutations of which were frequently associated with UV sensitivity. We focused our study on M442L mutation, which in association with Q444P strongly increases the UV sensitivity of the yeast cells. Importantly, mutated residues are localized within the conserved domains of Med17 based on multiple sequence alignments and secondary structure features (Bourbon, 2008). These residues correspond to functionally close amino acids in human Med17 protein, suggesting that molecular mechanisms might extend to other eukaryotes. It remains to be determined how these mutations influence Med17 conformation, as well as conformation of the entire Mediator complex leading to UV sensitivity phenotypes and observed changes in Rad2 and Pol II genome-wide occupancy.

Our results further document the central role of Mediator/Pol II interplay in transcription and DNA repair. We observed a global decrease in Pol II occupancy, similar for both *med17* mutants, but a noticeable change in Pol II distribution in *med17* UV^s mutant. It remains to be investigated if this change is related to UV sensitivity phenotype of this mutant. *med17* UV-sensitive mutants are also colethal with a *rpb9*Δ Pol II mutant, while other *med17* mutants are not. This suggests that Mediator might in part compensate the absence of Rpb9 subunit in Pol II and this function is impaired by specific mutations of Med17 Mediator subunit. Interestingly, *med17* UV-sensitive mutations result in stronger Pol II/Mediator interaction. Current structural models do not suggest a direct interaction between Med17 and Rpb9 subunits in PIC assembly. It would be interesting to determine the effects of these mutants on Mediator and Pol II structure. We show that *rpb9* deletion does not result in a global decrease in Pol II occupancy but leads to a global change in Pol II profile with some gene-specific effects. Rpb9 was proposed to have several functions such as transcription start site selection, stimulation of RNA cleavage or resolution of transcription-replication conflicts, in addition to its role in TCR, and the

potential role of Mediator in these processes could be considered.

Transcription-coupled repair mechanisms

Our results are particularly interesting as they shed a new light on the yeast TCR pathway. This work suggests that Mediator role in NER is at least in part independent on Rad26-related pathway and functionally linked to Rpb9 Pol II subunit. In contrast to mammalian cells, yeast cells are able to perform DNA repair of UV-induced damage on transcribed DNA strand even in the absence of *RAD7* GGR-specific and *RAD26* TCR-specific genes and this repair requires the presence of *RPB9* gene (Gaillard et al., 2009; Li and Smerdon, 2002). However, the mechanism involving Rpb9 in TCR remains to be determined (Li and Smerdon, 2002). Recent study showed that *rpb9*Δ, and other Pol II mutations, impaired replication fork progression, suggesting that Pol II itself can help to resolve transcription-replication conflicts (Felipe-Abrio et al., 2015). It is however not known whether this is linked to Rpb9 role in DNA repair. Preliminary results suggest that *med17* UV^s mutants are sensitive to hydroxyurea (**Supplementary Figure S3C**). It would therefore be interesting to determine whether Rpb9 and Mediator may be involved in the removal of stalled Pol II from damages and/or conflicts with the replication machinery.

This study clarifies the mechanism of Rad2 recruitment to transcribed regions. Other proteins involved in TCR, such as Rad26, are known to interact with elongating Pol II. However, in contrast to Rad26, Rad2 does not seem to have an impact on Pol II-dependent transcription (Eyboulet et al., 2013). TCR is a rapid process that requires efficient removal of stalled Pol II from DNA lesions. Recruitment of Rad2 to transcribed regions may thus be a way to maximize TCR efficiency and allow rapid resumption of transcription following damage. It would be interesting to know whether other TCR factors are also present on transcribed genes prior to DNA damage or to find mutants that may prevent Rad2 recruitment to transcribed regions without affecting transcription.

Acknowledgments

We thank C. Thermes, E. Van Dijk and Y. Jaszczyszyn for performing the high throughput-sequencing of ChIP samples, the SPI (CEA/Saclay) for monoclonal antibodies, M. Werner, A. Goldar, S. Marcand, A. Verger and R. Guerois for fruitful discussions, M. Werner for critical reading of the manuscript. This work was supported by the Agence Nationale de la Recherche (ANR-14-CE10-0012-01) and the Fondation ARC (grants n° SL220130607079 and PGA1 RF20170205342). A.G. was supported by a grant from the Fondation ARC (grant n° PDF20131200577), D.G. was supported by a grant from La Ligue Nationale Contre le Cancer.

Author contributions

J.S. designed the study, with contributions from A.G.; A.G., D.G., N.G.A. and M.-B.B. conducted the experiments; C.D.W. performed the bioinformatic analyses with contribution from D.G., E.N. and O.A.; J.S. and A.G. wrote the manuscript, with input from C.D.W. and D.G. All authors commented on the manuscript.

Experimental procedures

1. Strains and plasmids

2. All *S. cerevisiae* strains, plasmids and oligonucleotides used in this study can be found in **Supplemental Table S1**.

To generate yeast strains allowing to test *MED17* mutations, strains with *med17* deletion complemented by a URA-selectable plasmid allowing expression of wild type *MED17 (med17Δ/MED17 URA)* were transformed with a TRP-selectable plasmid allowing expression of wild type or mutated *MED17*. Transformed clones obtained on medium without tryptophan were grown for 2 days on a non-selective medium (YPD), at 25°C to avoid selection of suppressors, then replica-plated on 5-FOA containing medium. After 3 days, plates were replicated again on 5-FOA containing medium, and finally on medium without tryptophan after 3 more days. Incorporation of the plasmid and absence of undesirable mutations was checked by PCR and sequencing.

3. Random mutagenesis of Med17 and mutation screening

We amplified Med17 (382-681) domain in the presence of 7mM $MgCl_2$ and 0.1 (A) or 0.5mM (B) $MnCl_2$ for 30 PCR cycles. PCR product were purified and mixed with a linearized yeast expression vector pVV204 including the coding sequence of Med17 without its C-terminal domain and TRP auxotrophic marker. The mix was co-transformed in a *rad7Δ med17Δ/MED17 URA* yeast strain and plated to have 8000-10000 colonies. MED17 URA vector was then chased by replicating plates on 5-FOA containing medium. Selected colonies were finally replicated on three YPD plates, one kept at 30°C, one at 37°C, and one treated with 30 J/m^2 UVC before being incubated at 30°C in the dark. We looked for clones with either UV-sensitivity or temperature sensitivity phenotypes. Selected clones were streaked on medium without tryptophan (Casamino Acids medium supplemented with adenine and uracil, CAU), and their phenotypes were confirmed by spotting assay. The genomic DNA was then prepared and transformed in DH10b competent cells, using Ampicillin as selectable marker. Mutated vector was purified and retransformed in *rad7Δ med17Δ/MED17 URA* strain, before counterselecting MED17 URA vector on 5-FOA, in order to verify that the observed phenotypes were due to Med17 mutations. When it was the case, the plasmids were sequenced to determine Med17 mutations.

4. Site-directed mutagenesis of Med17

To generate specific mutations, we designed mutagenesis primers with 15-20 nucleotides overhangs surrounding the targeted base mutation in the forward and reverse orientation. Two PCR products were amplified, one with primers Med17-F-attB1 and reverse mutagenesis primer, the other with primer Med17-R-attB2 and forward mutagenesis primer, using Phusion Flash Mastermix (ThermoFisher), according to manufacturer's instructions (15 cycles), using 100ng pVV204-MED17 plasmid as template. PCR products were separated on an agarose gel, the desired gel bands were excised, pooled and purified using Qiaquick Gel Extraction Kit (Qiagen), according to manufacturer's instructions. 20µL of the combined PCR products were mixed with an equal amount of Phusion Flash Mastermix, and 7 PCR cycles were run without primers. 25pmol Med17-F-attB1 and Med17-R-attB2 (2.5µL of a 10µM stock), mixed with 5µL of Phusion Flash Mastermix, were then added to the PCR mix, and 15 PCR cycles were run. 5µL of the reaction were deposited on gel to confirm that the desired PCR product was obtained. The other 45µL were purified using Qiaquick PCR Purification Kit (Qiagen).

For truncations of *MED17* and *RAD2*, attB-containing primers were designed to amplify the desired portion of *MED17/RAD2*. Products were amplified using Phusion Flash Mastermix (ThermoFisher) for 30 cycles, using 100ng YPH500 genomic DNA as template.

PCR products containing attB sites were inserted in pDONR201 plasmid using Gateway BP Clonase II Enzyme mix (ThermoFisher). The obtained donor plasmid was then used to transfer mutated Med17 cassette in pVV212 (for GAL4-DBD fusion constructs), pVV213 (for GAL4-AD fusion constructs) or pVV204 (for yeast expression plasmids with *TRP* auxotrophic marker) Gateway Destination plasmids, using Gateway LR Clonase II Enzyme mix (ThermoFisher), according to manufacturer's instructions.

5. Yeast Two-Hybrid assay

For Yeast Two-Hybrid assay, haploid strains (Y187 and Y190) were respectively transformed with constructs expressing the desired gene in fusion with Gal4 DNA-binding domain (with *TRP* auxotrophic marker) or Gal4 activating domain (with *LEU* auxotrophic marker). Clones growing on (respectively) *-trp* or *-leu* medium were selected and integration of the plasmid was verified by PCR.

Haploid strains growing on *-trp* and *-leu* agar plates were scrapped and resuspended in sterile water. Y187 and Y190 derived strains were mated together by spotting 2.5µL of each suspension on a YPD plate and incubating at 30°C overnight. Patches were replica-plated on *-trp -leu* plates and incubated 3 days at 30°C. Sufficient amounts of diploid yeasts were scraped and resuspended in synthetic defined (SD) medium supplemented with 40mg/L Alanine (SD+2A). Optical Density at 600nm of the suspension was measured, and the suspension was diluted to obtain a OD_{600} of 0.1. 10µL of this dilution were then spotted on agar plates containing either SD+2A medium supplemented with 10mM, 25mM or 50mM 3-amino-1,2,4-triazole (3AT), or *-leu -trp* medium, and incubated for 3 days at 30°C.

When indicated, X-gal staining was done as follows: for one 120mm square petri dish, 10mL 1% Agarose in water was mixed with 10mL Phosphate Buffer (made from 6.15mL 1M K_2HPO_4 and 3.85mL 1M KH_2PO_4 aqueous solutions), both prewarmed at 50°C. 1.2mL N,N-dimethylformamide (DMF), 0.2mL 10% SDS solution (in ddH_2O) and 0.2mL of 4%X-Gal solution (in DMF, kept at -20°C) were successively added to the mix. The mix was then poured onto yeast spots. As soon as solidified, the plate was incubated at 30°C for 24h. Pictures were taken using an office scanner, plate open in direction of the scanner. Luminosity and contrast were adjusted using ImageJ software.

6. Spotting assay

Yeast were grown on YPD plates for 2-3 days at 25°C. Sufficient amounts of cells were scrapped and resuspended in water. Optical Density at 600nm of the suspension was measured, and the suspension was diluted to obtain an OD_{600} of 0.5. Serial dilutions were then led to obtain suspensions with OD_{600} of 0.05, 0.005, and 0.0005. 5µL of each dilution was spotted on YPD agar plates, sometimes supplemented with 4-NQO or hydroxyurea as indicated. Once dried, spots were irradiated with the indicated UV dose using a UV Stratalinker 1800 (Stratagene). Plates were then incubated at 25°C, 30°C or 37°C for 3 days, as indicated. Pictures were taken using an office scanner, plate open in direction of the scanner. Luminosity and contrast were adjusted using ImageJ software.

7. Coimmunoprecipitation

100mL exponentially growing cells were centrifugated, washed and lyzed by bead-beating for 30min at 4°C in WB+ buffer (10% Glycerol, 50mM Hepes-KOH pH 7.5, 150mM NaCl, 1mM EDTA, 0.05% NP-40, 1mM DTT, 1mM PMSF, cOmplete protease inhibitor cocktails (Roche)), as described previously (Eyboulet et al., 2013). Protein concentration was measured using Bradford method, taking bovine serum albumin (BSA) as reference.

Protein extracts were then used for co-IP as follows: 50µL Dynabeads pan-mouse IgG were washed 3 times in PBS containing 0.1% BSA, and incubated 1h with antibodies (1µL anti-HA (12CA5),

2µL anti-Myc (9E10) or 5µL anti-Rpb1-CTD (8WG16),) at 4°C. Beads were washed again three times in PBS/0.1% BSA, then 2 times in WB+ Buffer. 1.5mg of proteins were added to beads and WB+ buffer was added to adjust volume to have the same volume in all samples (at least 50µL). Beads and proteins were incubated together for 3h at 4°C with constant agitation (1300rpm). Beads were then washed 4 times in WB+ Buffer. 40µL SDS Sample Buffer (15% Glycerol, 3% SDS, 75mM Tris-HCl, pH 6.8, 15mM EDTA) was finally added to beads, and samples (with beads) were kept at -80°C until further analysis.

Just prior to SDS-PAGE analysis, samples were thawed, supplemented with 5µL 1M DTT and incubated at 95°C for 2 minutes. Separation was done on 8% bis-acrylamide gels in Tris-Glycine-SDS Buffer, and proteins were transferred on Amersham Protran 0.2 NC membranes (GE Healthcare) for Western blotting. Membranes were preblocked 1h in Tris-Buffered-Saline supplemented with 0.5% Tween 20 (TBS-T) and 5% Milk, then incubated overnight with the indicated antibody in TBS-T with 2% Milk (diluted at 1:10000 for anti-HA (12CA5), 1:5000 for anti-Myc (9E10), or 1:2000 for anti-Rpb1-CTD (8WG16)). After 3 washes in TBS-T, membranes were incubated 45 minutes in TBS-T with 2% Milk containing secondary antibodies diluted at 1:20000 (HRP-anti Mouse-IgG (H+L) (Promega)). After 3 more washes in TBS-T, detection was carried out using Amersham ECL or ECL-Prime reagents (GE Healthcare). Imaging was done using a Fusion FX7 imaging system. Luminosity and contrast were adjusted using ImageJ software.

8. Chromatin immunoprecipitation

Chromatin immunoprecipitation was done as previously described (Eyboulet et al., 2013) except for a sonication step performed on a S220 focused-ultrasonicator (Covaris) in 1mL milliTube (Covaris), for two cycles of 3 minutes spaced by a 30s rest time. Each cycle consisted of 150W pulses for 10% of the time (duty factor 10). Sonicated lysates were then transferred to a new 2mL safe-lock tube and centrifugation was performed at 15000g for 20 minutes. Supernatant was collected and combined with 300µL FA/SDS/PMSF. Sonicated chromatin was divided in 250µL aliquots, snap-frozen in liquid nitrogen and kept at -80°C until further use.

Immunoprecipitation, DNA precipitation and library preparation were done on an IP-Star compact automated system (Diagenode) using built-in programs and following manufacturer's instructions, with the following exceptions (Denby Wilkes et al., in preparation), except for *kin28 ts* and the corresponding wild-type samples prepared as previously described (Eyboulet et al., 2013).

IP was done using the ChIP_IPure_200_D program, at 22°C, with 1h "Ab coating" (Slow speed), 3h "IP reaction" (Medium speed) and 5 minutes "washes" (Fast speed). "Beads wash buffer" was PBS + 0.1% BSA, FA/SDS adjusted to 500mM NaCl was used for "IP Wash 1" and "IP Wash 2", "IP Wash 3" was done with IP Buffer (Tris 10mM pH8, LiCl 0.25M, EDTA 1mM, NP40 0.5%, Na-Deoxycholate 0.5%), "IP Wash 4" was done with TE (Tris 10mM pH 8, EDTA 1mM). "Elution buffer" was the elution buffer (A+B) of Auto iPure kit V2 (Diagenode). "Ab coating mix" was 1µL anti-HA (12CA5), 2µL anti-Myc (9E10) or 5µL anti-Rpb1-CTD (8WG16) completed to 100µL with "Beads wash buffer". "Sample" was 200µL sheared chromatin, supplemented with 4µL BSA and 4µL 50X Protease Inhibitor Cocktail (prepared by dissolving one cOmplete tablet in 1mL ddH_2O). 20µL DiaMag protein A-coated magnetic beads (Diagenode) were used per sample.

After program completion, strips containing the eluates were warmed to redissolve precipitated SDS, eluates were recovered using a magnetic stand, 5µL of

5M NaCl was added to eluates and they were incubated for 4h at 65°C to reverse crosslink. 1µL RNase A (ThermoFisher) was added to eluates and they were then incubated for 30 minutes at 37°C. DNA purification was done on IP-Star system using Auto iPure kit V2 (Diagenode), with iPure program selected (50µL elution), following manufacturer's instructions.

Library preparation for ChIP-seq was performed on IP-Star system using MicroPlex Library Preparation Kit v2 (Diagenode), following manufacturer's instructions.

The ChIP-seq data have been deposited to Array Express under accession number E-MTAB-7081.

ChIP-seq data analysis

ChIP-seq data were analysed using the following procedure. Reads were first trimmed with cutadapt (v1.12, http://dx.doi.org/10.14806/ej.17.1.200) then mapped on *S. cerevisiae* genome (University of California at Santa Cruz [UCSC] version sacCer3) using bowtie2 (v2.2.1, (Langmead and Salzberg, 2012)). Files were converted using Samtools (v1.16, (Li et al., 2009)) and deepTools (v2.4.2-4-99ec5d, (Ramirez et al., 2016)). Read counts were first normalized in RPM (Reads Per Million of mapped reads) then by qPCR data, on a set of selected regions, using the ratio between WT and mutant strains as previously described (Eyboulet et al., 2015). The number of mapped reads for each ChIP-seq experiment and normalization coefficients are indicated in **Supplementary Table S3**. Input DNA and DNA from ChIP with an untagged strain were used as negative controls.

The transcribed regions were determined using the TSS (Transcription Start Sites) and TES (Transcription End Sites) of mRNA genes taken from (Malabat et al., 2015; Pelechano et al., 2013) (n=5337). In each experiment, transcribed regions were grouped in deciles based on their average Pol II occupancy signal in the wild type. Med15 and Rad3 peaks were called from the data in (Eyboulet et al., 2013; Eyboulet et al., 2015; Eychenne et al., 2017) using MACS2 (v2.1.10) and filtered (fold-change >2.5 and p value < 1e-10) (n=561 for Med15 and n=2411 for Rad3). Peaks that were further than 1kb away from a TSS were discarded. Promoter regions (n=4068) were defined as corresponding intergenic regions in tandem or in divergent orientation in yeast genome excluding intergenic regions encompassing Pol III-transcribed genes. In order to avoid potential biases that could arise from low enrichment of Rad2 ChIP, we focused our analysis on the most Pol II-enriched decile. All correlations were calculated with Spearman method (Hollander, 1973). All figures were prepared using R packages (https://www.R-project.org/). Data visualization package for R ggplot2 was used to prepare Supplementary Figures S4 and S5 (Wickham, 2009).

References

Bourbon, H.M. (2008). Comparative genomics supports a deep evolutionary origin for the large, four-module transcriptional mediator complex. Nucleic Acids Res *36*, 3993-4008.

Chen, X., Ruggiero, C., and Li, S. (2007). Yeast Rpb9 plays an important role in ubiquitylation and degradation of Rpb1 in response to UV-induced DNA damage. Mol Cell Biol *27*, 4617-4625.

Cismowski, M.J., Laff, G.M., Solomon, M.J., and Reed, S.I. (1995). KIN28 encodes a C-terminal domain kinase that controls mRNA transcription in Saccharomyces cerevisiae but lacks cyclin-dependent kinase-activating kinase (CAK) activity. Mol Cell Biol *15*, 2983-2992.

Eyboulet, F., Cibot, C., Eychenne, T., Neil, H., Alibert, O., Werner, M., and Soutourina, J. (2013). Mediator links transcription and DNA repair by facilitating Rad2/XPG recruitment. Genes Dev *27*, 2549-2562.

Eyboulet, F., Wydau-Dematteis, S., Eychenne, T., Alibert, O., Neil, H., Boschiero, C., Nevers, M.C., Volland,

H., Cornu, D., Redeker, V., *et al.* (2015). Mediator independently orchestrates multiple steps of preinitiation complex assembly in vivo. Nucleic Acids Res *43*, 9214-9231.

Eychenne, T., Werner, M., and Soutourina, J. (2017). Toward understanding of the mechanisms of Mediator function in vivo: Focus on the preinitiation complex assembly. Transcription *8*, 328-342.

Felipe-Abrio, I., Lafuente-Barquero, J., Garcia-Rubio, M.L., and Aguilera, A. (2015). RNA polymerase II contributes to preventing transcription-mediated replication fork stalls. EMBO J *34*, 236-250.

Gaillard, H., Tous, C., Botet, J., Gonzalez-Aguilera, C., Quintero, M.J., Viladevall, L., Garcia-Rubio, M.L., Rodriguez-Gil, A., Marin, A., Arino, J., *et al.* (2009). Genome-wide analysis of factors affecting transcription elongation and DNA repair: a new role for PAF and Ccr4-not in transcription-coupled repair. PLoS Genet *5*, e1000364.

Hanawalt, P.C., and Spivak, G. (2008). Transcription-coupled DNA repair: two decades of progress and surprises. Nat Rev Mol Cell Biol *9*, 958-970.

Hollander, M.W., D.A. (1973). Nonparametric Statistical Methods (New York: John Wiley & Sons).

Imasaki, T., Calero, G., Cai, G., Tsai, K.L., Yamada, K., Cardelli, F., Erdjument-Bromage, H., Tempst, P., Berger, I., Kornberg, G.L., *et al.* (2011). Architecture of the Mediator head module. Nature *475*, 240-243.

Ito, S., Kuraoka, I., Chymkowitch, P., Compe, E., Takedachi, A., Ishigami, C., Coin, F., Egly, J.M., and Tanaka, K. (2007). XPG stabilizes TFIIH, allowing transactivation of nuclear receptors: implications for Cockayne syndrome in XP-G/CS patients. Molecular cell *26*, 231-243.

Jeronimo, C., Langelier, M.F., Bataille, A.R., Pascal, J.M., Pugh, B.F., and Robert, F. (2016). Tail and Kinase Modules Differently Regulate Core Mediator Recruitment and Function In Vivo. Molecular cell *64*, 455-466.

Jeronimo, C., and Robert, F. (2014). Kin28 regulates the transient association of Mediator with core promoters. Nature structural & molecular biology *21*, 449-455.

Kikuchi, Y., Umemura, H., Nishitani, S., Iida, S., Fukasawa, R., Hayashi, H., Hirose, Y., Tanaka, A., Sugasawa, K., and Ohkuma, Y. (2015). Human mediator MED17 subunit plays essential roles in gene regulation by associating with the transcription and DNA repair machineries. Genes Cells *20*, 191-202.

Koleske, A.J., and Young, R.A. (1994). An RNA polymerase II holoenzyme responsive to activators. Nature *368*, 466-469.

Kornberg, R.D. (2005). Mediator and the mechanism of transcriptional activation. Trends Biochem Sci *30*, 235-239.

Lagerwerf, S., Vrouwe, M.G., Overmeer, R.M., Fousteri, M.I., and Mullenders, L.H. (2011). DNA damage response and transcription. DNA Repair (Amst) *10*, 743-750.

Langmead, B., and Salzberg, S.L. (2012). Fast gapped-read alignment with Bowtie 2. Nat Methods *9*, 357-359.

Lariviere, L., Plaschka, C., Seizl, M., Wenzeck, L., Kurth, F., and Cramer, P. (2012a). Structure of the Mediator head module. Nature *492*, 448-451.

Lariviere, L., Seizl, M., and Cramer, P. (2012b). A structural perspective on Mediator function. Curr Opin Cell Biol *24*, 305-313.

Le May, N., Fradin, D., Iltis, I., Bougneres, P., and Egly, J.M. (2012). XPG and XPF endonucleases trigger chromatin looping and DNA demethylation for accurate expression

of activated genes. Molecular cell *47*, 622-632.

Le May, N., Mota-Fernandes, D., Velez-Cruz, R., Iltis, I., Biard, D., and Egly, J.M. (2010). NER factors are recruited to active promoters and facilitate chromatin modification for transcription in the absence of exogenous genotoxic attack. Molecular cell *38*, 54-66.

Li, H., Handsaker, B., Wysoker, A., Fennell, T., Ruan, J., Homer, N., Marth, G., Abecasis, G., Durbin, R., and Genome Project Data Processing, S. (2009). The Sequence Alignment/Map format and SAMtools. Bioinformatics *25*, 2078-2079.

Li, S., and Smerdon, M.J. (2002). Rpb4 and Rpb9 mediate subpathways of transcription-coupled DNA repair in Saccharomyces cerevisiae. EMBO J *21*, 5921-5929.

Malabat, C., Feuerbach, F., Ma, L., Saveanu, C., and Jacquier, A. (2015). Quality control of transcription start site selection by nonsense-mediated-mRNA decay. Elife *4*.

Malik, S., and Roeder, R.G. (2010). The metazoan Mediator co-activator complex as an integrative hub for transcriptional regulation. Nat Rev Genet *11*, 761-772.

Marteijn, J.A., Lans, H., Vermeulen, W., and Hoeijmakers, J.H. (2014). Understanding nucleotide excision repair and its roles in cancer and ageing. Nat Rev Mol Cell Biol *15*, 465-481.

Mietus, M., Nowak, E., Jaciuk, M., Kustosz, P., Studnicka, J., and Nowotny, M. (2014). Crystal structure of the catalytic core of Rad2: insights into the mechanism of substrate binding. Nucleic Acids Res *42*, 10762-10775.

Mullenders, L. (2015). DNA damage mediated transcription arrest: Step back to go forward. DNA Repair (Amst) *36*, 28-35.

Nonet, M.L., and Young, R.A. (1989). Intragenic and extragenic suppressors of mutations in the heptapeptide repeat domain of Saccharomyces cerevisiae RNA polymerase II. Genetics *123*, 715-724.

Nozawa, K., Schneider, T.R., and Cramer, P. (2017). Core Mediator structure at 3.4 A extends model of transcription initiation complex. Nature *545*, 248-251.

Pelechano, V., Wei, W., and Steinmetz, L.M. (2013). Extensive transcriptional heterogeneity revealed by isoform profiling. Nature *497*, 127-131.

Petrenko, N., Jin, Y., Wong, K.H., and Struhl, K. (2016). Mediator Undergoes a Compositional Change during Transcriptional Activation. Molecular cell *64*, 443-454.

Plaschka, C., Lariviere, L., Wenzeck, L., Seizl, M., Hemann, M., Tegunov, D., Petrotchenko, E.V., Borchers, C.H., Baumeister, W., Herzog, F., *et al.* (2015). Architecture of the RNA polymerase II-Mediator core initiation complex. Nature *518*, 376-380.

Poss, Z.C., Ebmeier, C.C., and Taatjes, D.J. (2013). The Mediator complex and transcription regulation. Crit Rev Biochem Mol Biol *48*, 575-608.

Ramirez, F., Ryan, D.P., Gruning, B., Bhardwaj, V., Kilpert, F., Richter, A.S., Heyne, S., Dundar, F., and Manke, T. (2016). deepTools2: a next generation web server for deep-sequencing data analysis. Nucleic Acids Res *44*, W160-165.

Robinson, P.J., Bushnell, D.A., Trnka, M.J., Burlingame, A.L., and Kornberg, R.D. (2012). Structure of the mediator head module bound to the carboxy-terminal domain of RNA polymerase II. Proc Natl Acad Sci U S A *109*, 17931-17935.

Robinson, P.J., Trnka, M.J., Bushnell, D.A., Davis, R.E., Mattei, P.J., Burlingame, A.L., and Kornberg, R.D. (2016). Structure of a Complete Mediator-RNA Polymerase II Pre-

Initiation Complex. Cell *166*, 1411-1422 e1416.

Robinson, P.J., Trnka, M.J., Pellarin, R., Greenberg, C.H., Bushnell, D.A., Davis, R., Burlingame, A.L., Sali, A., and Kornberg, R.D. (2015). Molecular architecture of the yeast Mediator complex. Elife *4*.

Ruan, W., Lehmann, E., Thomm, M., Kostrewa, D., and Cramer, P. (2011). Evolution of two modes of intrinsic RNA polymerase transcript cleavage. J Biol Chem *286*, 18701-18707.

Sarker, A.H., Tsutakawa, S.E., Kostek, S., Ng, C., Shin, D.S., Peris, M., Campeau, E., Tainer, J.A., Nogales, E., and Cooper, P.K. (2005). Recognition of RNA polymerase II and transcription bubbles by XPG, CSB, and TFIIH: insights for transcription-coupled repair and Cockayne Syndrome. Molecular cell *20*, 187-198.

Schiano, C., Casamassimi, A., Rienzo, M., de Nigris, F., Sommese, L., and Napoli, C. (2014). Involvement of Mediator complex in malignancy. Biochim Biophys Acta *1845*, 66-83.

Schneider, M., Hellerschmied, D., Schubert, T., Amlacher, S., Vinayachandran, V., Reja, R., Pugh, B.F., Clausen, T., and Kohler, A. (2015). The Nuclear Pore-Associated TREX-2 Complex Employs Mediator to Regulate Gene Expression. Cell *162*, 1016-1028.

Sogaard, T.M., and Svejstrup, J.Q. (2007). Hyperphosphorylation of the C-terminal repeat domain of RNA polymerase II facilitates dissociation of its complex with mediator. J Biol Chem *282*, 14113-14120.

Sollier, J., Stork, C.T., Garcia-Rubio, M.L., Paulsen, R.D., Aguilera, A., and Cimprich, K.A. (2014). Transcription-coupled nucleotide excision repair factors promote R-loop-induced genome instability. Molecular cell *56*, 777-785.

Soutourina, J. (2018). Transcription regulation by the Mediator complex. Nat Rev Mol Cell Biol *19*, 262-274.

Soutourina, J., Wydau, S., Ambroise, Y., Boschiero, C., and Werner, M. (2011). Direct interaction of RNA polymerase II and mediator required for transcription in vivo. Science *331*, 1451-1454.

Spaeth, J.M., Kim, N.H., and Boyer, T.G. (2011). Mediator and human disease. Semin Cell Dev Biol *22*, 776-787.

Svejstrup, J.Q. (2002). Mechanisms of transcription-coupled DNA repair. Nat Rev Mol Cell Biol *3*, 21-29.

Svejstrup, J.Q. (2007). Contending with transcriptional arrest during RNAPII transcript elongation. Trends Biochem Sci *32*, 165-171.

Thompson, C.M., Koleske, A.J., Chao, D.M., and Young, R.A. (1993). A multisubunit complex associated with the RNA polymerase II CTD and TATA-binding protein in yeast. Cell *73*, 1361-1375.

Trego, K.S., Groesser, T., Davalos, A.R., Parplys, A.C., Zhao, W., Nelson, M.R., Hlaing, A., Shih, B., Rydberg, B., Pluth, J.M., *et al.* (2016). Non-catalytic Roles for XPG with BRCA1 and BRCA2 in Homologous Recombination and Genome Stability. Molecular cell *61*, 535-546.

Tsai, K.L., Tomomori-Sato, C., Sato, S., Conaway, R.C., Conaway, J.W., and Asturias, F.J. (2014). Subunit architecture and functional modular rearrangements of the transcriptional mediator complex. Cell *157*, 1430-1444.

Tsai, K.L., Yu, X., Gopalan, S., Chao, T.C., Zhang, Y., Florens, L., Washburn, M.P., Murakami, K., Conaway, R.C., Conaway, J.W., *et al.* (2017). Mediator structure and rearrangements required for holoenzyme formation. Nature *544*, 196-201.

Verhage, R.A., van Gool, A.J., de Groot, N., Hoeijmakers, J.H., van de Putte, P.,

and Brouwer, J. (1996). Double mutants of Saccharomyces cerevisiae with alterations in global genome and transcription-coupled repair. Mol Cell Biol *16*, 496-502.

Vermeulen, W., and Fousteri, M. (2013). Mammalian transcription-coupled excision repair. Cold Spring Harb Perspect Biol *5*, a012625.

Wickham, H. (2009). ggplot2: Elegant Graphics for Data Analysis (Springer-Verlag New York).

Wong, K.H., Jin, Y., and Struhl, K. (2014). TFIIH Phosphorylation of the Pol II CTD Stimulates Mediator Dissociation from the Preinitiation Complex and Promoter Escape. Molecular cell *54*, 601-612.

Ziegler, L.M., Khaperskyy, D.A., Ammerman, M.L., and Ponticelli, A.S. (2003). Yeast RNA polymerase II lacking the Rpb9 subunit is impaired for interaction with transcription factor IIF. J Biol Chem *278*, 48950-48956.

II. Mediator's link to other NER proteins

To precise the link between Mediator and the NER machinery, we investigated whether Mediator functionally interacted with other NER proteins. We tested five NER proteins Rad1/XPF, Rad10/ERCC1, Rad26/CSB, Rad4/XPC and Rad14/XPA which have functions at different steps of the NER pathway. Rad26/CSB is a TC-NER specific protein, involved in damage recognition. Rad4/XPC is involved in damage recognition step of the GG-NER sub-pathway. Rad1/XPF and Rad10/ERCC1 form a dimer with a 5' endonuclease activity involved in damage excision. Rad14/XPA is implicated in damage verification and assembly of the NER machinery.

In this chapter the term NER proteins will be used for Rad1, Rad10, Rad26, Rad4, Rad14 and Rad2.

II.1 Physical interaction between Mediator and NER proteins

As a first step, we carried out coimmunoprecipitation (CoIP) experiments to identify new interacting partners of Mediator. We constructed strains containing Mediator Med17 subunit Myc-tagged in addition to HA-tagged or Flag-tagged NER proteins. To test whether the tagged versions of proteins are functional, we carried out a spotting assay with the cells irradiated or not with UV (Figure 21).

Rad26 is a TC-NER protein whose deletion does not lead to UV-sensitivity in yeast (van Gool *et al.,* 1994). Therefore, to test whether Rad26 HA-tagged proteins were functional, strains containing C-terminal or N-terminal HA-tagged version of Rad26 were constructed in a GG-NER deficient context (*rad7Δ*). We observed that *rad7Δ rad26Δ* strain was more sensitive than the *rad7Δ* strain (Figure 21A) as expected and previously reported (Eyboulet *et al.,* 2013). Furthermore in GG-NER deficient context, we observed that strain carrying N-terminal HA-tagged Rad26 (HA-Rad26) is very comparable to *rad7Δ* strain and less UV-sensitive than the *rad7Δ rad26Δ* strain (Figure 21), suggesting that the N-terminal HA-tagged Rad26 is functional. However, the strain carrying C-terminal HA-tagged Rad26 (Rad26-HA) is more sensitive than *rad7Δ,* suggesting that this tagged version of Rad26 may not be completely functional. Therefore, the N-terminal HA-tagged Rad26 was used.

The other NER proteins namely Rad1, Rad10, Rad4, Rad14 and Rad2 are either common to NER sub-pathways or act in GG-NER, therefore there was no need to carry out UV-sensitivity assay in GG-NER-deficient context. We observed that after UV-treatment, there was no difference in UV-sensitivity phenotype in tagged strains compared to untagged strain (NT). Therefore, these strains can be used for CoIP experiments.

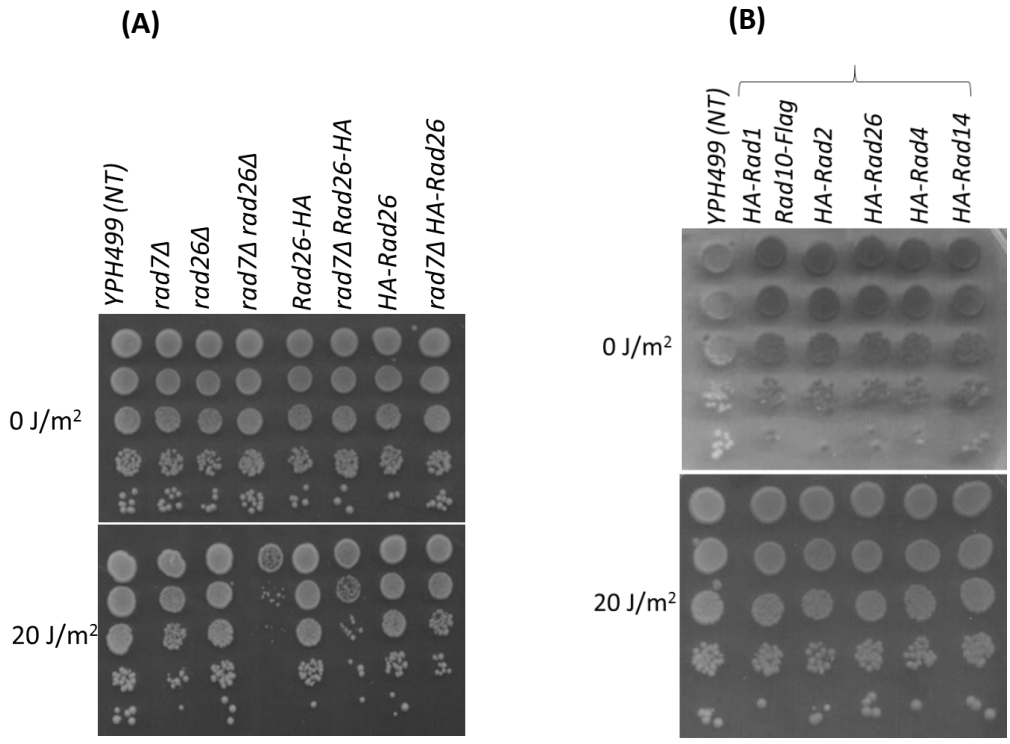

Figure 21: Growth phenotypes of strains carrying tagged NER proteins after UV treatment.

Strains were serially diluted, spotted on indicated agar plates, and incubated for 3 days at 30°C. For UV-sensitivity assays, cells were treated or not with 20J/m^2 of UV (UV Stratalinker 1800). (A) To test Rad26 strain sensitivity, strains carrying N-terminal or C-terminal HA-tagged version of Rad26 in GG-NER deficient context (*rad7Δ*) strains were constructed. (B) Strains carrying C-terminal Myc-tagged Med17 (Med17-Myc) and NER HA-tagged proteins were constructed. One strain contained three tags: C-terminal Myc-tagged Med17 (Med17-Myc), N-terminal HA-tagged Rad1 (HA-Rad1) and C-terminal Flag-tagged Rad10 (Rad10-Flag). A control strain that did not contain any tag (no tag, NT) was used.

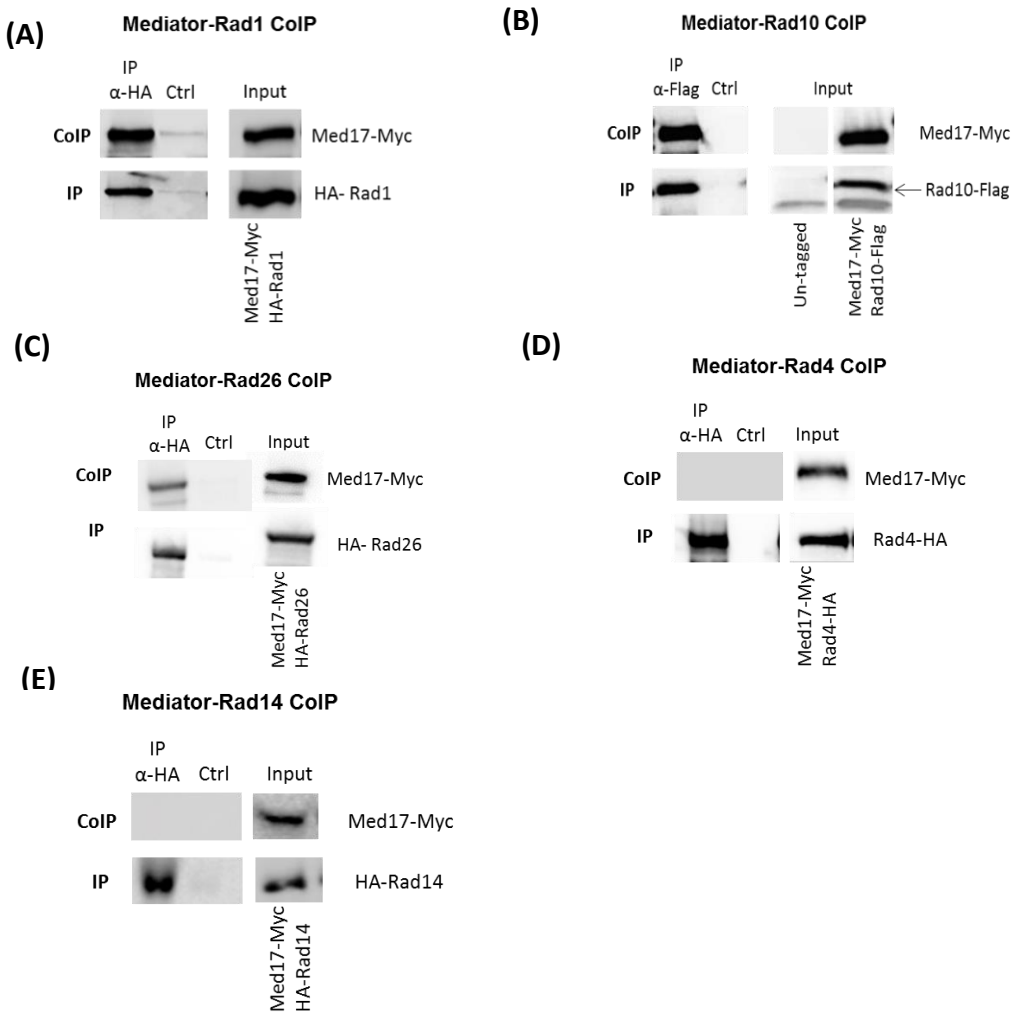

Figure 22: Interaction between the Mediator complex and NER proteins.

HA-tagged (A) Rad1, (C) Rad26, (D) Rad4 and (E) Rad14 were immunoprecipitated (IP) with α-HA antibody and (B) Rad10 with an α-Flag antibody from crude yeast extracts, from cells grown at 30°C, and analysed by Western blotting with α-Myc antibody against Med17-Myc (co-IP). Ctrl: Control IP was carried out on yeast extract lacking HA-tag or using IgG beads not coated with α-HA antibodies.

In our experimental conditions, the Mediator subunit remained associated within the complex. Though we reveal one subunit, it is the whole complex that interacts with the different NER proteins. Crude protein extracts from these strains were used to immunoprecipitate NER proteins with either α-HA antibody or α -Flag antibody and analysis by Western blotting revealed Mediator (Med17-Myc) if there is co-immunoprecipitation (Figure 22).

We observed that, in the absence of genotoxic stress, Mediator interacts with NER proteins Rad1, Rad10 and Rad26. Moreover, in our CoIP conditions, we do not observe any interaction with Rad14 and GG-NER protein Rad4.

In conclusion, we identified three more NER proteins (Rad1, Rad10, Rad26) interacting with the Mediator complex in addition to Rad2. Interestingly, Rad1 and Rad10 form a dimer with a 5' endonuclease activity while Rad2 is the 3' endonuclease in NER. Rad26, on the other

hand, is a TC-NER specific protein and previous results have suggested that Mediator might be in part implicated in Rad26-independent TC-NER (Article1).

II.2 Genome-wide occupancy analysis of Rad1, Rad10 and Rad26

To further characterise the new interactions between Mediator and NER proteins Rad1, Rad10 and Rad26, their genomic distribution profiles were compared. To date, no genome-wide data of Rad1, Rad10 and Rad26 occupancies are available, ChIP-seq experiments were hence performed. Moreover, for comparison of genomic profiles, ChIP-seq data already present in the laboratory for Mediator (Med15), Rad2 and RNA Pol II (Rpb1) were used (Eyboulet *et al.*, 2013).

First, quantitative ChIP analysis experiments were conducted on selected regions (Figure 23).

Quantitative ChIP experiments were carried out on selected RNA Pol II-transcribed (class II) genes and a RNA Pol II-transcribed (class III) gene. We tested the enrichment of C-terminal HA-tagged Rad1 and Rad10 and N-terminal HA-tagged Rad1 and Rad10 (Figure 23A, B). To note that none of these strains were UV-sensitive (data not shown), indicating that both HA-tagged versions of Rad1 and Rad10 were functional. We observed that Rad1 and Rad10 were predominantly enriched on ORFs (Open Reading Frames) of the tested class II genes, compared to the negative controls (*IGV*, *GAL1-O*). Rad1 and Rad10 were also enriched on the tested class III gene. Furthermore, we observed a better enrichment for C-terminal HA-tagged Rad1 (Rad1-HA) than the N-terminally tagged protein (HA-Rad1) (Figure 23A). For Rad10, the enrichment of both tagged versions were roughly similar, except for few regions where the C-terminally tagged version has a better enrichment (Figure 23B). Therefore, Rad1-HA and Rad10-HA were used for ChIP-seq experiments.

The N-terminal HA-tagged Rad26 strain was used as Rad26 C-terminal HA-tagged strain was UV-sensitive (Figure 21A). We observed that Rad26 was enriched on ORFs compared to the negative control (Figure 23C).

In conclusion, Rad1-HA, Rad10-HA and HA-Rad26 are particularly enriched on tested ORFs and ChIP-seq experiments was then carried out to get the genomic distribution of these NER proteins.

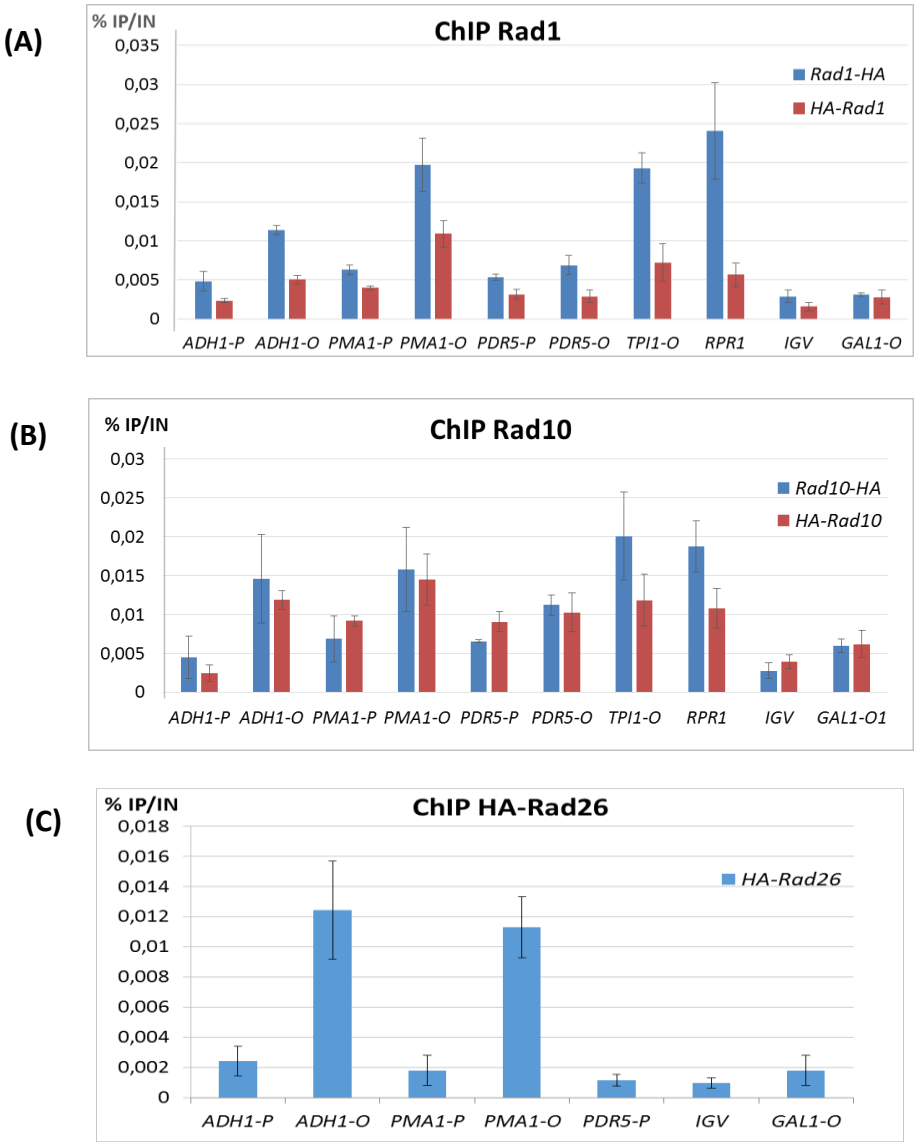

Figure 23: ChIP analysis of Rad1, Rad10 and Rad26 occupancies on selected class II genes.

(A) Quantitative ChIP analysis of (A) Rad1, (B) Rad10 and (C) Rad26 occupancies on selected genes. Yeast strains carrying either N-terminal HA-tagged proteins (HA-Rad1, HA-Rad10 and Rad26) or C-terminal HA-tagged versions (Rad1-HA, Rad10-HA) were grown in YPD complete medium at 30°C. Immunoprecipitated fragments, using α-HA antibody, from ChIP experiments were amplified with primers corresponding to selected class II gene promoters (P) or ORFs (O) and a class III gene (*RPR1*). A *GAL1* ORF and a non-transcribed region on chromosome V (IGV) were used as negative controls. The displayed values represent the percentage of immunoprecipitated fragments (IP) relative to the input (IN). Mean values and standard deviation (indicated by error bars) of three independent experiments are shown.

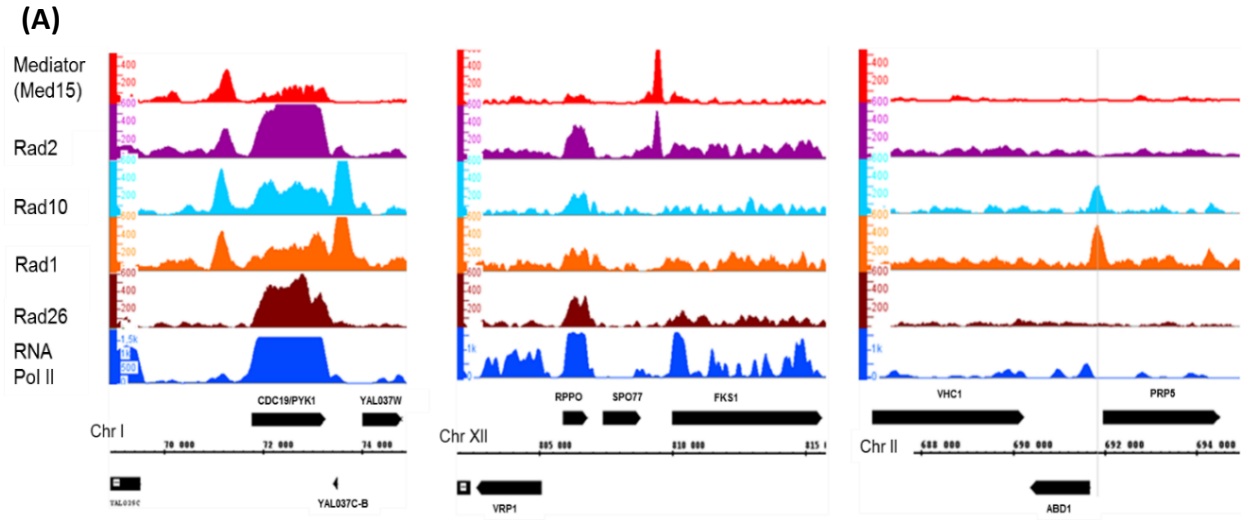

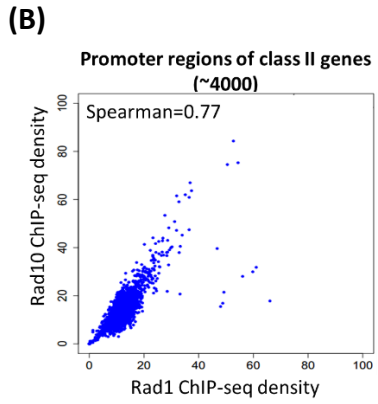

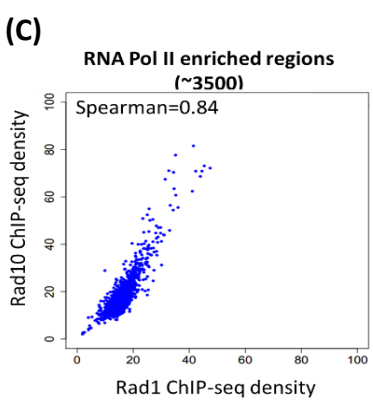

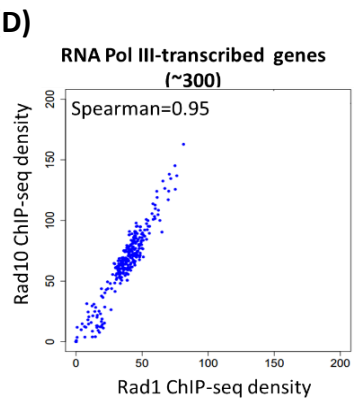

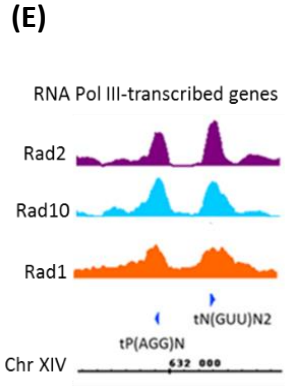

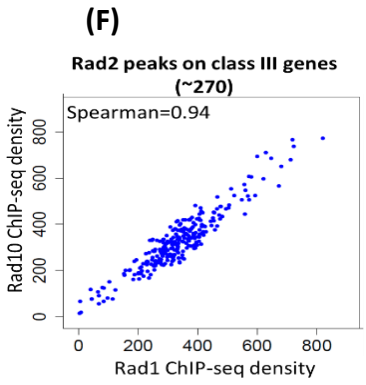

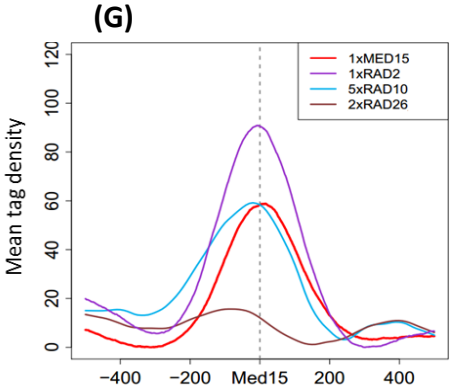

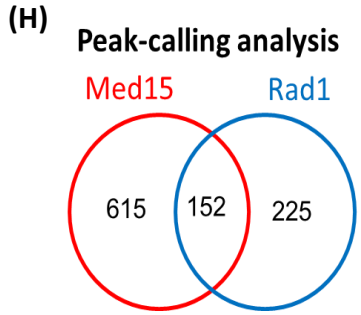

(I)

Spearman Correlation on class II transcribed regions

	Rad10	Rad26	Rad2	RNA Pol II
Rad10	1	0.83	0.74	0.58
Rad26	0.83	1	0.76	0.67
Rad2	0.74	0.76	1	0.78
RNA Pol II	0.58	0.67	0.78	1

Figure 24: Genome-wide analysis of Rad1, Rad10 and Rad26 chromatin occupancies.

Rad1, Rad10 and Rad26 enrichment profiles were assessed from ChIP-seq experiments with Rad1-HA, Rad10-HA and HA-Rad26 strains grown at 30°C in YPD complete medium. (A, E) Examples of ChIP-seq enrichment profiles of Rad1, Rad10 and Rad26. Densities of sequence tags were displayed after subtraction of data from the normalized untagged strain. These profiles were compared to that of Rad2, Mediator and RNA Pol II (Eyboulet *et al*., 2013). (B-D, F) Spearman correlation between Rad1 and Rad10 was calculated on tag densities scaled per million reads (RPM). The tag densities of Rad1 and Rad10 were calculated on (B) class II promoter regions of RNA Pol II-transcribed genes (4068 regions), (C) RNA Pol II-enriched transcribed regions (3552 regions), (D) RNA Pol III-transcribed genes (310 regions), and (F) on Rad2 enriched class III genes. Each point on the plot corresponds to one region. Promoter regions correspond to intergenic regions for RNA Pol II-transcribed genes in tandem or in divergent orientation, excluding intergenic regions encompassing RNA Pol II-transcribed genes. (G) Density profiles of Rad10 and Rad26 around the maximum of Med15 peaks (767), obtained by peak-calling software MACS2. The mean distribution profile of Rad10 was compared to that of Mediator and Rad2 on class II promoter regions. The peaks are oriented in respect to the TSS (Transcription Start Site). (H) Mediator and Rad10 enriched promoter regions were detected by peak-calling software, MACS2. (I) Pairwise Spearman correlation coefficients between NER proteins and RNA Pol II on transcribed regions of class II genes.

In vivo, Rad1 and Rad10 form a highly stable complex in yeast and complex formation is essential for their biological functions (Bailly *et al.,* 1992). Analysis of our ChIP-seq data showed that both Rad1 and Rad10 are enriched on promoter and transcribed regions of class II genes (RNA Pol II-transcribed genes) as illustrated in Figure 24A. Moreover, they were also found on class III genes (RNA Pol III-transcribed genes), similarly to Rad2 (Figure 24E). Genome-wide correlation analysis showed that Rad1 and Rad10 were strongly correlated, on a genome-wide scale, on the promoter regions (Spearman correlation coefficient = 0.77, Figure 24B) and on transcribed regions (Spearman correlation coefficient = 0.84, Figure 24C) of RNA Pol II-transcribed genes. In addition, Rad1 and Rad10 were very strongly correlated on class III genes as well (Spearman correlation coefficient = 0.95, Figure 24D). Rad2 was also reported to be enriched on class III genes (Eyboulet *et al.*, 2013, Figure 24E), therefore we tested whether Rad1 and Rad10 were present on class III genes enriched by Rad2. We used a peak-calling software, MACS2, which allowed the detection of Rad2 enrichment peaks over class III genes (272 peaks detected). The enrichment densities of Rad1 and Rad10 were calculated on these Rad2-encriched class III genes. We observed that Rad1 and Rad10 were highly correlated on Rad2-enriched class III genes (Figure 24F). Therefore, Rad1 and Rad10 co-occupied class III genes with Rad2. Thus, we showed that Rad1 and Rad10 are strongly correlated on a genome-wide scale on class II gene regions and class III genes, in agreement with their function as a dimer. For further analysis, Rad10 data was used as representative of Rad1 and Rad10 genomic behaviour, hereafter termed Rad1-Rad10, because the background noise was higher in Rad1 ChIP-seq data.

Mediator is essential for the transcription of almost all class II genes, and given that the object of this study is to characterise the link between NER proteins and Mediator, we focused our study on class II genes.

To investigate the link between Mediator, Rad2 and Rad1-Rad10, their genomic profiles were compared relative to Mediator enriched regions. Hence, we used a peak-calling software, MACS2, which allowed the detection of Mediator (Med15 subunit) enrichment peaks. The mean ChIP-seq tag densities for each protein were calculated for regions corresponding to oriented promoter regions of class II genes in tandem, excluding intergenic regions encompassing RNA Pol III transcribed genes, centered on Med15 enrichment peaks. The mean distributions of Rad2 and Mediator were also plotted and we observed an enrichment around Med15 peaks (Figure 24G), confirming previously obtained results (Eyboulet *et al*., 2013). We found that Rad1-Rad10 enrichment profile, around Med15 peaks, coincided with those of Rad2 and Mediator (Figure 24G), and hence showing that promoter regions were indeed co-occupied by Mediator and Rad1-Rad10 on a global scale.

Furthermore, we identified peaks of Rad1-Rad10 (377 peaks) and Mediator (767 peaks) by peak-calling software MACS2 on promoter regions of class II genes (Figure 24H). Furthermore, only a portion of RNA Pol II-transcribed gene promoters were co-occupied by Rad1-Rad10 and Mediator (152 common regions). Therefore, only 40% of Rad1-Rad10 enriched promoter regions were occupied by Mediator as well. This indicated that there were 3 categories of genes: a first category enriched with all four proteins, a second category enriched with Mediator and Rad2 only and a third category enriched with Rad1 and Rad10 only, as illustrated by example of enrichment profiles of these proteins in Figure 24A. To note that the promoter regions tested in qPCR (Figure 24A, B) for Rad1-Rad10 enrichment were also not enriched in our genome-wide analysis and present in the gene group where only Mediator and Rad2 are enriched.

Moreover, global analysis of class II transcribed regions, where most of RNA Pol II ChIP-seq signals are present, we observed a good correlation between Rad1-Rad10 and NER proteins (Rad2 and Rad26). However, no strong correlation was observed between Rad1-Rad10 and RNA Pol II (Figure 24I).

Another protein we have shown to interact with Mediator is Rad26. Analysis of Rad26 ChIP-seq data showed that it is mainly enriched on transcribed regions, as illustrated by examples of enrichment profiles of class II genes in Figure 24A. Moreover, Rad26 correlates well with other NER proteins (Rad1-Rad10, Rad2) on class II transcribed regions while less strongly correlated with RNA Pol II (Figure 24I). To note that among the NER proteins tested (Rad1, Rad10, Rad26 and Rad2), Rad2 is the most strongly correlated with RNA Pol II. Mean enrichment density was calculated for Rad26 around Med15 peaks and no particular enrichment of Rad26 was observed on these regions (Figure 24G). Indeed, there was no distinct peak of Rad26 around Mediator peaks, the low signal observed is more characteristic of a background noise.

In conclusion, NER proteins Rad1, Rad10 and Rad26 are present on the chromatin even in the absence of genotoxic stress, similarly to what has been previously observed for Rad2 (Eyboulet *et al.*, 2013). Moreover, Mediator co-occupies certain promoter regions with

Rad1-Rad10 (40%). Rad26 does not seem to be specifically enriched on promoter regions occupied by Mediator (Figure 24G). Rad1, Rad10 and Rad26 are all enriched on the transcribed regions, more or less linked to RNA Pol II presence as demonstrated by the varying correlation coefficients (Figure 24I).

II.3 Rad1 and Rad10 do not play a major role in yeast transcription

We showed that Rad1 and Rad10 interact with Mediator, a well-characterised transcriptional co-regulator. Therefore, we tested whether Rad1 and Rad10 have a role in transcription. *RAD1* and *RAD10* genes not being essential for yeast cell viability, we constructed *rad1* and *rad10* deletion mutants in *BY4741* and *YPH499* contexts, and tested different growth conditions.

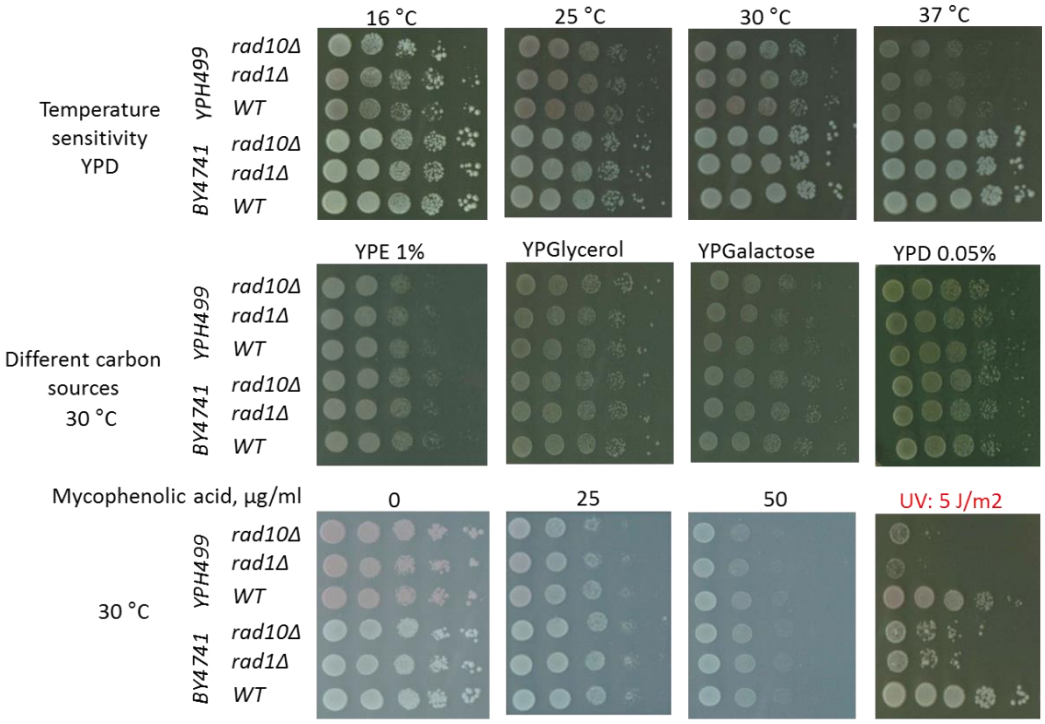

Figure 25: **Growth phenotypes of *rad1* and *rad10* deletion mutants in *BY4741* and *YPH499* contexts.**
Cells were serially diluted and spotted on different media (YP medium supplemented with glucose, galactose, ethanol, or glycerol) and incubated for 3 days or 5 days for MPA (Mycophenolic acid, nucleotide depletion drug) at indicated temperatures. Cells were also grown on YPD medium low in glucose. Cells were UV-irradiated at 5 J/m^2 and incubated for 3 days at 30°C.

We did not observe any growth differences between *rad1* deletion and *rad10* deletion strains and the wild-type strains on YPD medium grown under different temperatures (16°C, 25°C, 30°C, or 37°C), on different carbon sources (YP medium supplemented with glucose, galactose, ethanol, or glycerol) or on NTP depletion condition (mycophenolic acid) (Figure

25). The only observed phenotype was a heightened UV-sensitivity of *rad1* and *rad10* deletion mutants as expected for proteins involved in NER.

A role for Rad26 in transcription was previously proposed (Lee *et al.*, 2001). This work of Lee *et al*. showed that on YP medium supplemented with galactose, *rad26* deletion inhibited cell growth and a more severe growth defect was observed in the absence of Rad26 and TFIIS, a transcription elongation factor, similar results were obtained in the presence of a nucleotide depletion drug (6AU). Furthermore, it was shown that in the absence of Rad26, the mRNAs levels of inducible genes were lower than in the wild-type and that this defect was more severe in cells lacking both Rad26 and TFIIS. We conducted growth asssays for *rad26Δ,* similar to those conducted for *rad1Δ* and *rad10Δ* mutants, but did not observe any growth defect for *rad26Δ* even on YP medium supplemented with galactose. Similarly in the presence of mycophenolic acid, there was no growth difference between *rad26Δ* and the wild-type strain (data not shown). Therefore, our results do not confirm growth defect in *rad26Δ* mutant.

RNA Pol II and Mediator are essential components of the transcription machinery, we hence investigated the effect of *rad1* and *rad10* deletions on their chromatin presence. Quantitative analysis of RNA Pol II and Mediator ChIP experiments on selected class II genes showed that the occupancies of both RNA Pol II and Mediator were not affected in either *rad1* or *rad10* deletion mutants (Figure 26).

These results together with the lack of defect in growth phenotypes (Figure 26) suggested that Rad1 and Rad10 do not play a major role in yeast transcription, similar to Rad2.

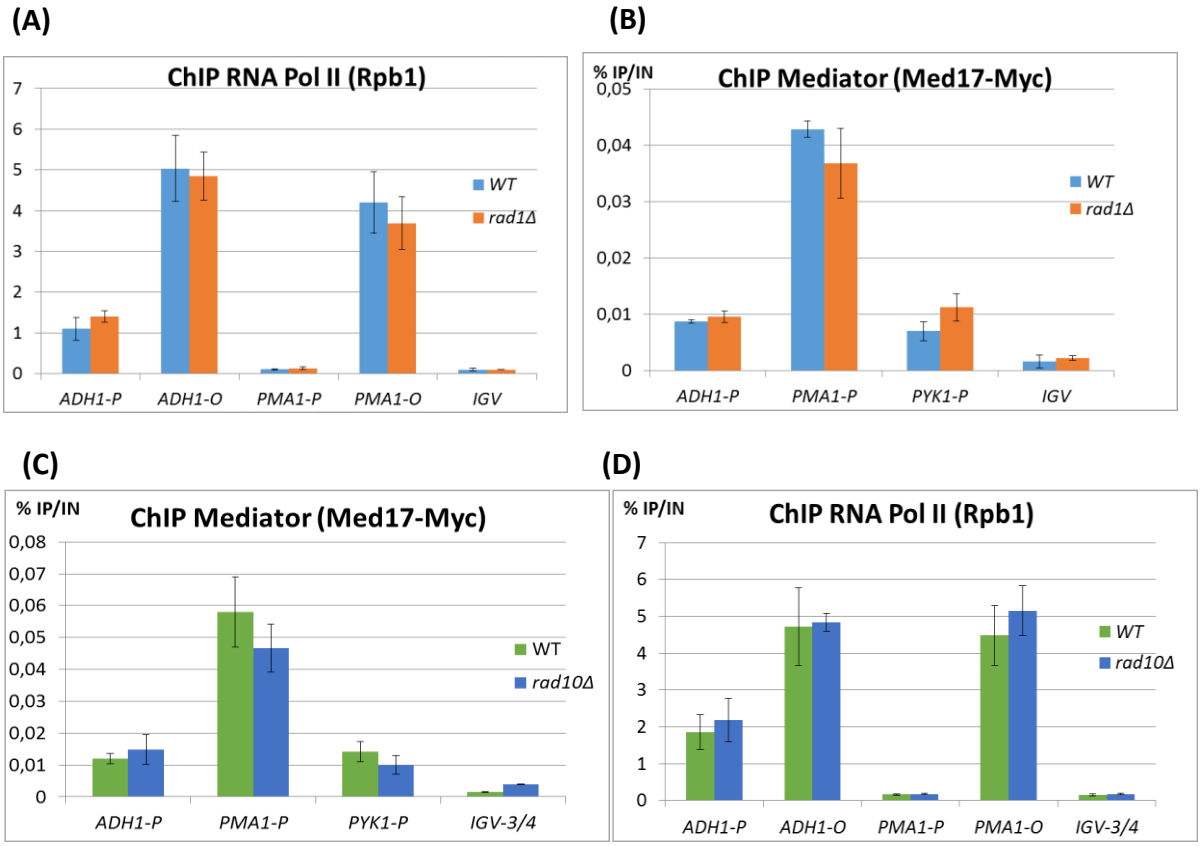

Figure 26: Effect of *RAD1* or *RAD10* deletion on RNA Pol II and Mediator occupancies.

Quantitative analysis of RNA Pol II and Mediator occupancies in *rad1Δ* (A, B) and *rad10Δ* (C, D) strains on selected class II regions. *rad1Δ* and *rad10Δ* and wild-type strains were grown in YPD medium at 30°C. Immunoprecipitations were performed using α-CTD antibody (RNA Pol II) (A, C) and α-Myc antibody against Med17-Myc (Mediator) (B, D). Fragments immunoprecipitated in Mediator and RNA Pol II ChIP experiments were amplified with primers corresponding to selected class II gene promoters (P) or ORFs (O). The displayed values represent the percentage of immunoprecipitated fragments (IP) relative to the input (IN). Mean values and standard deviation (indicated by error bars) of three independent experiments are shown. An intergenic region on chromosome V (IGV) was used as a negative control.

II.4 Functional characterisation of the physical interaction between Mediator and NER proteins (Rad1, Rad10 and Rad26)

II.4.1 Characterising Rad1, Rad10 and Rad26 chromatin binding

From the previous sections, we have identified new interactions between Rad1, Rad10 and Rad26 and Mediator. Rad1 and Rad10 are present on class II promoter regions as well as on transcribed regions in the absence of genotoxic stress. Rad26 seems to be more predominantly enriched on transcribed regions of class II genes. Hence in this section, results on the characterisation of the functional interplay between Rad1, Rad10, Rad26 and Mediator will be presented.

II.4.1.1 Presence of Rad1 and Rad10 on the chromatin is dependent on RNA Pol II transcription

Above, we demonstrated that Rad1, Rad10 and Rad26 were present on class II genes (Figure 24), hence we investigated whether the presence of these proteins on the chromatin is dependent on RNA Pol II transcription. We used an *rpb1-1* thermo-sensitive mutant as Rpb1 is essential for cell viability. Yeast cells were grown at 25°C and then transferred to the non-permissive temperature, 37°C for 90 min. Rad26 presence on chromatin has already been shown to be dependent on RNA Pol II transcription, in the absence of genotoxic stress (Malik *et al.*, 2010). It was shown that the induction of RNA Pol II transcription leads to the recruitment of Rad26 on the ORF. Furthermore, in *rpb1* mutant context, Rad26 chromatin occupancy was decreased.

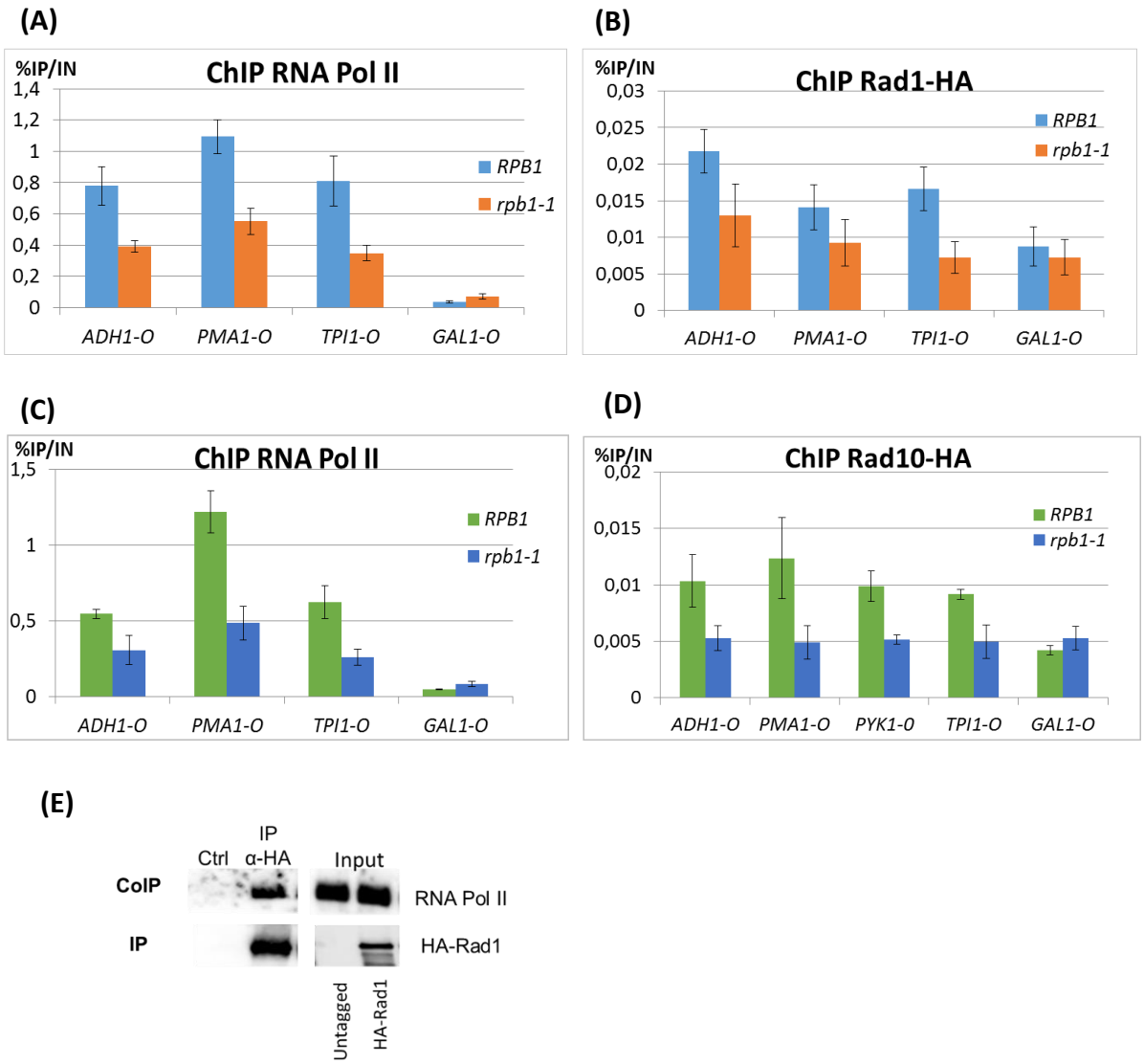

Figure 27: Effect of *rpb1-1* mutation on Rad1, Rad10 and RNA Pol II occupancies on selected transcribed regions.

Cells were grown in selective SD medium complemented with amino acids at 25°C and then shifted for 90 min at 37°C. Quantitative experiments were performed on immunoprecipitated fragments obtained from (A, C) RNA Pol II ChIP using α-Rpb1 antibody, and from (B, D) Rad1-HA and Rad10-HA ChIP using α-HA antibody. ChIP experiments were conducted for RNA Pol II in Rad1-HA strain and Rad10-HA strain to confirm that transcription is affected in both strains (A, C). The displayed values represent the percentage of immunoprecipitated fragments (IP) relative to the input (IN). Mean values and standard deviation (indicated by error bars) on selected class II gene ORFs (O) corresponding to three independent experiments are presented. A *GAL1* ORF was used as a negative control. (E) Cells were grown at 30°C in YPD. Rad1-HA was immunoprecipitated (IP) with α-HA antibody from crude yeast extracts and analysed by Western blotting with α-Rpb1 antibody against RNA Pol II (co-IP). Control IP was carried out with yeast extract from an untagged strain for HA (Med17-Myc).

The *rbp1-1* mutation was previously described as leading to rapid inhibition of transcription after a shift to 37°C, the non-permissive temperature (Nonet *et al.,* 1987). Two strains were constructed containing Rad1-HA or Rad10-HA in *rpb1-1* mutant context as well as in the wild-type. When cells were grown at 25°C and then shifted to 37°C for 90 min, we observed a marked decrease of RNA Pol II occupancy on transcribed regions (Figure 27A, C). Concomitantly, we observed a decrease of Rad1 and Rad10 on transcribed regions of class II genes (Figure 27B, D). We hence concluded that Rad1 and Rad10 occupancies is dependent on RNA Pol II transcription.

Next, we investigated whether RNA Pol II interacted with Rad1-Rad10. An interaction between Rad26 and RNA Pol II was previously reported (Malik *et al*., 2010).

HA-Rad1 was immunoprecipitated from wild-type cell extracts and RNA Pol II was revealed by Western blotting, using an antibody against Rpb1. We observed that RNA Pol II co-immunoprecipitated with Rad1 (Figure 27E).

Therefore, Rad1-Rad10 and Rad26 interact with RNA Pol II and their presence was dependent on RNA Pol II transcription.

II.4.1.2 Analysis of Rad1 and Rad10 presence on class II promoter and corresponding transcribed region in relation to Rad2 and Mediator

As previously shown (Figure 24) Rad1-Rad10 and Mediator only co-occupy a fraction of promoter regions, hence we attempted to characterise the different gene groups according to Rad1-Rad10 and Mediator-Rad2 chromatin binding. First, their average enrichment densities on class II promoter regions, excluding class III genes, were calculated. Second, given the strong correlation between Rad2 and Mediator shown previously (Eyboulet *et al.*, 2013), we added the enrichment densities over class II promoter regions of these two proteins forming one Mediator-Rad2 couple. Similar bioinformatics analyses were done for Rad1 and Rad10. Based on their enrichment profiles, gene promoters were categorised in five groups. A first group corresponding to gene promoters enriched with Rad1-Rad10 and Mediator-Rad2 pairs. A second group enriched for Mediator-Rad2 only and a third group enriched for Rad1-Rad10 only. In addition, a fourth group corresponding to gene promoters that are not enriched by any of the four proteins and a fifth group corresponding to genes bordering the four groups (Figure 28A). However, we could not identify any particular characteristics of these gene groups relative to promoter architecture (TATA box, TFIID (TAF1)-dependent genes), gene function, nucleosome occupancy and dynamics, and transcription factor dependency (data not shown). It would therefore seem that the different gene groups cannot be explained based solely on transcription. Further analyses have to be conducted to identify particular characteristics of these different gene categories.

To pursue in the characterisation of these gene groups, we tried to investigate whether there is a link between promoter presence of Rad1-Rad10 and their presence on the transcribed regions, suggested by visual analysis of ChIP-seq data. We used the previously defined five gene groups based on promoter enrichment of Mediator-Rad2 pair and Rad1-

Rad10 pair (Figure 28A) to investigate whether promoter enrichment of Rad1 and Rad10 affect their presence on the transcribed regions of class II genes.

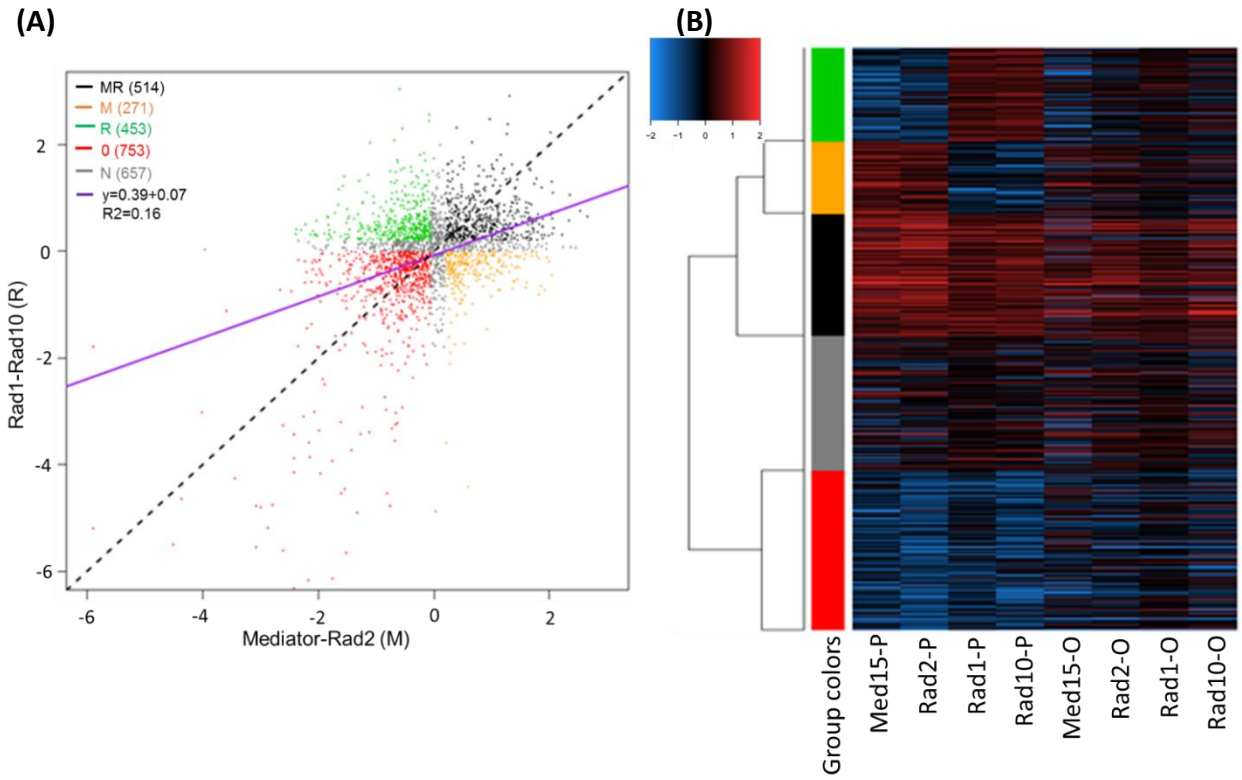

Figure 28: Enrichment of Mediator-Rad2 and Rad1-Rad10 pairs on promoter and corresponding transcribed regions of class II genes.

(A) Five groups of genes were defined based on the enrichment densities of each pair over promoter regions. The x-axis corresponds to the sum of enrichment densities of Mediator and Rad2 over promoter regions. The y-axis corresponds to the sum of Rad1 and Rad10 enrichment densities over promoter regions. MR group corresponds to gene promoters enriched by Mediator-Rad2 and Rad1-Rad10. M group corresponds to gene promoters enriched with Mediator-Rad2. R group to gene promoters enriched with Rad1-Rad10. 0 correspond to gene groups not enriched by either Rad1-Rad10 or Mediator-Rad2. N is the gene group at the borders of the other groups. The number of regions in each group is indicated in brackets, next to the group name. (B) Tag densities of each gene group were calculated over the promoter (P) and corresponding ORFs (O) of class II genes which are represented in above heat map. On the scale, the colour red indicates the highest protein enrichment on promoter regions.

To obtain a genome-wide insight of Rad1, Rad10, Rad2 and Mediator enrichment profiles on promoter regions of class II and their corresponding transcribed regions, the mean enrichment densities of each protein were calculated on these regions and represented in a heat map. The first part of the heat map corresponds to promoter regions and we observed that the five groups correctly represented the different categories based on protein enrichment, for example in the green group consists of promoter regions enriched with Rad1-Rad10. Moreover, we observed that there is a difference in enrichment of Rad1 and

Rad10 depending on the gene groups (Figure 28). Indeed, promoter regions enriched with both Rad1-Rad10 and Mediator-Rad2 pairs are also more enriched with Rad1-Rad10 on the transcribed regions (group in black in Figure 28B) compared to regions where only Rad10-Rad10 pair is present on promoters (group in green in Figure 28B). These results suggest that there is a link between protein enrichment on promoter regions and their presence on transcribed regions and that Mediator-Rad2 presence on promoter regions might influence Rad1-Rad10 presence on transcribed regions, by an unknown mechanism.

II.4.2 Functional interplay between Rad1, Rad10, Rad26, Mediator and RNA Pol II

Heat map analysis of Rad1 and Rad10 occupancies gave us a notion of the difference in the global distribution of these proteins in the different gene groups characterised by the presence or absence of Mediator-Rad2 on promoter regions (Figure 28). Further analysis is needed to characterise the link between their presence on promoter and corresponding transcribed regions. We used *kin28 ts* mutant (detailed in "Article 1") which we validated as an interesting tool to dissociate protein binding on promoter regions from its binding on transcribed regions. It allows to investigate the effect on Rad1 and Rad10 genomic occupancies when Mediator is stabilised on promoter regions and RNA Pol II occupancy is decreased on transcribed regions.

Moreover, we showed that Rad26 interacts with Mediator (Figure 22) but did not observe any particular enrichment on Mediator enriched UAS (Figure 24A, G). Moreover, Rad26 was highly enriched on transcribed regions (Figure 24A, I) and dependent on RNA Pol II transcription (Malik *et al.*, 2010). This is similar to what is observed for RNA Pol II and Mediator and it was demonstrated that Mediator transiently contacts core promoter-bound RNA Pol II (Article 1; Wong *et al.*, 2014; Jeronimo and Robert, 2014). We hypothesised that the interaction between Mediator and Rad26 on the chromatin might be dynamic, hence we used a *kin28 ts* mutant which stabilises Mediator on the chromatin to better characterise this interplay.

We performed Rad1, Rad10 and Rad26 ChIP-seq in *kin28 ts* context, to characterize the functional link between NER proteins, Mediator and RNA Pol II. We also performed Mediator and RNA Pol II ChIP in the same series of ChIP-seq. Only the ChIP-seq results of Rad10 were used for bioinformatics analyses as they were of better quality. Yeast cells were grown at 25°C then shifted to 37°C for 75 min.

For genome-wide analyses, we used Mediator peaks and Rad3 (TFIIH) peaks defined in a wild-type context corresponding to the UAS and core promoters, respectively. In the *kin28 ts* mutant compared to the wild-type, we observed that Mediator occupancy is increased on the UAS in the mutant compared to the wild-type (Figure 29, panel A), in agreement to previous studies (Article 1; Wong *et al.*, 2014; Jeronimo and Robert, 2014). Similarly, mean densities of Mediator calculated over core promoter regions showed that Mediator is also enriched on these regions (Figure 29, panel B). This suggests that an unstable intermediate containing Mediator is stabilized on the promoter regions in *kin28 ts* mutants affected for RNA Pol II phosphorylation. Moreover, in the *kin28 ts mutant*, we observed an important

decrease of RNA Pol II on the transcribed regions compared to the wild-type (Figure 29, panel C) as previously reported (Article 1; Wong *et al.*, 2014; Jeronimo and Robert, 2014).

Analysis of Rad10 and Rad26 genomic occupancies around Mediator peaks present on UAS showed that Rad10 and Rad26 occupancies were increased on UAS (Figure 29, panel A, 30D), though to a lesser extent for Rad26. On the other hand, on core promoter regions, Rad26 profile was modified in the mutant compared to the wild-type (Figure 29, panel B). Bioinformatics analysis conducted on 20% of RNA Pol II-most enriched genes, showed a slight increase in Rad26 occupancy in *kin28 ts* mutant compared to the wild-type (Figure 29G, H). Rad10 was enriched on core promoter regions in the *kin28 ts* mutant, as demonstrated by the ratios between mutant and wild-type (Figure 29F). On the transcribed regions, we observed that there was a very strong decrease of Rad26 similarly to RNA Pol II occupancy (Figure 29, panel C). The decrease over transcribed regions of Rad26 was stronger than what was observed for Rad2 (Article 1). No decrease of Rad1 was observed on the transcribed regions (Figure 29, panel C, F). Our results showed that Rad26 chromatin binding is increased on UAS and also slightly increased on core promoter regions. Its decrease on the transcribed region is very strong and similar to that observed for RNA Pol II, in agreement with Rad26 implication in transcription and its transcription-dependent presence on gene bodies. This experiment has also allowed us to visualize a slight stabilization of Rad26 on Mediator-bound UAS. In addition, the slight stabilization of Rad26 on promoter regions and decrease on transcribed region might indicate Rad26 binding to promoter regions and then loading on transcribed regions and not a transfer from transcribed regions to promoter regions.

To note that in these experiments, we observed that Rad26 was enriched on UAS in the wild-type but previously we did not find a specific enrichment over these regions (Figure 24G). One possible explanation is that yeast cells were previously grown at 30°C and in the current experiment, cells were grown at 25°C followed by a 75min shift at 37°C. It is possible that the difference in growth conditions can impact the localisation of Rad26, this point has to be further studied.

On the other hand, Rad10 was enriched on Mediator-bound UAS and core promoter in the *kin28* mutant. However, no decrease was observed on transcribed regions. This experiment was carried out to investigate whether Mediator's presence on promoter regions can influence Rad1-Rad10 presence on the transcribed regions. Therefore, additional analyses have to be carried out on the different gene groups previously defined (Figure 28) to address this question.

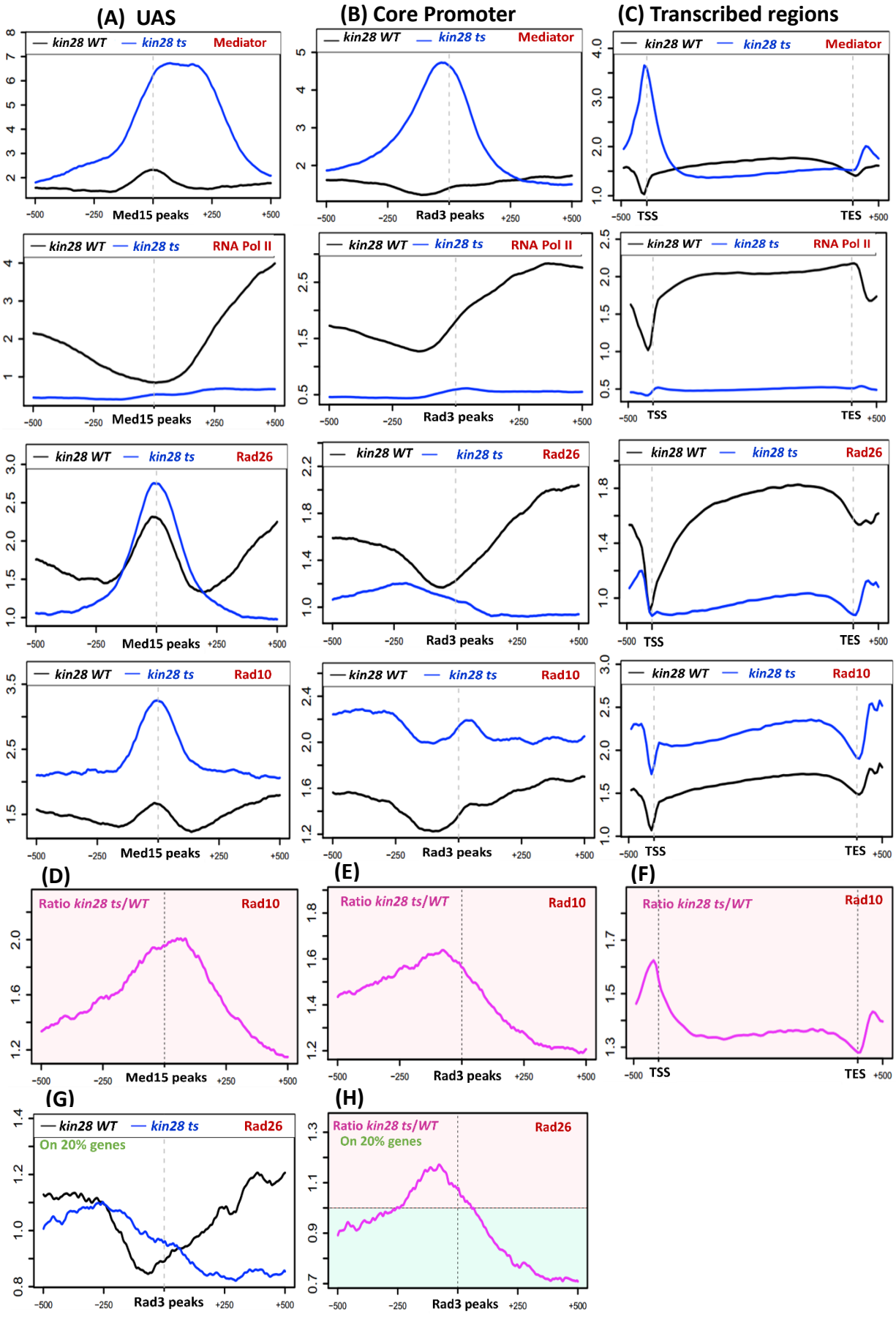
(A) UAS
(B) Core Promoter
(C) Transcribed regions
kin28 WT
kin28 ts
Mediator
RNA Pol II
Rad26
Rad10
Med15 peaks
Rad3 peaks
TSS
TES
(D)
(E)
(F)
Ratio kin28 ts/WT
(G)
(H)
On 20% genes

Figure 29: Impact of *kin28* mutation on Mediator, Rad1, Rad10, Rad26 and RNA Pol II genomic occupancies.

Cells were grown at 25°C and then shifted to 37°C for 75 min. Yeast chromatin fragments were immunoprecipitated using α-Myc antibody (Mediator Med17-Myc), α-Rpb1 antibody (RNA Pol II) and α-HA antibody (Rad10-HA, Rad26-HA). The mean densities of Mediator, Rad10, Rad26 and RNA Pol II were calculated around (A) Mediator peaks (UAS), (B) Rad3 peaks (core promoters), both regions are scaled to a 1000 bp window centered on the maximum of either Med15 or Rad3 peaks, and (C) on transcribed regions corresponding to 500 bp before TSS, scaled window between TSS and TES, and 500 bp after TES. The peaks of Mediator and Rad3 were oriented using the TSS of the nearest gene and intergenic regions encompassing RNA Pol III were excluded. (D-F) Rad10-HA occupancy ratios between *kin28 ts* mutant and the wild-type (WT) around (D) Med15 peaks (UAS), (E) Rad3 peaks (core promoters) and (F) transcribed regions. (G) The distribution of HA-Rad26 around Rad3 peaks, on 20% of genes most enriched with RNA Pol II. (H) HA-Rad26 occupancy ratios between *kin28 ts* mutant and the wild-type (WT) around Rad3 peaks. The pink background in the ratio plot indicated value above one, when the enrichment of the mutant is greater than the WT. The blue background for ratios lower than one, the WT is more enriched on these regions.

II.4.3 Effect of Mediator mutations on Rad1 and Rad10 occupancies

We sought to understand the significance of Mediator interactions with Rad1, Rad10 and Rad26 and a possible implication of these links in NER. As a first step in the characterisation of Mediator interactions with Rad1, Rad10 and Rad26, we proceeded to identify Mediator subunits implicated by two-hybrid assays. Mediator subunits were fused to the activating domain of transcription factor Gal4 (prey) and NER proteins were fused to the Gal4 DNA binding domain (bait). Experiments were also carried out with NER proteins being the prey and Mediator subunits being the bait. All 25 subunits of Mediator were tested but we were unable to reveal any positive contact (data not shown).

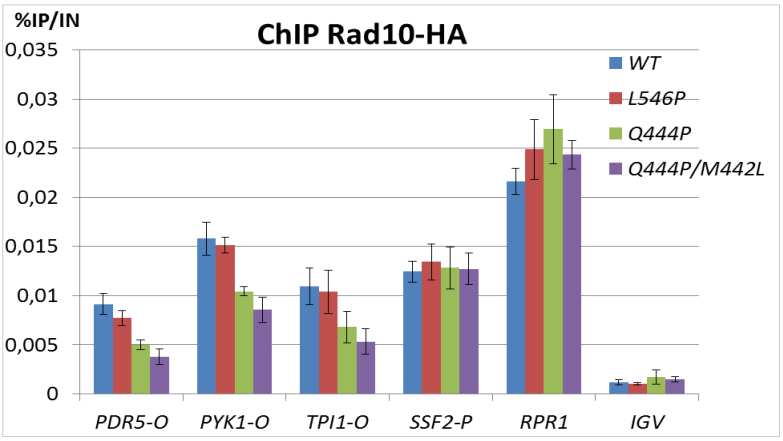

Figure 30: Effect of *med17* mutations on Rad10, RNA Pol II and Mediator occupancies. Quantitative ChIP analysis of Rad10 occupancy on selected regions. Cells were grown in YPD medium at 30°C and ChIP assays were performed on the extracted chromatin using α-HA antibody against Rad10-HA. Immunoprecipitated fragments from ChIP experiments were amplified with primers corresponding to selected class II gene promoter (P) or ORFs (O) and a selected class III gene (RPR1). The displayed values represent the percentage of immunoprecipitated fragments (IP) relative to the input (IN). Mean values and standard deviation (indicated by error bars) of three independent experiments are shown. A non-transcribed region on chromosome V (IGV) was used as a negative control.

Two-hybrid experiments performed did not lead to the identification of Mediator subunits involved in the interaction with Rad1, Rad10 and Rad26. Therefore, to get a functional insight on these interactions, we used previously characterised Mediator mutants in the laboratory that were UV-sensitive or not. We used three different mutants of Mediator Med17 subunit: *med17-L546P*, *med17-Q444P* and *med17-Q444P/M442L. med17-L546P* is only thermo-sensitive, *med17-Q444P* mutant is temperature-sensitive but does not have a pronounced UV-sensitive phenotype, whereas *med17-Q444P/M442L* is both thermo-sensitive and strongly UV-sensitive. These mutants were previously characterised in the laboratory and it was showed that all the mutants showed a decrease of RNA Pol II occupancy on transcribed regions. The *med17-Q444P* and *med17-Q444P/M442L* genomic distribution was characterised in Article 1. The results showed that on a global scale, Mediator was stabilised on UAS and RNA Pol II occupancy was decreased on transcribed regions in both mutants.

The first quantitative analysis of ChIP experiments showed that Rad10 was specifically decreased on transcribed regions of class II genes in UV-sensitive mutants but no decrease was observed for the non-UV sensitive *med17-L546P* mutant (Figure 30). Even though transcription was affected in all mutants, only the UV-sensitive mutants (*med17-Q444P* and *med17-Q444P/M442L*) showed a defect in Rad10 occupancy, with the highly UV-sensitive m*ed17-Q444P/M442L* mutant being more affected. These results suggest that Mediator influence Rad10 occupancy related to UV-sensitivity.

II.4.4 Occupancies of Rad1 and Rad10 are not dependent on Rad2

In NER it has been reported that the presence of Rad2 on the chromatin induces a conformation modification that is required for the recruitment of Rad1 and Rad10. Therefore, we tested whether the presence of Rad2 is required for Rad1 and Rad10 recruitment to the chromatin and their interactions with Mediator.

Rad2 is not essential for cell viability, hence we constructed *rad2Δ* mutant. We performed CoIP experiments on whole cell extracts from wild-type cells and *rad2Δ* mutant. Rad10 was immunoprecipitated via its Flag tag and Mediator was revealed by Western blotting using an antibody specific to Med17. We observed that in the absence of Rad2, Mediator co-immunoprecipitates with Rad10, at a comparable level to that in the wild-type strain (Figure 31A). Hence, we concluded that Rad2 is not necessary for Rad10 and Mediator interaction.

Next, we investigated whether the occupancy of Rad1 and Rad10 are dependent on Rad2 and vice-versa. Hence, we conducted ChIP experiments in *rad2Δ, rad1Δ* or *rad10Δ* contexts. For Rad10 ChIP in *rad2Δ*, we used primers over gene regions that were identified from our ChIP-seq experiments and were more or less enriched with Rad10. We observed that in the absence of Rad2, we do not observe any decrease of Rad10 recruitment to the chromatin (Figure 31B). Quite the inverse, we observed an increase of Rad10 in the mutant on all the regions tested including class III gene *RPR1*. Interestingly, in *rad1Δ* or *rad10Δ* contexts, there was an increase of Rad2 on the regions tested, the effect in the *rad1Δ* mutant was more pronounced than in the *rad10Δ* mutant. These results point towards a potential competition between Rad1-Rad10 and Rad2 for chromatin binding.

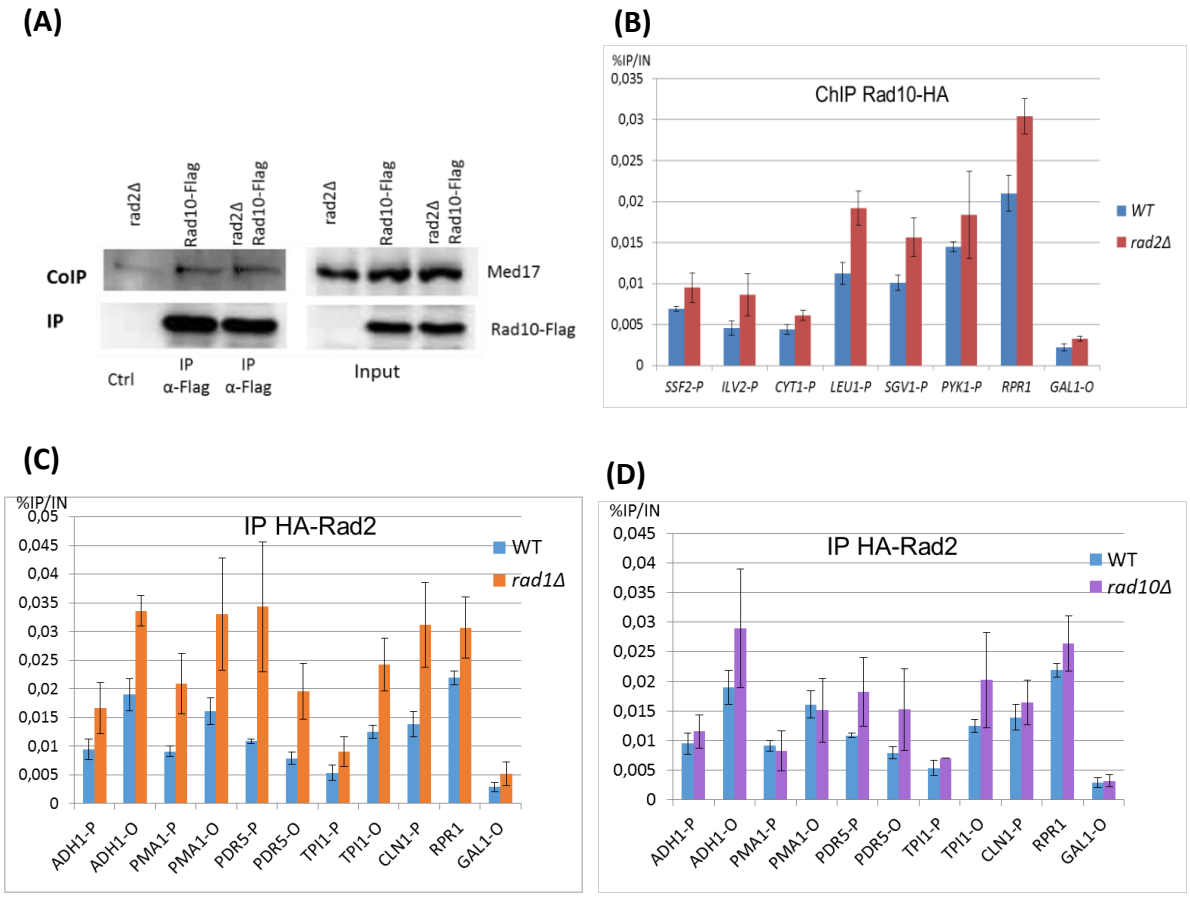

Figure 31: Effect of *rad2* deletion on Mediator-Rad10 interaction and Rad10 chromatin binding as well as *rad1* or *rad10* deletion on Rad2 chromatin occupancy.
(A) Coimmunoprecipitation experiments were conducted in *rad2Δ* strain. Rad10-Flag was immunoprecipitated with α-Flag antibody from crude extracts and analysed by Western blotting with an antibody against Med17 (co-IP). Ctrl: control immunoprecipitation in an untagged *rad2Δ* strain was carried out. (B) Occupancies of Rad10 in *rad2Δ* mutant and the occupancy of Rad2 in (C) *rad1Δ* and (D) *rad10Δ* mutants on selected transcribed regions. Quantitative experiments were performed on selected regions of class II and class III (*RPR1*) genes. Fragments were immunoprecipitated using α-HA antibody for Rad1-HA and Rad10-HA ChIP, in *rad2Δ* mutant (B) and for HA-Rad2 ChIP in *rad1Δ* and *rad10Δ* mutants (C, D). Mean values and standard deviation (indicated by error bars), on selected class II gene ORFs (O) and promoter region (P), corresponding to three independent experiments are presented. A *GAL1* ORF and a non-transcribed region on chromosome V (IGV) were used as negative controls.

II.5 Effect of UV-irradiation on Mediator interactions with NER proteins and chromatin binding

We have observed that NER proteins (Rad1, Rad10, Rad26 and Rad2) interact with Mediator in the absence of genotoxic stress. Therefore, we wished to test whether there was a modification in Mediator-NER protein interactions after damage induction. Another interesting aspect in the NER research field is the binding dynamics of NER proteins after induction of damage. Previously, we showed that NER proteins are present on the chromatin ahead of exogenous damage induction, therefore we sought to investigate changes in chromatin binding after UV stress.

II.5.1 Effect of UV-irradiation on Mediator interactions with NER proteins

UV-irradiation causes DNA damages and can also lead to protein degradation. Hence it was important to determine the optimal dose of UV that will not induce any degradation of our proteins of interest. We tested different doses of UV and either collected the cells directly after UV treatment (T0), after 30 min (T30) or 60 min (T60) incubation at 30°C. Non-irradiated cells (UV-) were also collected. We observed that the level of Med17 was constant at all the time-points and UV doses tested (Figure 32). Moreover, Rad2 level was constant at all time-points in cells irradiated at 50 J/m^2 (Figure 32). However, we observed that there was a slight decrease of Rad2, 30 min and 60 min after UV treatment when cells were irradiated at 100 J/m^2 or 150 J/m^2.

Therefore, we performed CoIP experiments on total yeast extracts from cells irradiated or not at 50 J/m^2, to be in optimal CoIP conditions.

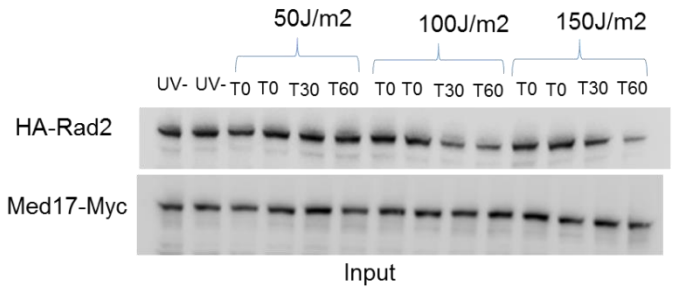

Figure 32: Western blotting analysis of Rad2 and Med17 protein levels in total yeast extract with or without UV-irradiation, visualised by Western blotting.

Cells were grown at 30°C and were either directly collected (UV-) or treated with UV at 50, 100 or 150 J/m^2. UV-treated cells were collected directly (T0, 2 extracts) or after 30 or 60 min incubation at 30°C.

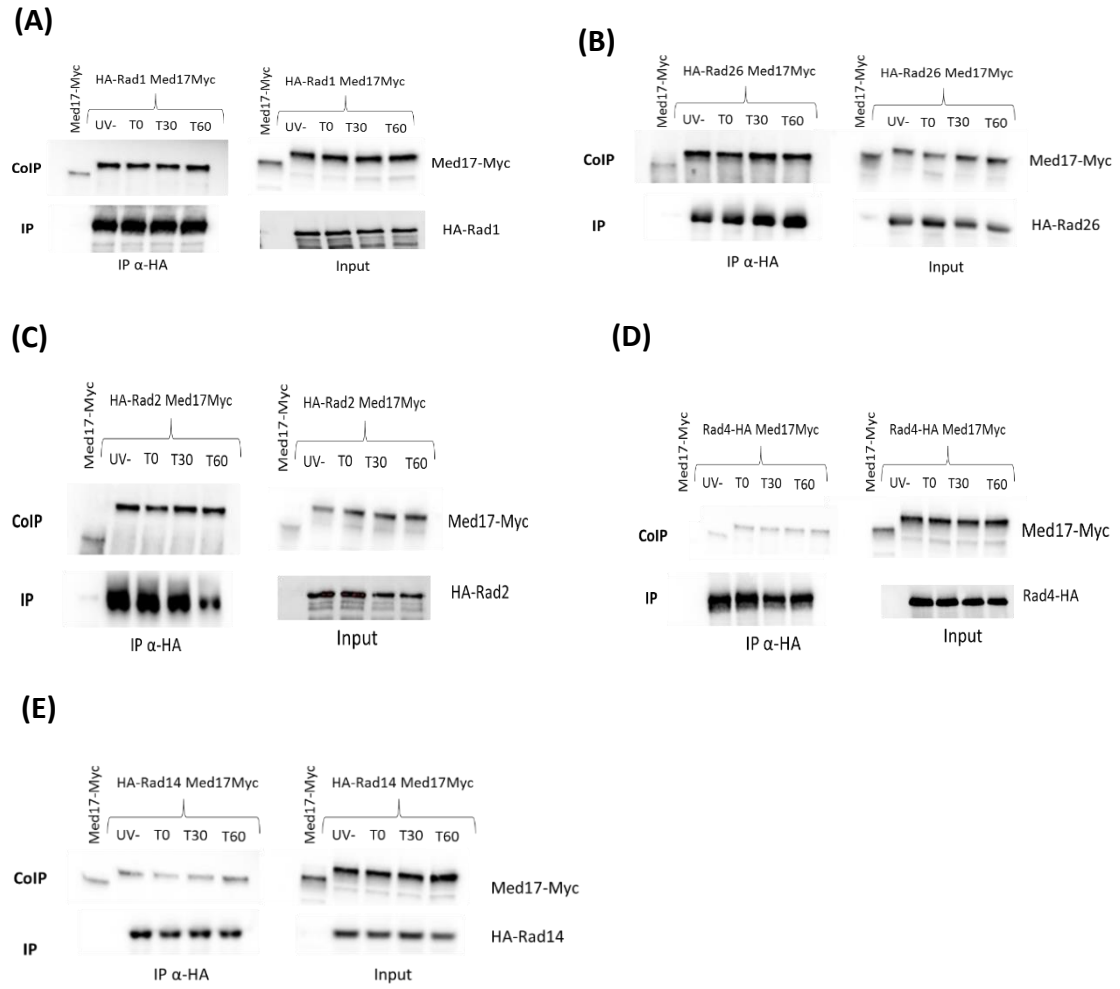

Figure 33: Interaction between the Mediator complex and NER proteins before and after UV irradiation.

Cells were grown at 30°C and were either directly collected (UV-) or treated with UV at 50 J/m^2 in PBS. UV-treated cells were either collected directly (T0) or after 30 min (T30) or 60 min (T60) incubation at 30°C, in YPD. Rad1, Rad26, Rad4, Rad14 were immunoprecipitated (IP) with α-HA antibody from crude yeast extracts and analysed by Western blotting with α-Myc antibody against Med17-Myc (co-IP). Control IP was carried out with yeast extract from an untagged strain for HA (Med17-Myc).

To investigate whether UV-irradiation could lead to any changes in Mediator interactions with Rad1, Rad10 and Rad26, we conducted CoIP experiments on total yeast extracts obtained from non-irradiated and irradiated cells collected at different time-points after UV stress (T0, T30 and T60). We also tested Mediator interaction with Rad2 as it was not tested in our previous study under UV stress conditions (Eyboulet *et al.,* 2013). We used an extract from Med17-Myc strain, containing no HA-tag, as control. The number of Myc repeats in this strain is lower than the double strain which explains the difference in migration pattern observed (Figure 33).

After the induction of UV-damage, we did not observe any major effect on Mediator interactions with Rad1, Rad26 and Rad2 (Figure 33A, B, C). Therefore, it seems that the

interaction with Mediator occurs prior to UV stress and persists after induction of DNA damage. Moreover after UV-irradiation, immunoprecipitation of HA-tagged Rad4 or Rad14 does not co-immunoprecipitate Mediator (Figure 33D, E). Indeed, we observed a signal of similar intensity in the control (untagged strain for HA-tag). Therefore, in our co-immunoprecipitation condition, Rad4 and Rad14 do not interact with Mediator in the absence or presence of UV-irradiation.

II.5.2 Effect of UV-irradiation on Mediator and NER proteins chromatin occupancies

Having previously shown that NER proteins (Rad1, Rad10, Rad26 and Rad2) were present on the chromatin before damage induction, we investigated whether the chromatin binding of NER proteins was modified after UV-irradiation. The changes in Mediator and RNA Pol II occupancies after UV irradiation were also analysed.

We performed ChIP-qPCR analysis and our first experiments indicate that there was a change in chromatin binding of the different proteins tested. We tested the highly transcribed *PYK1* gene, intermediate transcribed *BFR2* gene and inducible *GAL1* gene, non-transcribed in the presence of glucose in our growth condition. Indeed, we observed that Mediator occupancy on transcribed regions was increased but no changes were observed for the promoter region tested (Figure 34A). RNA Pol II, on the other hand, showed a decrease in occupancy at T0 on promoter and transcribed regions compared to UV-untreated cells (Figure 34B). Interestingly, Rad10 occupancy was increased 30 min after UV-irradiation on promoter and transcribed regions (Figure 34C). Just after UV-irradiation (T0), there was a decrease of Rad10 occupancy on the ORF of *PYK1*, but not on other regions tested. For Rad2, an increase in occupancy is observed at T0 and T30, no quantitative difference is observed between the two time-points after UV-irradiation on promoter and transcribed regions (Figure 34D). The results for Rad26 suggest a particular behaviour depending on the region examined (Figure 34E). No significant changes were observed on the tested promoter region. On the transcribed regions, there was an increase on regions that were not enriched for Rad26 before UV-irradiation (*GAL1*, *BFR2*) whereas the transcribed region (*PYK1*) where Rad26 was present prior to UV-irradiation, there was a decrease of Rad26 at T0 and T30.

In conclusion, we observed interesting changes in chromatin binding of the different proteins tested, but more regions should be tested to obtain a genome-wide view of their chromatin binding profiles.

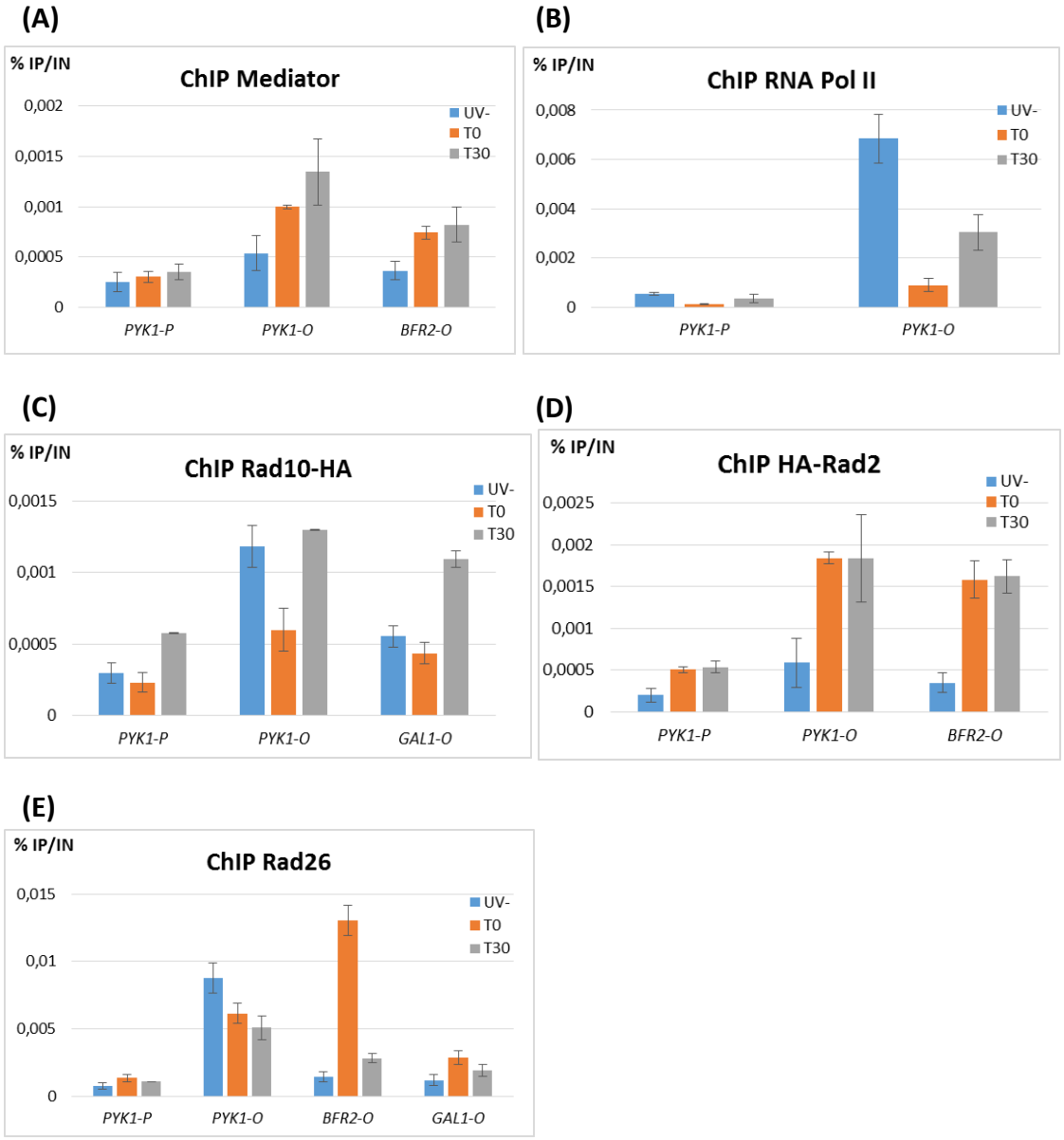

Figure 34: Chromatin binding of Mediator, RNA Pol II, Rad10, Rad26 and Rad2 in the absence or presence of UV-irradiation.

(A) ChIP experiments were conducted before and after UV damage. Cells were grown at 30°C and were collected directly (UV-) or after UV irradiation at 100 J/m^2 in PBS. After UV treatment, cells were collected without incubation (T0) or after incubation, in YPD, for 30 min at 30°C. (A-E) Quantitative experiments were performed on immunoprecipitated fragments and the occupancy of each protein were observed using primers of selected regions. Mean values and standard deviation (indicated by error bars), on selected class II gene ORFs (O) and promoter region (P), corresponding to three independent experiments are presented.

III. Is Mediator role in NER dependent on Mediator-TFIIH contact?

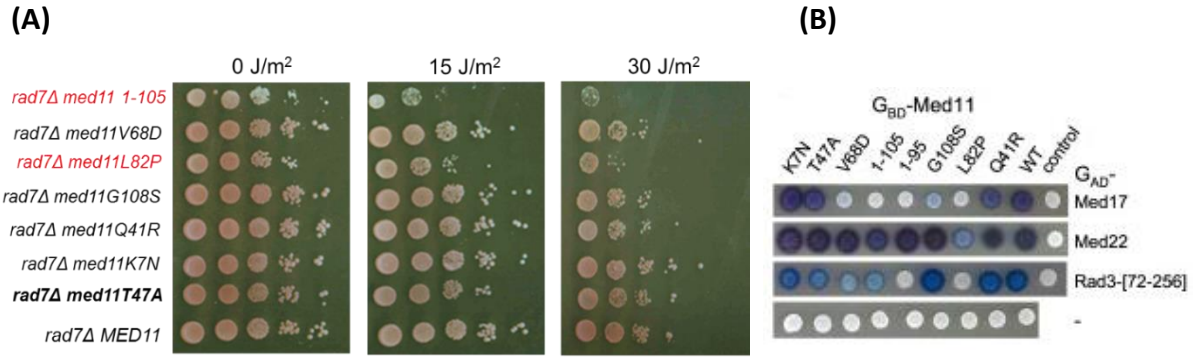

Figure 35: Effect of UV-irradiation on *med11* mutants.
(A) Serial dilutions of yeast cells were plated and grown for 3 days at 30°C without UV-irradiation or after UV-irradiation at either 15 J/m^2 or 30 J/m^2. (B) Interactions between Med11 and its known interacting partners (Med17, Med22 and Rad3 (TFIIH)) were tested in *med11* mutants, in two-hybrid assays (Figure from Esnault *et al.,* 2008).

TFIIH is one of the well-known complexes with dual role in transcription and DNA repair. It plays an essential role in transcription as a general transcription factor and is also an essential NER factor. Moreover, the laboratory has previously identified an interaction between Rad3 subunit of TFIIH and Med11 subunit of Mediator, necessary for recruitment of TFIIH to the PIC in transcription (Esnault *et al.,* 2008). We therefore investigated whether this interaction between Rad3 and Med11 is important for NER. We tested several mutants of *med11* that are affected for different interactions, determined by two-hybrid analysis (Figure 35B, Esnault *et al.*, 2008). Within the Mediator complex, Med11 interacts with Med17 and Med22. Briefly, *med11 T47A* is specifically impaired for Rad3 interaction and hence of particular interest for this study. *med11 K7N* is also mildly affected for Rad3 interaction. *med11 Q41R, med11 G108S* and *med11 V68D* are affected for Med17 interaction. *med11 1-105* is impaired for Med17 and Rad3 interactions. *med11 L82P* is affected for all three interactions (Med17, Med22 and Rad3).

We observed that in a GG-NER deficient context, *med11 T47A,* specifically affected for Rad3 interaction, did not display any increase UV-sensitivity (Figure 35A). Therefore the role of Mediator in NER seems to be independent of the Rad3-Med11 interaction in this particular mutant. Interestingly, two other mutants displayed a heightened UV-sensitivity namely *med11 L82P* and *med11 1-105* (Figure 35A). These mutants are affected for two-hybrid interactions of Med11 with Rad3 as well as Med17. However, other mutants affected only for one of these interactions were not UV-sensitive.

In conclusion, these results show that Mediator subunit Med11, in addition to Med17, could be implicated in NER as mutations of Med11 lead to UV-sensitivity. Moreover, Mediator's role in NER might be independent of Mediator functional link with TFIIH. Further experiments are needed to clarify whether Mediator-TFIIH interplay might be important for NER.

Discussion and Perspectives

I. Molecular mechanisms of RNA Pol II and Rad2 interplay

The laboratory has previously shown a physical interaction between RNA Pol II and Rad2 (Eyboulet *et al.,* 2013). In addition, in Article 1 we have proposed a mechanism in which Rad2 shuttles between regulatory and transcribed regions via a functional interplay with Mediator and RNA Pol II, thereby showing a functional link between RNA Pol II and Rad2. Our results show that in *kin28* TFIIH, and *med17* Mediator mutants, Rad2 presence on the transcribed regions is diminished and that in *rpb9* mutant there seem to be a gene-dependent effect. In *med17* and *kin28* mutants, we observed an important decrease in RNA Pol II occupancy on transcribed regions whereas the decrease in Rad2 occupancy is not that drastic (Article 1).

Our results indicate that Rad2 and RNA Pol II are well-correlated on transcribed regions (Figure 24I and that Rad2 is transferred on transcribed regions via an interaction with RNA Pol II (Article 1). However, the decrease on transcribed region in *kin28* mutant context is much less drastic that RNA Pol II (Article 1). Hence, it will be interesting to characterise the relationship between Rad2 and RNA Pol II on transcribed regions. To address this question, sequential ChIP (or Re-ChIP) experiments can be performed. It consists to sequentially immunoprecipitate two proteins using different antibodies, allowing to visualise the simultaneous presence of two proteins on the same genomic region. High-throughput sequencing can also be carried out for a genome-wide view. One of the limitations of this technique is that the amount of immunoprecipitated DNA fragments from the first ChIP has to be subsequent enough for the second ChIP. RNA Pol II can be immunoprecipitated first as its ChIP is very efficient and a Rad2 ChIP on these fragments can reveal whether these two proteins are present on the same genomic region at the same time.

The difference in occupancy, on transcribed regions, between Rad2 and RNA Pol II also raises the question of whether Rad2 presence on transcribed regions is only dependent on RNA Pol II or is influenced by other factors. To shed light on Rad2 presence on transcribed regions, mutants that specifically affect Rad2-RNA Pol II interaction can be used. However, this will require the identification of the subunit(s) of RNA Pol II interacting with Rad2 to be able to characterize the interaction interface between Rad2 and RNA Pol II. Mutants of Rad2 or RNA Pol II, which specifically disrupt this interaction can hence be constructed. These mutants can be used to assess the loss of Rad2-RNA Pol II interaction on Rad2 chromatin presence. In the case where disrupting Rad2-RNA Pol II interaction does not or slightly decrease Rad2 presence on transcribed regions, it will suggest that there is another mechanism independent of RNA Pol II that is responsible for Rad2 presence on transcribed regions.

II. Better characterising the physical interaction between Mediator and NER proteins

In this work, we identified interactions between Mediator and NER proteins. We hence sought to define the interaction interface to specifically affect these contacts for functional analysis. As a first step, protein two-hybrid experiments were conducted to identify Mediator subunit(s) interacting with NER proteins, using full length of Mediator subunits and NER proteins. We tested all 25 Mediator subunits as bait (fused to Gal4 DNA binding domain) and as prey (fused to Gal4 activating domain), but these experiments did not allow to identify the Mediator subunits interacting with Rad1, Rad10 and Rad26. One possible explanation is that full-length proteins were used, and the use of protein fragments can sometimes be better to detect interactions in two-hybrid experiments. For example, the interaction between Mediator Med17 and Rad2 is detectable using a fragment of Rad2 and not the full length protein. The two-hybrid screening of Mediator subunits with a yeast genomic library, conducted previously in the laboratory, that detected Med17-Rad2 interaction, did not detect the other interactions between Mediator and NER proteins (Rad1, Rad10 and Rad26). One possible explanation could be that Mediator subunits were used as bait (protein fused to Gal4 DNA binding domain) and two-hybrid assays can have varying sensitivity based on whether the Gal4 activating domain or DNA binding domain was fused to the protein of interest. Hence, it will be worthwhile to perform a two-hybrid screening using Rad1, Rad10 and Rad26 as baits against Mediator subunits (fragments), which can lead to the identification of interacting domains. Another possibility is to do a two-hybrid screen with fragments of Rad1, Rad10 and Rad26.

III. Test the competition hypothesis proposed for Rad1-Rad10 and Rad2 recruitment to the chromatin

In the absence of genotoxic stress, Rad2 interaction with either Rad1 or Rad10 was previously tested and no evidence of complex formation was reported (Bailly *et al.,* 1992). In our study, we observed an increase of Rad2 occupancy in the absence of either Rad1 or Rad10, and conversely of Rad1 and Rad10 in the absence of Rad2, suggesting a competition mechanism for their DNA binding (Figure 31). A competition assay can be used with an inducible form of Rad1 or Rad2 to validate this hypothesis. In *S. cerevisiae*, a system with a fusion bacterial LexA DNA-binding protein, the human estrogen receptor (ER) and an activation domain (AD) has been developed (Ottoz *et al.*, 2014). This system allows the regulated expression of a gene (low, intermediate or high levels) with the hormone β-estradiol and by adjusting the number of LexA-binding sites in the target promoter. Moreover, the LexA DNA binding site is not dependent on yeast metabolism and hence, this system can be used under different growth conditions.

A system allowing an inducible and regulated expression of Rad1 or Rad2 can be used to assess the relationship between Rad1-Rad10 and Rad2. For example, a strain containing a constitutive version and an inducible version of the *RAD2* and constitutive versions of *RAD1* and *RAD10* can be used. In case of competition for chromatin binding between Rad1-Rad10 and Rad2, production of increasing amounts of the inducible version of Rad2 will lead to a decrease of Rad1-Rad10 presence on chromatin.

IV. In-depth characterisation of Mediator link with NER proteins Rad1, Rad10 and Rad26

IV.1 Effect of kin28 TFIIH mutation on Rad1, Rad10 and Rad26 genomic occupancies

We have shown that the presence of Rad1 and Rad10 on RNA Pol II-transcribed regions was dependent on transcription. Rad26 chromatin occupancy was also reported to be dependent on transcription (Malik *et al.,* 2010). To uncover the functional interplay between Rad1, Rad10 and Rad26 chromatin binding relative to Mediator and RNA Pol II, we used a *kin28 ts* mutant in which RNA Pol II promoter escape was hindered.

This experiment was performed to investigate whether there was a link between Mediator-Rad2 co-occupying gene promoters with Rad1-Rad10 and the presence of Rad1-Rad10 on the transcribed regions. We observed that Rad10 was stabilized on Mediator-bound UAS and core promoter regions, similarly to Rad2. However, no decrease was observed on the transcribed regions (Figure 29). These analyses were carried out on all transcribed regions, hence to address our question, bioinformatics analyses have to be performed on the different gene groups that were defined based on Rad1-Rad10 and Mediator-Rad2 enrichment.

Another aspect worth investigating is whether these proteins are present on promoter regions at the same time. We have defined the different gene groups according to their presence on promoter regions. However, we do not know whether Mediator, Rad2, Rad1 and Rad10 are present on the same genomic region at the same time. To address this question, sequential ChIP (or Re-ChIP) experiments can be performed. Sequential immunoprecipitation of Rad1-Rad10 followed by immunoprecipitation of Mediator will allow to visualize the simultaneous presence of two proteins on the same genomic region. As mentioned above, the sequential ChIP technique requires sufficient material to be obtained from the first ChIP for a second immunoprecipitation. Both Rad1-Rad10 and Mediator ChIPs are challenging. One reason for low Mediator enrichment can be that Mediator does not bind directly to DNA but via transcription factors or PIC components and it is not known whether the binding of Rad1-Rad10 to DNA is direct, in the absence of UV stress.

In *kin28 ts* mutant, Rad26 presence was increased on Mediator-bound UAS, to a lesser extent than Rad10 and Rad2 (Figure 29). Moreover, Rad26 was present on some core promoter regions (Figure 29). Therefore, the effect of Mediator stabilized on promoter regions was minimal on Rad26 occupancy compared to what is observed for Rad1-Rad10 and Rad2. The effect was observed on a group of genes, hence bioinformatics analyses can be carried out to identify those genes. On the transcribed regions, Rad26 occupancy was greatly decreased, similar to the decrease observed for RNA Pol II, in line with previous results showing that Rad26 interacts with RNA Pol II and that its presence on transcribed regions is dependent on RNA Pol II transcription (Malik *et al*., 2010). The strong decrease of Rad26 on transcribed regions, similar to RNA Pol II, suggest a close link between Rad26 and RNA Pol II. To investigate whether Rad26 travels with RNA Pol II on transcribed regions, a re-ChIP experiment can be conducted (technique detailed in section "Further characterization of RNA Pol II and Rad2 interplay" of the discussion).

Coimmunoprecipitation experiments can also be conducted to test whether the interactions between these proteins are modified in *kin28 ts* mutant compared to wild-type. This can help in understanding, at least in part, the difference in protein chromatin binding observed in the mutant compared to the wild-type.

IV.2 Is chromatin binding of NER proteins dependent on their interaction with Mediator?

To investigate the link between Mediator and NER proteins Rad1, Rad10 and Rad26, we used UV-sensitive Mediator mutants. Our first results showed that Rad10 occupancy is specifically reduced in UV-sensitive mutants, on RNA Pol II-transcribed regions (Figure 30). This experiment has to be conducted on a genome-wide scale to get the chromatin binding profiles of Rad10 in UV-sensitive Mediator mutants compared to UV-insensitive mutants. CoIP experiments can also be carried out to investigate whether the reduced Rad10 occupancy observed in UV-sensitive mutants could be linked to a decrease in interaction between Mediator and Rad10 that will help to clarify the functional link between Rad10 and Mediator in DNA repair.

To investigate whether the Rad26-Mediator physical interaction is implicated in NER, co-immunoprecipitation and ChIP experiments can be performed in Mediator UV-sensitive and UV-insensitive mutants to investigate whether there was a decrease in Rad26-Mediator interaction and in Rad26 chromatin presence. If this decrease is specifically observed in UV-sensitive mutants, it will indicate that the Rad26-Mediator interaction is involved in NER.

Mediator is an essential transcription co-regulator. Hence, it is important to investigate whether the Rad26-Mediator interaction is implicated in NER or transcription.

The presence, in the laboratory, of UV-sensitive and UV-insensitive *med17* and *med11* Mediator mutants is an asset and can be used to address this question. Genetic characterisation of *med17* mutants revealed that the temperature-sensitive phenotype cannot be dissociated from the UV-sensitive phenotype (Article 1). However, UV-sensitivity

of *med17* mutants is not a consequence of transcriptional defects as not all *med17* temperature sensitive mutants are UV-sensitive. Moreover, we have shown that in GG-NER deficient context, combined *med17* mutation and *rad26* deletion led to an increase in UV-sensitivity phenotype compared to either *rad26* or *med17* mutants. However, there was no increase in temperature sensitivity in these mutants, therefore genetic tests suggest that the link between Rad26 and Mediator is NER-related (Article 1). It should be noted that a genome-wide screen, in *S. cerevisiae*, identified a positive genetic interaction between Med11 Mediator and Rad26 (Costanzo *et al.*, 2016). *med11* temperature-sensitive mutant was crossed with *rad26* deletion mutant and the meiotic progeny harbouring both mutations were scored for fitness, by quantifying colony sizes. The progeny exhibited greater fitness than expected by the combination of the corresponding single mutants. Further studies are needed to precise the mechanisms involved.

In addition, we showed that the *med11* mutations lead to a UV-sensitivity in a GG-NER deficient background (Figure 35). We also tested whether the link between TFIIH and Mediator was implicated in NER, we used a mutant in which the interaction between of Med11 and Rad3 was disrupted, since Rad3 subunit is implicated in NER. However, using a mutant that was specifically affected for Rad3-Med11 interaction, we did not observe an increase in UV-sensitivity. This was observed for one mutant, it will be interesting to test other mutants that specifically affect the Rad3-Med11 interaction. Med11 is part of the head module of Mediator and recently, high resolution structural data of TFIIH in complex with Mediator head and middle module was obtained (Schilbach *et al.*, 2017). This structure can be used to target Mediator-TFIIH interaction.

V. Physical interaction between Mediator and NER proteins in the presence of UV-irradiation

We have looked at NER protein interactions with Mediator in the absence or presence of UV-irradiation, and did not observe any change (Figure 33). Therefore, the interactions between Mediator and NER proteins occur before the induction of exogenous damages and persist after damage induction.

RNA Pol II is the first TC-NER factor that encounters the damage. Therefore, it will be interesting to investigate whether the interactions between NER proteins (Rad, Rad10, Rad26 and Rad2) and RNA Pol II are modified after UV-irradiation.

Moreover, we carried out co-immunoprecipitation using whole cell extracts, hence we do not know whether the interaction between Mediator and NER proteins are direct or not. To address this question, we can use purified proteins for co-immunoprecipitation experiments.

VI. Effect of UV-irradiation on chromatin binding of Mediator, Rad1-Rad10, Rad26, Rad2 and RNA Pol II

Our ChIP experiments after UV-stress showed that the occupancy of tested proteins (Mediator, Rad1-Rad10, Rad26 and RNA Pol II) is modified after UV-irradiation (Figure 34). These experiments will be performed on a genome-wide scale to get the global trend of protein binding (Mediator, Rad1-Rad10, Rad26, Rad2 and RNA Pol II) after UV-damage induction.

Interestingly from our ChIP-qPCR analysis, we observed that Mediator is localized on transcribed regions after UV irradiation. To confirm this result, Mediator signal over the transcribed regions can be compared with that of a control immunoprecipitation with an untagged strain. Hence, it will be interesting to also check whether the interaction between Mediator and RNA Pol II is modified after UV stress. This can give a hint on how Mediator is transferred on the transcribed regions after UV-damage induction. Moreover, to further characterize the role of Mediator in NER, it will be interesting to perform a CPD ChIP in UV-sensitive and non UV-sensitive mutants, at different time-points, to investigate the difference in repair kinetics and hence precise Mediator's role in NER. CPD ChIP uses antibodies directed specifically against CPD lesions which are the most abundant UV-induced damage. This technique also requires considerable amount of immunoprecipitated fragments from the first protein ChIP to perform a second ChIP on CPD. Relatively high doses of UV have to be used so that a consequent amount of CPD is generated for immunoprecipitation (around 100 J/m^2).

The presence of RNA Pol II can block access of the downstream NER proteins to the damage sites or the passage of subsequent RNA Pol II, hence RNA Pol II has to be processed to free DNA damaged sites. Two mechanisms have been previously described in yeast for RNA Pol II clearing at DNA damage sites: Translesion bypass (Walmacq *et al*., 2012) and Def1-dependent RNA Pol II degradation (Woudstra *et al.*, 2002; Somesh *et al.*, 2005). Our results show a decrease of RNA Pol II immediately after UV-irradiation and its occupancy increases at 30 min post-UV stress. These results suggest a clearance of RNA Pol II immediately after UV-damage which is followed by an arrival of RNA Pol II within 30 min post-UV stress. To test whether the observed decrease of RNA Pol II is due to its degradation, a *def1* deletion mutant can be used to investigate whether RNA Pol II is still present on the chromatin in the presence of UV-irradiation. In case of rapid RNA Pol II eviction and degradation post-UV stress, we do not expect to see the decrease in RNA Pol II occupancy. Moreover, it will be interesting to correlate the change in RNA Pol II binding with transcriptional level post-UV irradiation (Elaborated in the next section) which can help in understanding the arrival of RNA Pol II signal 30 min post-UV irradiation. Indeed in human cells, it has been suggested that a *de novo* wave of elongating RNA Pol II is released, after UV-irradiation (Lavigne *et al.,* 2017) which has been proposed to allow a faster sensing and favoring a more open chromatin conformation due to the progression of RNA Pol II. Therefore, analysis of RNA

transcript produced can be assessed to get a direct measurement on a transcription level and help in understanding RNA Pol II genomic profile.

Rad26 is a TC-NER specific factor, involved in DNA damage recognition and hence intervening at a very early stage of TC-NER. ChIP-qPCR analysis on selected genes showed that there is a difference in occupancy after UV-irradiation and the effect seems to be related to transcription level. It was shown that its occupancy increased on lowly transcribed genes and decreased on highly transcribed genes. In both cases, there was a decrease 30 min after UV-irradiation, in accordance with an early requirement of Rad26. Hence, it is crucial to determine a genome-wide profile in understanding of Rad26 chromatin binding profile, after UV-irradiation. Moreover, it will be interesting to correlate the change in protein binding with transcriptional level post-UV irradiation (Elaborated in the next section).

Interestingly, we showed that Rad2, 3' endonuclease, and Rad1-Rad10, 5' endonuclease, have different chromatin binding dynamics. Rad2 occupancy is increased immediately after UV-irradiation and persists 30 min post-UV irradiation. This is interesting as the human homolog of Rad2, XPG, has been described as having a role in both damage recognition in TC-NER, in cooperation with CSB (homolog of yeast Rad26), and in damaged DNA cleavage as a 3'endonuclease. In yeast, Rad2 involvement in NER has been, for now, restricted to its 3' endonuclease activity. The early presence of Rad2 on chromatin suggests an early requirement and its persistence might reflect a role at later stages. Therefore having a genome-wide distribution profile of Rad2 in the presence of UV-irradiation together with testing its interactions with Rad26 and RNA Pol II after UV will be useful to understand Rad2 role after UV stress.

On the other hand, Rad1-Rad10 occupancy is increased 30 min after UV-irradiation, suggesting a role in later stages. The binding of Rad10 to UV-induced damage sites has been visualized by fluorescence microscopy in *S. cerevisiae* (Mardiros *et al.,* 2011). The formation of Rad10 foci was observed after 15 min with a peak 2h post-UV irradiation. Hence, other time-points, after UV-irradiation, can be performed to see the kinetics of Rad10 binding.

Furthermore, to better link the change in protein occupancy to UV-induced damage sites, a ChIP of a protein of interest followed by a CPD ChIP-seq can be performed. Hence, a genome-wide view of Mediator and NER proteins binding relative to DNA lesions can be obtained.

VII. Transcription level after UV-irradiation

In yeast, it has been proposed that RNA Pol II can bypass lesions or is degraded to allow efficient repair (Walmacq *et al*., 2012; Woudstra *et al.*, 2002; Somesh *et al.*, 2005). Therefore, it will be interesting to link the transcription level, after UV-irradiation, with the genome-wide distribution of RNA Pol II and the other NER proteins.

For profiling gene expression in the presence and absence of UV-irradiation, SLAM-sequencing (thiol (SH)-linked alkylation for the metabolic sequencing of RNA) can, for example, be used to evaluate RNA Pol II transcription (Herzog *et al.*, 2017). This approach has the advantage of taking into account RNA metabolism (RNA synthesis, processing and decay) and uses 4-thiouridine (s^4U), as nucleotide analogue, to label and hence track RNA molecules. s^4U can enter metazoan cells via nucleoside transporters. However, in yeast the hENT1 (human Equilibriative Nucleoside Transporter) has to be expressed and it has been demonstrated that this transporter can mediate the efficient uptake of s^4U (Miller *et al.,* 2011).

Briefly, total RNA extracted from cells are labelled with s^4U followed by a modification of its thiol by alkylation. cDNA libraries are generated by reverse transcription, which are then amplified by PCR and subjected to high-throughput sequencing. During reverse transcription, a guanine is added opposite to the alkylated s^4U and hence, there is an increase in thymine to cytosine conversion in newly synthesized RNA. Therefore, this technique can be used to quantitatively assess newly synthesized RNA after UV-irradiation.

3' mRNA library can be prepared that takes into account full-length transcript. However, some transcripts can be truncated due to RNA Pol II stalled in elongation and lack 3' polyAdenylated tail. Cap-seq library, compatible with SLAM-seq, mapping the 5' end of RNA anchored to RNA Pol II can be used to detect all transcripts.

VIII. Conservation of Mediator's role in NER in human cells

The laboratory has previously demonstrated the conservation of the interaction between Mediator and XPG (counterpart of Rad2) in human fibroblasts and HeLa cells by co-immunoprecipitation experiments (unpublished data). The new Mediator interactions showed with NER proteins (Rad1/XPF, Rad10/ERCC1 and Rad26/CSB) in yeast can also be tested in human cells. Moreover, genome-wide distributions of NER proteins can be compared to that of Mediator.

In Article 1, we have presented the interaction surface between Mediator and Rad2 and have identified residues important for Mediator-Rad2 interaction, whose mutations can lead to transcription defect and UV-sensitive phenotype. These yeast Mediator mutations can be transposed to human cells and their effect on Mediator interactions with NER proteins as well as their effects on the genomic occupancies of NER proteins can be analyzed. These experiments will help to understand the impact of Mediator mutations on DNA repair.

Furthermore, XP or XP/CS cell lines derived from patients' fibroblasts can be used to test the effect of mutations of NER factors on their interaction with Mediator and the impact of these mutations on the chromatin localization of Mediator and NER proteins. These experiments can help to characterize the molecular mechanisms affected in these patients.

One interesting question is the specific recruitment of Mediator to DNA damage, in different mutant contexts. In human cells, UV-damage foci can be induced in the nucleus and the recruitment of Mediator and the NER proteins to damage sites can be analyzed by fluorescence microscopy. Mediator UV-sensitive mutants can be used to investigate Mediator's requirement for the recruitment of different NER proteins to DNA damage sites. Experiments performed at different time points can give the kinetics of recruitment of the different factors.

To note that fluorescence microscopy experiments are trickier to put in place in yeast due to its small size and high background auto-fluorescence.

IX. Chromatin binding of NER proteins Rad1, Rad10, Rad26 and Rad2 can be linked to R-loops

Our ChIP-seq results showed that Rad1-Rad10 are present on class II genes and their presence is dependent on RNA Pol II transcription. We determined different gene categories based on the enrichment of Rad1-Rad10 and Mediator-Rad2 on their promoters. However, we did not find transcription-related differences of the different groups.

Interestingly, we also found that Rad1-Rad10 are present on class III genes, similarly to Rad2 (Eyboulet *et al.*, 2013). A temperature-sensitive mutant of RNA Pol III that considerably reduces transcription after a shift to non-permissive temperature, 37°C, was used to assess Rad2 presence on class III genes (unpublished data). It was shown that Rad2 presence on class III genes is not dependent on RNA Pol III transcription. It has to be investigated whether Rad1-Rad10 presence on class III genes is dependent on RNA Pol III transcription.

Given the presence of Rad2 and Rad1-Rad10 on class II and III genes, one possible line of investigation is their implication in R-loops processing. R-loops, found in organisms from bacteria to mammals, are DNA:RNA hybrids formed between nascent RNA and the transcribed strand, leaving the non-transcribed strand single-stranded. R-loops have been reported to have regulatory roles such as gene expression, DNA repair and can result from transcription of all three RNA Pols (Sollier and Cimprich, 2015). Moreover, modifications in R-loops regulation can lead to DNA damage and genome instability. In addition in human cells, it was proposed that TC-NER proteins process R-loops generated during transcription into double-strand breaks (Sollier *et al.*, 2014). Indeed, it was demonstrated that NER factors XPA (homolog of Rad14), TFIIH subunits XPD and XPB, flap endonucleases XPF and XPG (homologs of Rad1 and Rad2) are implicated in R-loop processing. A similar role was also demonstrated for yeast Rad2, suggesting conservation in R-loop processing. Moreover, TC-NER specific factor CSB (homolog of Rad26) was also involved in R-loop processing, but not GG-NER specific XPC (Sollier *et al.*, 2014).

In yeast, genome-wide distribution of R-loops has been reported to preferentially accumulate at certain genomic positions including RNA Pol III transcribed tRNAs, 5S rDNA (El Hage *et al.*, 2014). Interestingly, R-loops were detected in the wild-type strain in 5S rDNA

and were enriched over ORFs of highly transcribed class II genes with high GC-rich content (Chan *et al*., 2014; El Hage *et al.*, 2014). In the absence of RNase H, which resolve R-loops by cleaving the DNA: RNA hybrid, R-loops were increased over 5S rDNA and other RNA Pol III-transcribed genes.

Hence, it will be interesting to use the genome-wide data available on R-loops, in *S. cerevisiae*, to analyze the different gene groups, based on Rad2 and Rad1-Rad10 enrichment, to investigate whether there was a link between Rad2 and Rad1-Rad10 presence and R-loops-enriched regions. Moreover, Rad26 ChIP-seq signal can be correlated with the presence of R-loops, which are also formed on class II ORFs, where Rad26 is enriched.

Furthermore, we have not analyzed the sequence composition of the different gene groups enriched with Rad1-Rad10. This analysis can be performed, even more that R-loops have been reported to form preferentially on GC-rich class II genes (Chan *et al*., 2014).

Moreover, it will be interesting to investigate whether Mediator is implicated in R-loop processing. Genetic test can be performed as a first step by combining Mediator mutations and mutations in a gene involved in R-loop processing. For example, RNase H, which cleaves the DNA:RNA hybrid, or Topoisomerase I, which resolves negative DNA torsion behind RNA polymerase, can be mutated.

X. Concluding remarks

The NER pathway is closely linked to transcription, as illustrated by some of the factors having a role in NER as well as in transcription, for example, RNA Pol II and TFIIH.

Previously, the laboratory has identified a role for Mediator in NER, via a functional link with Rad2/XPG (Eyboulet *et al*., 2013). In this work, we have strengthened the link between Mediator, RNA Pol II and Rad2/XPG. We have also suggested a role for Mediator in TC-NER that is, at least in part, independent of Rad26. Moreover, we have provided results showing that the link between Mediator and the NER machinery can be extended to other NER proteins namely Rad1/XPF, Rad10/ERCC1 and Rad26/CSB proteins.

Interestingly, our study showed that NER proteins (Rad1, Rad10, Rad26 and Rad2) are present at the chromatin ahead of UV-induced damage, and that their presence depends on RNA Pol II transcription. Therefore, the targeting of NER factors on transcribing regions in the absence of damage, can facilitate repair of these regions after damage induction.

In addition, the role of Mediator can be extended to other DNA repair pathway, such as BER (Base Excision Repair) (unpublished data from collaborators). The role of Mediator in transcription and DNA repair illustrates the close link between these two fundamental processes. It also opens new possibilities to better understand the molecular basis of pathologies such as XP/CS (XP combined with CS) which have defects that are not limited to the NER pathway.

Material & Methods

I. Cell culture for ChIP, ChIP-seq and CoIP experiments

Yeast cells were grown to a final optical density (OD_{600}) of 0.6-0.8, corresponding to the exponential phase. The temperature at which the different strains were grown varies.

For experiments involving:

-Only wild-type cells, for example those conducted to obtain the genomic distribution of Rad1, Rad10 and Rad26 presented in Figure 24, cells were also grown at 30°C.

- *rad2*, *rad1* and *rad10* deletion mutants as well as the *med17* mutants, and the corresponding wild-types were also grown at 30°C.

- In *RPB1* wild-type and rpb1-1 mutant contexts, cells were grown at 25°C to 0.4-0.5 OD_{600} and then shifted to 37°C for 90min.

- In *KIN28* wild-type and *kin28* mutant contexts, cells were grown at 25°C to 0.4-0.5 OD_{600} and then shifted to 37°C for 75min.

II. Cell preparation for UV experiments

For co-immunoprecipitation: Yeast cells were grown at 30°C till 0.6-0.8 OD_{600}, collected by centrifugation and resuspended in PBS 1X. 100 mL of culture was used per condition. Cells were either directly collected (UV-) or treated with UV at 50 J/m^2 in PBS 1X. UV-treated cells were either collected directly (T0) or after 30 min (T30) or 60 min (T60) incubation at 30°C, in YPD.

For ChIP: Cells were grown at 30°C to OD600 0.6-0.8, collected by centrifugation and resuspended in PBS 1X. 100 mL of culture was used per condition. Cells were either directly collected (UV-) or treated with UV at 50 J/m2 in PBS 1X. UV-treated cells were either collected directly (T0) or after 30 min (T30) or 60 min (T60) incubation at 30°C, in YPD.

III. Coimmunoprecipitation

Cell extract preparation

- 100 mL of yeast cells were collected by centrifugation at 3200g (4000 rpm) for 3 min and washed with 100 mL of water.
- Cells were resuspended in 10 mL of WB- buffer and centrifugated.
- Cells were resuspended in 1 mL of WB- buffer (10% Glycerol, 50mM Hepes-KOH pH 7.5, 150mM NaCl, 1mM EDTA, 0.05% NP-40, 1 mM DTT) and transferred to 2 mL-Eppendorf tube.
- Cells were resuspended in 500 µL of PMSF-containing buffer WB+ (WB buffer supplemented with DTT, PMSF (Serine protease inhibitor) and cOmplete (Protease

Inhibitor Cocktail)) and transferred to a tube containing 400 µL of glass beads (425-600 µm, Sigma).
- Cell lysis was performed by bead-beating for 30 min (maximum) at 4°C.
- The cell extract was then centrifugated at 15000g (13200 rpm) for 15 min at 4°C. The supernatant was collected and then a centrifugation step was repeated again.
- Protein concentration was measured using Bradford method, taking BSA (Bovine Serum Albumin) as reference.

Protein immunoprecipitation
- 50 µL of anti-mouse IgG coated beads ((Dynabeads Pan mouse IgG, Invitrogen) was washed with 500 µL of PBS-BSA 0.1%, at 4°C.
- The beads were resuspended in 100 µL of PBS-BSA 0.1%, at 4°C and 1 µL of anti-HA (12CA5) was added.
- Beads and antibodies were incubated for 1h under agitation, 1300 rpm for 30 min at 4°C.
- The antibody-coated beads were then washed thrice, with 500 µL of PBS-BSA 0.1%, at 4°C, for 5 min with constant agitation.
- Two additional rapid washes were done in WB+ buffer.
- Protein extract was centrifugated for 15 min at rpm 13200g (12000 rpm) and 1.5 mg of protein extract was added on antibody-coated beads.
- Incubation was done with constant agitation at 1300 rpm, 4°C, for 3h. After 1h30min, PMSF 100X was added for a final concentration of 1X.
- Four washes with WB+ buffer, with agitation at 1300 rpm, for 5min at 40C. The tube is changed after the first wash.
- 40µL SDS Sample Buffer (15% Glycerol, 3% SDS, 75mM Tris-HCl, pH 6.8, 15mM EDTA) was added to beads, and samples (with beads) were kept at -80°C.

Western blotting
- Prior to SDS-PAGE, proteins were eluted by incubation at 85°C for 2 min.
- 20 µg of input and 10 µL of immunoprecipitated sample was loaded on a bis-acrylamide gel in Tris-Glycine-SDS Buffer.
- Proteins were transferred on Amersham Protran 0.2 NC membranes (GE Healthcare) for Western blotting.
- Membranes were incubated for 1h in Tris-Buffered-Saline buffer supplemented with 0.5% Tween 20 (TBS-T) and 5% milk.
- Membranes were incubated with antibodies in TBS-T with 2% milk overnight with the indicated antibody (diluted at 1:10000 for anti-HA (12CA5), 1:5000 for anti-Myc (9E10), or 1:2000 for anti-Rpb1-CTD (8WG16)).
- Membranes were washed three times in TBS-T and then incubated for 45 min -1h in TBS-T with 2% milk containing secondary antibodies diluted at 1:20000 (HRP-anti Mouse-IgG (H+L) (Promega)). After 3 more washes in TBS-T, detection was carried out using Amersham ECL or ECL-Prime reagents (GE Healthcare). Imaging was done using a Fusion FX7 imaging system.

IV. ChIP and ChIP-seq experiments

Chromatin immunoprecipitation (ChIP) is carried out to evaluate the binding of a protein on chromatin, additional library preparation and sequencing steps allow the visualisation of protein binding on a genome-wide scale (ChIP-seq). The experiments were performed in triplicates.

Cell culture and cross-link

- 100 mL of three independent cultures were grown as indicated above, depending on the strain used.
- Covalent crosslinks between DNA and protein was carried out by formaldehyde: 3 mL of formaldehyde 37% was added to the culture and let to agitate for 10 min.
- To stop the crosslink, 2.5M glycine was added and let to agitate for 5 min.
- Cells were collected in 50 mL falcons by centrifugation for 3 min at 3200g (4000 rpm).
- Cells were resuspended in 50 mL Tris 20 mM pH8 at 4°C, and centrifugated as above. This step was repeated.
- Cells were resuspended in 5 mL of FA/SDS buffer (Hepes KOH 50 mM (pH 7.5), NaCl 150 mM, EDTA 1 mM, Triton 100X 1%, Déoxycholate de Na 0,1%, SDS 0,1%) containing PMSF (FA-SDS+PMSF), a serine protease inhibitor.
- Cells were transferred to 1.5 mL Eppendorf tubes and centrifugated.
- Cells were frozen in liquid nitrogen and stored at -80°C.

Chromatin preparation

- Cells were resuspended in 1 mL of FA-SDS+PMSF and 500 µL were transferred to two 2mL Eppendorf tubes, each containing 750 µL of glass beads (425-600 µm, Sigma).
- Cells were lysed by bead-beating for 30 min (maximum) at 4°C.
- Eppendorf tubes were pierced with a heated needle (0,7x30mm).
- Each tube was placed in a 14 mL falcon and centrifugated for 800g (2000 rpm) for 1 min.
- The beads were washed twice with 200 µL of FA-SDA+PMSF and centrifugated.
- The cellular suspensions, two per condition, were then regrouped in a 2 mL Eppendorf tube.
- The cell extracts were then centrifugated at 13200g (12000 rpm) for 20 min, at 4°C.
- The supernatant was discarded. The cross-linked chromatin appears as a transparent ring around the opaque pellet.
- The opaque pellet and chromatin ring are transferred using a glass Pasteur pipettes, with a sealed end, to a 2 mL Eppendorf tube. The tube was washed with 800 µL of FA-SDS +PMSF.
- The pellet was resuspended using a Pasteur pipette and finishing with few aspirations with a P1000 pipette.
- The cells were then placed on a rotating wheel for 1-1 ½ h.
- The cellular suspension was then centrifugated for 20 min at 4°C. The supernatant was discarded.

Chromatin sonication

Chromatin preparation include of a step of chromatin shearing, to obtain fragments of about 200 bases mean size as illustrated in Figure 36.

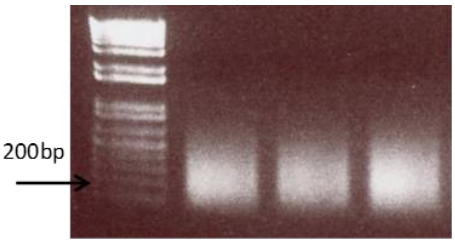

Figure 36: Size of sonicated fragments.
The fragments obtained after sonication were analysed on an agarose gel**.**

- The pellet was resuspended and transferred to a 1mL milliTube Covaris.
- Chromatin were sheared using a S220 focused-ultrasonicator (Covaris), for 10 min at 150W pulses for 10% of the time (duty factor 10).
- After sonication, the suspension was transferred to a 1.5 mL Eppendorf tube and collected by centrifugation at 9300g (10000 rpm) for 30 min, at 4°C.
- The sonicated chromatin was now soluble, hence the supernatant was collected and 1.2 mL of FA-SDS+PMSF was added. Aliquots of 650 µL were stored at -80°C.

Chromatin immunoprecipitation

- 50 µL of anti-mouse IgG coated beads ((Dynabeads Pan mouse IgG, Invitrogen) was washed with 500 µL of PBS-BSA 0.1%, at 4°C.
- The beads were resuspended in 100 µL of PBS-BSA 0.1%, at 4°C and antibodies were added. 1 µL of anti-HA (12CA5) or 2 µL of anti-Myc (9E10) or 5 µL of anti-Rpb1 (8WG16).
- Beads and antibodies were incubated for 1h under agitation, 1300 rpm for 30 min at 30°C.
- The antibody-coated beads were then washed twice, with 500 µL of PBS-BSA 0.1%, at 4°C.
- An additional wash was done with agitation, 1300 rpm for 10 min at 30°C, followed by another quick wash.
- 500 µL of chromatin suspension was added on the antibody-coated beads and 50 µL of PBS-BSA 10 mg/ml was added.
- The mix was incubated for 2h at 21°C, with constant agitation (1300 rpm).
- The supernatant was removed and the beads were resuspended in 500 µL of FA-SDS.
- Two rapid washes were done with FA-SDS + 500 mM NaCl. An additional was at 1300 rpm agitation for 10 min at 21°C.
- The beads were then washed with 500 µL IP Buffer (Tris 10mM pH8, LiCl 0.25M, EDTA 1mM, NP40 0.5%, Na-Deoxycholate 0.5%), followed by TE buffer Tris 10mM pH 8, EDTA 1mM).
- Elution was carried out at 65° C for 20 min, at 600 rpm constant agitation in a pronase buffer.

- 6.25 µL of Pronase was added to the eluate. For input, to 100 µL of chromatin (not immunoprecipitated), 25 µL of pronase buffer 5X was added. Incubation at 37 °C for 30 min-1h, for pronase to act.
- 3.3 µL of RNase immunoprcipitated DNA (IP) and Input DNA (IN), incubation at 37 °C for 1h.
- DNA was purified using Qiagen kit for PCR purification, according to manufacturer's protocol.
- qPCR analysis was conducted using qPCR MasterMix SYBR® Green (Taykon).

V. ChIP-seq data analysis of Rad1, Rad10 and Rad26

Sequences were aligned on *S. cerevisiae* genome (University of California at Santa Cruz [UCSC] version sacCer3) with Bowtie version 0.12.7. Only uniquely mapped tags were used, allowing a maximum of two mismatches. To avoid possible sequencing artifacts, reads beyond five repetitions at the same position of the genome were removed. Samtools and deepTools were used to generate different file formats.

Data normalization:

- For examples of enrichment profiles, screen shots of the profiles were taken from IGB (Integrated Genome Browser). The protein enrichment profiles were presented after subtraction of the signal from the ChIP of an untagged strain. It the yeast genome, there are some regions that display an apparent enrichment, most of which are RNA Pol II highly-transcribed regions. To correct for this background distribution, the normalized signal of the untagged strain was subtracted from each protein ChIP signal. qPCR normalisation using the ratio between the protein ChIP and the untagged strain ChIP was done. Normalisation values are presented in Table 3.

- For metagene data analysis, data was normalized in RPM (Reads Per Million of mapped reads). These normalized bigwig files were used for calculating densities genome-wide analysis.

Metagene analysis

To get a global view of the occupancy of a protein of interest, and compare genomic profiles of different proteins, metagene analysis were conducted.

- **Enrichment peak identification and Venn diagram**

To detect protein enrichment peaks, MACS2 (Peakcalling software) can be used on bam or bed files. MACS2 allows the identification of peaks in protein ChIP file compared to control file (for example, input), to ensure the detection of specific peaks.

Script:

```
macs2 callpeak -t IP-Prot.bed -c Input-Prot.bed -n Name -g 12495682  --
keep-dup=all –m 2,100  --bw 300 –q 0.05
```

Parameters:

```
-t/--treatment: Protein ChIP file

-c/--control: Control file

-n/--name: Name of the output file

-g/--gsize: Size of the reference genome

--keep-dup: Parameter for duplicated reads. If the option "all" is
selected, MACS2 keep all the reads. If a number is specified, MACS2 keep
that number of reads at each position.

--m/--mfold: Parameter used to define fold change, enrichment compared to
background

--bw : Bandwidth used to scan the genome

-q/--qvalue : Significant peak detection threshold
```

Annotated peaks can be used to generate Venn diagrams to have a qualitative analysis of different protein enrichments. A script "plotVennDiag" written by Olivier Alibert was used. This script uses the peak files generated by MACS2 and calculate the intersection between different lists and display the result in the form of a Venn diagram. These lists of genes can be used for gene ontology analysis. For example, to categorise genes enriched for different proteins based on their molecular function or biological process in which they are implicated.

- **Correlation plots and density profiles**

For the generation of correlation plots and average density profiles, the read densities over regions of interest were calculated. A "get-tag_density" script written by Olivier Alibert (IRCM, Evry) was used to generate enrichment over promoter or transcribed regions. This script can output average densities over a region as well as give density per position, taking into consideration the strand orientation.

For correlation plots, the promoter regions corresponding to intergenic regions of tandem and divergent genes that do not overlap class III genes were used (4068). The transcribed regions correspond to RNA Pol II-enriched regions (3552).

For mean density plots around Med15 peaks (767), intergenic regions in tandem were used, which allowed to take into consideration strand orientation. Also, tandem intergenic regions

can be unambiguously assigned to one gene promoter. For oriented density plots, it is important to take into consideration the strand directionality.

Script for calculating read densities:

```
get_tag_density -s -f IP-Prot.bw Annotated_interest_regions.bed > Read_density.tsv
```

Parameters:

```
-s : take into consideration the strand orientation

-f : input file of protein of interest in bigwig

Annotated_interest_regions.bed: File containing the regions of interest, in bed format, on which the densities will be obtained

Read_density.tsv: Output file containing the densities. This file, namely, contains information on the genomic region, the start and end coordinates of the region, the strand orientation, the average densities over the genomic
```

Using these densities, correlation and mean density plots were generated in R. For correlation profiles, the density per position was used, and for mean density profile plot, the average density over a region was used. The output file of the "get_tag_density" contains both information, therefore the required density values have to be extracted from those files. The script below is an example for extracting density per position for the protein of interest. .

```
cut -f4,7 Tag-density_IP-Prot.tsv | sed 's/\;/\t/g' > densityvalues-IP-Prot.tsv
```

Parameters:

```
cut -f4,7 : Allows to retrieve columns 4, corresponding to the name of the region, and column 7, containing the densities per position from the input file.

sed 's/\;/\t/g' : Replaces « ; » in the input file to tabs in the output file. This file can be used with R packages to generate the different plots.
```

Rad1-Rad10 and Mediator-Rad2 groups

Genes were categorized in different groups using their average densities over promoter regions (Elizaveta Novikova). To categorize gene promoters according to the enrichment of Rad1, Rad10, Rad2 and Mediator (Med15), five gene groups were generated. First, the average densities of each protein over promoter regions were calculated using the "get-tag_density" script. Given that there is a very good genome-wide correlation between Rad1

and Rad10 and Mediator and Rad2, the $\log_2$ ratio of the average densities of Rad1 and Rad10 were added, and similarly for Mediator and Rad2. Then four groups were generated based on the enrichment values and a fifth group consists of promoter regions at the border of these groups. The four gene groups were defined based on the enrichment of the protein pairs (Rad1-Rad10 pair and Mediator-Rad2 pair) on promoter regions: Rad1-Rad10 and Mediator-Rad2 enriched (MR), Rad1-Rad10 enriched (R), Mediator-Rad2 enriched (M) and a group without any of the protein enrichment (0). The dot plot and heatmap were generated in R.

kin28 mutant ChIP-seq experiments for Rad10, Rad26, RNA Pol II and Mediator

The data normalization and bioinformatics analyses were carried out as described in Article 1 and qPCR normalization protocol was based on Eyboulet *et al.*, 2013. For data normalization: Densities were scaled per million reads (RPM) and then read numbers were normalized relative to qPCR data on a set of selected regions using the ratio between wild-type (WT) and mutant strains. The ratio of ChIP-qPCR values (V) between WT and mutant strains was calculated for each selected region (RqPCR = VqPCRmut/VqPCRWT). For the same region, the ratio of ChIP-seq reads (N) between WT and mutant strains (Rseq =Nseqmut/Nseqwt) was determined. The ratio of the ChIP-qPCR and ChIP-seq read was calculated for each region (Q=RqPCR/Rseq). The mean of these ratios corresponds to the normalization coefficient, displayed in table 3, which is then used for ChIPseq data normalization.

Protein	Normalization coefficient
Rad1	1.85
Rad10	1.02
Rad26	0.65
RNA Pol II (*kin28* experiments)	3.59
Med17 (*kin28* experiments)	0.955
Rad26 (*kin28* experiments)	1.55
Rad10 (*kin28* experiments)	0.69

Table 3: Normalization values applied to ChIP-seq data.

References

Adam, S., Polo, S.E., and Almouzni, G. (2013). Transcription Recovery after DNA Damage Requires Chromatin Priming by the H3.3 Histone Chaperone HIRA. Cell *155*, 94–106.

Adar, S., Hu, J., Lieb, J.D., and Sancar, A. (2016). Genome-wide kinetics of DNA excision repair in relation to chromatin state and mutagenesis. Proc. Natl. Acad. Sci. U.S.A. *113*, E2124-2133.

Akoulitchev, S., Chuikov, S., and Reinberg, D. (2000a). TFIIH is negatively regulated by cdk8-containing mediator complexes. *407*, 8.

Alekseev, S., Nagy, Z., Sandoz, J., Weiss, A., Egly, J.-M., Le May, N., and Coin, F. (2017). Transcription without XPB Establishes a Unified Helicase-Independent Mechanism of Promoter Opening in Eukaryotic Gene Expression. Molecular Cell *65*, 504-514.e4.

Andrade-Lima, L.C., Veloso, A., Paulsen, M.T., Menck, C.F.M., and Ljungman, M. (2015). DNA repair and recovery of RNA synthesis following exposure to ultraviolet light are delayed in long genes. Nucleic Acids Research *43*, 2744–2756.

Andrau, J.-C., van de Pasch, L., Lijnzaad, P., Bijma, T., Koerkamp, M.G., van de Peppel, J., Werner, M., and Holstege, F.C.P. (2006). Genome-Wide Location of the Coactivator Mediator: Binding without Activation and Transient Cdk8 Interaction on DNA. Molecular Cell *22*, 179–192.

Anindya, R., Mari, P.-O., Kristensen, U., Kool, H., Giglia-Mari, G., Mullenders, L.H., Fousteri, M., Vermeulen, W., Egly, J.-M., and Svejstrup, J.Q. (2010). A Ubiquitin-Binding Domain in Cockayne Syndrome B Required for Transcription-Coupled Nucleotide Excision Repair. Molecular Cell *38*, 637–648.

Araujo, S.J., Nigg, E.A., and Wood, R.D. (2001). Strong Functional Interactions of TFIIH with XPC and XPG in Human DNA Nucleotide Excision Repair, without a Preassembled Repairosome. Molecular and Cellular Biology *21*, 2281–2291.

Araújo, S.J., Tirode, F., Coin, F., Pospiech, H., Syväoja, J.E., Stucki, M., Hübscher, U., Egly, J.-M., and Wood, R.D. (2000). Nucleotide excision repair of DNA with recombinant human proteins: definition of the minimal set of factors, active forms of TFIIH, and modulation by CAK. Genes Dev *14*, 349–359.

Armache, K.-J., Kettenberger, H., and Cramer, P. (2003). Architecture of initiation-competent 12-subunit RNA polymerase II. Proceedings of the National Academy of Sciences *100*, 6964–6968.

Asturias, F.J., Jiang, Y.W., Myers, L.C., Gustafsson, C.M., and Kornberg, R.D. (1999). Conserved Structures of Mediator and RNA Polymerase II Holoenzyme. Science *283*, 985–987.

Baek, H.J., Kang, Y.K., and Roeder, R.G. (2006). Human Mediator enhances basal transcription by facilitating recruitment of transcription factor IIB during preinitiation complex assembly. J. Biol. Chem. *281*, 15172–15181.

Baek, H.J., Kang, Y.K., and Roeder, R.G. (2006). Human Mediator enhances basal transcription by facilitating recruitment of transcription factor IIB during preinitiation complex assembly. J. Biol. Chem. *281*, 15172–15181.

Bailly, V., Sommers, C.H., Sung, P., Prakash, L., and Prakash, S. (1992). Specific complex formation between proteins encoded by the yeast DNA repair and recombination genes RADI and RADIO. Proc. Natl. Acad. Sci. USA 5.

Barberis, A., Pearlberg, J., Simkovich, N., Farrell, S., Reinagel, P., Bamdad, C., Sigal, G., and Ptashne, M. (1995). Contact with a component of the polymerase II holoenzyme suffices for gene activation. Cell *81*, 359–368.

Bardwell, A.J., Bardwell, L., Iyer, N., Svejstrup, J.Q., Feaver, W.J., Kornberg, R.D., and Friedberg, E.C. (1994). Yeast nucleotide excision repair proteins Rad2 and Rad4 interact with RNA polymerase II basal transcription factor b (TFIIH). Molecular and Cellular Biology *14*, 3569–3576.

Baumeister, W., Herzog, F., et al. (2015). Architecture of the RNA polymerase II–Mediator core initiation complex. Nature *518*, 376–380.

Berti, L., Mittler, G., Przemeck, G.K.H., Stelzer, G., Günzler, B., Amati, F., Conti, E., Dallapiccola, B., Hrabé de Angelis, M., Novelli, G., et al. (2001). Isolation and Characterization of a Novel Gene from the DiGeorge Chromosomal Region That Encodes for a Mediator Subunit. Genomics *74*, 320–332.

Bhatia, P.K., Verhage, R.A., Brouwer, J., and Friedberg, E.C. (1996). Molecular cloning and characterization of Saccharomyces cerevisiae RAD28, the yeast homolog of the human Cockayne syndrome A (CSA) gene. Journal of Bacteriology *178*, 5977–5988.

Bohr, V. (1985). DNA repair in an active gene: Removal of pyrimidine dimers from the DHFR gene of CHO cells is much more efficient than in the genome overall. Cell *40*, 359–369.

Boiteux, S., and Jinks-Robertson, S. (2013). DNA Repair Mechanisms and the Bypass of DNA Damage in Saccharomyces cerevisiae. Genetics *193*, 1025–1064.

Boube, M., Joulia, L., Cribbs, D.L., and Bourbon, H.-M. (2002). Evidence for a Mediator of RNA Polymerase II Transcriptional Regulation Conserved from Yeast to Man. Cell *110*, 143–151.

Bourbon, H.-M. (2008). Comparative genomics supports a deep evolutionary origin for the large, four-module transcriptional mediator complex. Nucleic Acids Research *36*, 3993–4008.

Bourbon, H.-M., Aguilera, A., Ansari, A.Z., Asturias, F.J., Berk, A.J., Bjorklund, S., Blackwell, T.K., Borggrefe, T., Carey, M., Carlson, M., et al. (2004). A Unified Nomenclature for Protein Subunits of Mediator Complexes Linking Transcriptional Regulators to RNA Polymerase II. Molecular Cell *14*, 553–557.

Boyce, R.P., and Howard-Flanders, P. (1964). Genetic control of dna breakdown and repair in e. Coli k-12 treated with mitomycin c or ultraviolet light. Z. Vererbungsl. *95*, 345–350.

Bregman, D.B., Halaban, R., van Gool, A.J., Henning, K.A., Friedberg, E.C., and Warren, S.L. (1996). UV-induced ubiquitination of RNA polymerase II: a novel modification deficient in Cockayne syndrome cells. Proceedings of the National Academy of Sciences *93*, 11586–11590.

Budd, M.E., and Campbell, J.L. (1995). DNA polymerases required for repair of UV-induced damage in Saccharomyces cerevisiae. Molecular and Cellular Biology *15*, 2173–2179.

Bukowska, B., and Karwowski, B.T. (2018). Actual state of knowledge in the field of diseases related with defective nucleotide excision repair. Life Sciences *195*, 6–18.

Bushnell, D.A., and Kornberg, R.D. (2003). Complete, 12-subunit RNA polymerase II at 4.1-A resolution: Implications for the initiation of transcription. Proceedings of the National Academy of Sciences *100*, 6969–6973.

Cai, G., Imasaki, T., Takagi, Y., and Asturias, F.J. (2009). Mediator Structural Conservation and Implications for the Regulation Mechanism. Structure *17*, 559–567.

Ceccaldi, R., Rondinelli, B., and D'Andrea, A.D. (2016). Repair Pathway Choices and Consequences at the Double-Strand Break. Trends in Cell Biology *26*, 52–64.

Chaudhuri, S., Wyrick, J.J., and Smerdon, M.J. (2009). Histone H3 Lys79 methylation is required for efficient nucleotide excision repair in a silenced locus of Saccharomyces cerevisiae. Nucleic Acids Research *37*, 1690–1700.

Chen, F.X., Smith, E.R., and Shilatifard, A. (2018). Born to run: control of transcription elongation by RNA polymerase II. Nature Reviews Molecular Cell Biology *19*, 464–478.

Chen, X., Ruggiero, C., and Li, S. (2007). Yeast Rpb9 Plays an Important Role in Ubiquitylation and Degradation of Rpb1 in Response to UV-Induced DNA Damage. Molecular and Cellular Biology *27*, 4617–4625.

Chinchilla, K., Rodriguez-Molina, J.B., Ursic, D., Finkel, J.S., Ansari, A.Z., and Culbertson, M.R. (2012). Interactions of Sen1, Nrd1, and Nab3 with Multiple Phosphorylated Forms of the Rpb1 C-Terminal Domain in Saccharomyces cerevisiae. Eukaryotic Cell *11*, 417–429.

Christiansen, M. (2003). Functional consequences of mutations in the conserved SF2 motifs and post-translational phosphorylation of the CSB protein. Nucleic Acids Research *31*, 963–973.

Chu, G., and Chang, E. (1988). Xeroderma pigmentosum group E cells lack a nuclear factor that binds to damaged DNA. Science *242*, 564–567.

Citterio, E., Van Den Boom, V., Schnitzler, G., Kanaar, R., Bonte, E., Kingston, R.E., Hoeijmakers, J.H.J., and Vermeulen, W. (2000). ATP-Dependent Chromatin Remodeling by the Cockayne Syndrome B DNA Repair-Transcription-Coupling Factor. Molecular and Cellular Biology *20*, 7643–7653.

Clapier, C.R., and Cairns, B.R. (2009). The Biology of Chromatin Remodeling Complexes. Annual Review of Biochemistry *78*, 273–304.

Cleaver, J.E. (2005). Opinion: Cancer in xeroderma pigmentosum and related disorders of DNA repair. Nature Reviews Cancer *5*, 564–573.

Coin, F., De Santis, L.P., Nardo, T., Zlobinskaya, O., Stefanini, M., and Egly, J.-M. (2006). p8/TTD-A as a Repair-Specific TFIIH Subunit. Molecular Cell *21*, 215–226.

Costanzo, M., VanderSluis, B., Koch, E.N., Baryshnikova, A., Pons, C., Tan, G., Wang, W., Usaj, M., Hanchard, J., Lee, S.D., et al. (2016). A global genetic interaction network maps a wiring diagram of cellular function. Science *353*, aaf1420–aaf1420.

Craighead, J.L., Chang, W., and Asturias, F.J. (2002). Structure of Yeast RNA Polymerase II in Solution: Implications for Enzyme Regulation and Interaction with Promoter DNA.

Cramer, P. (2000). Architecture of RNA Polymerase II and Implications for the Transcription Mechanism. Science *288*, 640–649.

Cramer, P. (2004). RNA polymerase II structure: from core to functional complexes. Current Opinion in Genetics & Development *14*, 218–226.

Crowley, D.J., Boubriak, I., Berquist, B.R., Clark, M., Richard, E., Sullivan, L., DasSarma, S., and McCready, S. (2006). The uvrA, uvrB and uvrC genes are required for repair of ultraviolet light induced DNA photoproducts in Halobacterium sp. NRC-1. Saline Syst. *2*, 11.

de Laat, W.L., Appeldoorn, E., Sugasawa, K., Weterings, E., Jaspers, N.G.J., and Hoeijmakers, J.H.J. (1998). DNA-binding polarity of human replication protein A positions nucleases in nucleotide excision repair. Genes & Development *12*, 2598–2609.

den Dulk, B., van Eijk, P., de Ruijter, M., Brandsma, J.A., and Brouwer, J. (2008). The NER protein Rad33 shows functional homology to human Centrin2 and is involved in modification of Rad4. DNA Repair *7*, 858–868.

Dinant, C., Ampatziadis-Michailidis, G., Lans, H., Tresini, M., Lagarou, A., Grosbart, M., Theil, A.F., van Cappellen, W.A., Kimura, H., Bartek, J., et al. (2013). Enhanced Chromatin Dynamics by FACT Promotes Transcriptional Restart after UV-Induced DNA Damage. Molecular Cell *51*, 469–479.

Ding, B., LeJeune, D., and Li, S. (2010). The C-terminal Repeat Domain of Spt5 Plays an Important Role in Suppression of Rad26-independent Transcription Coupled Repair. J. Biol. Chem. *285*, 5317–5326.

Dotson, M.R., Yuan, C.X., Roeder, R.G., Myers, L.C., Gustafsson, C.M., Jiang, Y.W., Li, Y., Kornberg, R.D., and Asturias, F.J. (2000). Structural organization of yeast and mammalian mediator complexes. Proceedings of the National Academy of Sciences *97*, 14307–14310.

Douki, T., Angelov, D., and Cadet, J. (2001). UV laser photolysis of DNA: effect of duplex stability on charge-transfer efficiency. J. Am. Chem. Soc. *123*, 11360–11366.

Douziech, M., Coin, F., Chipoulet, J.-M., Arai, Y., Ohkuma, Y., Egly, J.-M., and Coulombe, B. (2000). Mechanism of Promoter Melting by the Xeroderma Pigmentosum Complementation Group B Helicase of Transcription Factor IIH Revealed by Protein-DNA Photo-Cross-Linking. Molecular and Cellular Biology *20*, 8168–8177.

Dubaele, S., Proietti De Santis, L., Bienstock, R.J., Keriel, A., Stefanini, M., Van Houten, B., and Egly, J.-M. (2003). Basal transcription defect discriminates between xeroderma pigmentosum and trichothiodystrophy in XPD patients. Mol. Cell *11*, 1635–1646.

Dunand-Sauthier, I., Hohl, M., Thorel, F., Jaquier-Gubler, P., Clarkson, S.G., and Schärer, O.D. (2005). The Spacer Region of XPG Mediates Recruitment to Nucleotide Excision Repair Complexes and Determines Substrate Specificity. Journal of Biological Chemistry *280*, 7030–7037.

Duncan, J., Hamilton, L., and Friedberg, E.C. (1976). Enzymatic degradation of uracil-containing DNA. II. Evidence for N-glycosidase and nuclease activities in unfractionated extracts of Bacillus subtilis. J. Virol. *19*, 338–345.

Ebmeier, C.C., and Taatjes, D.J. (2010). Activator-Mediator binding regulates Mediator-cofactor interactions. Proceedings of the National Academy of Sciences *107*, 11283–11288.

Edwards, A.M., Kane, C.M., Young, R.A., and Kornberg, R.D. (1991). Two dissociable subunits of yeast RNA polymerase II stimulate the initiation of transcription at a promoter in vitro. J. Biol. Chem. *266*, 71–75.

Eick, D., and Geyer, M. (2013). The RNA Polymerase II Carboxy-Terminal Domain (CTD) Code. Chemical Reviews *113*, 8456–8490.

Emmert, S., Slor, H., Busch, D.B., Batko, S., Albert, R.B., Coleman, D., Khan, S.G., Abu-Libdeh, B., DiGiovanna, J.J., Cunningham, B.B., et al. (2002). Relationship of Neurologic Degeneration to Genotype in Three Xeroderma Pigmentosum Group G Patients11An abstract of this study was presented at the annual meeting of the Society for Investigative Dermatology, May 2000, Chicago, IL, and published in J Invest Dermatol 114:825, 2000. Journal of Investigative Dermatology *118*, 972–982.

Enzlin, J.H. (2002). The active site of the DNA repair endonuclease XPF-ERCC1 forms a highly conserved nuclease motif. The EMBO Journal *21*, 2045–2053.

Esnault, C., Ghavi-Helm, Y., Brun, S., Soutourina, J., Van Berkum, N., Boschiero, C., Holstege, F., and Werner, M. (2008). Mediator-Dependent Recruitment of TFIIH Modules in Preinitiation Complex. Molecular Cell *31*, 337–346.

Evans, E. (1997). Open complex formation around a lesion during nucleotide excision repair provides a structure for cleavage by human XPG protein. The EMBO Journal *16*, 625–638.

Eyboulet, F., Cibot, C., Eychenne, T., Neil, H., Alibert, O., Werner, M., and Soutourina, J. (2013). Mediator links transcription and DNA repair by facilitating Rad2/XPG recruitment. Genes Dev. *27*, 2549–2562.

Eyboulet, F., Wydau-Dematteis, S., Eychenne, T., Alibert, O., Neil, H., Boschiero, C., Nevers, M.-C., Volland, H., Cornu, D., Redeker, V., et al. (2015). Mediator independently orchestrates multiple steps of preinitiation complex assembly in vivo. Nucleic Acids Research *43*, 9214–9231.

Eychenne, T., Novikova, E., Barrault, M.-B., Alibert, O., Boschiero, C., Peixeiro, N., Cornu, D., Redeker, V., Kuras, L., Nicolas, P., et al. (2016). Functional interplay between Mediator and

TFIIB in preinitiation complex assembly in relation to promoter architecture. Genes & Development *30*, 2119–2132.

Eychenne, T., Werner, M., and Soutourina, J. (2017). Toward understanding of the mechanisms of Mediator function *in vivo* : Focus on the preinitiation complex assembly. Transcription *8*, 328–342.

Fagbemi, A.F., Orelli, B., and Schärer, O.D. (2011). Regulation of endonuclease activity in human nucleotide excision repair. DNA Repair *10*, 722–729.

Felsenfeld, G., and Groudine, M. (2003). Controlling the double helix. Nature *421*, 448–453.

Fitch, M.E., Nakajima, S., Yasui, A., and Ford, J.M. (2003). *In Vivo* Recruitment of XPC to UV-induced Cyclobutane Pyrimidine Dimers by the *DDB2* Gene Product. Journal of Biological Chemistry *278*, 46906–46910.

Fondell, J.D., Ge, H., and Roeder, R.G. (1996). Ligand induction of a transcriptionally active thyroid hormone receptor coactivator complex. Proceedings of the National Academy of Sciences *93*, 8329–8333.

Fousteri, M., Vermeulen, W., van Zeeland, A.A., and Mullenders, L.H.F. (2006). Cockayne Syndrome A and B Proteins Differentially Regulate Recruitment of Chromatin Remodeling and Repair Factors to Stalled RNA Polymerase II In Vivo. Molecular Cell *23*, 471–482.

Furter-Graves, E.M., Hall', B.D., and Furter, R (1994). Role of a small RNA pol 11 subunit in TATA to transcription start site spacing.

Gaillard, P.-H.L. (2001). Activity of individual ERCC1 and XPF subunits in DNA nucleotide excision repair. Nucleic Acids Research *29*, 872–879.

Gaillard, P.-H.L., Martini, E.M.-D., Kaufman, P.D., Stillman, B., Moustacchi, E., and Almouzni, G. (1996). Chromatin Assembly Coupled to DNA Repair: A New Role for Chromatin Assembly Factor I. Cell *86*, 887–896.

Galbraith, M.D., Donner, A.J., and Espinosa, J.M. (2010). CDK8: A positive regulator of transcription. Transcription *1*, 4–12.

Gaudreau, L., Adam, M., and Ptashne, M. (1998). Activation of Transcription In Vitro by Recruitment of the Yeast RNA Polymerase II Holoenzyme. Molecular Cell *1*, 913–916.

Georgaki, A., Strack, B., Podust, V., and Hübscher, U. (1992). DNA unwinding activity of replication protein A. FEBS Letters *308*, 240–244.

Gibbons, B.J., Brignole, E.J., Azubel, M., Murakami, K., Voss, N.R., Bushnell, D.A., Asturias, F.J., and Kornberg, R.D. (2012). Subunit architecture of general transcription factor TFIIH. Proceedings of the National Academy of Sciences *109*, 1949–1954.

Gill, G., and Ptashne, M. (1988). Negative effect of the transcriptional activator GAL4. Nature *334*, 721.

Gillette, T.G., Yu, S., Zhou, Z., Waters, R., Johnston, S.A., and Reed, S.H. (2006). Distinct functions of the ubiquitin–proteasome pathway influence nucleotide excision repair. The EMBO Journal.

Glover-Cutter, K., Larochelle, S., Erickson, B., Zhang, C., Shokat, K., Fisher, R.P., and Bentley, D.L. (2009). TFIIH-Associated Cdk7 Kinase Functions in Phosphorylation of C-Terminal Domain Ser7 Residues, Promoter-Proximal Pausing, and Termination by RNA Polymerase II. Molecular and Cellular Biology *29*, 5455–5464.

Greber, B.J., Nguyen, T.H.D., Fang, J., Afonine, P.V., Adams, P.D., and Nogales, E. (2017). The cryo-electron microscopy structure of human transcription factor IIH. Nature *549*, 414–417.

Green, C.M. (2002). When repair meets chromatin: First in series on chromatin dynamics. EMBO Reports *3*, 28–33.

Green, C.M. (2003). Local action of the chromatin assembly factor CAF-1 at sites of nucleotide excision repair in vivo. The EMBO Journal *22*, 5163–5174.

Gregersen, L.H., and Svejstrup, J.Q. (2018). The Cellular Response to Transcription-Blocking DNA Damage. Trends in Biochemical Sciences 43, 327–341.

Groisman, R., Kuraoka, I., Chevallier, O., Gaye, N., Magnaldo, T., Tanaka, K., Kisselev, A.F., Harel-Bellan, A., and Nakatani, Y. (2006). CSA-dependent degradation of CSB by the ubiquitin–proteasome pathway establishes a link between complementation factors of the Cockayne syndrome. Genes & Development *20*, 1429–1434.

Groisman, R., Polanowska, J., Kuraoka, I., Sawada, J., Saijo, M., Drapkin, R., Kisselev, A.F., Tanaka, K., and Nakatani, Y. (2003). The Ubiquitin Ligase Activity in the DDB2 and CSA Complexes Is Differentially Regulated by the COP9 Signalosome in Response to DNA Damage. Cell *113*, 357–367.

Grünberg, S., Warfield, L., and Hahn, S. (2012). Architecture of the RNA polymerase II preinitiation complex and mechanism of ATP-dependent promoter opening. Nature Structural & Molecular Biology *19*, 788–796.

Guermah, M., Tao, Y., and Roeder, R.G. (2001). Positive and Negative TAFII Functions That Suggest a Dynamic TFIID Structure and Elicit Synergy with TRAPs in Activator-Induced Transcription. Molecular and Cellular Biology *21*, 6882–6894.

Guglielmi, B., van Berkum, N.L., Klapholz, B., Bijma, T., Boube, M., Boschiero, C., Bourbon, H.-M., Holstege, F.C.P., and Werner, M. (2004). A high resolution protein interaction map of the yeast Mediator complex. Nucleic Acids Research *32*, 5379–5391.

Gunz, D., Hess, M.T., and Naegeli, H. (1996). Recognition of DNA Adducts by Human Nucleotide Excision Repair: evidence for a thermodynamic probing mechanism. Journal of Biological Chemistry *271*, 25089–25098.

Guo, R., Chen, J., Mitchell, D.L., and Johnson, D.G. (2011). GCN5 and E2F1 stimulate nucleotide excision repair by promoting H3K9 acetylation at sites of damage. Nucleic Acids Research *39*, 1390–1397.

Guzder, S.N., Sommers, C.H., Prakash, L., and Prakash, S. (2006). Complex Formation with Damage Recognition Protein Rad14 Is Essential for Saccharomyces cerevisiae Rad1-Rad10 Nuclease To Perform Its Function in Nucleotide Excision Repair In Vivo. Molecular and Cellular Biology *26*, 1135–1141.

Guzder, S.N., Sung, P., Prakash, L., and Prakash, S. (1997). Yeast Rad7-Rad16 Complex, Specific for the Nucleotide Excision Repair of the Nontranscribed DNA Strand, Is an ATP-dependent DNA Damage Sensor. Journal of Biological Chemistry *272*, 21665–21668

Guzder, S.N., Sung, P., Prakash, L., and Prakash, S. (1998). The DNA-dependent ATPase Activity of Yeast Nucleotide Excision Repair Factor 4 and Its Role in DNA Damage Recognition. Journal of Biological Chemistry *273*, 6292–6296.

Guzder, S.N., Sung, P., Prakash, L., and Prakash, S. (1999). Synergistic Interaction between Yeast Nucleotide Excision Repair Factors NEF2 and NEF4 in the Binding of Ultraviolet-damaged DNA. Journal of Biological Chemistry *274*, 24257–24262.

Gyenis, Á., Umlauf, D., Újfaludi, Z., Boros, I., Ye, T., and Tora, L. (2014). UVB Induces a Genome-Wide Acting Negative Regulatory Mechanism That Operates at the Level of Transcription Initiation in Human Cells. PLoS Genetics *10*, e1004483.

Habraken, Y., Sung, P., Prakash, S., and Prakash, L. (1996). Transcription factor TFIIH and DNA endonuclease Rad2 constitute yeast nucleotide excision repair factor 3: implications for nucleotide excision repair and Cockayne syndrome. Proceedings of the National Academy of Sciences *93*, 10718–10722.

Hahn, S. (2004). Structure and mechanism of the RNA polymerase II transcription machinery. Nature Structural & Molecular Biology *11*, 394–403.

Hahn, S., and Young, E.T. (2011). Transcriptional Regulation in *Saccharomyces cerevisiae* : Transcription Factor Regulation and Function, Mechanisms of Initiation, and Roles of Activators and Coactivators. Genetics *189*, 705–736.

Hanawalt, P., and Wax, R. (1964). Transcription of a repressed gene: evidence that it requires dna replication. Science *145*, 1061–1063.

Hanawalt, P.C., and Spivak, G. (2008). Transcription-coupled DNA repair: two decades of progress and surprises. Nature Reviews Molecular Cell Biology *9*, 958–970.

Haradhvala, N.J., Polak, P., Stojanov, P., Covington, K.R., Shinbrot, E., Hess, J.M., Rheinbay, E., Kim, J., Maruvka, Y.E., Braunstein, L.Z., et al. (2016). Mutational Strand Asymmetries in Cancer Genomes Reveal Mechanisms of DNA Damage and Repair. Cell *164*, 538–549.

Harreman, M., Taschner, M., Sigurdsson, S., Anindya, R., Reid, J., Somesh, B., Kong, S.E., Banks, C.A.S., Conaway, R.C., Conaway, J.W., et al. (2009). Distinct ubiquitin ligases act sequentially for RNA polymerase II polyubiquitylation. Proceedings of the National Academy of Sciences *106*, 20705–20710.

Hartzog, G.A., Wada, T., Handa, H., and Winston, F. (1998). Evidence that Spt4, Spt5, and Spt6 control transcription elongation by RNA polymerase II in Saccharomyces cerevisiae. Genes & Development *12*, 357–369.

Hashimoto, S., Boissel, S., Zarhrate, M., Rio, M., Munnich, A., Egly, J.-M., and Colleaux, L. (2011). MED23 mutation links intellectual disability to dysregulation of immediate early gene expression. Science *333*, 1161–1163.

He, J., Zhu, Q., Wani, G., and Wani, A.A. (2017). UV-induced proteolysis of RNA polymerase II is mediated by VCP/p97 segregase and timely orchestration by Cockayne syndrome B protein. Oncotarget *8*.

He, Z., Henricksen, L.A., Wold, M.S., and Ingles, C.J. (1995). RPA involvement in the damage-recognition and incision steps of nucleotide excision repair. Nature 374, 566.

Hengartner, C.J., Myer, V.E., Liao, S.-M., Wilson, C.J., Koh, S.S., and Young, R.A. (1998). Temporal Regulation of RNA Polymerase II by Srb10 and Kin28 Cyclin-Dependent Kinases. Molecular Cell *2*, 43–53.

Hengartner, C.J., Thompson, C.M., Zhang, J., Chao, D.M., Liao, S.M., Koleske, A.J., Okamura, S., and Young, R.A. (1995). Association of an activator with an RNA polymerase II holoenzyme. Genes & Development *9*, 897–910.

Henry, N.L., Campbell, A.M., Feaver, W.J., Poon, D., Weil, P.A., and Kornberg, R.D. (1994). TFIIF-TAF-RNA polymerase II connection. Genes & Development *8*, 2868–2878.

Higa, M., Tanaka, K., and Saijo, M. (2018). Inhibition of UVSSA ubiquitination suppresses transcription-coupled nucleotide excision repair deficiency caused by dissociation from USP7. The FEBS Journal *285*, 965–976.

Hoeijmakers, J.H.J. (2001). Genome maintenance mechanisms for preventing cancer. *411*, 9.

Hohl, M., Thorel, F., Clarkson, S.G., and Schärer, O.D. (2003). Structural Determinants for Substrate Binding and Catalysis by the Structure-specific Endonuclease XPG. Journal of Biological Chemistry *278*, 19500–19508.

Holstege, F.C.., Jennings, E.G., Wyrick, J.J., Lee, T.I., Hengartner, C.J., Green, M.R., Golub, T.R., Lander, E.S., and Young, R.A. (1998). Dissecting the Regulatory Circuitry of a Eukaryotic Genome. Cell *95*, 717–728.

Holstege, F.C.P. (1997). Three transitions in the RNA polymerase II transcription complex during initiation. The EMBO Journal *16*, 7468–7480.

Hu, J., Adebali, O., Adar, S., and Sancar, A. (2017). Dynamic maps of UV damage formation and repair for the human genome. Proceedings of the National Academy of Sciences 201706522.

Huibregtse, J.M., Yang, J.C., and Beaudenon, S.L. (1997). The large subunit of RNA polymerase II is a substrate of the Rsp5 ubiquitin-protein ligase. Proc. Natl. Acad. Sci. U.S.A. *94*, 3656–3661.

Hull, M.W., McKune, K., and Woychik, N.A. (1995). RNA polymerase II subunit RPB9 is required for accurate start site selection. Genes & Development *9*, 481–490.

Ibarra, A., and Hetzer, M.W. (2015). Nuclear pore proteins and the control of genome functions. Genes & Development *29*, 337–349.

Ikegami, T., Kuraoka, I., Saijo, M., Kodo, N., Kyogoku, Y., Morikawa, K., Tanaka, K., and Shirakawa, M. (1998). Solution structure of the DNA- and RPA-binding domain of the human repair factor XPA. Nature Structural &Amp; Molecular Biology 5, 701.

Ito, S., Kuraoka, I., Chymkowitch, P., Compe, E., Takedachi, A., Ishigami, C., Coin, F., Egly, J.-M., and Tanaka, K. (2007). XPG Stabilizes TFIIH, Allowing Transactivation of Nuclear Receptors: Implications for Cockayne Syndrome in XP-G/CS Patients. Molecular Cell *26*, 231–243.

Iyer, N., Reagan, M.S., Wu, K.-J., Canagarajah, B., and Friedberg, E.C. (1996). Interactions Involving the Human RNA Polymerase II Transcription/Nucleotide Excision Repair Complex TFIIH, the Nucleotide Excision Repair Protein XPG, and Cockayne Syndrome Group B (CSB) Protein †. Biochemistry *35*, 2157–2167.

Jackson, S.P., and Bartek, J. (2009). The DNA-damage response in human biology and disease. Nature *461*, 1071–1078.

Jans, J., Schul, W., Sert, Y.-G., Rijksen, Y., Rebel, H., Eker, A.P.M., Nakajima, S., van Steeg, H., de Gruijl, F.R., Yasui, A., et al. (2005). Powerful Skin Cancer Protection by a CPD-Photolyase Transgene. Current Biology *15*, 105–115.

Jasiak, A.J., Hartmann, H., Karakasili, E., Kalocsay, M., Flatley, A., Kremmer, E., Strässer, K., Martin, D.E., Söding, J., and Cramer, P. (2008). Genome-associated RNA Polymerase II Includes the Dissociable Rpb4/7 Subcomplex. Journal of Biological Chemistry *283*, 26423–26427.

Jensen, G.J. (1998). Structure of wild-type yeast RNA polymerase II and location of Rpb4 and Rpb7. The EMBO Journal *17*, 2353–2358.

Jeronimo, C., and Robert, F. (2014). Kin28 regulates the transient association of Mediator with core promoters. Nature Structural & Molecular Biology *21*, 449–455.

Jeronimo, C., Langelier, M.-F., Bataille, A.R., Pascal, J.M., Pugh, B.F., and Robert, F. (2016). Tail and Kinase Modules Differently Regulate Core Mediator Recruitment and Function In Vivo. Molecular Cell *64*, 455–466.

Jia, Y., Viswakarma, N., and Reddy, J.K. (2014). Med1 Subunit of the Mediator Complex in Nuclear Receptor-Regulated Energy Metabolism, Liver Regeneration, and Hepatocarcinogenesis. Gene Expression *16*, 63–75.

Jiang, Y., Wang, X., Bao, S., Guo, R., Johnson, D.G., Shen, X., and Li, L. (2010). INO80 chromatin remodeling complex promotes the removal of UV lesions by the nucleotide excision repair pathway. Proceedings of the National Academy of Sciences *107*, 17274–17279.

Kagey, M.H., Newman, J.J., Bilodeau, S., Zhan, Y., Orlando, D.A., van Berkum, N.L., Ebmeier, C.C., Goossens, J., Rahl, P.B., Levine, S.S., et al. (2010). Mediator and cohesin connect gene expression and chromatin architecture. Nature *467*, 430–435.

Kang, J.S., Kim, S.H., Hwang, M.S., Han, S.J., Lee, Y.C., and Kim, Y.-J. (2001). The Structural and Functional Organization of the Yeast Mediator Complex. Journal of Biological Chemistry *276*, 42003–42010.

Kapetanaki, M.G., Guerrero-Santoro, J., Bisi, D.C., Hsieh, C.L., Rapic-Otrin, V., and Levine, A.S. (2006). The DDB1-CUL4ADDB2 ubiquitin ligase is deficient in xeroderma pigmentosum

group E and targets histone H2A at UV-damaged DNA sites. Proceedings of the National Academy of Sciences *103*, 2588–2593.

Kedinger, M., Gniazdowski, C., Mandel, M., L. Jr., Gissinger, J. Jr., and Chambon, P. (1970). α-Amanitin: A specific inhibitor of one of two DNA-dependent RNA polymerase activities from calf thymus.

Kelleher, R.J., Flanagan, P.M., and Kornberg, R.D. (1990). A novel mediator between activator proteins and the RNA polymerase II transcription apparatus. Cell *61*, 1209–1215.

Kelman, Z. (1997). PCNA: structure, functions and interactions. Oncogene *14*, 629–640.

Kelner, A. (1949). Photoreactivation of ultraviolet-irradiated escherichia coli, with special reference to the dose-reduction principle and to ultraviolet-induced mutation. J. Bacteriol. *58*, 511–522.

Kemp, M.G., Reardon, J.T., Lindsey-Boltz, L.A., and Sancar, A. (2012). Mechanism of Release and Fate of Excised Oligonucleotides during Nucleotide Excision Repair. J. Biol. Chem. *287*, 22889–22899.

Khazak, V., Sadhale, P.P., Woychik, N.A., Brent, R., and Golemis, E.A. (1995). Human RNA polymerase II subunit hsRPB7 functions in yeast and influences stress survival and cell morphology. Molecular Biology of the Cell *6*, 759–775.

Kikuchi, Y., Umemura, H., Nishitani, S., Iida, S., Fukasawa, R., Hayashi, H., Hirose, Y., Tanaka, A., Sugasawa, K., and Ohkuma, Y. Human mediator MED17 subunit plays essential roles in gene regulation by associating with the transcription and DNA repair machineries. Genes to Cells *20*, 191–202.

Kim, M.Y. (2005). Poly(ADP-ribosyl)ation by PARP-1: `PAR-laying' NAD+ into a nuclear signal. Genes & Development *19*, 1951–1967

Kim, Y.K., Bourgeois, C.F., Isel, C., Churcher, M.J., and Karn, J. (2002). Phosphorylation of the RNA Polymerase II Carboxyl-Terminal Domain by CDK9 Is Directly Responsible for Human Immunodeficiency Virus Type 1 Tat-Activated Transcriptional Elongation. Molecular and Cellular Biology *22*, 4622–4637.

Kimura, A., Umehara, T., and Horikoshi, M. (2002). Chromosomal gradient of histone acetylation established by Sas2p and Sir2p functions as a shield against gene silencing. Nature Genetics *32*, 370–377.

Koch, S.C., Simon, N., Ebert, C., and Carell, T. (2016). Molecular mechanisms of xeroderma pigmentosum (XP) proteins. Quarterly Reviews of Biophysics *49*.

Koh, S.S., Ansari, A.Z., Ptashne, M., and Young, R.A. (1998). An Activator Target in the RNA Polymerase II Holoenzyme. Molecular Cell *1*, 895–904.

Koschubs, T., Seizl, M., Larivière, L., Kurth, F., Baumli, S., Martin, D.E., and Cramer, P. (2009). Identification, structure, and functional requirement of the Mediator submodule Med7N/31. The EMBO Journal *28*, 69–80.

Krivega, I., and Dean, A. (2017). LDB1-mediated enhancer looping can be established independent of mediator and cohesin. Nucleic Acids Research *45*, 8255–8268.

Krokan, H.E., and Bjoras, M. (2013). Base Excision Repair. Cold Spring Harbor Perspectives in Biology *5*, a012583–a012583.

Kwak, H., and Lis, J.T. (2013). Control of Transcriptional Elongation. Annu. Rev. Genet. *47*, 483–508.

Lacombe, T., Poh, S.L., Barbey, R., and Kuras, L. (2013). Mediator is an intrinsic component of the basal RNA polymerase II machinery in vivo. Nucleic Acids Research *41*, 9651–9662.

Lafrance-Vanasse, J., Arseneault, G., Cappadocia, L., Legault, P., and Omichinski, J.G. (2013). Structural and functional evidence that Rad4 competes with Rad2 for binding to the Tfb1 subunit of TFIIH in NER. Nucleic Acids Research *41*, 2736–2745.

Lainé, J.-P., and Egly, J.-M. (2006). When transcription and repair meet: a complex system. Trends in Genetics *22*, 430–436.

Lake, R.J., Geyko, A., Hemashettar, G., Zhao, Y., and Fan, H.-Y. (2010). UV-Induced Association of the CSB Remodeling Protein with Chromatin Requires ATP-Dependent Relief of N-Terminal Autorepression. Molecular Cell *37*, 235–246.

Lan, L., Nakajima, S., Kapetanaki, M.G., Hsieh, C.L., Fagerburg, M., Thickman, K., Rodriguez-Collazo, P., Leuba, S.H., Levine, A.S., and Rapić-Otrin, V. (2012). Monoubiquitinated Histone H2A Destabilizes Photolesion-containing Nucleosomes with Concomitant Release of UV-damaged DNA-binding Protein E3 Ligase. Journal of Biological Chemistry *287*, 12036–12049.

Laugel, V. (2013). Cockayne syndrome: The expanding clinical and mutational spectrum. Mechanisms of Ageing and Development *134*, 161–170.

Lavigne, M.D., Konstantopoulos, D., Ntakou-Zamplara, K.Z., Liakos, A., and Fousteri, M. (2017). Global unleashing of transcription elongation waves in response to genotoxic stress restricts somatic mutation rate. Nature Communications *8*.

Le May, N., Mota-Fernandes, D., Vélez-Cruz, R., Iltis, I., Biard, D., and Egly, J.M. (2010). NER Factors Are Recruited to Active Promoters and Facilitate Chromatin Modification for Transcription in the Absence of Exogenous Genotoxic Attack. Molecular Cell *38*, 54–66.

Le May, N., Fradin, D., Iltis, I., Bougnères, P., and Egly, J.-M. (2012). XPG and XPF Endonucleases Trigger Chromatin Looping and DNA Demethylation for Accurate Expression of Activated Genes. Molecular Cell *47*, 622–632.

Leadon, S.A., Zolan, M.E., and Hanawalt, P.C. (1983). Restricted repair of aflatoxin B1 induced damage in alpha DNA of monkey cells. Nucleic Acids Research 11, 5675–5689.

Lee, J.-H. (2003). NMR study on the interaction between RPA and DNA decamer containing cis-syn cyclobutane pyrimidine dimer in the presence of XPA: implication for damage verification and strand-specific dual incision in nucleotide excision repair. Nucleic Acids Research *31*, 4747–4754.

Lee, K.-B., Wang, D., Lippard, S.J., and Sharp, P.A. (2002). Transcription-coupled and DNA damage-dependent ubiquitination of RNA polymerase II in vitro. Proceedings of the National Academy of Sciences *99*, 4239–4244.

Léonard, V.H.J., Kohl, A., Hart, T.J., and Elliott, R.M. (2006). Interaction of Bunyamwera Orthobunyavirus NSs Protein with Mediator Protein MED8: a Mechanism for Inhibiting the Interferon Response. J. Virol. *80*, 9667.

Levine, M., and Tjian, R. (2003). Transcription regulation and animal diversity. Nature *424*, 147–151.

Li, C.-L., Golebiowski, F.M., Onishi, Y., Samara, N.L., Sugasawa, K., and Yang, W. (2015). Tripartite DNA Lesion Recognition and Verification by XPC, TFIIH, and XPA in Nucleotide Excision Repair. Molecular Cell *59*, 1025–1034.

Li, S., and Smerdon, M.J. (2002). Rpb4 and Rpb9 mediate subpathways of transcription-coupled DNA repair in Saccharomyces cerevisiae. EMBO J. *21*, 5921–5929.

Li, S., and Smerdon, M.J. (2004). Dissecting Transcription-coupled and Global Genomic Repair in the Chromatin of Yeast *GAL1-10* Genes. Journal of Biological Chemistry *279*, 14418–14426.

Li, S., Ding, B., Chen, R., Ruggiero, C., and Chen, X. (2006). Evidence that the Transcription Elongation Function of Rpb9 Is Involved in Transcription-Coupled DNA Repair in Saccharomyces cerevisiae. Molecular and Cellular Biology *26*, 9430–9441.

Li, W., Adebali, O., Yang, Y., Selby, C.P., and Sancar, A. (2018). Single-nucleotide resolution dynamic repair maps of UV damage in *Saccharomyces cerevisiae* genome. Proceedings of the National Academy of Sciences *115*, E3408–E3415.

Li, W., Selvam, K., Rahman, S.A., and Li, S. (2016). Sen1, the yeast homolog of human senataxin, plays a more direct role than Rad26 in transcription coupled DNA repair. Nucleic Acids Research *44*, 6794–6802.

Liang, X., Peng, L., Tsvetanova, B., Li, K., Yang, J.-P., Ho, T., Shirley, J., Xu, L., Potter, J., Kudlicki, W., et al. (2012). Recombination-based DNA assembly and mutagenesis methods for metabolic engineering. Methods Mol. Biol. *834*, 93–109.

Liu, Y., Ranish, J.A., Aebersold, R., and Hahn, S. (2001). Yeast Nuclear Extract Contains Two Major Forms of RNA Polymerase II Mediator Complexes. Journal of Biological Chemistry *276*, 7169–7175.

Lommel, L., Ortolan, T., Chen, L., Madura, K., and Sweder, K.S. (2002). Proteolysis of a nucleotide excision repair protein by the 26S proteasome. Current Genetics *42*, 9–20.

Loney, E.R., Inglis, P.W., Sharp, S., Pryde, F.E., Kent, N.A., Mellor, J., and Louis, E.J. (2009). Repressive and non-repressive chromatin at native telomeres in Saccharomyces cerevisiae. Epigenetics & Chromatin *2*, 18.

Lue, N.F., and Kornberg, R.D. (1987). Accurate initiation at RNA polymerase II promoters in extracts from Saccharomyces cerevisiae. Proceedings of the National Academy of Sciences *84*, 8839–8843.

Luijsterburg, M.S., Lindh, M., Acs, K., Vrouwe, M.G., Pines, A., van Attikum, H., Mullenders, L.H., and Dantuma, N.P. (2012). DDB2 promotes chromatin decondensation at UV-induced DNA damage. The Journal of Cell Biology *197*, 267–281.

Luo, J., Cimermancic, P., Viswanath, S., Ebmeier, C.C., Kim, B., Dehecq, M., Raman, V., Greenberg, C.H., Pellarin, R., Sali, A., et al. (2015). Architecture of the Human and Yeast General Transcription and DNA Repair Factor TFIIH. Molecular Cell *59*, 794–806.

Luo, Z., Zheng, J., Lu, Y., and Bregman, D.B. (2001). Ultraviolet radiation alters the phosphorylation of RNA polymerase II large subunit and accelerates its proteasome-dependent degradation. Mutation Research/DNA Repair *486*, 259–274.

Luse, D.S., and Roeder, R.G. (1980). Accurate transcription initiation on a purified mouse β-globin DNA fragment in a cell-free system. Cell 20, 691–699.

Malabat, C., Feuerbach, F., Ma, L., Saveanu, C., and Jacquier, A. (2015). Quality control of transcription start site selection by nonsense-mediated-mRNA decay. eLife 4, e06722.

Malik, S., Chaurasia, P., Lahudkar, S., Durairaj, G., Shukla, A., and Bhaumik, S.R. (2010). Rad26p, a transcription-coupled repair factor, is recruited to the site of DNA lesion in an elongating RNA polymerase II-dependent manner in vivo. Nucleic Acids Res *38*, 1461–1477.

Mao, P., Smerdon, M.J., Roberts, S.A., and Wyrick, J.J. (2016). Chromosomal landscape of UV damage formation and repair at single-nucleotide resolution. Proceedings of the National Academy of Sciences *113*, 9057–9062.

Mardiros, A., Benoun, J.M., Haughton, R., Baxter, K., Kelson, E.P., and Fischhaber, P.L. (2011). Rad10-YFP focus induction in response to UV depends on RAD14 in yeast. Acta Histochemica *113*, 409–415.

Masutani, C. (1999). Xeroderma pigmentosum variant (XP-V) correcting protein from HeLa cells has a thymine dimer bypass DNA polymerase activity. The EMBO Journal *18*, 3491–3501.

Masutani, C., Kusumoto, R., Yamada, A., Dohmae, N., Yokoi, M., Yuasa, M., Araki, M., Iwai, S., Takio, K., and Hanaoka, F. (1999). The XPV (xeroderma pigmentosum variant) gene encodes human DNA polymerase η. Nature 399, 700.

MatsuiS, T., Segallg, J., Weill, P.A., and Roederll, R. Multiple Factors Required for Accurate Initiation of Transcriptibony Purified RNA Polymerase 11. 5.

Mayne, L.V., and Lehmann, A.R. (1982). Failure of RNA Synthesis to Recover after UV Irradiation: An Early Defect in Cells from Individuals with Cockayne's Syndrome and Xeroderma Pigmentosum. *42*, 7.

Mellon, I., and Hanawalt, P.C. (1989). Induction of the Escherichia coli lactose operon selectively increases repair of its transcribed DNA strand. Nature 342, 95.Mellon, I. (1987). Selective removal of transcription-blocking DNA damage from the transcribed strand of the mammalian DHFR gene. Cell *51*, 241–249.

Menck, C.F., and Munford, V. (2014). DNA repair diseases: what do they tell us about cancer and aging? Genetics and Molecular Biology *37*, 220–233.

Miętus, M., Nowak, E., Jaciuk, M., Kustosz, P., Studnicka, J., and Nowotny, M. (2014). Crystal structure of the catalytic core of Rad2: insights into the mechanism of substrate binding. Nucleic Acids Research *42*, 10762–10775.

Miller, C., Schwalb, B., Maier, K., Schulz, D., Dumcke, S., Zacher, B., Mayer, A., Sydow, J., Marcinowski, L., Dolken, L., et al. (2014). Dynamic transcriptome analysis measures rates of mRNA synthesis and decay in yeast. Molecular Systems Biology *7*, 458–458.

Min, J.-H., and Pavletich, N.P. (2007). Recognition of DNA damage by the Rad4 nucleotide excision repair protein. Nature *449*, 570–575.

Mitchell, D.L., Jen, J., and Cleaver, J.E. (1992). Sequence specificity of cyclobutane pyrimidine dimers in DNA treated with solar (ultraviolet B) radiation. Nucleic Acids Research *20*, 225–229.

Mittler, G., Stühler, T., Santolin, L., Uhlmann, T., Kremmer, E., Lottspeich, F., Berti, L., and Meisterernst, M. (2003). A novel docking site on Mediator is critical for activation by VP16 in mammalian cells. EMBO J *22*, 6494.

Mocquet, V., Lainé, J.P., Riedl, T., Yajin, Z., Lee, M.Y., and Egly, J.M. (2008). Sequential recruitment of the repair factors during NER: the role of XPG in initiating the resynthesis step. The EMBO Journal *27*, 155–167.

Moriel-Carretero, M., Herrera-Moyano, E., and Aguilera, A. (2015). A unified model for the molecular basis of Xeroderma pigmentosum-Cockayne Syndrome. Rare Diseases *3*, e1079362.

Moser, J., Volker, M., Kool, H., Alekseev, S., Vrieling, H., Yasui, A., van Zeeland, A.A., and Mullenders, L.H.F. (2005). The UV-damaged DNA binding protein mediates efficient targeting of the nucleotide excision repair complex to UV-induced photo lesions. DNA Repair *4*, 571–582.

Murakami, K.S., and Darst, S.A. (2003). Bacterial RNA polymerases: the wholo story. Current Opinion in Structural Biology *13*, 31–39.

Myers, L.C., Gustafsson, C.M., Hayashibara, K.C., Brown, P.O., and Kornberg, R.D. (1999). Mediator protein mutations that selectively abolish activated transcription. Proceedings of the National Academy of Sciences *96*, 67–72.

Naegeli, H., Bardwell, L., and Friedberg, E.C. (1992). The DNA helicase and adenosine triphosphatase activities of yeast Rad3 protein are inhibited by DNA damage. A potential mechanism for damage-specific recognition. J. Biol. Chem. *267*, 392–398.

Nakazawa, Y., Sasaki, K., Mitsutake, N., Matsuse, M., Shimada, M., Nardo, T., Takahashi, Y., Ohyama, K., Ito, K., Mishima, H., et al. (2012). Mutations in UVSSA cause UV-sensitive syndrome and impair RNA polymerase IIo processing in transcription-coupled nucleotide-excision repair. Nature Genetics *44*, 586–592.

Nesser, N.K., Peterson, D.O., and Hawley, D.K. (2006). RNA polymerase II subunit Rpb9 is important for transcriptional fidelity in vivo. Proceedings of the National Academy of Sciences *103*, 3268–3273.

Ng, J.M.Y. (2003). A novel regulation mechanism of DNA repair by damage-induced and RAD23-dependent stabilization of xeroderma pigmentosum group C protein. Genes & Development *17*, 1630–1645.

Nishi, R., Okuda, Y., Watanabe, E., Mori, T., Iwai, S., Masutani, C., Sugasawa, K., and Hanaoka, F. (2005). Centrin 2 Stimulates Nucleotide Excision Repair by Interacting with Xeroderma Pigmentosum Group C Protein. Molecular and Cellular Biology *25*, 5664–5674.

Nishikawa, J.L., Boeszoermenyi, A., Vale-Silva, L.A., Torelli, R., Posteraro, B., Sohn, Y.-J., Ji, F., Gelev, V., Sanglard, D., Sanguinetti, M., et al. (2016). Inhibiting fungal multidrug resistance by disrupting an activator–Mediator interaction. Nature *530*, 485.

Nonet, M.L., and Young, R.A. (1989) Intragenic and Extragenic Suppressorosf Mutations in the Heptapeptide Repeat Domain of Saccharomyces cerervisiae RNA Polymerase I. Genetics 123: 715-724

Nozawa, K., Schneider, T.R., and Cramer, P. (2017). Core Mediator structure at 3.4 Å extends model of transcription initiation complex. Nature *545*, 248–251.

Ogi, T., Limsirichaikul, S., Overmeer, R.M., Volker, M., Takenaka, K., Cloney, R., Nakazawa, Y., Niimi, A., Miki, Y., Jaspers, N.G., et al. (2010). Three DNA Polymerases, Recruited by Different Mechanisms, Carry Out NER Repair Synthesis in Human Cells. Molecular Cell *37*, 714–727.

Ohkuma, Y., hashimoto, S., wang, C.K., horikoshi, M., and Roeder, R.G. (1995). Analysis of the Role of TFIIE in Basal Transcription and TFIIH-Mediated Carboxy-Terminal Domain Phosphorylation through Structure-Function Studies of TFIIE. MOL. CELL. BIOL. *15*, 11.

Oksenych, V., and Coin, F. (2010). The long unwinding road: XPB and XPD helicases in damaged DNA opening. Cell Cycle *9*, 90–96.

Oksenych, V., de Jesus, B.B., Zhovmer, A., Egly, J.-M., and Coin, F. (2009). Molecular insights into the recruitment of TFIIH to sites of DNA damage. The EMBO Journal *28*, 2971–2980.

Ottoz, D.S.M., Rudolf, F., and Stelling, J. (2014). Inducible, tightly regulated and growth condition-independent transcription factor in Saccharomyces cerevisiae. Nucleic Acids Research *42*, e130–e130.

Overmeer, R.M., Moser, J., Volker, M., Kool, H., Tomkinson, A.E., van Zeeland, A.A., Mullenders, L.H.F., and Fousteri, M. (2011). Replication protein A safeguards genome integrity by controlling NER incision events. The Journal of Cell Biology *192*, 401–415.

Oztas, O., Selby, C.P., Sancar, A., and Adebali, O. (2018). Genome-wide excision repair in Arabidopsis is coupled to transcription and reflects circadian gene expression patterns. Nature Communications *9*.

Park, C.H., and Sancar, A. (1994). Formation of a ternary complex by human XPA, ERCC1, and ERCC4(XPF) excision repair proteins. Proc Natl Acad Sci U S A *91*, 5017–5021.

Patrick, S.M., and Turchi, J.J. (2002). Xeroderma Pigmentosum Complementation Group A Protein (XPA) Modulates RPA-DNA Interactions via Enhanced Complex Stability and Inhibition of Strand Separation Activity. Journal of Biological Chemistry *277*, 16096–16101.

Pelechano, V., Wei, W., and Steinmetz, L.M. (2013). Extensive transcriptional heterogeneity revealed by isoform profiling. Nature *497*, 127–131.

Peng, J., and Zhou, J.-Q. (2012). The tail-module of yeast Mediator complex is required for telomere heterochromatin maintenance. Nucleic Acids Research *40*, 581–593.

Petrenko, N., Jin, Y., Wong, K.H., and Struhl, K. (2016). Mediator Undergoes a Compositional Change during Transcriptional Activation. Molecular Cell *64*, 443–454.

Pfeifer, G.P., Drouin, R., Riggs, A.D., and Holmquist, G.P. (1992). Binding of transcription factors creates hot spots for UV photoproducts in vivo. Molecular and Cellular Biology *12*, 1798–1804.

Pines, A., Vrouwe, M.G., Marteijn, J.A., Typas, D., Luijsterburg, M.S., Cansoy, M., Hensbergen, P., Deelder, A., de Groot, A., Matsumoto, S., et al. (2012). PARP1 promotes nucleotide excision repair through DDB2 stabilization and recruitment of ALC1. The Journal of Cell Biology *199*, 235–249.

Piruat, J.I., Chavez, S. and Aguilera A (1997). The Yeast HRSl Gene Is Involved in Positive and Negative Regulation of Transcriptionand Shows Genetic Characteristics Similar to SIN4 and GAL1. Genetics 147: 1585-1594.

Polo, S.E., and Almouzni, G. (2015). Chromatin dynamics after DNA damage: The legacy of the access–repair–restore model. DNA Repair *36*, 114–121.

Powell, J.R., Bennett, M.R., Evans, K.E., Yu, S., Webster, R.M., Waters, R., Skinner, N., and Reed, S.H. (2015). 3D-DIP-Chip: a microarray-based method to measure genomic DNA damage. Scientific Reports *5*.

Prakash, S., and Prakash, L. (2000). Nucleotide excision repair in yeast. Mutation Research/Fundamental and Molecular Mechanisms of Mutagenesis *451*, 13–24.

Proietti-De-Santis, L., Drané, P., and Egly, J.-M. (2006). Cockayne syndrome B protein regulates the transcriptional program after UV irradiation. The EMBO Journal *25*, 1915–1923.

Ramanathan, B. and Smerdon, M. J. (1989) Enhanced DNA Repair Synthesis in Hyperacetylated Nucleosomes. J. Biol. Chem. 264, 11026.

Ramanathan, B., and Smerdon, M.J. (1986). Changes in nuclear protein acetylation in u.v.-damaged human cells. Carcinogenesis *7*, 1087–1094.

Ramsey, K.L., Smith, J.J., Dasgupta, A., Maqani, N., Grant, P., and Auble, D.T. (2004). The NEF4 Complex Regulates Rad4 Levels and Utilizes Snf2/Swi2-Related ATPase Activity for Nucleotide Excision Repair. Molecular and Cellular Biology *24*, 6362–6378.

Ranish, J.A., Hahn, S., Lu, Y., Yi, E.C., Li, X., Eng, J., and Aebersold, R. (2004). Identification of TFB5, a new component of general transcription and DNA repair factor IIH. Nature Genetics *36*, 707–713.

Rasmussen, R.E., and Painter, R.B. (1964). Evidence for repair of ultra-violet damaged deoxyribonucleic acid in cultured mammalian cells. Nature *203*, 1360–1362.

Ravanat, J.-L., and Douki, T. (2016). UV and ionizing radiations induced DNA damage, differences and similarities. Radiation Physics and Chemistry *128*, 92–102.

Ray, A., Milum, K., Battu, A., Wani, G., and Wani, A.A. (2013). NER initiation factors, DDB2 and XPC, regulate UV radiation response by recruiting ATR and ATM kinases to DNA damage sites. DNA Repair (Amst.) *12*, 273–283.

Ray, A., Mir, S.N., Wani, G., Zhao, Q., Battu, A., Zhu, Q., Wang, Q.-E., and Wani, A.A. (2009). Human SNF5/INI1, a Component of the Human SWI/SNF Chromatin Remodeling Complex, Promotes Nucleotide Excision Repair by Influencing ATM Recruitment and Downstream H2AX Phosphorylation. Molecular and Cellular Biology *29*, 6206–6219.

Reed, S.H., Akiyama, M., Stillman, B., and Friedberg, E.C. (1999). Yeast autonomously replicating sequence binding factor is involved in nucleotide excision repair. Genes & Development *13*, 3052–3058.

Riedl, T. (2003). The comings and goings of nucleotide excision repair factors on damaged DNA. The EMBO Journal *22*, 5293–5303.

Rimel, J.K., and Taatjes, D.J. (2018). The essential and multifunctional TFIIH complex: Essential and Multi-Functional TFIIH. Protein Science *27*, 1018–1037.

Risley, M.D., Clowes, C., Yu, M., Mitchell, K., and Hentges, K.E. (2010). The Mediator complex protein Med31 is required for embryonic growth and cell proliferation during mammalian development. Developmental Biology *342*, 146–156.

Robins, P., Jones, C.J., Biggerstaff, M., Lindahl, T., and Wood, R.D. (1991). Complementation of DNA repair in xeroderma pigmentosum group A cell extracts by a protein with affinity for damaged DNA. EMBO J. *10*, 3913–3921.

Rockx, D.A.P., Mason, R., van Hoffen, A., Barton, M.C., Citterio, E., Bregman, D.B., van Zeeland, A.A., Vrieling, H., and Mullenders, L.H.F. (2000). UV-induced inhibition of transcription involves repression of transcription initiation and phosphorylation of RNA polymerase II. Proceedings of the National Academy of Sciences *97*, 10503–10508.

Roeder, R.G., and rutter, W.J. (1969). Multiple Forms of DNA-dependent RNA Polymerase in Eukaryotic Organisms. Nature 224, 234.

Saijo, M., Hirai, T., Ogawa, A., Kobayashi, A., Kamiuchi, S., and Tanaka, K. (2007). Functional TFIIH Is Required for UV-Induced Translocation of CSA to the Nuclear Matrix. Molecular and Cellular Biology *27*, 2538–2547.

Salmon-Divon, M., Dvinge, H., Tammoja, K., and Bertone, P. (2010). PeakAnalyzer: genome-wide annotation of chromatin binding and modification loci. BMC Bioinformatics *11*, 415.

Sarkar, S., Kiely, R., and McHugh, P.J. (2010). The Ino80 chromatin-remodeling complex restores chromatin structure during UV DNA damage repair. The Journal of Cell Biology *191*, 1061–1068.

Sarker, A.H., Tsutakawa, S.E., Kostek, S., Ng, C., Shin, D.S., Peris, M., Campeau, E., Tainer, J.A., Nogales, E., and Cooper, P.K. (2005). Recognition of RNA Polymerase II and Transcription Bubbles by XPG, CSB, and TFIIH: Insights for Transcription-Coupled Repair and Cockayne Syndrome. Molecular Cell *20*, 187–198.

Sayre, M.H., TschochnerQ, H., and Kornberg, R.D. Reconstitutionof Transcriptionwith Five Purified Initiation Factors and RNA Polymerase I1 from Saccharomyces cerevisiae".

Schärer, O.D. (2009). XPG: Its Products and Biological Roles. In Molecular Mechanisms of Xeroderma Pigmentosum, S.I. Ahmad, and F. Hanaoka, eds. (New York, NY: Springer New York), pp. 83–92.

Scheibye-Knudsen, M., Croteau, D.L., and Bohr, V.A. (2013). Mitochondrial deficiency in Cockayne syndrome. Mechanisms of Ageing and Development *134*, 275–283.

Scherly, D., Nouspikel, T., Corlet, J., Ucla, C., Bairoch, A., and Clarkson, S.G. (1993). Complementation of the DNA repair defect in xeroderma pigmentosum group G cells by a human cDNA related to yeast RAD2. Nature 363, 182.

Schilbach, S., Hantsche, M., Tegunov, D., Dienemann, C., Wigge, C., Urlaub, H., and Cramer, P. (2017). Structures of transcription pre-initiation complex with TFIIH and Mediator. Nature *551*, 204–209.

Schneider, M., Hellerschmied, D., Schubert, T., Amlacher, S., Vinayachandran, V., Reja, R., Pugh, B.F., Clausen, T., and Köhler, A. (2015). The Nuclear Pore-Associated TREX-2 Complex Employs Mediator to Regulate Gene Expression. Cell *162*, 1016–1028.

Schwertman, P., Lagarou, A., Dekkers, D.H.W., Raams, A., van der Hoek, A.C., Laffeber, C., Hoeijmakers, J.H.J., Demmers, J.A.A., Fousteri, M., Vermeulen, W., et al. (2012). UV-sensitive syndrome protein UVSSA recruits USP7 to regulate transcription-coupled repair. Nature Genetics *44*, 598–602.

Schwertman, P., Vermeulen, W., and Marteijn, J.A. (2013). UVSSA and USP7, a new couple in transcription-coupled DNA repair. Chromosoma *122*, 275–284.

Scrima, A., Koníčková, R., Czyzewski, B.K., Kawasaki, Y., Jeffrey, P.D., Groisman, R., Nakatani, Y., Iwai, S., Pavletich, N.P., and Thomä, N.H. (2008). Structural Basis of UV DNA-Damage Recognition by the DDB1–DDB2 Complex. Cell *135*, 1213–1223.

Seebode, C., Lehmann, J., and Emmert, S. (2016). Photocarcinogenesis and Skin Cancer Prevention Strategies. Anticancer Res. *36*, 1371–1378.

Selby, C.P., and Sancar, A. (1997). Human Transcription-Repair Coupling Factor CSB/ERCC6 Is a DNA-stimulated ATPase but Is Not a Helicase and Does Not Disrupt the Ternary Transcription Complex of Stalled RNA Polymerase II. J. Biol. Chem. *272*, 1885–1890.

Setlow, R.B., and Carrier, W.L. (1964). The disappearance of thymine dimers from dna: an error-correcting mechanism. PNAS 51, 226–231.

Setlow, R.B., and Carrier, W.L. (2003). The disappearance of thymine dimers from DNA: an error-correcting mechanism. 1963. DNA Repair (Amst.) *2*, 1274–1279.

Sidik, K., and Michael, J.S. (1984). Nuclease sensitivity of repair-incorporated nucleotides in chromatin and nucleosome rearrangement in human cells damaged by methyl methanesulfonate and methylnitrosourea. Carcinogenesis *5*, 245–253.

Sijbers, A.M., de Laat, W.L., Ariza, R.R., Biggerstaff, M., Wei, Y.-F., Moggs, J.G., Carter, K.C., Shell, B.K., Evans, E., de Jong, M.C., et al. (1996). Xeroderma Pigmentosum Group F Caused by a Defect in a Structure-Specific DNA Repair Endonuclease. Cell *86*, 811–822.

Smerdon, M.J., and Thoma, F. (1990). Site-specific DNA repair at the nucleosome level in a yeast minichromosome. Cell *61*, 675–684.

Smerdon, M.J. (1991). DNA repair and the role of chromatin structure. Current Opinion in Cell Biology *3*, 422–428.

Sollier, J., and Cimprich, K.A. (2015). Breaking bad: R-loops and genome integrity. Trends in Cell Biology *25*, 514–522.

Sollier, J., Stork, C.T., García-Rubio, M.L., Paulsen, R.D., Aguilera, A., and Cimprich, K.A. (2014). Transcription-Coupled Nucleotide Excision Repair Factors Promote R-Loop-Induced Genome Instability. Molecular Cell *56*, 777–785.

Somesh, B.P., Reid, J., Liu, W.-F., Søgaard, T.M.M., Erdjument-Bromage, H., Tempst, P., and Svejstrup, J.Q. (2005). Multiple Mechanisms Confining RNA Polymerase II Ubiquitylation to Polymerases Undergoing Transcriptional Arrest. Cell *121*, 913–923.

Soutourina, J. (2018). Transcription regulation by the Mediator complex. Nat. Rev. Mol. Cell Biol. *19*, 262–274.

Soutourina, J., Wydau, S., Ambroise, Y., Boschiero, C., and Werner, M. (2011). Direct Interaction of RNA Polymerase II and Mediator Required for Transcription in Vivo. Science *331*, 1451–1454.

Spaeth, J.M., Kim, N.H., and Boyer, T.G. (2011). Mediator and human disease. Semin Cell Dev Biol *22*, 776-787.

Stantial, N., Dumpe, J., Pietrosimone, K., Baltazar, F., and Crowley, D.J. (2016). Transcription-coupled repair of UV damage in the halophilic archaea. DNA Repair *41*, 63–68.

Staresincic, L., Fagbemi, A.F., Enzlin, J.H., Gourdin, A.M., Wijgers, N., Dunand-Sauthier, I., Giglia-Mari, G., Clarkson, S.G., Vermeulen, W., and Schärer, O.D. (2009). Coordination of dual incision and repair synthesis in human nucleotide excision repair. The EMBO Journal *28*, 1111–1120.

States, J.C., and Reed, E. (1996). Enhanced XPA mRNA levels in cisplatin-resistant human ovarian cancer are not associated with XPA mutations or gene amplification. Cancer Letters *108*, 233–237.

Stefanini, M., Botta, E., Lanzafame, M., and Orioli, D. (2010). Trichothiodystrophy: From basic mechanisms to clinical implications. DNA Repair *9*, 2–10.

Steinmetz, E.J., Warren, C.L., Kuehner, J.N., Panbehi, B., Ansari, A.Z., and Brow, D.A. (2006). Genome-wide distribution of yeast RNA polymerase II and its control by Sen1 helicase. Mol. Cell *24*, 735–746.

Steurer, B., and Marteijn, J.A. (2017). Traveling Rocky Roads: The Consequences of Transcription-Blocking DNA Lesions on RNA Polymerase II. Journal of Molecular Biology *429*, 3146–3155.

Stewart, D.J. (2007). Mechanisms of resistance to cisplatin and carboplatin. Critical Reviews in Oncology/Hematology *63*, 12–31.

Sugasawa, K. (2001). A multistep damage recognition mechanism for global genomic nucleotide excision repair. Genes & Development *15*, 507–521.

Sugasawa, K., Akagi, J., Nishi, R., Iwai, S., and Hanaoka, F. (2009). Two-Step Recognition of DNA Damage for Mammalian Nucleotide Excision Repair: Directional Binding of the XPC Complex and DNA Strand Scanning. Molecular Cell *36*, 642–653.

Sugasawa, K., Ng, J.M.., Masutani, C., Iwai, S., van der Spek, P.J., Eker, A.P.., Hanaoka, F., Bootsma, D., and Hoeijmakers, J.H.. (1998). Xeroderma Pigmentosum Group C Protein Complex Is the Initiator of Global Genome Nucleotide Excision Repair. Molecular Cell *2*, 223–232.

Suzuki, Y., and Nishizawa, M. (1994). The yeast GAL11 protein is involved in regulation of the structure and the position effect of telomeres. Molecular and Cellular Biology *14*, 3791–3799.

Svejstrup, J.Q., Wang, Z., Feave, W.J., Wu, X., Bushnell, D.A., Donahue, T.F., Friedberg, E.C., and Kornberg, R.D. (1995). Different forms of TFIIH for transcription and DNA repair: Holo-TFIIH and a nucleotide excision repairosome. Cell *80*, 21–28.

Tagami, H., Ray-Gallet, D., Almouzni, G., and Nakatani, Y. (2004). Histone H3.1 and H3.3 complexes mediate nucleosome assembly pathways dependent or independent of DNA synthesis. Cell *116*, 51–61.

Takagi, Y., and Kornberg, R.D. (2006). Mediator as a General Transcription Factor. Journal of Biological Chemistry *281*, 80–89.

Takahashi, H., Parmely, T.J., Sato, S., Tomomori-Sato, C., Banks, C.A.S., Kong, S.E., Szutorisz, H., Swanson, S.K., Martin-Brown, S., Washburn, M.P., et al. (2011). Human Mediator Subunit MED26 Functions as a Docking Site for Transcription Elongation Factors. Cell *146*, 92–104.

Tang, J., and Chu, G. (2002). Xeroderma pigmentosum complementation group E and UV-damaged DNA-binding protein. DNA Repair *1*, 601–616.

Tantin, D. (1998). RNA Polymerase II Elongation Complexes Containing the Cockayne Syndrome Group B Protein Interact with a Molecular Complex Containing the Transcription Factor IIH Components Xeroderma Pigmentosum B and p62. Journal of Biological Chemistry *273*, 27794–27799.

Tatum, D., Li, W., Placer, M., and Li, S. (2011). Diverse Roles of RNA Polymerase II-associated Factor 1 Complex in Different Subpathways of Nucleotide Excision Repair. Journal of Biological Chemistry *286*, 30304–30313.

Teng, Y., Liu, H., Gill, H.W., Yu, Y., Waters, R., and Reed, S.H. (2008). Saccharomyces cerevisiae Rad16 mediates ultraviolet-dependent histone H3 acetylation required for efficient global genome nucleotide-excision repair. EMBO Reports *9*, 97–102.

Thakur, J.K., Arthanari, H., Yang, F., Chau, K.H., Wagner, G., and Näär, A.M. (2009). Mediator Subunit Gal11p/MED15 Is Required for Fatty Acid-dependent Gene Activation by Yeast Transcription Factor Oaf1p. Journal of Biological Chemistry *284*, 4422–4428.

Thomas, M.C., and Chiang, C.-M. (2006). The General Transcription Machinery and General Cofactors. Critical Reviews in Biochemistry and Molecular Biology *41*, 105–178.

Thompson, C.M., Koleske, A.J., Chao, D.M., and Young, R.A. (1993). A multisubunit complex associated with the RNA polymerase II CTD and TATA-binding protein in yeast. Cell *73*, 1361–1375.

Thorel, F., Constantinou, A., Dunand-Sauthier, I., Nouspikel, T., Lalle, P., Raams, A., Jaspers, N.G.J., Vermeulen, W., Shivji, M.K.K., Wood, R.D., et al. (2004). Definition of a Short Region of XPG Necessary for TFIIH Interaction and Stable Recruitment to Sites of UV Damage. Molecular and Cellular Biology *24*, 10670–10680.

Tijsterman, M. (1996). Transcription-coupled and global genome repair in the Saccharomyces cerevisiae RPB2 gene at nucleotide resolution. Nucleic Acids Research *24*, 3499–3506.

Tijsterman, M., Verhage, R.A., van de Putte, P., Jong, J.G.T. -d., and Brouwer, J. (1997). Transitions in the coupling of transcription and nucleotide excision repair within RNA polymerase II-transcribed genes of Saccharomyces cerevisiae. Proceedings of the National Academy of Sciences *94*, 8027–8032.

Tirode, F., Busso, D., Coin, F., and Egly, J.M. (1999). Reconstitution of the transcription factor TFIIH: assignment of functions for the three enzymatic subunits, XPB, XPD, and cdk7. Mol. Cell *3*, 87–95.

Toyooka, T., and Ibuki, Y. (2005). Co-exposure to benzo[a]pyrene and UVA induces phosphorylation of histone H2AX. FEBS Lett. *579*, 6338–6342.

Tripsianes, K., Folkers, G., Ab, E., Das, D., Odijk, H., Jaspers, N.G.J., Hoeijmakers, J.H.J., Kaptein, R., and Boelens, R. (2005). The Structure of the Human ERCC1/XPF Interaction Domains Reveals a Complementary Role for the Two Proteins in Nucleotide Excision Repair. Structure *13*, 1849–1858.

Troelstra, C., Vermeulen, W., Bootsma, D., and Hoeijmakers, J.H.J. ERCCG, a Member of a Subfamily of Putative Helicases, Is Involved in Cockaynes Syndrome and Preferential Repair of Active Genes. 15.

Tsai, K.-L., Sato, S., Tomomori-Sato, C., Conaway, R.C., Conaway, J.W., and Asturias, F.J. (2013). A conserved Mediator–CDK8 kinase module association regulates Mediator–RNA polymerase II interaction. Nature Structural & Molecular Biology *20*, 611–619.

Tsai, K.-L., Tomomori-Sato, C., Sato, S., Conaway, R.C., Conaway, J.W., and Asturias, F.J. (2014). Subunit Architecture and Functional Modular Rearrangements of the Transcriptional Mediator Complex. Cell *157*, 1430–1444.

Tudor, M., Murray, P.J., Onufryk, C., Jaenisch, R., and Young, R.A. (1999). Ubiquitous expression and embryonic requirement for RNA polymerase II coactivator subunit Srb7 in mice. Genes & Development *13*, 2365–2368.

Unrau, P., Wheatcroft, R., and Cox, B.S. (1971). The excision of pyrimidine dimers from DNA of ultraviolet irradiated yeast. Mol. Gen. Genet. *113*, 359–362.

Ursic, D. (2004). Multiple protein/protein and protein/RNA interactions suggest roles for yeast DNA/RNA helicase Sen1p in transcription, transcription-coupled DNA repair and RNA processing. Nucleic Acids Research *32*, 2441–2452.

van de Peppel, J., Kettelarij, N., van Bakel, H., Kockelkorn, T.T.J.P., van Leenen, D., and Holstege, F.C.P. (2005). Mediator Expression Profiling Epistasis Reveals a Signal Transduction Pathway with Antagonistic Submodules and Highly Specific Downstream Targets. Molecular Cell *19*, 511–522.

van der Horst, G.T.., van Steeg, H., Berg, R.J.., van Gool, A.J., de Wit, J., Weeda, G., Morreau, H., Beems, R.B., van Kreijl, C.F., de Gruijl, F.R., et al. (1997). Defective Transcription-Coupled Repair in Cockayne Syndrome B Mice Is Associated with Skin Cancer Predisposition. Cell *89*, 425–435.

Van Gool (1994) RAD26 the functional S.cerevisiae homolog of the cockayne syndrome B gene ERCC6.pdf.

Verhage, R., Zeeman, A.M., de Groot, N., Gleig, F., Bang, D.D., van de Putte, P., and Brouwer, J. (1994). The RAD7 and RAD16 genes, which are essential for pyrimidine dimer removal from the silent mating type loci, are also required for repair of the nontranscribed strand of an active gene in Saccharomyces cerevisiae. Molecular and Cellular Biology *14*, 6135–6142.

Verhage, R.A., van Gool, A.J., de Groot, N., Hoeijmakers, J.H., van de Putte, P., and Brouwer, J. (1996). Double mutants of Saccharomyces cerevisiae with alterations in global genome and transcription-coupled repair. Molecular and Cellular Biology *16*, 496–502.

Verma, R., Oania, R., Fang, R., Smith, G.T., and Deshaies, R.J. (2011). Cdc48/p97 Mediates UV-Dependent Turnover of RNA Pol II. Molecular Cell *41*, 82–92.

Wakasugi, M., Kawashima, A., Morioka, H., Linn, S., Sancar, A., Mori, T., Nikaido, O., and Matsunaga, T. (2002). DDB Accumulates at DNA Damage Sites Immediately after UV Irradiation and Directly Stimulates Nucleotide Excision Repair. Journal of Biological Chemistry *277*, 1637–1640.

Walmacq, C., Cheung, A.C.M., Kireeva, M.L., Lubkowska, L., Ye, C., Gotte, D., Strathern, J.N., Carell, T., Cramer, P., and Kashlev, M. (2012). Mechanism of Translesion Transcription by RNA Polymerase II and Its Role in Cellular Resistance to DNA Damage. Molecular Cell *46*, 18–29.

Walmacq, C., Wang, L., Chong, J., Scibelli, K., Lubkowska, L., Gnatt, A., Brooks, P.J., Wang, D., and Kashlev, M. (2015). Mechanism of RNA polymerase II bypass of oxidative cyclopurine DNA lesions. Proceedings of the National Academy of Sciences of the United States of America 112, E410–E419.

Wang, H., Zhai, L., Xu, J., Joo, H.-Y., Jackson, S., Erdjument-Bromage, H., Tempst, P., Xiong, Y., and Zhang, Y. (2006). Histone H3 and H4 Ubiquitylation by the CUL4-DDB-ROC1 Ubiquitin Ligase Facilitates Cellular Response to DNA Damage. Molecular Cell *22*, 383–394.

Wang, X., Sun, Q., Ding, Z., Ji, J., Wang, J., Kong, X., Yang, J., and Cai, G. (2014). Redefining the modular organization of the core Mediator complex. Cell Research *24*, 796–808.

Wang, Z., Wei, S., Reed, S.H., Wu, X., Svejstrup, J.Q., Feaver, W.J., Kornberg, R.D., and Friedberg, E.C. (1997). The RAD7, RAD16, and RAD23 genes of Saccharomyces cerevisiae: requirement for transcription-independent nucleotide excision repair in vitro and interactions between the gene products. Molecular and Cellular Biology *17*, 635–643.

Weinmann, R., and Roeder, R.G. (1974). Role of DNA-Dependent RNA Polymerase III in the Transcription of the tRNA and 5S RNA Genes. Proceedings of the National Academy of Sciences *71*, 1790–1794.

Wellinger, R.E. (1997). Nucleosome structure and positioning modulate nucleotide excision repair in the non-transcribed strand of an active gene. The EMBO Journal *16*, 5046–5056.

Werner, F., and Grohmann, D. (2011). Evolution of multisubunit RNA polymerases in the three domains of life. Nature Reviews Microbiology *9*, 85–98.

Whyte, W.A., Orlando, D.A., Hnisz, D., Abraham, B.J., Lin, C.Y., Kagey, M.H., Rahl, P.B., Lee, T.I., and Young, R.A. (2013). Master Transcription Factors and Mediator Establish Super-Enhancers at Key Cell Identity Genes. Cell *153*, 307–319.

Wong, K.H., Jin, Y., and Struhl, K. (2014). TFIIH Phosphorylation of the Pol II CTD Stimulates Mediator Dissociation from the Preinitiation Complex and Promoter Escape. Molecular Cell *54*, 601–612.

Woontner and Jaehning (1989) Accurate initiation by RNA polymerase II in a whole cell extract from Saccharomyces cerevisiae

Woudstra, E.C., Gilbert, C., Fellows, J., Jansen, L., Brouwer, J., Erdjument-Bromage, H., Tempst, P., and Svejstrup, J.Q. (2002). A Rad26±Def1 complex coordinates repair and RNA pol II proteolysis in response to DNA damage. *415*, 7.

Woychik, N.A., and Young, R.A. (1989). RNA polymerase II subunit RPB4 is essential for high- and low-temperature yeast cell growth. Molecular and Cellular Biology *9*, 2854–2859.

Woychik, N.A., Lane, W.S., and Young, R.A. (1991). Yeast RNA polymerase II subunit RPB9 is essential for growth at temperature extremes. J. Biol. Chem. *266*, 19053–19055.

Wu, X., Braithwaite, E., and Wang, Z. (1999). DNA Ligation during Excision Repair in Yeast Cell-Free Extracts Is Specifically Catalyzed by the *CDC9* Gene Product †. Biochemistry *38*, 2628–2635.

Xie, Z. (2004). Roles of Rad23 protein in yeast nucleotide excision repair. Nucleic Acids Research *32*, 5981–5990.

Xu, J., Lahiri, I., Wang, W., Wier, A., Cianfrocco, M.A., Chong, J., Hare, A.A., Dervan, P.B., DiMaio, F., Leschziner, A.E., et al. (2017). Structural basis for the initiation of eukaryotic transcription-coupled DNA repair. Nature.

Yang, F., Vought, B.W., Satterlee, J.S., Walker, A.K., Jim Sun, Z.-Y., Watts, J.L., DeBeaumont, R., Mako Saito, R., Hyberts, S.G., Yang, S., et al. (2006). An ARC/Mediator subunit required for SREBP control of cholesterol and lipid homeostasis. Nature *442*, 700–704.

Yang, Y., Adebali, O., Wu, G., Selby, C.P., Chiou, Y.-Y., Rashid, N., Hu, J., Hogenesch, J.B., and Sancar, A. (2018). Cisplatin-DNA adduct repair of transcribed genes is controlled by two circadian programs in mouse tissues. PNAS 201804493.

Yin, J. -w., and Wang, G. (2014). The Mediator complex: a master coordinator of transcription and cell lineage development. Development *141*, 977–987.

Yin, J. -w., Liang, Y., Park, J.Y., Chen, D., Yao, X., Xiao, Q., Liu, Z., Jiang, B., Fu, Y., Bao, M., et al. (2012). Mediator MED23 plays opposing roles in directing smooth muscle cell and adipocyte differentiation. Genes & Development *26*, 2192–2205.

Yokoi, M., Masutani, C., Maekawa, T., Sugasawa, K., Ohkuma, Y., and Hanaoka, F. (2000). The Xeroderma Pigmentosum Group C Protein Complex XPC-HR23B Plays an Important Role in the Recruitment of Transcription Factor IIH to Damaged DNA. Journal of Biological Chemistry *275*, 9870–9875.

You, J.-S., Wang, M., and Lee, S.-H. (2003). Biochemical Analysis of the Damage Recognition Process in Nucleotide Excision Repair. Journal of Biological Chemistry *278*, 7476–7485.

Yu, S., Owen-Hughes, T., Friedberg, E.C., Waters, R., and Reed, S.H. (2004). The yeast Rad7/Rad16/Abf1 complex generates superhelical torsion in DNA that is required for nucleotide excision repair. DNA Repair *3*, 277–287.

Yu, S., Smirnova, J.B., Friedberg, E.C., Stillman, B., Akiyama, M., Owen-Hughes, T., Waters, R., and Reed, S.H. (2009). ABF1-binding sites promote efficient global genome nucleotide excision repair. J. Biol. Chem. *284*, 966–973.

Yu, S., Teng, Y., Waters, R., and Reed, S.H. (2011). How Chromatin Is Remodelled during DNA Repair of UV-Induced DNA Damage in Saccharomyces cerevisiae. PLoS Genetics *7*, e1002124.

Yu, Y., Deng, Y., Reed, S.H., Millar, C.B., and Waters, R. (2013). Histone variant Htz1 promotes histone H3 acetylation to enhance nucleotide excision repair in Htz1 nucleosomes. Nucleic Acids Research *41*, 9006–9019.

Zaborowska, J., Egloff, S., and Murphy, S. (2016). The pol II CTD: new twists in the tail. Nature Structural & Molecular Biology *23*, 771–777.

Zhang, X., Horibata, K., Saijo, M., Ishigami, C., Ukai, A., Kanno, S., Tahara, H., Neilan, E.G., Honma, M., Nohmi, T., et al. (2012). Mutations in UVSSA cause UV-sensitive syndrome and destabilize ERCC6 in transcription-coupled DNA repair. Nature Genetics *44*, 593–597.

Zhao, Q., Wang, Q.-E., Ray, A., Wani, G., Han, C., Milum, K., and Wani, A.A. (2009). Modulation of Nucleotide Excision Repair by Mammalian SWI/SNF Chromatin-remodeling Complex. Journal of Biological Chemistry *284*, 30424–30432.

Zhou, B.-B.S., and Elledge, S.J. (2000). The DNA damage response: putting checkpoints in perspective. *408*, 7.

Zhou, M., and Law, J.A. (2015). RNA Pol IV and V in gene silencing: Rebel polymerases evolving away from Pol II's rules. Current Opinion in Plant Biology *27*, 154–164.

Zhou, Y., Kou, H., and Wang, Z. (2007). Tfb5 interacts with Tfb2 and facilitates nucleotide excision repair in yeast. Nucleic Acids Research *35*, 861–871.

Zhu, X., Zhang, Y., Bjornsdottir, G., Liu, Z., Quan, A., Costanzo, M., Dávila López, M., Westholm, J.O., Ronne, H., Boone, C., et al. (2011). Histone modifications influence mediator interactions with chromatin. Nucleic Acids Research *39*, 8342–8354.

Zolan, M.E., Cortopassi, G.A., Smith, C.A., and Hanawalt, P.C. (1982). Deficient repair of chemical adducts in α DNA of monkey cells. Cell 28, 613 – 619

Zotter, A., Luijsterburg, M.S., Warmerdam, D.O., Ibrahim, S., Nigg, A., van Cappellen, W.A., Hoeijmakers, J.H.J., van Driel, R., Vermeulen, W., and Houtsmuller, A.B. (2006). Recruitment of the Nucleotide Excision Repair Endonuclease XPG to Sites of UV-Induced DNA Damage Depends on Functional TFIIH. Molecular and Cellular Biology *26*, 8868–8879.

Annexes

I. Article 1 : Supplementary data.

Supplementary Information

Supplementary text for random mutagenesis of Med17 C-terminal domain

A linearized plasmid containing *med17* N-terminal domain and *TRP1* gene (for auxotrophic selection), and *med17* C-terminal domain amplified by error-prone PCR (30 cycles in presence of 0.1 mM (condition A) or 0.5mM (condition B) $MnCl_2$ and 7mM $MgCl_2$) were co-transformed in *rad7*Δ *med17*Δ*/MED17 URA* yeasts (**Supplementary Figure S2C**). The amplified *med17* C-terminal domain had extremities overlapping the introduced plasmid to allow recombination and reformation of a circular plasmid expressing *med17* and *TRP1* genes. Yeasts forming clones on CAU plates (Casamino Acids medium supplemented with adenine and uracil, lacking tryptophan) were scrapped, resuspended in YPD, supplemented with 6.5% DMS0, aliquoted and kept at -80°C until further use.

To screen colonies, 25 YPD plates per condition were seeded to have 200 colonies per plate and incubated at 30°C for 2 days. Plates were replicated on 5-FOA to select yeast without *MED17 URA* plasmid. About 20% colonies in condition A, 40% in condition B did not grow on 5-FOA, indicating that they had integrated non-viable versions of *med17*. After 3 days, plates were replicated on CAU (3 plates), 5-FOA and CAW (lacking uracil) to check that *MED17 URA* plasmid was eliminated. One YPD plate was irradiated with 30 J/m^2 UV-C (254 nm) and incubated at 30°C, the others were incubated at 30°C and 37°C, respectively (**Supplementary Figure S2D**). 3 days after treatment, plates were examined for colonies growing on the control plate (30°C) but not on one of the two other plates (37°C or UV). Detected colonies were replicated from the 5-FOA plate. The phenotype was confirmed using a spotting assay. When the phenotype was consistent, genomic DNA was prepared and used to transform competent cells that were selected on Ampicillin medium to recover *med17 TRP* plasmid. Isolated plasmids were used to retransform *rad7*Δ *med17*Δ*/MED17 URA* yeasts. After elimination of *MED17 URA*, the phenotypes were tested again on three clones to confirm that they were associated to the generated mutations of *med17*. Plasmids associated to a confirmed phenotype were then sequenced to determine causal mutations. Clones with similar mutations were removed, and a total of 121 new mutants of *med17* were identified and characterized for their sensitivity to UV-C (30 J/m^2), growth at 37°C (ts) and growth at 16°C (cs) (Supplementary Table S2, including 27 previously characterized mutants).

Using spotting assay (**Supplementary Figure S2E**), we found 10 *med17* mutants exhibiting increased UV-sensitivity and normal growth at 37°C. However, all these mutants had reduced growth at 16°C, and sequencing showed they all had single-base insertions or deletions resulting in premature stop codons. 23 other mutants also had predictions of premature stop codons. As *med17* C-terminal truncation mutants are not viable, we examined Med17 protein expression in three of these mutants by Western Blot (**Supplementary Figure S2F**). We found that a majority of expressed Med17 protein was indeed truncated, but that a small proportion of expressed Med17 had the size of full length Med17, suggesting that ribosomal sliding rescued these mutants. Apart from these 33 nonsense mutants, no mutant predicted to express full length Med17 caused UV sensitivity without also causing temperature sensitivity.

To identify positions that may play a bigger role in phenotypes, we represented the number of occurrences of mutations

affecting each residue, and the associated phenotype. Most residues were involved in less than 4 mutants, but a few positions were more frequently mutated in particular F437, M442, K517 and I541. Interestingly, whereas F437, M442 and I541 were more frequently associated to UV sensitivity, K517 and nearby residues were more frequently found with temperature-sensitive only mutants. Most frequently mutated residues in a majority of UV sensitive mutants were selected for further analysis using two-hybrid approach (**Supplementary Figure S3**).

Supplementary Figure S1

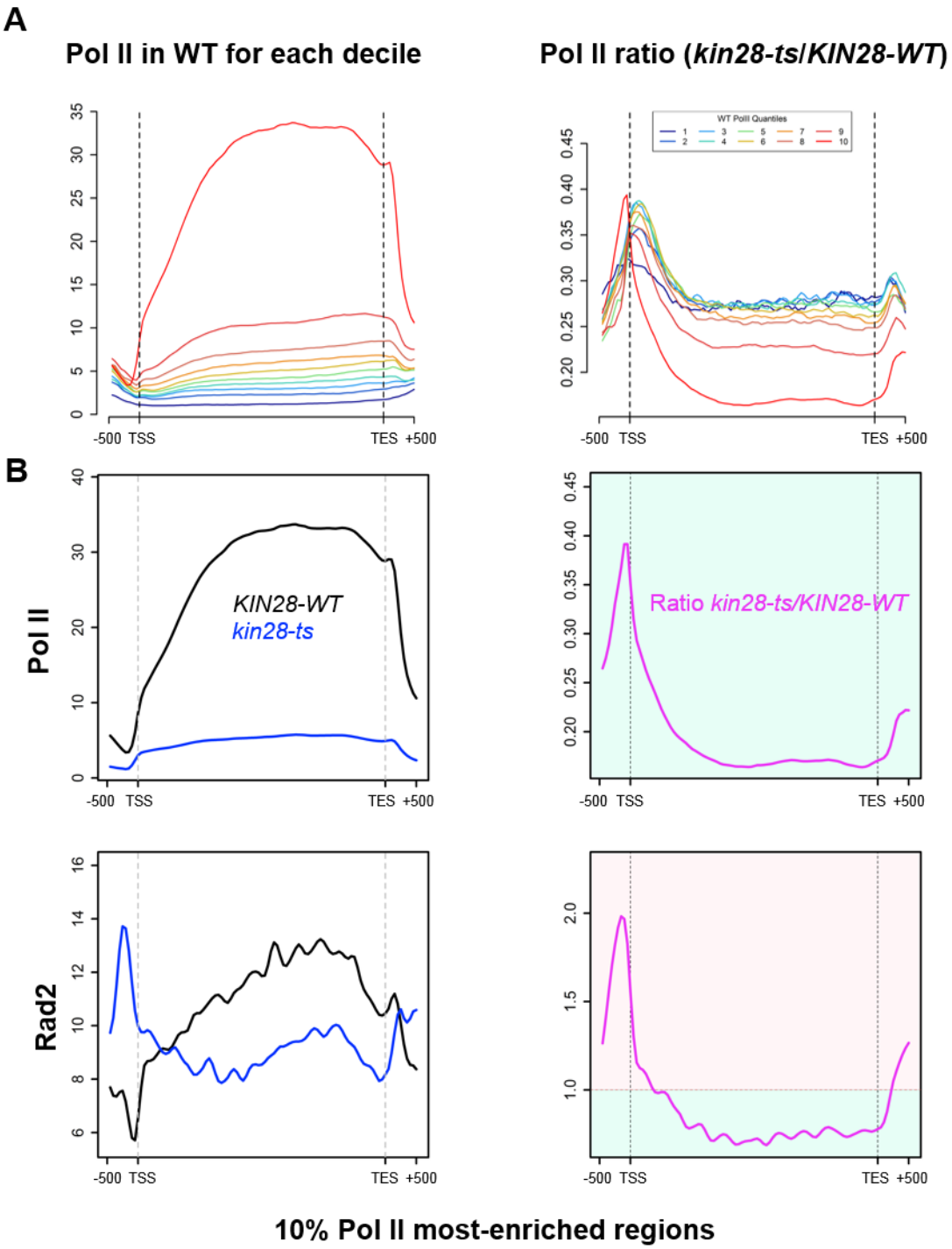

Genome-wide analysis of Pol II profiles in *kin28 ts* mutant compared to the wild-type as a function of Pol II enrichment.
(**A**) Average tag density in Rpb1 Pol II ChIP (left panel) in wild type strain on transcribed regions (500bp before TSS, scaled window between TSS and TES, and 500 bp after TES) was calculated for deciles of genes defined according to the Pol II enrichment in the wild-type (from a 1st decile group with lowest enrichment in violet corresponding to 10% lowest Pol II enrichment to a 10th decile group with highest enrichment in red corresponding to 10% highest Pol II enrichment). The right panel shows metagene analysis for Pol II ratio between *kin28-ts* mutant and the wild-type on all decile groups.
(**B**) Average tag density in Rpb1 Pol II ChIP or Rad2 ChIP (left panels) on transcribed regions of 10% Pol II most-enriched genes (500bp before TSS, scaled window between TSS and TES, and 500 bp after TES). Average tag density in wild type strains is indicated in black, whereas average tag density in *kin28 ts* strains is indicated in blue. The right panels show Pol II and Rad2 ratios (in pink) between *kin28-ts* mutant and the wild-type. For clarity, the background of the plot for ratios >1 is coloured in clear red and the background of the plot for ratios <1 is coloured in clear green.

Supplementary Figure S2

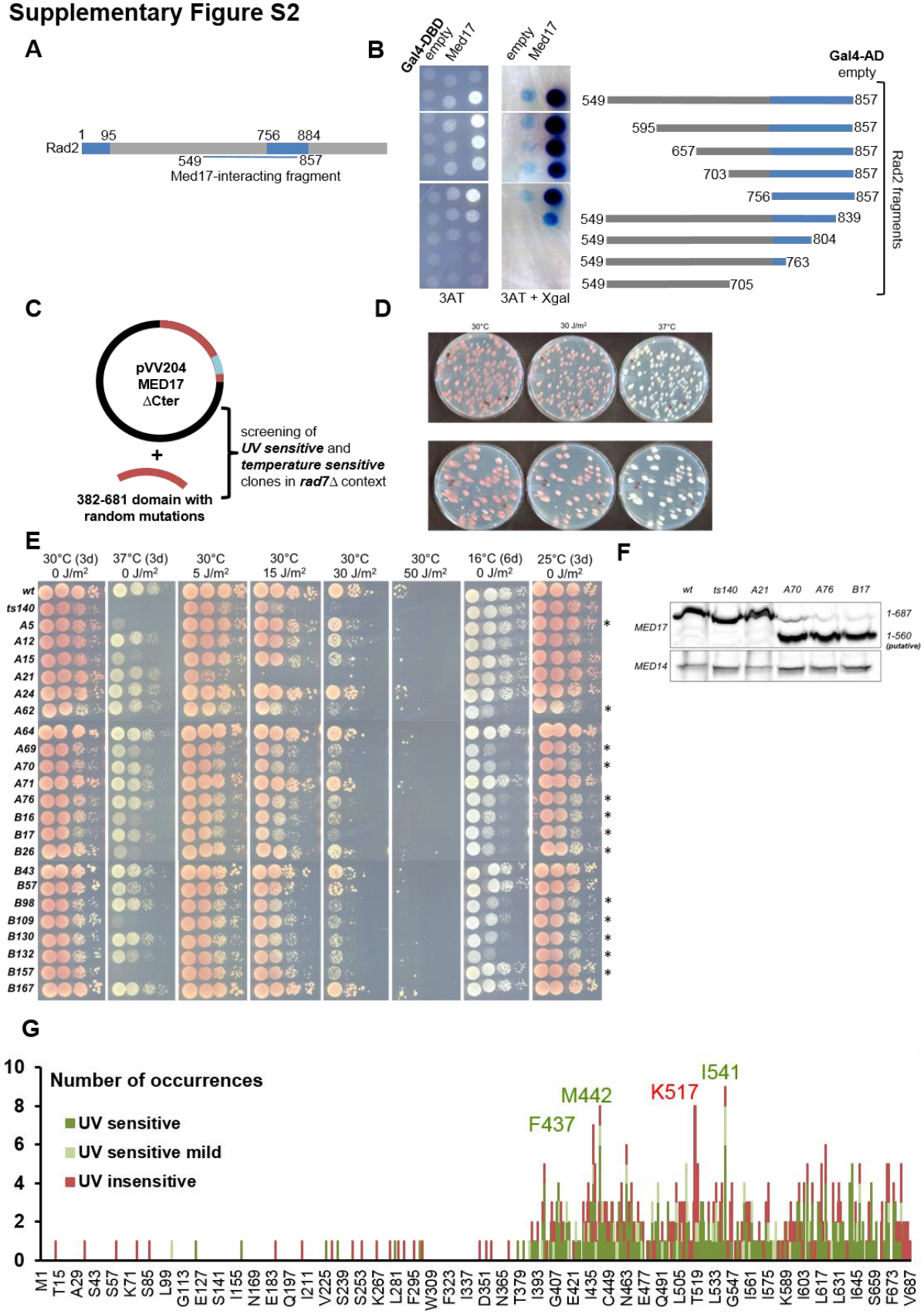

Random mutational screening of Med17-Rad2 interaction interface.
(**A, B**) Definition of Rad2 region interacting with Med17 fragment in yeast two-hybrid assay.

(**A**) Illustration of the position of Rad2 fragment interacting with Med17 in two-hybrid assay. Catalytic N and I domains of Rad2 are highlighted in blue. Rad2 fragment spans part of "linker" and "catalytic I" domains of Rad2. (**B**) Serial truncations of Rad2 fragment 549-857 were assayed for interaction with full length Med17 and Med17 fragment (382-687) based on Figure 1. Gal4 Activating domain (Gal4-AD), alone or in fusion with Rad2 fragments, was co-expressed with Gal4 DNA-Binding Domain (Gal4 DBD), alone, in fusion with full length Med17 or residues 382 to 687 of Med17. Spotted yeasts were grown on SD+2A medium supplemented with 25mM 3-AT for 3 days (left panel), then stained with X-Gal for 24h (middle panel). Residues 756 to 857 appear necessary to have a full interaction of Rad2 with both full length Med17 and Med17 fragment.
(**C-G**) Random mutational screening to identify *med17* UV-sensitive mutants.
(**C**) Illustration of the strategy to obtain mutants of *med17* C-terminal domain.
(**D**) Examples of screening for UV and temperature sensitive clones. Example of plates for the three conditions (30°C without treatment, 30°C after UV, 37°C without treatment) are shown. Clones selected for further examination are indicated by a red arrow. (**E**) Example of phenotype confirmation by spotting assay. Selected clones were spotted on medium without tryptophan (CAU, Casamino Acids medium supplemented with adenine and uracil), irradiated or not with various doses of UV-C, and incubated at 16°C, 25°C, 30°C, or 37°C for 3 days (except 16°C for 6 days). Asterisks indicate the clones for which the observed phenotype could be attributed to *med17 TRP* plasmid (after purification and retransformation). (**F**) Western blot analysis of Med17 protein expression in wild type or mutant strains. Crude extracts from isolated clones or the wild type strain were prepared, separated by SDS-PAGE and transferred to a nitrocellulose membrane for Western blotting. Antibodies again Med17 and Med14 were used. The putative Med17 products are indicated on the right, based on DNA sequencing of the corresponding plasmids. (**G**) Pile histogram representing the number of occurrences of Med17 residues in the mutants. The number of mutation occurrences is indicated for each amino acid position. Only mutants predicted to express full length Med17 were considered. The colours correspond to the associated phenotypes as follows: UV-sensitive in green, mild UV-sensitive in clear green and UV-insensitive in red. Most frequently mutated residues are indicated.

Supplementary Figure S3

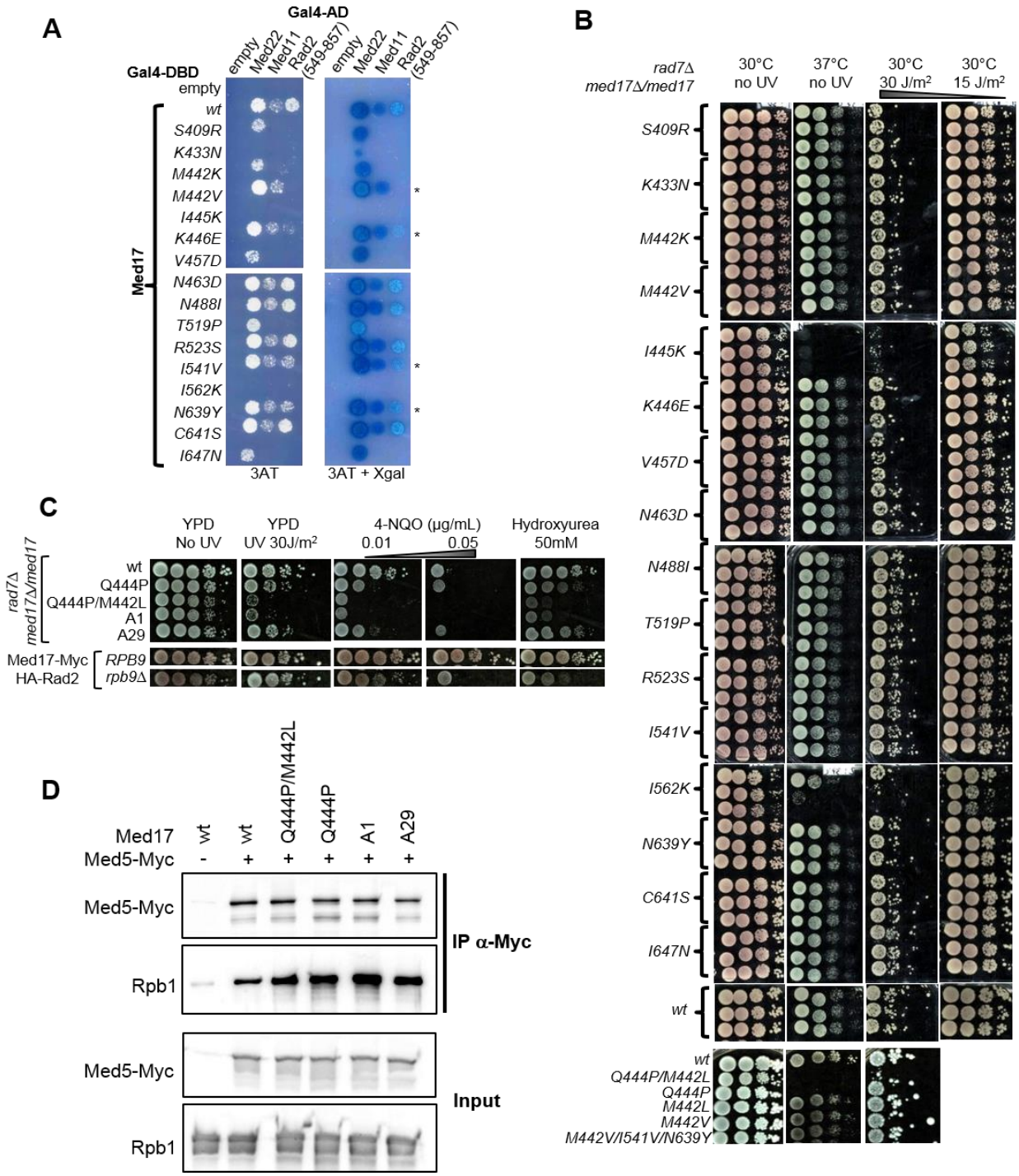

Analysis by site-directed mutagenesis of Med17 interaction with Rad2 fragment.

(**A**) Mutational analysis of Rad2-interacting Med17 fragment in yeast two-hybrid assay. Gal4 DNA binding (Gal4-DBD) domain, alone or in fusion with full length Med17, wild-type or with indicated mutation, was co-expressed with Gal4 Activation Domain (Gal4 AD), alone or in fusion with Med22, Med11 or residues 549 to 857 of Rad2. Yeast strains were spotted on SD+2A medium supplemented with 25mM 3-AT, grown for 3 days (left panel), and then stained with X-Gal for 24h (right panel). Med17 mutants with a decrease in interaction observed only with Rad2 fragment without disturbing the interactions with Med22 and Med11 are indicated with an asterisk (M442V, K446E, I541V and N639Y).

9. (**B**) Growth phenotypes of *med17* mutants. Spotting assay to determine UV and temperature sensitivity of yeast strains expressing either wild type or mutant versions of Med17 in *rad7*Δ context. Spotted yeasts were irradiated or not with 15 J/m^2 or 30 J/m^2 UV-C (254 nm) and incubated at 30°C or 37°C for 3 days. Single mutations affecting Med17-Rad2 interaction in two-hybrid assay had no UV^s or ts phenotypes. A triple mutant (M442V/I541V/N639Y) that specifically affect Med17-Rad2 Y2H interaction also gave no phenotype *in vivo.*

(**C**) Effects of *med17* mutations or *rpb9* deletion on the sensitivity of yeast to UV, 4-NQO or hydroxyurea. Yeast strains expressing wild type or mutated versions of Med17 in a *rad7*Δ context, or tagged versions of Med17 and Rad2 in a wild type or *rpb9*Δ context, were spotted on YPD agar plates supplemented or not with 0.01µg/mL 4-NQO, 0.05µg/mL 4-NQO or 50mM hydroxyurea, as indicated. Yeast cells were spotted on YPD agar plates, irradiated or not with 30 J/m^2 UV-C (254 nm) and incubated at 30°C for 3 days.

(**D**) Western blot analysis of Mediator interaction with Pol II in standard growth conditions.

Crude extracts were prepared from yeasts expressing tagged (+) or untagged (-) versions Med5 (Myc) in *MED17-wt*, *med17-Q444P*, *med17-Q444P/M442L*, *med17-A1* or *med17-A29* context in exponential phase, and samples were immunoprecipitated with α-Myc antibody (IP Myc). Immunoprecipitates and Inputs were analysed by SDS-PAGE followed by Western blotting using α-Myc and α-Rpb1 antibodies.

Supplementary Figure S4

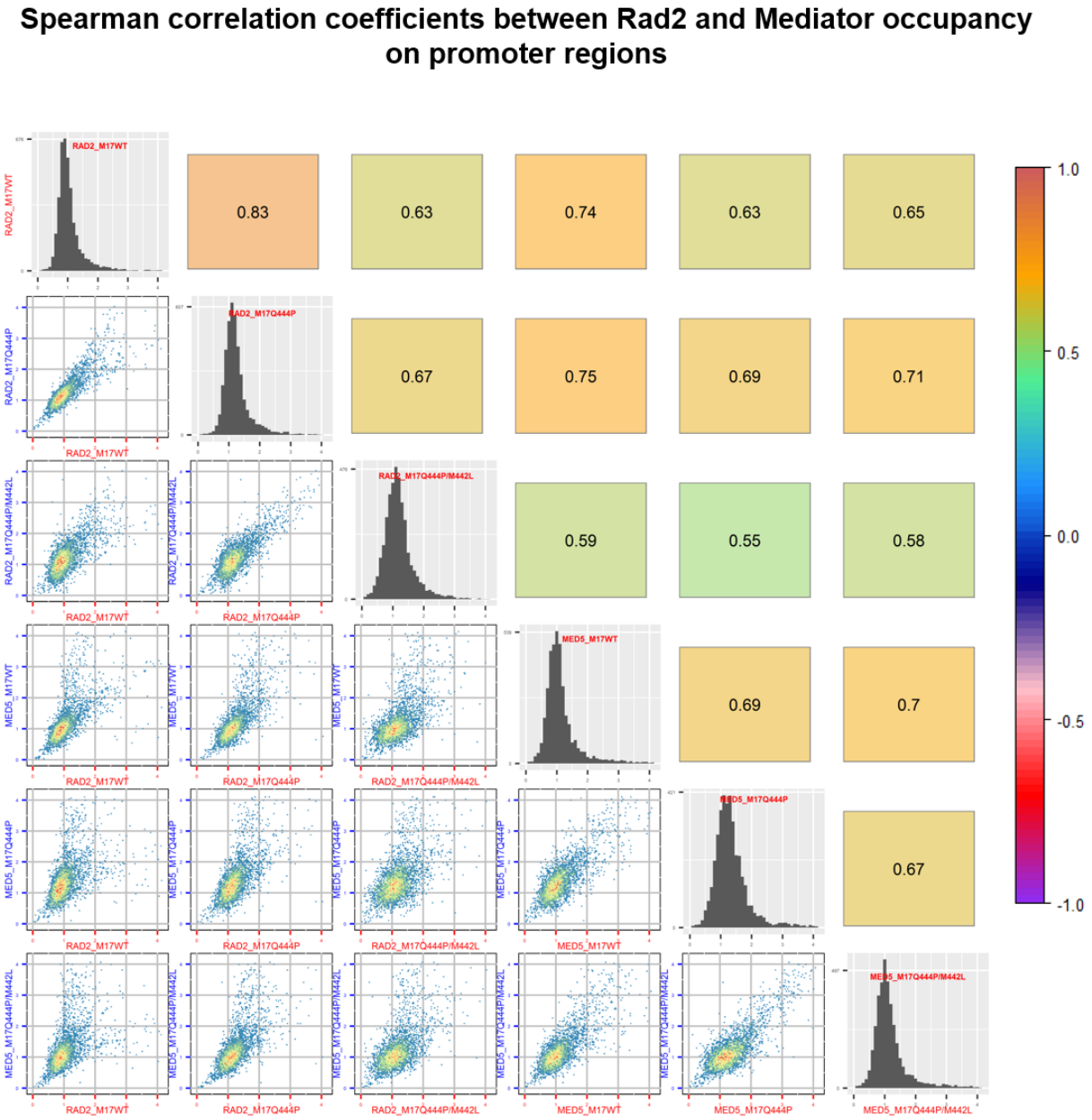

Correlation analysis between Rad2 and Mediator occupancy on promoter regions in *med17* mutants compared to the wild-type.
Pair-wise Spearman correlation coefficients (top-right part) of ChIP-seq data between *med17* mutants and wild-type were calculated for Rad2 and Mediator occupancy on promoter regions. The bottom-left part shows the scatter plots corresponding to each pair-wise combination. Tag density distribution for each ChIP-seq dataset is shown on the diagonal. The colours correspond to the scale for Spearman correlation coefficients indicated on the right.

Supplementary Figure S5

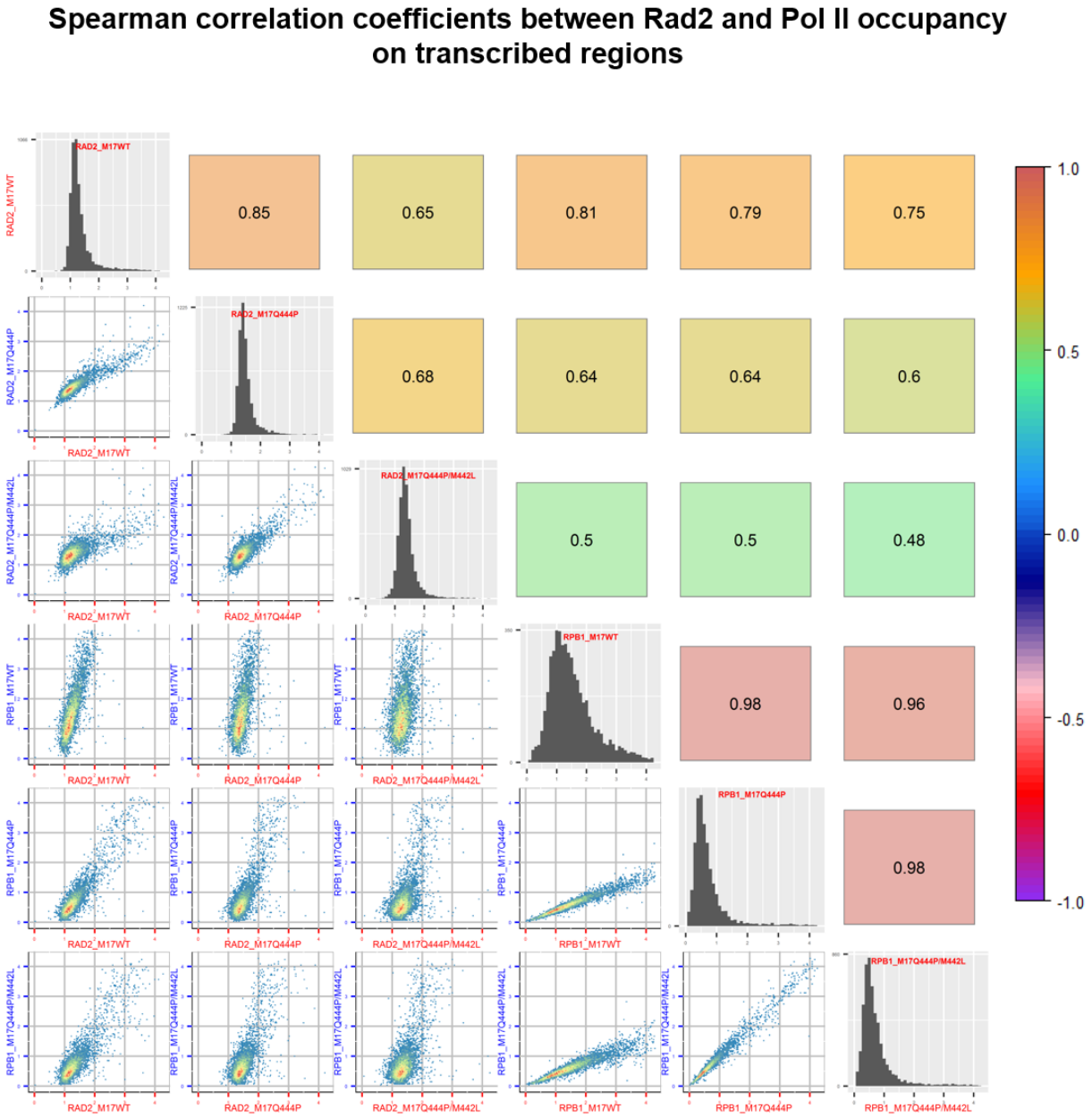

Correlation analysis between Rad2 and Pol II occupancy on transcribed regions in *med17* mutants compared to the wild-type.
Pair-wise Spearman correlation coefficients (top-right part) of ChIP-seq data between *med17* mutants and wild-type were calculated for Rad2 and Pol II occupancy on transcribed regions. The bottom-left part shows the scatter plots corresponding to each pair-wise combination. Tag density distribution for each ChIP-seq dataset is shown on the diagonal. The colours correspond to the scale for Spearman correlation coefficients indicated on the right.

Supplementary Figure S6

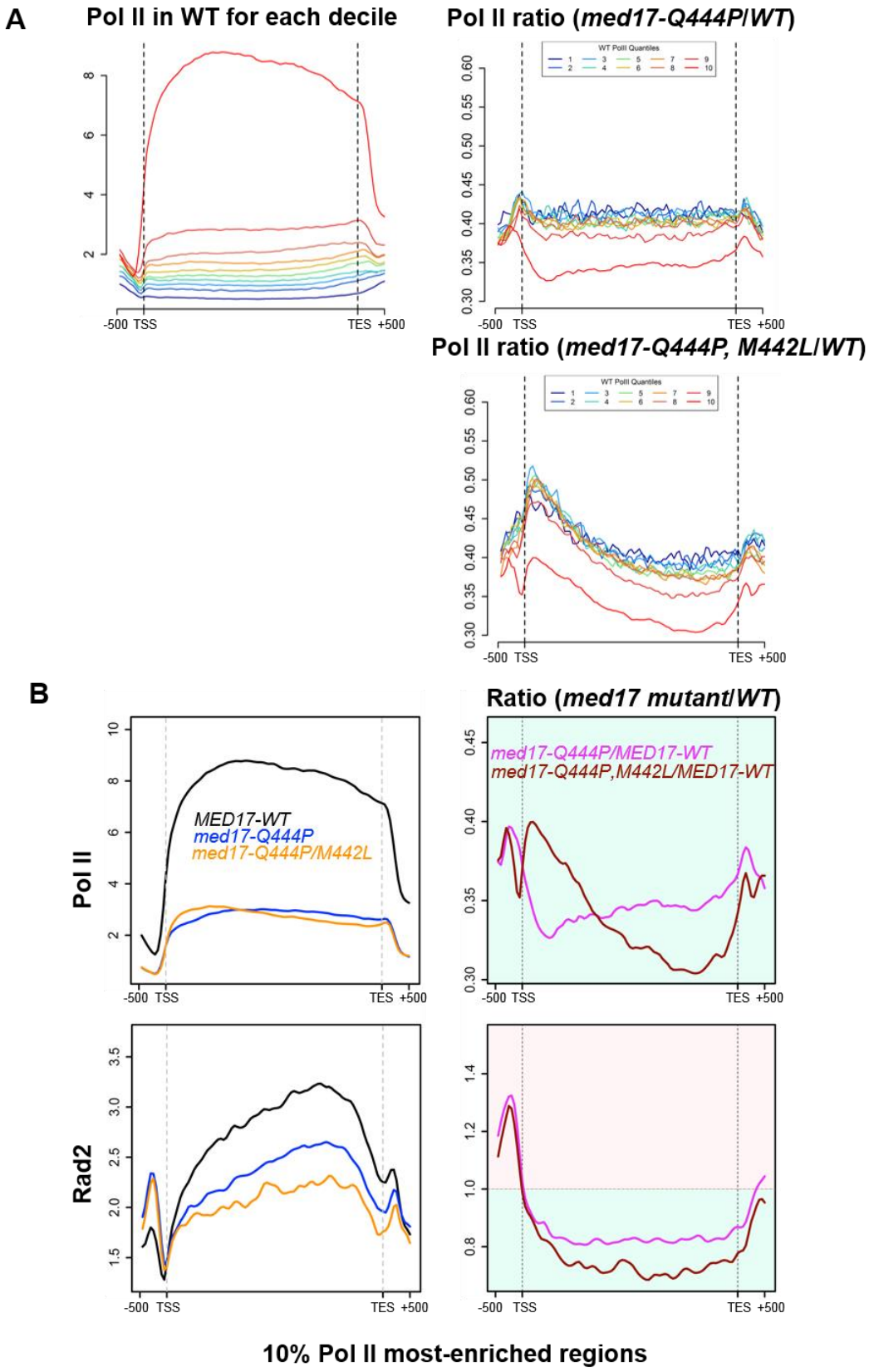

Genome-wide analysis of Pol II and Rad2 profiles in *med17* mutants compared to the wild-type.

(**A**) Average tag density in Rpb1 Pol II ChIP (left panel) in wild type strain on transcribed regions (500bp before TSS, scaled window between TSS and TES, and 500 bp after TES) was calculated for deciles of genes defined according to the Pol II enrichment in the wild-type (from a 1st decile group with lowest enrichment in violet corresponding to 10% lowest Pol II enrichment to a 10th decile group with highest enrichment in red corresponding to 10% highest Pol II enrichment). The right panel shows metagene analysis for Pol II ratio between *med17-Q444P* or *med17-Q444P/M442L* mutants and the wild-type on the 10 groups.

(**B**) Average tag density in Rpb1 Pol II ChIP or Rad2 ChIP (left panels) on transcribed regions (500bp before TSS, scaled window between TSS and TES, and 500 bp after TES) was calculated for 10% Pol II most-enriched genes defined according to the Pol II enrichment in the wild-type. Average tag density in wild type, *med17-Q444P* and *med17-Q444P/M442L* strains is indicated in black, blue and orange, respectively. The right panels show Pol II or Rad2 occupancy ratio between *med17-Q444P* or *med17-Q444P/M442L* mutants and the wild-type (in pink and brown, respectively). For clarity, the background of the plot for ratios >1 is coloured in clear red and the background of the plot for ratios <1 is coloured in clear green.

Supplementary Figure S7

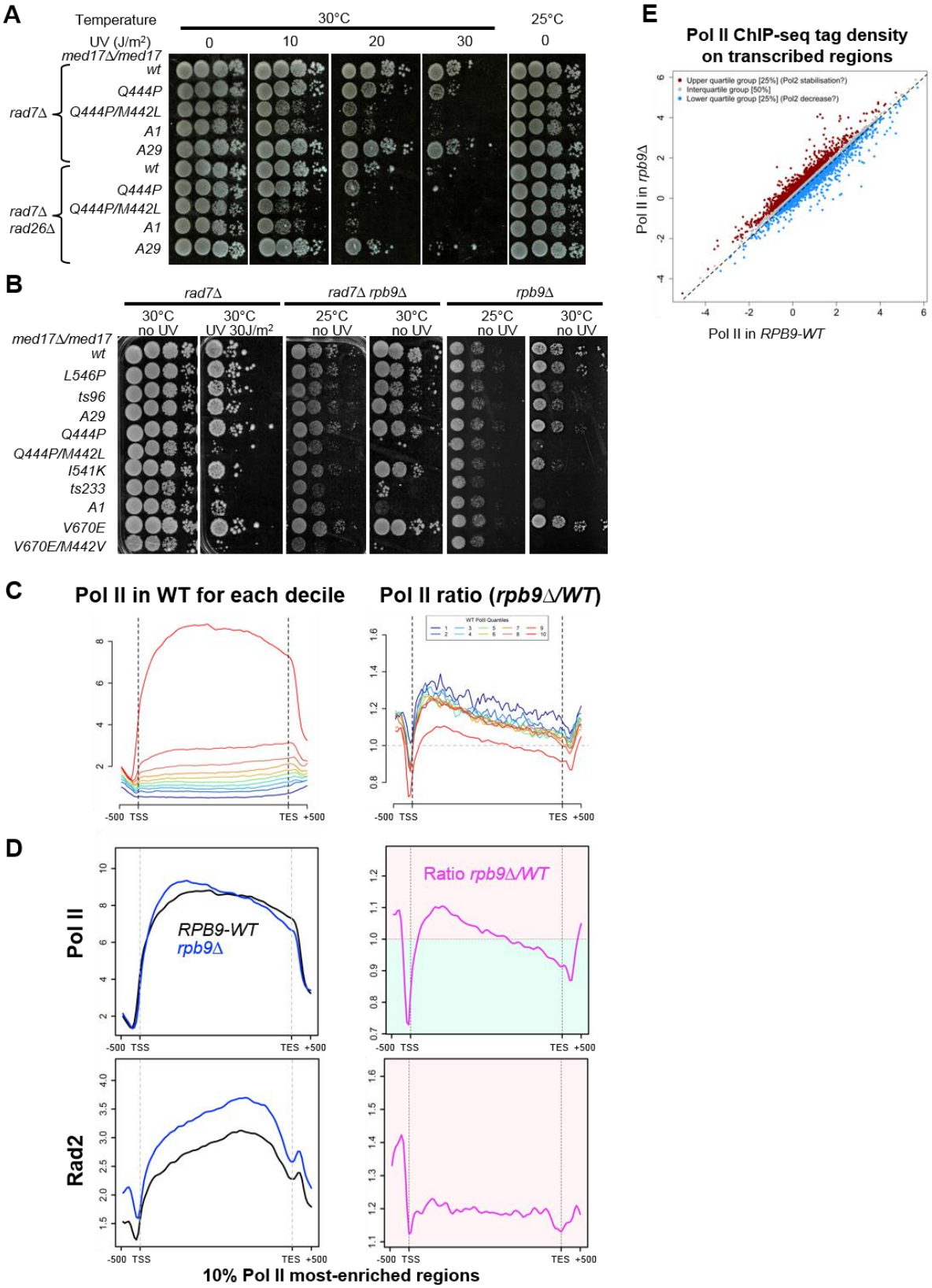

Genetic interactions between *med17* and *rpb9*Δ and genome-wide analysis of Pol II and Rad2 profiles in *rpb9*Δ mutant.

(**A**) Spotting assay to determine UV and temperature sensitivity of yeast strains expressing wild type or mutant versions of Med17 in *rad7*Δ or *rad7*Δ *rad26*Δ contexts. Yeast cells were spotted on YPD agar plates, irradiated or not with 10, 20 or 30 J/m^2 UV-C (254 nm) and incubated at 30°C or 25°C for 3 days. (**B**) Spotting assay to determine UV and temperature sensitivity of yeast strains expressing wild type or mutant versions of Med17 in *rad7*Δ, *rad7*Δ *rpb9*Δ or *rpb9*Δ contexts. Yeast cells were spotted on YPD agar plates, irradiated or not with 30 J/m^2 UV-C (254 nm) and incubated at 30°C or 25°C for 3 days. Med17 mutants unable to grow after UV treatment in *rad7*Δ context are also unable to grow at 30°C, in the absence of UV treatment, in *rad7*Δ *rpb9*Δ and *rpb9*Δ contexts.

(**C**) Average tag densities in Rpb1 Pol II ChIP (left panel) on transcribed regions (500bp before TSS, scaled window between TSS and TES, and 500 bp after TES) were calculated for deciles of genes defined according to the Pol II enrichment in the wild-type (from a 1st decile group with lowest enrichment in violet corresponding to 10% lowest Pol II enrichment to a 10th decile group with highest enrichment in red corresponding to 10% highest Pol II enrichment). The right panel shows metagene analysis for Pol II ratio between *rpb9*Δ mutant and the wild-type on all decile groups.

(**D**) Average tag densities in Rpb1 Pol II ChIP Rad2 ChIP (left panels) on transcribed regions of 10% Pol II most-enriched genes (500bp before TSS, scaled window between TSS and TES, and 500 bp after TES). Average tag density in wild type strains is indicated in black, whereas average tag density in *rpb9*Δ strains is indicated in blue. The right panels show Pol II or Rad2 occupancy ratio (in pink) between *rpb9*Δ mutant and the wild-type. For clarity, the background of the plot for ratios >1 is coloured in clear red and the background of the plot for ratios <1 is coloured in clear green.

(**E**) Pol II ChIP-seq tag densities in the *rpb9* mutant versus the wild type were plotted with $\log_2$ scales. Three groups of genes were defined according to the Pol II occupancy ratios on the transcribed regions between the *rpb9*Δ mutant and the wild type: the lowest 25% (lower quartile group in blue), the highest 25% (upper quartile group in red), and the ratios between 25% and 75% (interquartile group in grey). Blue points correspond to the lowest 25% of mutant/wild-type ratio values, and grey points correspond to values between 25% and 75% of the mutant/wild type ratio. The red points correspond to the 25% of the genes that have the highest mutant/wild-type ratio.

Supplementary Table S1 (Excel file). → NOT INCLUDED
Yeast strains, plasmids and primers used in the study.

Supplementary Table S2 (Excel file). → NOT INCLUDED
Med17 mutants with associated phenotypes and amino acid changes.

Supplementary Table S3.

Number of mapped reads and normalisation coefficients for ChIP-seq experiments.

Sample	Mapped reads	Normalization coefficient
NT_HA_Med5_Myc	13901150	1
RAD2_Med17WT	18626551	1
RAD2_Med17Q444P	18178665	0.875
RAD2_Med17Q444PM442L	2218097	0.926
MED5_Med17WT	6554659	1
MED5_Med17Q444P	3595899	0.788
MED5_Med17Q444PM442L	5889040	0.963
RPB1_Med17WT	17782766	1
RPB1_Med17Q444P	16398788	2.572
RPB1_Med17 Q444PM442L	17118260	2.667
INPUT_MED5Myc_RAD2HA_Med17WT	21248003	1
INPUT_MED5Myc_RAD2HA_Med17Q444P	22347006	1
INPUT_Med5Myc_RAD2HA_ Med17Q444PM442L	21850931	1
RAD2_Rpb9WT	18615433	1
RAD2_Rpb9D	18114259	0.754
MED17_Rpb9WT	5051300	1
MED17_Rpb9D	4989850	1.390
RPB1_Rpb9WT	16135457	1
RPB1_Rpb9D	16065910	0.920
INPUT_Med17Myc_RAD2HA_Rpb9WT	16259254	1
INPUT_Med17Myc_RAD2HA_Rpb9D	16700462	1
RAD2_Kin28WT	6872051	1
RAD2_Kin28TS	5455286	0.660
MED17_Kin28WT	2404471	1
MED17_Kin28TS	2816153	1.156
POL2_Kin28WT	20729886	1
POL2_Kin28TS	21394019	4.216

II. Résumé en français

II.1 Introduction

Nos cellules subissent des dizaines de milliers de dommages tous les jours, qui peuvent avoir des effets néfastes. Ces dommages peuvent être d'origine exogène (tels que les rayons ultraviolets, radiations ionisantes et des substances génotoxiques) ou d'origine endogène (tels que les radicaux libres issus du métabolisme cellulaire). Il est ainsi essentiel que les dommages soient réparés ou tolérés car ils peuvent interférer avec les processus cellulaires vitaux (la transcription, la réplication, …) ou avoir des effets mutagènes. Plusieurs mécanismes de réparation existent pour prendre en charge les dommages à l'ADN et maintenir l'intégrité de notre génome.

Dans le laboratoire, nous nous intéressons à la voie de réparation par excision de nucléotides (NER). Cette voie est très conservée et répare les dommages à l'ADN qui distordent la double hélice. La voie NER est divisée en deux sous-voies notamment le GG-NER (Global Genome Repair) et la TC-NER (Transcription Coupled Repair). La sous-voie GG-NER répare les dommages dans l'ensemble du génome y compris sur le brin non-transcrit d'un gène actif. La sous-voie TC-NER répare les lésions présentes sur le brin transcrit d'un gène actif. Les deux sous-voies du NER se différencient à la première étape de reconnaissance mais les étapes successives sont communes. Dans la sous-voie GG-NER, la reconnaissance requiert un complexe composé de XPC et RAD23B dans les cellules humaines et leurs homologues Rad4 et Rad23 chez la levure. Dans la TC-NER, l'ARN Pol II bloquée par le dommage est le premier signal qui permet le recrutement des protéines du NER notamment de Rad26/CSB. Chez l'homme CSB coopère avec XPG pour la reconnaissance du dommage et pour recruter des facteurs agissant en aval. En effet, l'étape initiale de reconnaissance des dommages, est suivie de l'ouverture de la double hélice d'ADN et de la vérification du dommage par TFIIH, Rad14/XPA et RPA. L'incision en 5' du dommage est réalisée par un dimère XPF-ERCC1 et leurs homologues Rad1-Rad10 chez la levure. Ensuite, l'incision en 5' est réalisée par Rad2/XPG. Un fragment de 25-30 nucléotides est excisé. La resynthèse du fragment d'ADN et la ligation permet de sceller la coupure. Ces étapes décrites séparément ne sont pas nécessairement indépendantes.

A noter que chez la levure, des mécanismes de TC-NER non-dépendantes de Rad26 ont été aussi proposées dont un mécanisme médié par une sous-unité non-essentielle de l'ARN Pol II, Rpb9 (Li and Smerdon, 2002).

Les mutations de la voie NER peut conduire à des pathologies graves telles que le xeroderma pigmentosum (XP) et le syndrome de Cockayne (CS). Ces pathologies se caractérisent notamment par une sensibilité accrue aux UV.

La voie NER est étroitement liée à la transcription et certains facteurs ont un rôle dans les deux processus notamment l'ARN Pol II, le Médiateur et TFIIH.

La transcription est un processus très conservé et est la première étape de l'expression des gènes. L'ARN Pol II est responsable de la transcription des gènes codant pour les protéines et certains ARN non-codants. La transcription comporte trois étapes : l'initiation, l'élongation et la terminaison. L'initiation consiste à la mise en place du PIC (complexe de pré-initiation) au niveau du promoteur et cette étape nécessite les facteurs généraux et spécifiques de la transcription. Pendant l'étape d'élongation, l'ARN Pol II parcourt le brin transcrit en synthétisant l'ARN. La terminaison de la transcription consiste en la libération de l'ARN Pol II de son matrice d'ADN et de l'ARN néo-synthétisé. Ces trois étapes sont régulées et ne sont pas nécessairement indépendantes.

Comme mentionné dans le paragraphe précédent, deux groupes de facteurs sont nécessaires à l'initiation de la transcription : les facteurs généraux de la transcription (GTFs) et les facteurs spécifiques de la transcription. Les GTFs sont requis pour l'initiation de tous les gènes et sont au nombre de six : TFIIA, TFIIB, TFIID, TFIIE, TFIIF et TFIIH. Ils se lient au promoteur cœur, région d'ADN minimum requise pour la transcription, et sont suffisants pour la transcription de base *in vitro*. TFIIH est donc impliqué dans la réparation de l'ADN et dans l'initiation de la transcription. Les facteurs spécifiques de la transcription se fixent sur l'UAS (Upstream Activating Sequence) ou l'enhancer et stimulent la transcription par l'intermédiaire des co-activateurs.

Nous nous intéressons particulièrement au Médiateur qui est un co-activateur essentiel pour la transcription dépendante de l'ARN Pol II. Le Médiateur est un complexe conservé de la levure à l'Homme faisant un lien physique entre les activateurs et la machinerie de base de la transcription. Le Médiateur interagit avec les GTFs et est requis pour la mise en place du PIC. Le Médiateur facilite aussi la phosphorylation de l'ARN Pol II par le module kinase de TFIIH. Cette phosphorylation diminue l'affinité du Médiateur pour l'ARN Pol II, ce qui permet au dernier de s'échapper du promoteur et de passer en élongation.

II.2 Avant-propos

Notre équipe vise à comprendre les mécanismes qui lient la transcription et la réparation de l'ADN. En effet, nous avons découvert un lien fonctionnel entre le Médiateur de la transcription et une protéine du NER, Rad2, chez *S. cerevisiae* (Eyboulet *et al.*, 2013).

Notre laboratoire travaille depuis des années sur le Médiateur et a aidé à une meilleure caractérisation de son rôle dans la transcription. Le Médiateur transmet les signaux des facteurs de transcription à la machinerie de transcription de l'ARN polymérase II. L'équipe a notamment mis en évidence des interactions entre le Médiateur et la machinerie de base de la transcription (TFIIH, TFIIB et l'ARN Pol II) in vivo, nécessaires au recrutement de ces facteurs lors de l'initiation de la transcription (Esnault *et al.,* 2008; Soutourina *et al*., 2011; Eyboulet *et al*., 2015 ; Eychenne *et al*., 2016).

Dans la première partie du projet, nous avons analysé de manière approfondie le lien fonctionnel entre Rad2, le Médiateur et l'ARN Pol II. Les analyses génomiques ont montré que la présence de Rad2 et du Médiateur était fortement corrélée au niveau des régions régulatrices (UAS) des gènes. Rad2, contrairement au Médiateur, est aussi présent au niveau des régions transcrites des gènes, tout comme l'ARN Pol II (Eyboulet *et al*., 2013). De plus, il a été démontré que le Médiateur et Rad2 interagissent avec l'ARN Pol II (Soutourina *et al.*, 2011; Eyboulet *et al.,* 2013). Ainsi, il existe un réseau d'interactions impliquant l'ARN Pol II, le Médiateur et Rad2. Un de nos objectifs consiste à mieux caractériser l'interaction fonctionnelle entre ces facteurs, en particulier à comprendre le mode de recrutement de Rad2 à la chromatine. Pour répondre à cette question, nous avons utilisé des mutants de *kin28* (sous-unité de TFIIH), *rpb9* (sous-unité de l'ARN Pol II) et *med17* (sous-unité du Médiateur). Ma contribution dans ce projet a consisté à analyser les effets de la mutation *kin28* sur la distribution génomique de l'ARN Pol II, du Médiateur et de Rad2 et les interactions entre ces protéines. Kin28 est une sous-unité de TFIIH possédant une activité kinase. La phosphorylation du CTD (Carboxy- Terminal Domain) de l'ARN Pol II par Kin28 est nécessaire à l'échappement de l'ARN Pol II du promoteur. Des expériences précédentes ont montré que l'inhibition de l'activité catalytique de Kin28 ou la diminution de sa quantité nucléaire permet de stabiliser l'association transitoire du Médiateur avec le complexe de pré-initiation au niveau du promoteur cœur (Wong *et al*., 2014; Jeronimo and Robert, 2014, Jeronimo *et al*., 2016; Petrenko *et al*., 2016).

Dans une deuxième partie, nous avons voulu savoir si le lien entre le Médiateur et la machinerie de réparation NER pouvait s'étendre à d'autres protéines. Pour cela nous avons utilisé des approches de génétique, de biologie moléculaire et de bio-informatique. Nous avons aussi testé les interactions entre le Médiateur et les protéines du NER après l'induction des dommages à l'ADN par les UV et analyser leur distribution chromatinienne.

II.3 Résultats

II.3.1 Lien fonctionnel entre Rad2, le Médiateur et l'ARN Pol II

Afin d'étudier le lien fonctionnel entre Rad2, le Médiateur et l'ARN Pol II, nous avons voulu déterminer comment la distribution chromatinienne de Rad2 change quand la présence du Médiateur est stabilisée sur le promoteur cœur et le départ de l'ARN Pol II en élongation est affecté. Nous avons utilisé un mutant thermosensible de Kin28 (*kin28 ts*) dans lequel le passage de 25°C à 37°C diminue considérablement la phosphorylation du CTD de l'ARN Pol II. Par des expériences de ChIP-seq, nous avons déterminé le changement de profil génomique de l'ARN Pol II, du Médiateur et de Rad2 dans le mutant *kin28 ts*. Nous avons observé qu'il y a une baisse globale de l'occupation de l'ARN Pol II au niveau des régions transcrites. La comparaison des ratios d'occupation de l'ARN Pol II dans le mutant *kin28 ts* sur la souche sauvage, a montré qu'il y a une baisse moins importante au niveau 5' des gènes. Ces résultats sont en accord avec une diminution de phosphorylation du CTD de l'ARN Pol II menant à un défaut d'échappement du promoteur de l'ARN Pol II. En comparaison avec la souche sauvage, nous avons observé que l'occupation du Médiateur est augmentée au niveau de l'UAS et au niveau du promoteur cœur, suggérant la stabilisation d'un intermédiaire contenant le Médiateur sur le promoteur cœur. Au niveau génomique, nous avons aussi observé un changement de la distribution de Rad2. Ainsi, au niveau des régions transcrites, nous avons observé une baisse de la présence de Rad2. De plus, l'occupation de Rad2 est augmentée au niveau de l'UAS autour des pics du Médiateur et au niveau du promoteur cœur mais l'augmentation est moins prononcée que pour le Médiateur. Ensuite, nous avons cherché à savoir si les changements de liaison à la chromatine de l'ARN Pol II, du Médiateur et de Rad2 observés peuvent être liés à une modification des interactions entre ces protéines. En conséquence, nous avons réalisé des expériences de co-immunoprécipitation eu utilisant des extraits bruts. Nous avons observé que dans le mutant *kin28 ts*, le Médiateur co-immunoprécipite davantage avec l'ARN Pol II et inversement, moins de Rad2 co-immunoprécipite avec l'ARN Pol II. Ces résultats sont en accord avec les données ChIP-seq. Nos résultats montrent que la présence de Rad2 à la chromatine est influencée à la fois par le Médiateur et par l'ARN Pol II. Rad2 semble suivre le Médiateur au niveau des régions promotrices et l'ARN Pol II au niveau des régions transcrites.

Nous avons aussi utilisé un mutant de la sous-unité Med17 du Médiateur qui présente un défaut d'interaction entre Rad2 et le Médiateur et un mutant d'une sous-unité non-essentielle de l'ARN Pol II, Rpb9.

Nous avons précédemment démontré que la sensibilité aux UV des mutants de med17 est corrélée à une baisse de l'occupation de Rad2 à la chromatine et une diminution de l'interaction entre le Médiateur et Rad2 (Eyboulet *et al.,* 2013). Dans cette étude, nous avons analysé l'effet des mutations de *med17* sur la distribution génomique de l'ARN Pol II, du Médiateur et de Rad2. Deux mutants du Médiateur ont été utilisés : *med17 Q444P*

(mutant légèrement sensible aux UV) et *med17 Q444P/M442L* (mutant ayant une sensibilité accrue aux UV).

Nous avons observé qu'il y a une augmentation de la présence de Rad2 au niveau de l'UAS qui accompagne une augmentation de l'occupation du Médiateur sur ces régions. Au niveau des régions transcrites, une baisse de l'occupation de Rad2 et de l'ARN Pol II a été observée. Cette baisse de Rad2 était plus prononcée dans le mutant qui est fortement sensible aux UV en comparaison avec le mutant légèrement UV-sensible.

De plus, des expériences génétiques ont montré que le phénotype de thermo-sensibilité, associé à des défauts transcriptionnels, ne peut être dissocié du phénotype de sensibilité aux UV. Néanmoins, les mutants thermo-sensibles du Médiateur ne sont pas tous UV-sensibles, donc le phénotype de sensibilité aux UV n'est pas une conséquence d'un défaut transcriptionnel. La sensibilité aux UV des mutants *med17* du Médiateur n'est visible que dans un contexte GG-NER déficient, suggérant un rôle du Médiateur dans la TC-NER. De ce fait, nous avons investigué si les mutations du Médiateur et de Rad26 sont épistatiques. Nous avons observé que dans un contexte GG-NER déficient, le mutant UV-sensible du Médiateur présente un phénotype synthétique de la sensibilité aux UV avec la délétion de *RAD26*, gène codant pour un facteur spécifique de la sous-voie TC-NER. Ce résultat suggère que la fonction du Médiateur dans le NER est au moins en partie indépendante de la voie TC-NER liée à Rad26.

De nombreuses études ont suggéré l'existence de voie TC-NER indépendante de Rad26 (Jansen *et al.*, 2002; Verhage *et al.*, 1996). Une voie TC-NER dépendante de la sous-unité non-essentielle de l'ARN Pol II, Rpb9, a été suggérée chez la levure (Li and Smerdon, 2002). Etant donné du lien fonctionnel qui existe entre le Médiateur et l'ARN Pol II, nous avons testé si les mutations de *med17* et *rpb9* sont épistatiques. De manière intéressante, nous avons observé une co-létalité entre *rpb9Δ* et le mutant *med17 Q444P/M442L* qui est fortement UV-sensible, ainsi que d'autres mutants *med17* sensibles aux UV. Ce qui indique un lien fonctionnel entre le Médiateur et Rpb9 dans la sous-voie TC-NER. En outre, l'occupation génomique de Rad2, du Médiateur et de l'ARN Pol II a été investiguée dans le mutant rpb9. La baisse de l'occupation de Rad2 et de l'ARN Pol II sur les régions transcrites était gène-dépendant. De plus, nous avons observé un enrichissement de Rad2 sur les UAS dans le mutant mais pas de changement dans l'occupation du Médiateur sur ces régions.

Dans l'ensemble, ces résultats issus des trois mutants (*kin28*, *rpb9* et *med17*) nous ont permis de proposer un modèle dans lequel Rad2 est recruté au niveau des régions régulatrices où le Médiateur est enrichi, et Rad2 est ensuite transféré au niveau de la région transcrite de manière dépendante à l'ARN Pol II.

II.3.2 Lien fonctionnel entre le Médiateur et d'autres protéines de la machinerie NER

Nous avons investigué si le lien fonctionnel entre le Médiateur et la machinerie NER peut être étendu à d'autres protéines. Cinq protéines du NER ont été testées : Rad1/XPF,

Rad10/ERCC1, Rad14/XPA, Rad26/CSB et Rad4/XPC. Rad1/XPF et Rad10/ERCC1 forme un dimère avec une activité 5' endonucléasique qui est requis pour les deux sous-voies du NER. Rad14/XPA est impliqué dans la vérification du dommage et l'assemblage du complexe de réparation. Rad4/XPC et Rad26/CSB sont impliqués dans la reconnaissance des dommages dans les voies GG-NER et TC-NER respectivement.

Tout d'abord, nous avons testé l'interaction physique entre le Médiateur et les protéines du NER par des expériences de co-immunoprécipitation. Nous avons montré que Rad1, Rad10 et Rad26 interagissent avec le Médiateur. Par contre dans nos conditions de co-immunoprécipitation, nous n'avons pas vu d'interaction entre le Médiateur et Rad4 ou Rad14.

Etant donné que le Médiateur a un rôle dans la transcription, nous avons vérifié que Rad1 et Rad10 n'avaient pas un rôle transcriptionnel. Nous avons délété les gènes *RAD1* ou *RAD10* car ces gènes sont non-essentiels tout comme RAD2. Nous n'avons pas observé de différence de croissance entre les mutants *rad1Δ* ou *rad10Δ* et la souche sauvage sur différents milieux de culture (contenant du glucose, galactose, glycérol, ou appauvri en glucose), à différentes températures (16°C, 25°C, 30°C, 37°C) ou en présence d'un inhibiteur de synthèse de nucléotide (acide mycophénolique). Le seul phénotype observé est la sensibilité aux UV, comme attendu pour des protéines de la voie NER. Nous avons aussi observé que dans les mutants *rad1Δ* et *rad10Δ*, l'ARN Pol II et le Médiateur sont correctement recrutés à la chromatine. Nous avons ainsi conclu que Rad1 et Rad10 n'ont pas de rôle majeur dans la transcription. Un rôle dans la transcription a déjà été proposé pour Rad26 (Lee *et al.*, 2001). Les auteurs ont montré que sur un milieu de culture contenant le galactose, la délétion de *RAD26* conduisait à un défaut de croissance cellulaire et ce défaut était accru en absence de Rad26 et TFIIS, un facteur général de la transcription. D'autre part dans le mutant *rad26Δ*, le niveau d'ARN messagers des gènes inductibles GAL était aussi réduit et l'effet était augmenté en absence de Rad26 et TFIIS. De plus, la croissance du mutant *rad26Δ* était aussi affectée en présence d'une drogue qui réduit la concentration intracellulaire des nucléotides (6-azauracil) (Lee *et al*., 2001). Néanmoins nous n'avons pas observé de défaut de croissance en comparaison avec la souche sauvage sur différents milieux de culture y compris galactose ou en présence d'un inhibiteur de synthèse de nucléotide (acide mycophénolique) comme précedemment fait pour les mutants *rad1Δ* et *rad10Δ*. Pour le test de croissance en présence de l'acide mycophénolique, nous avons observé que le mutant délété pour TFIIS avait bien un défaut de croissance mais pas *rad26Δ*. Ainsi, nos résultats ne confirment pas un défaut de croissance dans un mutant *rad26Δ*.

Pour approfondir le lien entre les protéines du NER et le Médiateur, nous avons réalisé des expériences de ChIP-seq (immunoprécipitation de la chromatine suivi d'un séquençage à haut débit). Nous avons comparé les distributions génomiques de Rad1, Rad10 et Rad26 à ceux de Rad2 et du Médiateur. Nous avons observé que Rad1, Rad10, Rad2 et le Médiateur sont présents au niveau de l'UAS de certains gènes, représentant 40% des pics de Rad1-

Rad10. Par contre, nous n'avons pas vu d'enrichissement spécifique de Rad26 au niveau de l'UAS.

De plus au niveau génomique, nous avons observé que Rad1, Rad10 et Rad26 sont enrichis au niveau des régions transcrites tout comme Rad2 et l'ARN Pol II. Des études précédentes ont montré une interaction entre l'ARN Pol II et Rad2 et Rad26 (Eyboulet *et al.,* 2013; Malik *et al*., 2010). Dans notre étude, nous avons observé une interaction entre Rad1 et l'ARN Pol II. Ainsi, nous avons testé si la présence de Rad1 et Rad10 dépend de la transcription de l'ARN Pol II en utilisant un mutant thermosensible de l'ARN Pol II, *rpb1-1*. Les cellules ont été cultivées à 25°C puis transférées à 37°C, température non-permissive, pendant 90 min. Nous avons observé une baisse de la présence Rad1 et Rad10 au niveau des régions transcrites des gènes dépendants de l'ARN Pol II dans le mutant par rapport à la souche sauvage. La présence de Rad1 et de Rad10 à la chromatine est dépendante de la transcription. La liaison à la chromatine de Rad26 est aussi dépendante de la transcription (Malik *et al*., 2010).

Pour mieux caractériser les gènes en fonction de leur enrichissement en Rad1, Rad10, Rad2 et le Médiateur sur les régions promotrices, nous avons divisé ces gènes en différents groupes. Un premier groupe enrichi en Rad1, Rad10, Rad2 et le Médiateur. Un deuxième groupe enrichi en Rad1 et Rad10 et un troisième groupe enrichi en Rad2 et le Médiateur. Un quatrième groupe de gènes qui n'est pas enrichi par aucune des quatre protéines. Un cinquième groupe correspondant aux gènes à l'interface des quatre groupes. Nous avons investigué si la présence de Rad1 et Rad10 sur les régions promotrices affecte leur présence sur les régions transcrites des gènes de classe II. Nous avons observé que les régions promotrices enrichies par Rad1-Rad10 et le Mediator-Rad2 sont aussi enrichies par Rad1-Rad10 au niveau des régions transcrites, en comparaison avec des régions promotrices enrichies uniquement en Rad1-Rad10. Ces résultats suggèrent un lien entre l'enrichissement de Rad1-Rad10 sur les régions promotrices et leur présence au niveau des régions transcrites et que la présence de Médiateur-Rad2 peut influencer la présence de Rad1-Rad10 sur les régions transcrites.

Pour mieux comprendre l'interaction fonctionnelle entre Rad1, Rad10, Rad26 et le Médiateur, nous avons utilisé le mutant *kin28 ts* précédemment décrit (partie 1 des résultats). Nous avons observé que dans ce mutant, il y a une stabilisation de Rad10 au niveau des régions promotrices (UAS et promoteur cœur) au niveau génomique. La présence de Rad26 est aussi stabilisée au niveau de l'UAS et il y a une petite stabilisation au niveau du promoteur cœur pour 20% des gènes. Le profil de ces protéines suit celui du Médiateur et Rad2 au niveau des régions promotrices mais de moindre amplitude. Dans le mutant au niveau de la région transcrite, il y a une baisse de l'occupation de Rad26 aussi observée pour l'ARN Pol II et cette baisse est plus importante que pour Rad2. On n'a pas observée de baisse de Rad10 au niveau des régions transcrites. Des analyses plus approfondies sont nécessaires, notamment sur les groupes de gènes définis en fonction de leur enrichissement en Rad1-Rad10 et Rad2-Médiateur.

Pour comprendre l'importance de l'interaction entre les protéines de la voie NER (Rad1, Rad10 et Rad26) et le Médiateur, nous avons essayé d'identifier les sous-unités du Médiateur interagissant avec les protéines du NER par des expériences de double hybride. Cependant, nous n'avons pas pu identifier d'interaction. Nous avons ainsi utilisé des mutants de *med17* avec différents niveau de sensibilité aux UV pour regarder l'influence de ces mutations sur la présence de Rad10 sur la chromatine. Alors que ces mutants sont tous défectueux pour la transcription, l'occupation des régions transcrites de Rad10 est affectée uniquement dans les mutants UV-sensibles. Ces résultats suggèrent que le Médiateur influence la présence de Rad10 sur la chromatine. Des expériences similaires doivent être faites pour Rad26 pour mieux caractériser son lien avec le Médiateur.

Le laboratoire a précédemment démontré une interaction fonctionnelle entre la sous-unité Med11 du Médiateur et la sous-unité Rad3 de TFIIH (Esnault *et al*., 2008). Etant donné que TFIIH a un rôle à la fois dans l'initiation de la transcription et dans le NER, nous avons voulu savoir si le rôle du Médiateur dans le NER impliquait cette interaction entre Rad3 et Med11. Des expériences de survie aux UV des mutants de *med11* dans un contexte GG-NER déficient n'ont pas montré d'augmentation de la sensibilité dans le mutant affecté pour l'interaction Med11-Rad3. Ainsi, le lien du Médiateur avec la voie NER peut être indépendant de cette interaction avec TFIIH. Il faut noter que deux autres mutants de *med11* ont une sensibilité accrue aux UV, suggérant une implication de la sous-unité Med11 du Médiateur en plus de Med17 dans le NER.

Les protéines du NER ont un rôle dans la réparation des dommages induits par les UV. Nous avons donc voulu savoir s'il y avait un changement d'interaction entre le Médiateur et les protéines du NER après un stress UV. Nous avons irradié les cellules à 50 J/m^2 et les cellules ont été récupérées juste après l'irradiation (T0) ou 30 min (T30) ou 60 min (T60) après incubation à 30°C. Les expériences de co-immunoprécipitation montrent que l'interaction entre le Médiateur et les protéines de réparation persiste après l'induction de dommages mais il n'y a pas de modification de l'interaction.

Précédemment, nous avons montré que les protéines du NER (Rad1, Rad10, Rad26 et Rad2) sont présentes à la chromatine avant l'induction des dommages à l'ADN. Nous avons réalisé des expériences de ChIP pour savoir s'il y avait un changement de liaison à l'ADN de Rad1, Rad10, Rad26, Rad2, l'ARN Pol II et le Médiateur après l'irradiation aux UV. Les cellules ont été récupérées juste après les UV (T0) et 30 min après incubation à 30°C (T30). Les premières analyses sur plusieurs gènes sélectionnés montrent qu'il y a effectivement un changement de profil de liaison de ces protéines après induction de dommage et la cinétique de recrutement n'est pas la même pour les différentes protéines. Nous avons observé une augmentation de l'occupation de Rad2 dès T0, par contre l'augmentation de Rad10 est observée à T30 sur les régions promotrices et transcrites. Il y a une baisse de l'occupation de l'ARN Pol II à T0 au niveau de la région transcrite et promotrice en comparaison avec les cellules non-irradiées. De manière intéressante, nous avons observé une augmentation de l'occupation du Médiateur au niveau de la région transcrite après

irradiation. En conclusion, nous avons observé des modifications de liaison à l'ADN de ces protéines sur certaines régions après l'irradiation UV. Ces expériences seront faites à l'échelle du génome pour avoir une vue plus globale des changements de distribution de ces protéines.

II.4 Conclusion

La transcription et la réparation de l'ADN sont deux processus fondamentaux dont les dysfonctionnements sont impliqués dans les pathologies graves. A travers notre projet, nous proposons de faire le lien entre ces deux processus par la compréhension du mode d'action du Médiateur et de ces partenaires dans la réparation de l'ADN couplée à la transcription. En effet, nous avons solidifié le lien entre la machinerie du NER et le Médiateur en démontrant des nouvelles interactions entre le Médiateur et Rad1, Rad10 et Rad26. Nous avons démontré que la présence de ces protéines du NER sur la chromatine est dépendante de la transcription et du Médiateur. De plus, la présence de ces protéines sur la chromatine en l'absence de stress génotoxique peut faciliter la réparation de ces régions après l'induction des dommages à l'ADN.

Titre : Etude des mécanismes moléculaires liant la transcription et la réparation de l'ADN chez la levure *Saccharomyces cerevisiae*
Mots clés : Réparation par excision de nucléotides, Transcription, Médiateur, ARN Polymérase II, Rad2, Rad1, Rad10, Rad26

Résumé : La voie de réparation par excision de nucléotides (NER) répare les lésions qui distordent la double hélice d'ADN notamment ceux induits par l'irradiation UV. Le NER est subdivisé en deux sous-voies : GG-NER (Global Genome Repair) et TC-NER (Transcription-Coupled Repair). La sous-voie GG-NER enlève les dommages dans l'ensemble du génome. La sous-voie TC-NER répare les dommges qui interfèrent avec la progression de la Pol II. Les défauts de la voie NER peuvent conduire à l'apparition de pathologies graves. Par exemple, des mutations dans le gène XPG, codant une 3' endonucléase impliquée dans la voie NER, peuvent mener au xeroderma pigmentosum associé ou non au syndrome de Cockayne .

Récemment, le laboratoire a découvert un lien fonctionnel entre Rad2, homologue chez la levure *S. cerevisiae* de la protéine XPG humaine, et le Médiateur (Eyboulet *et al.*, 2013). Le Médiateur est un complexe multiprotéique nécessaire à la régulation de la transcription dépendante de la Pol II. Cette étude a suggéré que le Médiateur est impliqué dans la sous-voie TC-NER en facilitant le recrutement de Rad2 au niveau des régions transcrites.

Mon projet de thèse visait à investiguer le lien fonctionnel entre le Médiateur et la machinerie du NER chez *S. cerevisiae*.

Lors du TC-NER, l'ARN Pol II est le premier facteur signalant le dommage à l'ADN. De plus, le Médiateur et Rad2 interagissent avec la Pol II. Pour déterminer le lien fonctionnel entre ces composants, nous avons utilisé des approches de génétique et génomique dans les mutants de TFIIH (*kin28*), de l'ARN Pol II (*rpb9*) and du Médiateur (*med17*). Nos résultats nous ont permis de proposer un modèle dans lequel Rad2 est recruté au niveau des régions régulatrices enrichies par le Médiateur, et Rad2 est ensuite transféré au niveau des régions transcrites par un mécanisme dépendant de la Pol II (Georges, Gopaul *et al*., en révision. De plus, ces résultats suggèrent que le rôle du Médiateur dans la transcription est fortement lié à son rôle dans la réparation de l'ADN.

Nous avons ensuite montré un lien entre le Médiateur et d'autres protéines du NER notamment en démontrant une interaction physique entre le Médiateur et Rad1, Rad10 ou Rad26, en l'absence des UV. Tout comme Rad2, nous avons montré que Rad1 et Rad10 n'ont pas de rôle majeur dans la transcription. Pour approfondir le lien entre ces protéines du NER et le Médiateur, des expériences de ChIP-sequencing ont été réalisées. Nous avons observé que le Médiateur est présent au niveau de certaines régions promotrices qui sont aussi enrichies par ces protéines du NER. Après l'induction des dommages par UV, les interactions entre le Médiateur et la machinerie du NER reste inchangées par rapport aux conditions en l'absence des UV. De plus grâce à nos expériences de ChIP, nous avons observé un changement de distribution chromatinienne des protéines du NER et du Médiateur après l'irradiation aux UV. Des expériences de ChIP-sequencing seront réalisées pour avoir une vue globale de ces changements.

En conclusion, nous avons solidifié le lien fonctionnel entre Rad2, le Médiateur et l'ARN Pol II par rapport à la réparation couplée à la transcription. Nous avons aussi démontré que le Médiateur interagit avec d'autres protéines du NER et colocalise avec eux sur certaines régions de la chromatine. Notre projet place le Médiateur à l'interface de la transcription et de la réparation de l'ADN, deux processus essentiels dont les défauts peuvent mener à des pathologies graves.

Title : Study of the molecular mechanisms linking transcription and DNA repair in *Saccharomyces cerevisiae*
Keywords: Nucleotide Excision Repair, Transcription, Mediator, RNA Polymerase II, Rad2, Rad1, Rad10, Rad26

Abstract: Nucleotide excision repair (NER) is a conserved pathway that removes helix-distorting DNA lesions such as those arising upon UV irradiation. Global genome repair subpathway (GG-NER) removes the DNA lesions in the genome overall, and transcription-coupled repair (TC-NER) removes the DNA lesions interfering with Pol II progression through actively-transcribed regions. Defects in the NER pathway may lead to severe human pathologies. For instance, mutations in human XPG gene, encoding a 3' endonuclease essential for NER, give rise to xeroderma pigmentosum sometimes associated with Cockayne syndrome. Recently, the laboratory discovered a functional link between Rad2/XPG and Mediator in *Saccharomyces cerevisiae* (Eyboulet *et al.*, 2013). Mediator is a large multisubunit complex essential for transcription regulation. We suggest that Mediator is involved in TC-NER by facilitating Rad2 recruitment to transcribed genes.

My PhD work aimed at addressing the molecular mechanisms of this link between transcription and DNA repair, especially by investigating the functional interplay between Mediator and the NER machinery in *S. cerevisiae*.

Pol II is the first complex of TC-NER that encounters the DNA damage. Moreover, both Mediator and Rad2/XPG interact with Pol II. However, a functional interplay between all these components related to TC-NER remains to be determined. Using genetic and genomic approaches, in particular ChIP-sequencing in TFIIH (*kin28*), Pol II (*rpb9*) and Mediator (*med17*) mutants, our work led us to propose a model where Rad2 shuttles between Mediator on upstream activating sequence (UAS) and Pol II on transcribed regions (Georges, Gopaul *et al*., under review). Our results also suggest that Mediator's functions in transcription and DNA repair are closely related. Moreover, we showed that Mediator's link to NER can be extended to other NER proteins. Indeed, we identified a physical interaction between Mediator and other NER proteins, including Rad1, Rad10 and Rad26 in the absence of UV irradiation. Similarly to Rad2, we demonstrated that Rad1 and Rad10 do not have a major role in yeast transcription. To further study the functional link between Mediator and the NER machinery, we obtained the genomic distribution of different NER proteins by ChIP-sequencing. We found that some promoter regions are co-occupied by Mediator and these NER proteins, and that relationships between Mediator and these NER proteins are more complex than between Mediator and Rad2. We also investigated if physical interactions between Mediator and NER proteins are modified after UV, we did not observe any significant change. Furthermore, we observed that the chromatin binding profiles of NER proteins and Mediator are modified after UV stress. ChIP-seq will be carried out to get a genome-wide view.

In conclusion, we have strengthened the link between Rad2, Mediator and Pol II, providing mechanistic insights into functional interplay between these components related to TC-NER, and showed that the link between Mediator and the NER machinery can be extended to other proteins. Taken together, our results suggest a close relation between Mediator's functions in transcription and in NER, two fundamental processes whose dysfunction leads to human diseases.